AER/AGS Report 100

Hydrogeological Mapping of Saline Aquifers in West-Central Alberta

AER/AGS Report 100

Hydrogeological Mapping of Saline Aquifers in West-Central Alberta

N. Nakevska, J. Brinsky and A. Singh

Alberta Energy Regulator
Alberta Geological Survey

March 2021

ISBN 978-1-4601-4514-2

If you use information from this publication in other publications or presentations, please acknowledge the AER/AGS. We recommend the following reference format:

Nakevska, N., Brinsky, J. and Singh, A. (2021): Hydrogeological mapping of saline aquifers in west-central Alberta; Alberta Energy Regulator / Alberta Geological Survey, AER/AGS Report 100, 148 p.

Published March 2021 by:
Alberta Energy Regulator
Alberta Geological Survey 4th
Floor, Twin Atria Building
4999 – 98th Avenue
Edmonton, AB T6B 2X3
Canada

Tel: 780.638.4491 Fax:
780.422.1459 Email:
AGS-Info@aer.ca Website:
www.ags.aer.ca

Contents

Tables

Figures

Acknowledgements

The authors wish to acknowledge the following individuals at the Alberta Geological Survey for their contributions to this report:

- S. Stewart for assistance with data compilation
- M. Babakhani for providing the bedrock formation surfaces
- D. Palombi and R. Huff for advice on culling criteria and ongoing discussion about the workflow for regional-scale hydrogeological mapping
- R. Huff, B. Smerdon, T. Lemay, and M. Grobe for reviewing earlier versions of this report

Abstract

This report presents the results and findings of a hydrogeological mapping project conducted by the Alberta Geological Survey to better understand groundwater conditions in an area of west-central Alberta, centred on the Town of Fox Creek. This study used fluid pressure, fluid chemistry, and temperature data to map the hydrogeological properties of 24 bedrock formations or grouped geological units spanning from the Upper Cretaceous Wapiti Formation, at depths of less than 500 m, to the base of the Cambrian succession, at depths of over 4000 m. For each formation or unit, maps were created showing aquifer delineation based on water-recovering drillstem tests, potentiometric surface, total dissolved solids, and water driving force. In addition to the hydrogeological mapping, pressure-elevation plots were created to examine vertical pressure gradients and hydraulic communication between formations. Water chemistry data were also analyzed using Piper plots and major ion data to determine the chemical composition of the formation water. The pressure gradients and Piper plots provide a summary of groundwater conditions at the regional-scale and can be used to understand the hydrogeological characteristics for deep saline formations in west-central Alberta.

1 Introduction

Unconventional resource plays in the Duvernay and Montney formations are undergoing development in west-central Alberta. Multistage hydraulic fracturing used in unconventional resource recovery has led to an increase in water demand, from both surface water and nonsaline groundwater sources. The amount of water used for hydraulic fracturing varies widely depending on the completion practice and the properties of the target formation. Reported water volumes used for hydraulic fracturing wells in the Duvernay unconventional resource play range from 10 000 to 60 000 m^3 per well (Alessi et al., 2017). The increase in water use and need for adequate disposal zones for flowback and produced water has led to a demand for hydrogeological information in this area. In addition, since 2006, the Alberta Government has encouraged oil and gas operators to minimize the use of nonsaline water in enhanced oil and bitumen recovery processes, and search for alternative water sources and technological alternatives (Alberta Government, 2014).

This report describes the methodology, results, and interpretation of the regional hydrogeological investigation of saline (>4000 mg/L total dissolved solids [TDS]) and mixed (nonsaline and saline) aquifers within a portion of west-central Alberta (Figure 1, Table 1), completed by the Alberta Geological Survey (AGS). Based on the permeability inferred from the general lithology of the investigated stratigraphic units, sandstone- and carbonate-dominated formations are considered aquifers, whereas shales and evaporites are considered aquitards. This study introduces further delineation of aquifers based on the location of water-recovering drillstem tests, and the amount of recovered water. This delineation represents a reasonable approximation of where a formation has shown it is capable of producing water, and provided an aquifer extent within which further mapping was completed.

The primary objective of this study is to portray groundwater information through a series of hydrogeological maps depicting different attributes, which can in turn be utilized to further characterize aquifer potential and support the development of water source and disposal scenarios. In addition to water sourcing and disposal, this hydrogeological information is beneficial for the planning and management of other development activities in the subsurface including CO_2 sequestration, geothermal resources evaluation, and evaluation of mineral resources found in formation waters.

This study produced up to four maps for each aquifer:

- a map showing the location of water-recovering drillstem tests (DSTs) and delineated aquifers
- a hydraulic head map (predevelopment), created to illustrate hydraulic head conditions excluding any production/injection-influenced data
- a TDS map, depicting the distribution of salinity
- a water driving force map, illustrating the net vectoral water driving force considering the density of fluid, hydraulic potential, and structural gradient within each aquifer

In addition, pressure-elevation plots, major ion plots and Piper diagrams, as well as schematic hydrogeological cross-sections, were created to support further analysis of groundwater compositions and conditions. For completeness, all maps, plots, summary tables, and supporting documentation are presented in the appendices at the end of this report as follows:

Appendix 1 – Hydrogeological Maps

Appendix 2 – Water Chemistry Plots

Appendix 3 – Summary Tables of Results

Appendix 4 – Culling Steps

Appendix 5 – Sources of Errors, Uncertainties, and Limitations

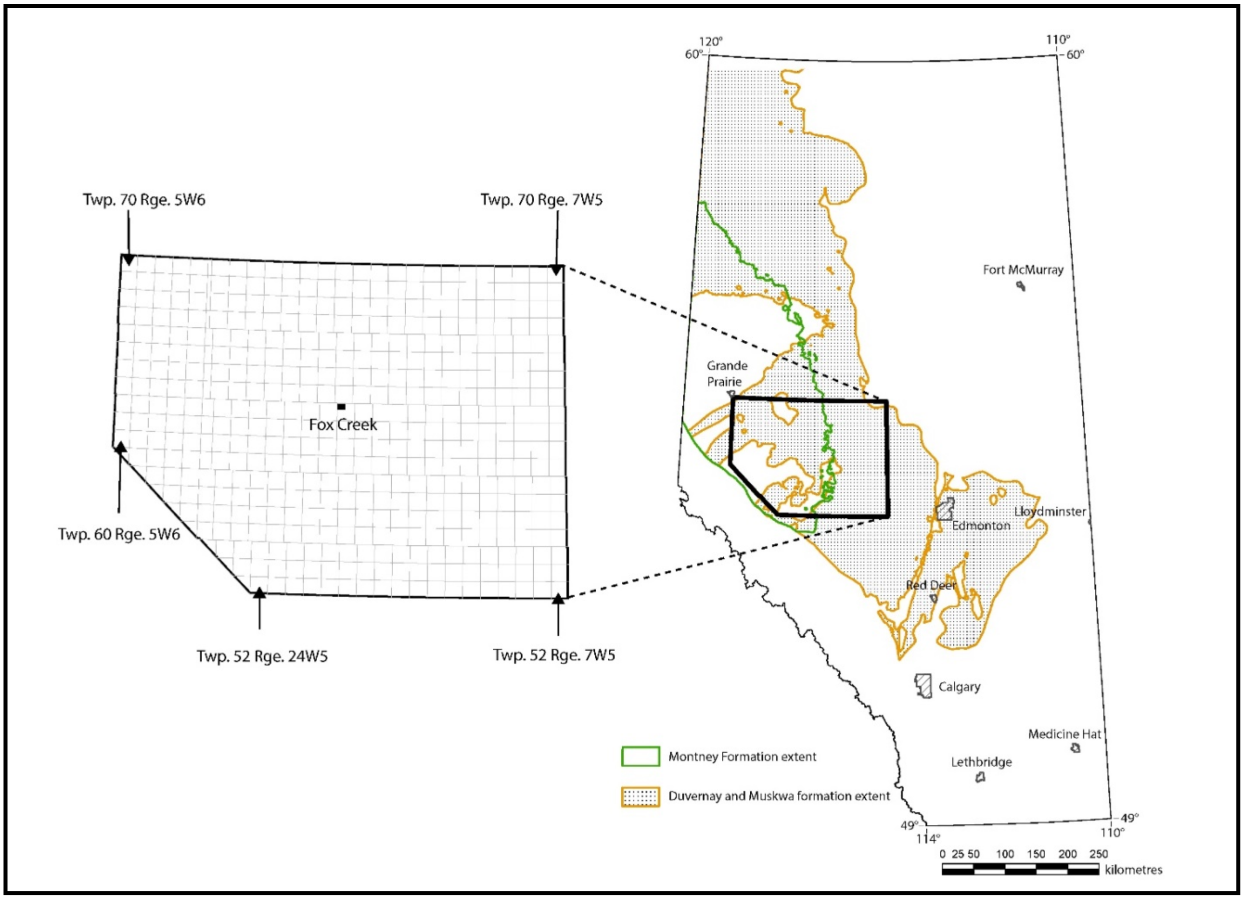

Figure 1. Location of the study area relative to the extents of the Duvernay, Muskwa, and Montney formations in Alberta. Formation extents from Alberta Geological Survey (2019a).

Table 1. Aquifers examined as part of the study, west-central Alberta.

Cretaceous	Mississippian–Jurassic	Cambrian–Devonian
Wapiti	Nordegg	Wabamun
Cardium	Middle–Upper Triassic	Blue Ridge
Dunvegan	Montney	Nisku
Viking	Belloy	Leduc
Spirit River	Debolt	Swan Hills
Bluesky	Shunda	Elk Point
Gething	Pekisko	Cambrian
Cadomin	Banff	
Nikanassin		

2 Location of the Study Area

The study area is located in west-central Alberta, centred on the Town of Fox Creek, and extends from Township 52, Range 7, west of the 5th Meridian in the southeastern corner to Township 70, Range 5, west of the 6th Meridian in the northwestern corner (Figure 1). The area covers parts of the subsurface extents of both the Duvernay and Montney formations. The topography within the study area is highly variable (Figure 2), ranging from 490 to 1606 m asl, with high elevations in the benchlands bordering the eastern edge of the Rocky Mountains in the southwest and the Swan Hills in the northeast, and low elevations in the valleys of the Athabasca River and tributaries to the Peace River. Several sandstone-dominated Cretaceous formations subcrop underneath Quaternary sediments north of the study area, in the vicinity of the Peace River valley (Figure 2), and may influence hydrogeological flow patterns and water chemistry within the study area.

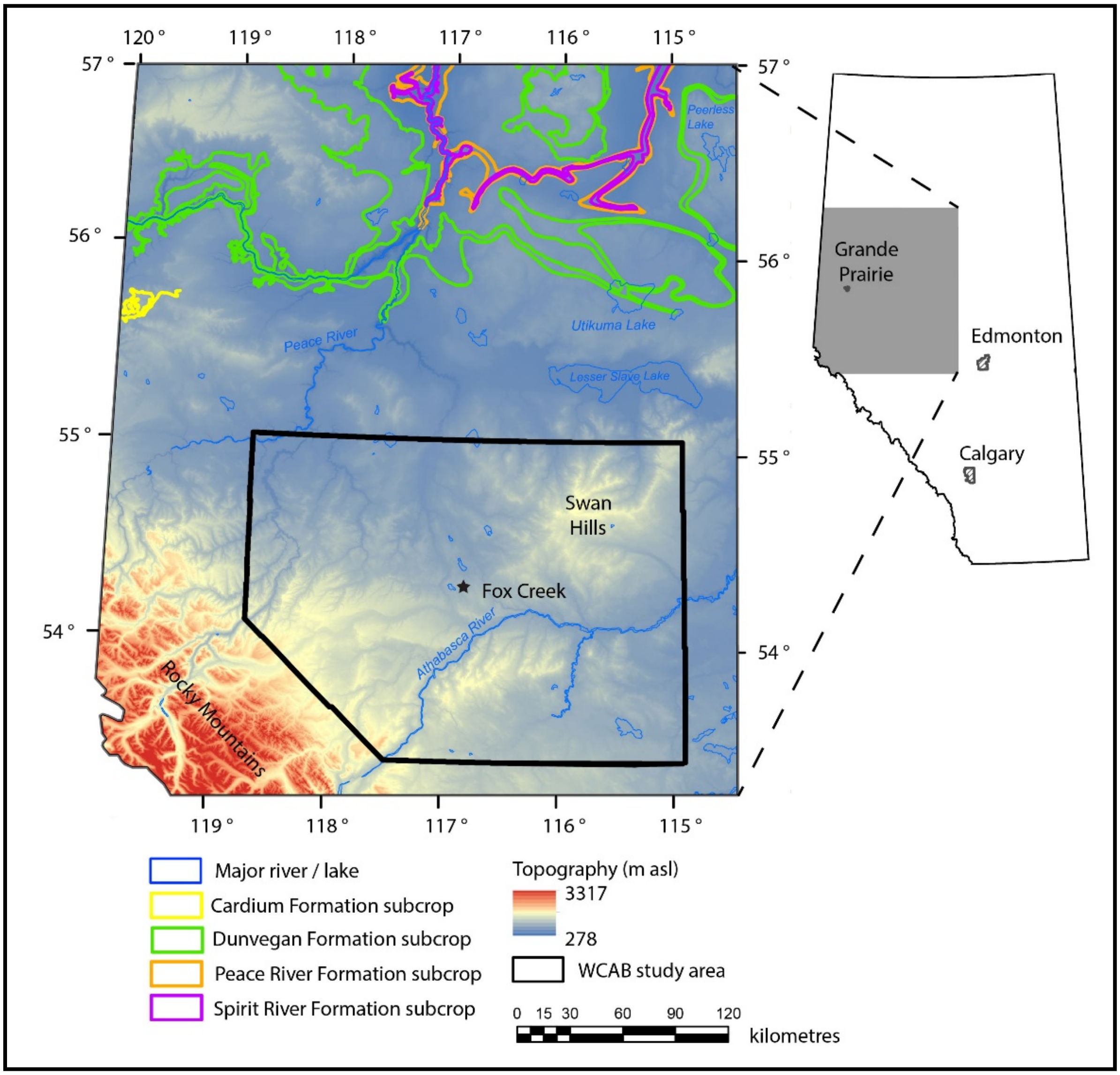

Figure 2. Location of subcrop areas of sandstone-dominated Cretaceous formations in relation to the west-central Alberta (WCAB) study area. Topography from provincial digital elevation model (DEM; Alberta Environment and Parks, 2015) and subcrop locations from *Bedrock Geology of Alberta* (Prior et al., 2013).

3 Hydrostratigraphy

The stratigraphic succession in the study area is divided into three hydrostratigraphic groups, based on similar lithology, hydrogeological attributes, and the presence of aquitards. This hydrostratigraphic breakdown consists of aquifers from the Cretaceous, Mississippian–Jurassic, and Cambrian–Devonian successions (Figures 3–5). Similar hydrostratigraphic breakdowns have been made in other parts of the Alberta Basin and throughout the province (Hitchon et al., 1990; Bachu, 1995; Michael, 2002).

The mapped Cretaceous succession in the study area (Figure 3) begins, at the top, with the Wapiti Formation, which, based on the general sandstone lithology, represents a relatively continuous aquifer, which subcrops beneath Quaternary sediments in the northern portion of the study area where it also reaches its zero edge. The Wapiti aquifer attains a thickness greater than 1300 m along the edge of the Rocky Mountain Foothills and thins towards the east (Dawson et al., 1994).

The Wapiti aquifer is underlain by the shales of the Lea Park and Wapiabi formations, which are part of a major continuous aquitard throughout the Alberta Basin (Bachu, 1995, 1999). The sandstone-dominated Cardium, Dunvegan, and Viking aquifers are isolated from each other by the Shaftesbury–Kaskapau aquitard. Within the three-dimensional (3D) geological model of west-central Alberta (Babakhani et al., 2019; Corlett et al., 2019), which was used as the geological framework for data allocation in the present study, the sandstone-dominated Viking Formation and the sandstone-dominated Paddy and Cadotte members of the Peace River Formation have been mapped as a single combined interval. As a result, the hydrogeological data used for mapping of the Viking aquifer were also combined. The Viking aquifer extends over the entire study area. The relatively thin Joli Fou aquitard, which includes shales of the Joli Fou Formation and Harmon Member of the lower Peace River Formation (Corlett et al., 2019), separates the Viking aquifer from the underlying Spirit River aquifer. The Spirit River aquifer comprises strata of the Spirit River Formation and correlative upper Mannville Group (Corlett et al., 2019). The Wilrich aquitard, where present, separates the Spirit River aquifer from the underlying Bluesky, Gething, and Cadomin aquifers. In the southeastern part of the study area, the Gething Formation transitions to the Ellerslie Member and Ostracod Beds (Corlett et al., 2019). In the western part of the study area, the lower Mannville Group–equivalent sandstones and conglomerates directly overlie the sandstones of the Upper Jurassic to Lower Cretaceous Nikanassin Formation at the sub-Cretaceous (sub-Aptian) unconformity, and are referred to as the Nikanassin–lower Mannville aquifer (Figure 3).

A summary of the general stratigraphy and hydrostratigraphy of the Mississippian–Jurassic succession is shown in Figure 4. The Mississippian–Jurassic succession is separated from the Cretaceous succession by the Fernie aquitard, which is present throughout the majority of the study area and pinches out in the east. The limestone aquifer of the Nordegg Member is found below the Fernie aquitard. The Nordegg aquifer is present throughout the study area and overlies subcropping formations of various ages, a result of major unconformities being present within the study area such as the sub-Jurassic, sub-Triassic, and sub-Permian unconformities. The Middle to Upper Triassic succession (Charlie Lake, Halfway, and Doig formations) is present in the northwestern part of the study area where it is eroded by the sub-Jurassic unconformity and subsequently pinches out (Corlett et al., 2019). The Middle to Upper Triassic succession in this area is characterized by variable lithology consisting of sandstones, evaporites, and carbonates. As a result, this succession acts as an aquifer in some areas and an aquitard in others. The Lower Triassic Montney Formation extends from the western to the central part of the study area, thinning eastwards as a result of depositional pinchout and erosion below the sub-Jurassic unconformity (Corlett et al., 2019). The general lithology of the Montney Formation changes from sandstone in the centre of the study area to siltstone and shale towards the west (Edwards et al., 1994). The Montney Formation can be considered an aquifer in the central part of the study area and an aquitard in the western part. In the west, the thick Montney aquitard separates the Middle–Upper Triassic aquifer from the underlying Permian Belloy aquifer. In the central and eastern parts of the study area, the Montney and Belloy formations form a continuous aquifer with the underlying Mississippian carbonates of the Debolt, Shunda, Pekisko, and Banff formations, which, with the exception of the Banff Formation, all have their zero-thickness edge within the study area (Michael, 2002).

The Cambrian–Devonian succession is confined by the aquitard formed by the overlying shales of the Devonian–Mississippian Exshaw Formation and lower portion of the Mississippian Banff Formation, and the underlying crystalline Precambrian basement, which acts as an aquiclude (Hitchon et al., 1990; Bachu, 1995). The Devonian succession from top to bottom consists of Wabamun, Winterburn, Woodbend, Beaverhill Lake, and Elk Point groups (Figure 5). Generally, the carbonates act as aquifers, whereas the intervening evaporites and basinal shales act as aquitards.

The Wabamun aquifer comprises a thick succession of predominantly limestone and dolostone. The Wabamun aquifer overlies the siltstone of the upper Graminia Formation (Graminia Silt member), which may form a thin aquitard between the Blue Ridge and Wabamun aquifers. The Blue Ridge Member of the Graminia Formation underlies the Graminia Silt member and was mapped in this study as the Blue Ridge aquifer. The Blue Ridge aquifer is underlain by the Calmar Formation shales, which form a thin aquitard separating the Blue Ridge aquifer from the Nisku aquifer. Underlying the Nisku aquifer are Woodbend Group strata consisting of dolomitized Leduc Formation reef buildups forming the Leduc aquifer, and shale deposits of the Ireton, Duvernay, and Majeau Lake formations, which form the Woodbend aquitard.

The Swan Hills Formation carbonate reef buildups and basinal carbonates of the Slave Point Formation were mapped together as one geological unit within the 3D geological model for the study area (Corlett et al., 2019). As a result, the hydrogeological data from the two formations were combined to map the Swan Hills aquifer. This aquifer is underlain by the mixed nearshore clastics and carbonates of the Elk Point Group, representing the Elk Point aquifer, and the underlying upper portion of the Cambrian succession, representing the Cambrian aquifer. A summary of the stratigraphy and hydrostratigraphy of the Cambrian–Devonian succession is shown in Figure 5.

4 Data and Methodology

The majority of data used to map hydraulic head and salinity originate from drillstem tests (DSTs) of oil and gas wells, accessed through AccuMap™ (IHS Markit, 2019). Some of the data used to map the shallower part of the Wapiti aquifer originate from the Alberta Water Well Information Database (AWWID; Alberta Environment and Parks, 2013). Stratigraphic allocation of data was completed using the 3D geological model of west-central Alberta (Babakhani et al., 2019). In this model, the stratigraphic interval between the top of the Precambrian and the top of the Watt Mountain Formation has not been subdivided, and includes strata of the Elk Point Group and the underlying Cambrian succession. As a result, hydrogeological data were first allocated based on the top of the Watt Mountain Formation followed by additional screening of individual tests to allocate data to either the Elk Point aquifer or the underlying Cambrian aquifer.

Representative pressure data was extracted from DST data in order to calculate hydraulic head values. The raw DST data were subjected to culling criteria modified from Jensen et al. (2013) to identify representative aquifer pressure tests. In addition to the automated culling, select DSTs were individually examined on an aquifer-by-aquifer basis to remove any remaining nonrepresentative fluid pressures. The DSTs passing the culling criteria were subsequently examined using a cumulative interference index (CII) methodology (Singh et al., 2017) to determine if pressures were influenced by production or injection activities.

Formation water analyses data were analyzed in order to select samples representative of formation water chemistry. Total dissolved solids (TDS) values were calculated by summing the major chemical constituents (Ca^{2+}, Mg^{2+}, Na^{+}, K^{+}, CO_3^{-}, HCO_3^{-}, Cl^{-}, and SO_4^{2-}) as reported in the dataset extracted from AccuMap. Chemical analyses were subjected to a culling procedure used in previous studies (Hitchon and Brulotte, 1994; Hitchon, 1996; Palombi, 2008) to identify potential contamination of formation water by drilling fluids, such as acid water, corrosion inhibitors, mud filtrates, and alcohols.

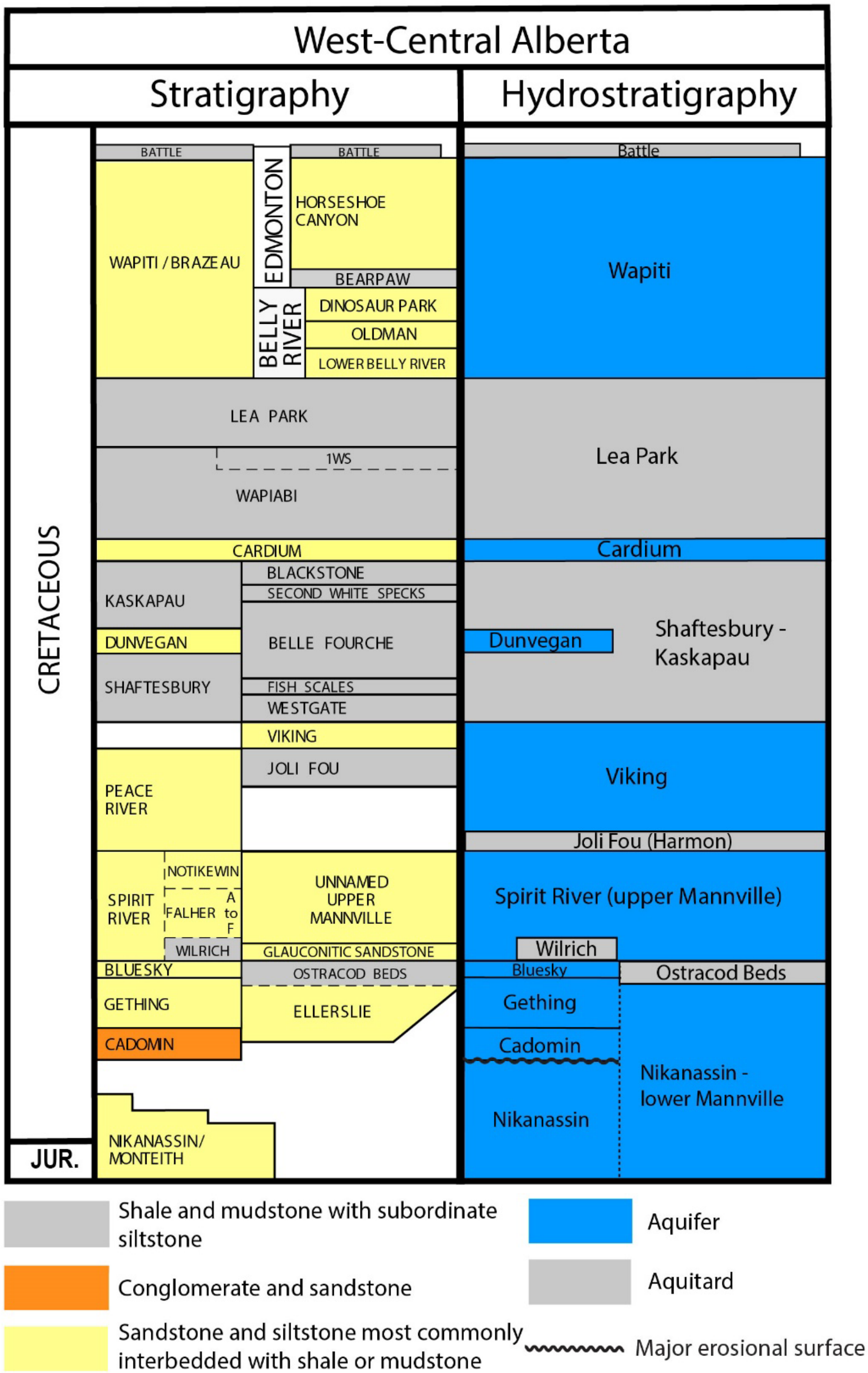

Figure 3. Stratigraphy and hydrostratigraphy of the Cretaceous succession in west-central Alberta (stratigraphy modified after Alberta Geological Survey, 2019b). Abbreviations: 1WS, First White Speckled Shale; JUR., Jurassic.

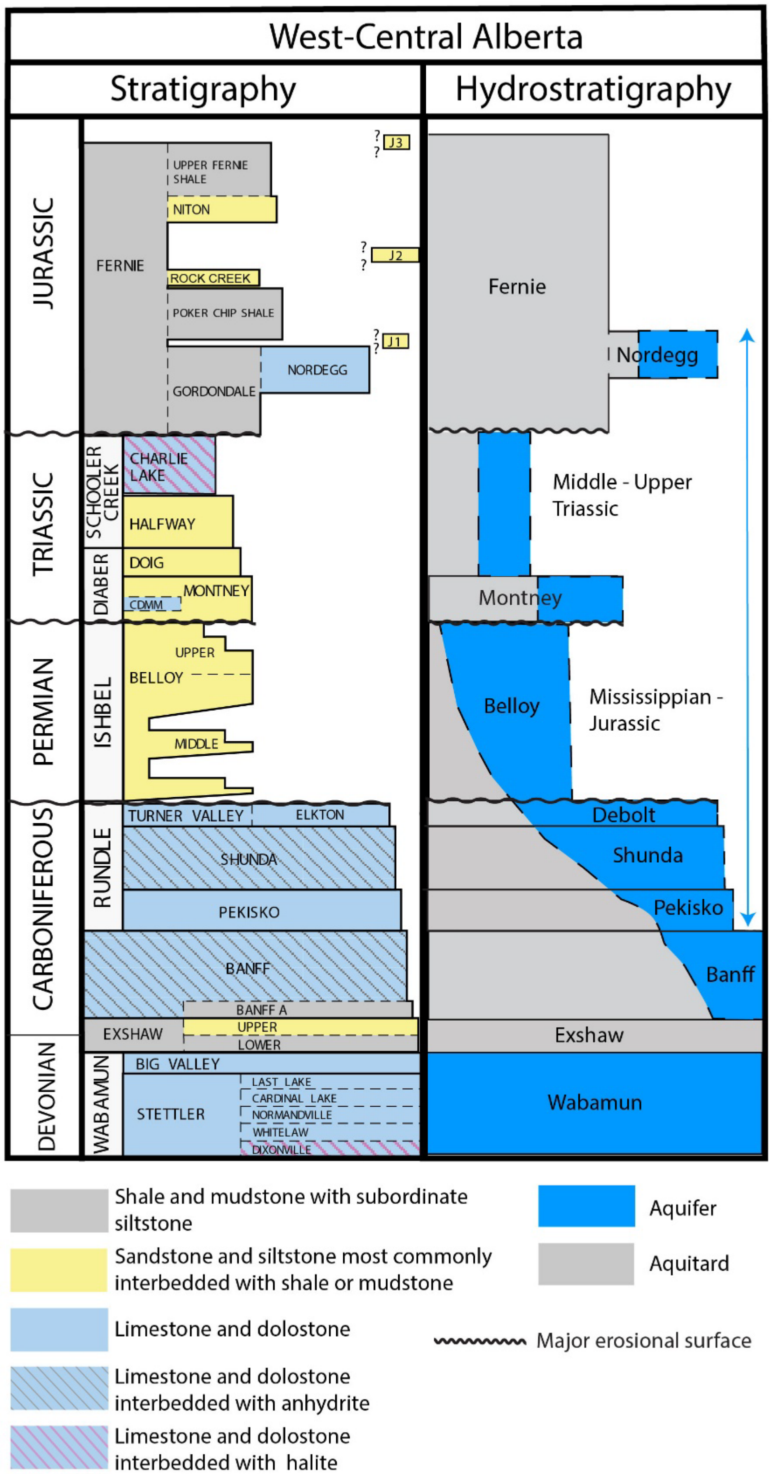

Figure 4. Stratigraphy and hydrostratigraphy of the Mississippian–Jurassic succession in west-central Alberta (stratigraphy modified after Alberta Geological Survey, 2019b). Abbreviation: CDMM, Coquinal Dolomite Middle Member.

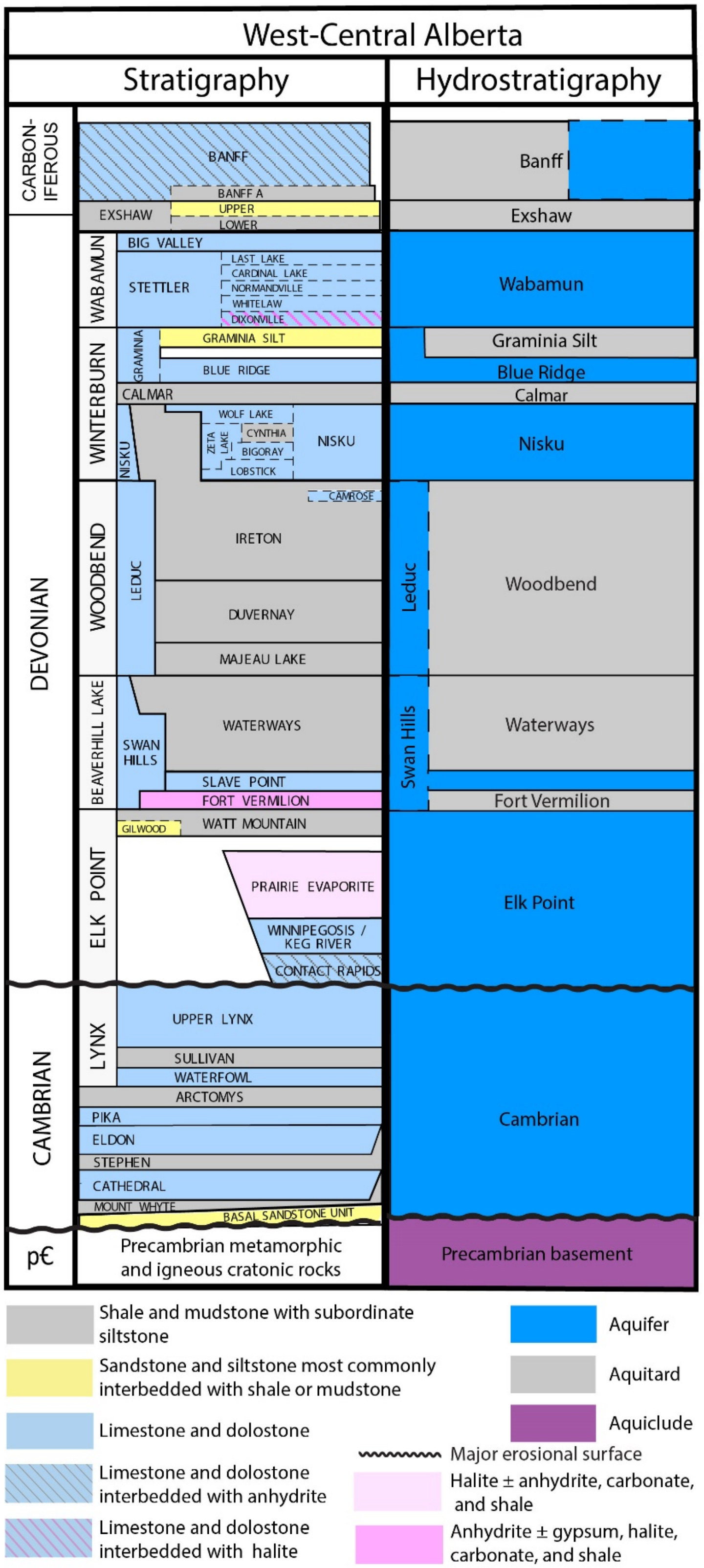

Figure 5. Stratigraphy and hydrostratigraphy of the Cambrian–Devonian succession in west-central Alberta (stratigraphy modified after Alberta Geological Survey, 2019b). Abbreviation: p€, Precambrian.

4.1 Aquifer Delineation Using DST Water Recovery

The first step in the aquifer mapping process was the delineation of regions within each formation where water was expected to be the predominant fluid present. This delineation was based on the locations of drillstem and other industry tests (initial production and wireline formation tests) that recovered formation water. An arbitrary cutoff of a minimum of 100 m of water recovery was used for this delineation. It was assumed that DSTs recovering 100 m of water or more indicate formations where water is the dominant fluid. Smaller recoveries may incorrectly be reported as formation water, and may instead be water and drilling mud introduced in the drilling process. The delineation represents a reasonable approximation of where the formation has shown it is capable of producing water, and provided an aquifer extent within which further mapping was completed. Since the resulting aquifer extent is controlled by the locations of DSTs, which often explicitly target areas of potential hydrocarbon pools, the actual aquifer might extend beyond the limit defined in this study. Maps showing the location of water-recovering DSTs and delineated aquifers can be found in Appendix 1.1. Information on water-recovering DSTs for each formation is summarized in Appendix 3, Table 2.

4.2 Hydraulic Head

Regional hydraulic head maps were created using pressure data from DSTs. Pressure data were converted to equivalent freshwater hydraulic heads using the relationship:

$$hydraulic\ head\ (m\ asl) = \frac{pressure\ (kPa)}{\rho g} + elevation\ (m\ asl) \qquad (1)$$

where ρ = fluid density (1000 kg/m^3 for freshwater); *g* = gravitational acceleration (9.81 m^2/s); and *m asl* = metres above sea level.

Density variations of the formation water and their effect on groundwater flow were taken into consideration with the construction and interpretation of water driving force (WDF) maps (Section 4.6).

Hydraulic head maps were created for all aquifers for which there was a sufficient amount of data. The maps were created using kriging or inverse distance weighting interpolation methods, depending on the number and spatial distribution of data points. The aquifer extent (as defined in Section 4.1) and the spatial distribution of representative pressure data determine the extent of the hydraulic head maps. Hydraulic head maps can be found in Appendix 1.2. The results of hydraulic head mapping for each aquifer are summarized in Appendix 3, Table 3.

4.3 Cumulative Interference Index (CII)

The results of a DST at a given location can be influenced by nearby production or injection activity. In order to identify potential production and injection influences, the CII methodology (Singh et al., 2017) was used. A 5 km and a 10 km search radius around locations where DSTs were conducted were used to assess the CII. Data from DSTs that were interpreted to have been influenced by production or injection were removed from the dataset, resulting in a hydraulic head map representative of predevelopment conditions.

4.4 Pressure-Elevation Plots

Pressure-elevation plots are useful for understanding basin-scale flow dynamics, inferring the potential for cross-formational flow or hydraulic connectivity. Pressure data, obtained from the culled hydraulic head dataset, are plotted against elevation, and their linear trend is compared to a reference gradient that is calculated using an ambient reference density, which is calculated using the Chierici equation (Chierici, 1994). If the data fall on a gradient with a slope greater than the reference hydrostatic gradient, an upward component of flow is indicated (superhydrostatic). If the data plot on a gradient less than the reference gradient, a downward component of flow is indicated (subhydrostatic). Data that plot on a gradient equal or close to the hydrostatic gradient indicate constant hydraulic head between data points and, therefore, no vertical flow potential.

4.5 Total Dissolved Solids (TDS) and Water Chemistry

Maps showing the distribution of total dissolved solids (TDS) were created for all aquifers for which there was a sufficient amount of data. The maps were created using kriging or inverse distance weighting interpolation methods, depending on the number and spatial distribution of TDS data points. The aquifer extent (as defined in Section 4.1) and the spatial distribution of representative formation water analyses determine the extent of the TDS maps. Maps showing the distribution of TDS in various aquifers can be found in Appendix 1.3. Water chemistry is also displayed graphically in Piper plots and major ion plots (Appendix 2). The results of TDS mapping for each aquifer are summarized in Appendix 3, Table 2.

4.6 Water Driving Force (WDF)

Although using freshwater density is common practice when mapping regional groundwater flow, neglecting density variations can have considerable effect on groundwater flow direction and magnitude, particularly in aquifers containing dense brines, having a steep structural dip, or having small hydraulic gradients (Bachu and Michael, 2002).

The WDF approach incorporates the effects of hydraulic gradient and density-related buoyant forces on the direction and magnitude of groundwater flow (Singh et al., 2017). The WDF is defined as

$$WDF = \nabla h + \frac{\Delta\rho}{\rho_o}\nabla E \qquad (2)$$

where h = freshwater hydraulic head; $\Delta\rho$ = density difference between in situ brine and freshwater; ρ_o = density of freshwater; and E = structural elevation of the aquifer base. The first term represents the force due to the hydraulic gradient whereas the second term represents the force due to buoyancy.

In order to identify areas where density-driven flow might be important and can change the inferred magnitude and direction of groundwater flow, WDF maps (Appendix 1.4) were created to accompany the hydraulic head maps. Arrows shown in the WDF maps illustrate the direction and relative magnitude of the WDF. The background colour in WDF maps indicates the angle between the WDF vector and hydraulic gradient vector. Smaller angles between the WDF vector and hydraulic gradient vector (<30˚) indicate no significant effect of buoyancy on groundwater flow. For more details about the WDF method and its implementation refer to Singh et al. (2017). The results of the WDF mapping for each aquifer are summarized in Appendix 3, Table 4.

5 Regional Groundwater Flow and Chemistry Interpretation

The results from this study build upon the knowledge and insights of previous studies (Hitchon et al., 1989, 1990; Thompson, 1989; Anfort, 1998; Anfort et al., 2001; Michael and Bachu, 2001; Michael, 2002; Michael and Buschkuehle, 2008) to interpret regional groundwater flow and chemistry within the west-central Alberta study area. Although previous work was performed in overlapping areas, there is no published work for the eastern part of the study area where Mississippian formations subcrop. In addition to the hydraulic head, TDS, and WDF maps, pressure-elevation plots were created and interpreted to evaluate regional flow patterns and the vertical component of groundwater flow. The effectiveness of intervening aquitards to impede flow (i.e., aquitard strength) was examined by comparing hydrogeological attributes and pressure-elevation trends of the aquifers.

Figure 6 shows the location of the present study area in relation to the locations of some previously completed studies. A summary of the flow of formation waters in the Alberta Basin is presented in Bachu (1995). This summary separates flow within the post-Jurassic hydrostratigraphic succession from that in the pre-Cretaceous hydrostratigraphic succession (Figure 7). Flow patterns observed in pre-Cretaceous aquifers in the Alberta Basin indicate flow away from the deformation front towards the northeast, and deep recharge from high elevations in Montana, discharging in northern Alberta as part of the Grosmont drain along the Peace River valley (Hitchon et al., 1989). Flow in these aquifers is driven by basin-scale topography with strong buoyancy forces (blue arrows in the schematic cross-section in Figure 7). The post-Jurassic succession is characterized by local-scale topographic flow (black arrows in schematic cross-section), and an area of flow opposing the topographic gradient towards an underpressured area in the 'deep basin' part (orange arrows in the schematic cross-section) of the province (Bachu, 1995). All of these flow regimes are observed in the west-central Alberta study area.

5.1 Cretaceous Aquifers

The presence of several sandstone units separated by shale results in several Cretaceous aquifers isolated by aquitards. The Wapiti, Cardium, Dunvegan, Viking, and Spirit River aquifers, which are separated by aquitards, were analyzed independently, whereas the Bluesky, Gething, Cadomin, and Nikanassin aquifers were analyzed together and comprise the Nikanassin–lower Mannville aquifer (Figure 3). The hydrochemistry and groundwater flow from these aquifers are discussed below.

5.1.1 Wapiti Aquifer

5.1.1.1 Groundwater Flow

Local-scale flow systems in the Alberta Basin developed in areas with topographic highs, such as the Cypress Hills, Pelican Mountain, Caribou Mountains, and Swan Hills, with flow being directed to the nearest topographic low, usually a river valley (Bachu, 1999). In the west-central Alberta study area, groundwater flow in the Wapiti aquifer is directed from topographic highs, such as the Swan Hills, toward topographic lows, such as the Athabasca River valley (Figure 52).

The pressure-elevation plot (Figure 8) shows that most of the pressure data in the Wapiti aquifer plot along a trend with a pressure gradient of 10.2 kPa/m. Some scatter in the data is observed with upward and downward deviations from this trend line representing components of recharge and discharge, respectively. Data from the shallow (<150 m depth) water wells (shown in turquoise) do not align with this trend line. The low salinity and resulting low density of Wapiti formation water causes no observable buoyancy effects on the groundwater flow in the Wapiti aquifer (Figure 93).

5.1.1.2 Hydrochemistry

The concentration of TDS in the Wapiti aquifer varies from around 660 mg/L in the northern portion of the study area to over 8000 mg/L in the southern portion (Figure 73). Examination of the Wapiti aquifer Piper plot (Figure 112) revealed the presence of two distinct water types, one dominated by Na^+ and Cl^-, and the other by Na^+ and HCO_3^-. Major ion plots for the Wapiti aquifer (Figure 135) show a strong linear (positive correlation) relationship of Na^+ and K^+ with TDS values, with Na^+ being the dominant cation with values up to 3820 mg/L. A slight trend of increasing cationic percentage of Ca^{2+} with decreasing TDS values can be seen, with the highest values just exceeding 10%. The anionic percentage of HCO_3^- increases exponentially with decreasing TDS values. At TDS values of less than 3000 mg/L, HCO_3^- makes up over 80% of the total anions. A slight increase in SO_4^- concentration is also observed in lower salinity waters, with maximum anionic percentages of around 19% SO_4^-.

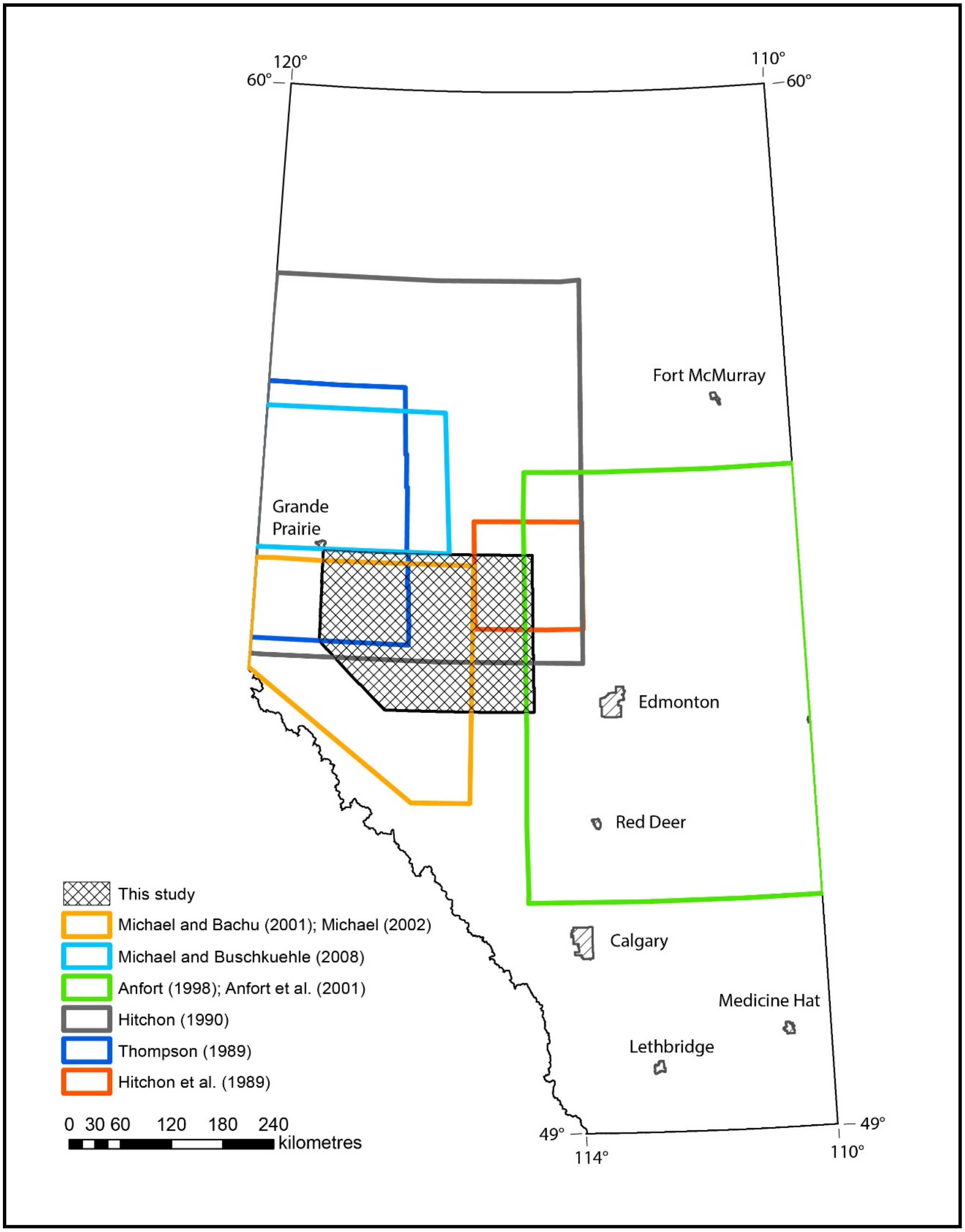

Figure 6. Location of the west-central Alberta study area in relation to locations of previously completed studies.

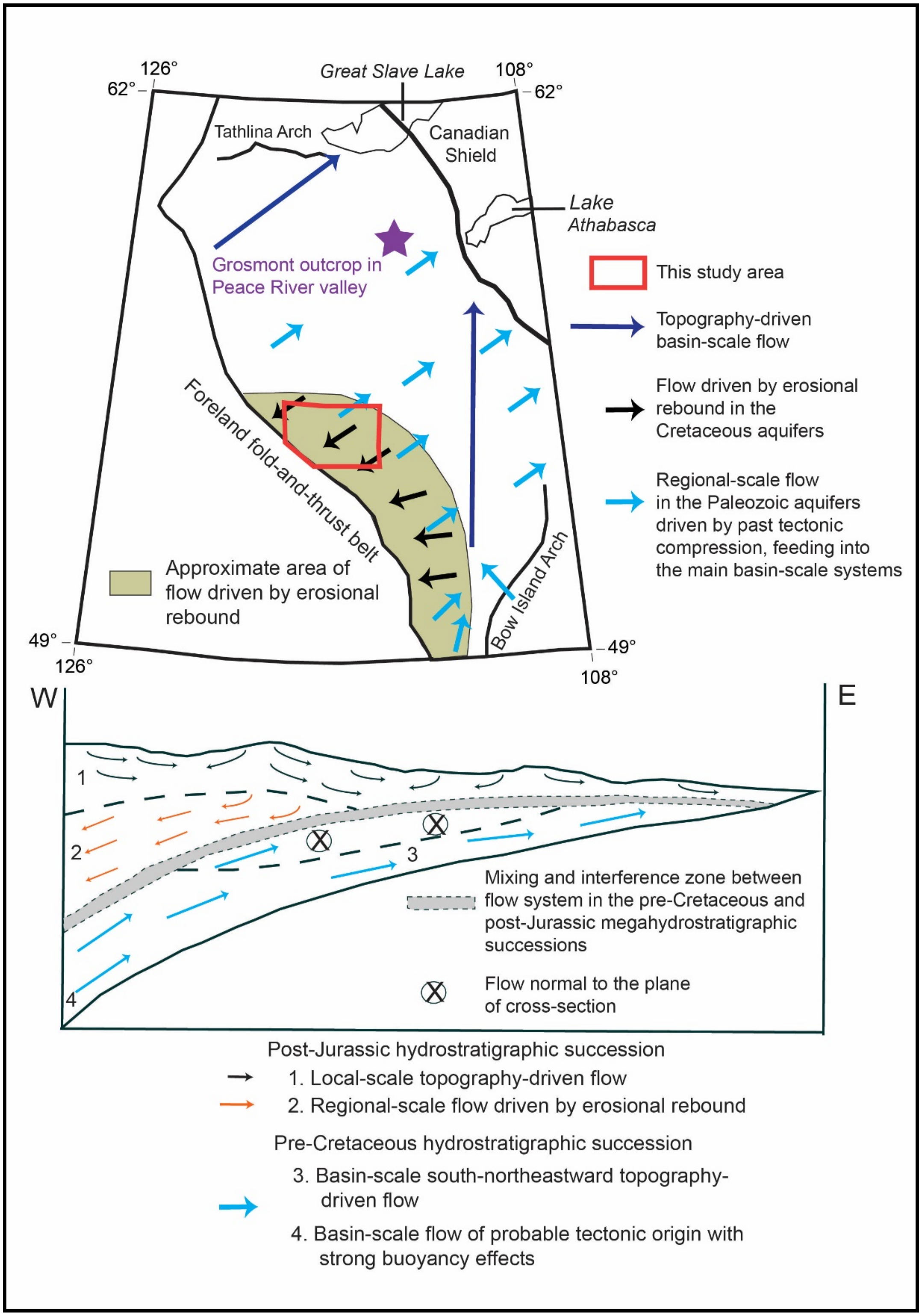

Figure 7. Map and cross-sectional view of flow systems in the Alberta Basin (modified after Bachu, 1995).

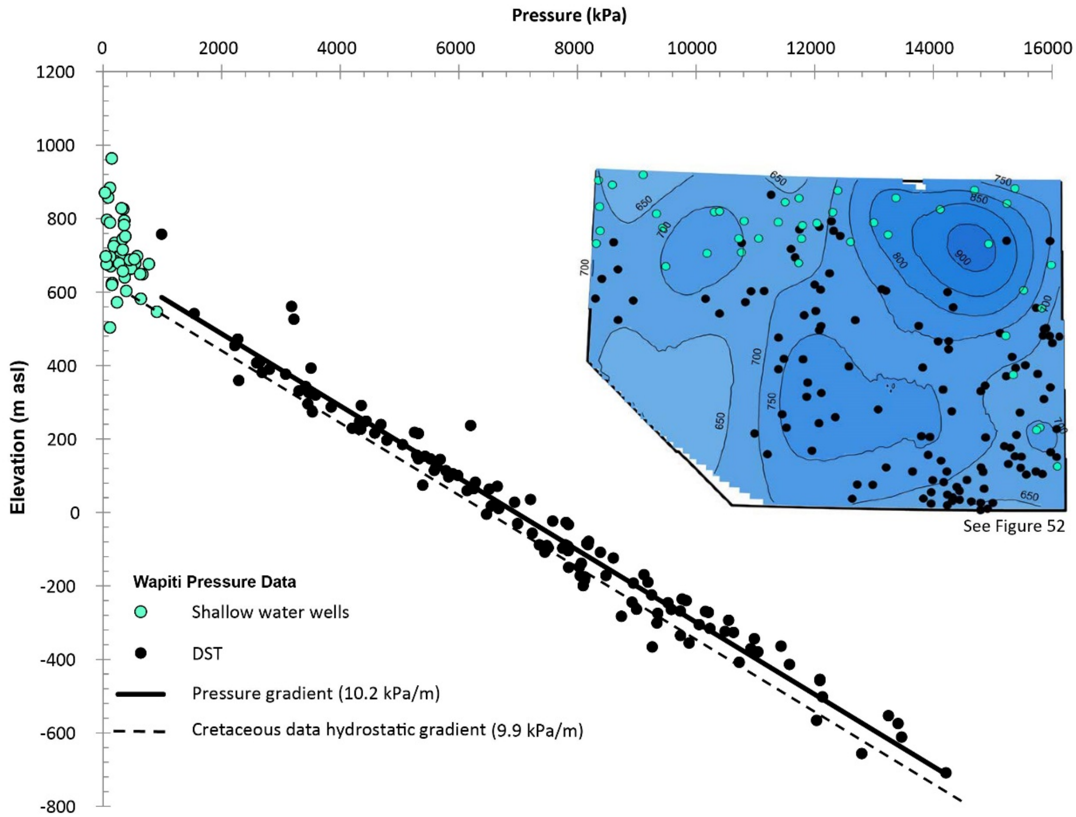

Figure 8. Pressure-elevation plot for the Wapiti aquifer in the west-central Alberta study area with the hydraulic head map shown as an inset.

5.1.2 Cardium Aquifer

5.1.2.1 Groundwater Flow

The Cardium aquifer occupies only a small portion on the western side of the study area (Figure 53). Hydraulic head throughout the majority of the Cardium aquifer ranges from 700 to 750 m asl corresponding to the elevation of Cardium subcrop found northwest of the study area. The similarities between the hydraulic head and the Cardium subcrop elevation were also observed by Michael (2002) and may relate to recharge occurring in the subcrop area. Further formation-scale mapping of the Cardium aquifer shows a continuation of the low hydraulic gradient and decreasing salinity (<4000 mg/L) towards the Cardium subcrop northwest of the study area (Brinsky, in press a, b).

Pressure data in the Cardium aquifer plot along a trend with a pressure gradient of 10.2 kPa/m, which is similar to the reference (hydrostatic) pressure gradient of 9.9 kPa/m for the Cretaceous succession (Figure 9). The pressure-elevation plot and hydraulic head distribution map reveal an abrupt change in the pressure regime in the southeastern portion of the aquifer. Michael (2002) related this pressure transition to a permeability barrier caused by the change from Cardium aquifer barrier sandstone in the west to isolated offshore barrier sandstone surrounded by fine sedimentary rocks to the east. Sufficient permeability in the Cardium aquifer through this barrier-bar sandstone (in the west) may be the reason for the low hydraulic gradient within the western portion of the aquifer. Towards the east, the decrease in permeability related to the fine sedimentary rocks that surround the isolated offshore barrier sandstones may isolate the eastern portion of the Cardium aquifer from the lower TDS and higher hydraulic head observed in the western portion. The low salinity and resulting low density of Cardium formation water causes no observable buoyancy effects on the groundwater flow in the Cardium aquifer (Figure 94).

5.1.2.2 Hydrochemistry

Salinity in the Cardium aquifer increases from TDS values of less than 9000 mg/L in the north to more than 20 000 mg/L in the south (Figure 74). Examination of the Cardium aquifer Piper plot (Figure 113) revealed that Na^+ and Cl^- are the major components of Cardium formation water. Major ion plots for the Cardium aquifer (Figure 136) show that Na^+ forms a strong linear (positive correlation) relationship with TDS values and has maximum concentrations exceeding 30 000 mg/L. Both K^+ and Mg^{2+} are minor components with highest measured values of 242 and 591 mg/L, respectively. The Ca^{2+} content appears more variable as the cationic percentage ranges from less than 1% to over 20%. The anionic percentage of SO_4^{2-} is low with values of less than 6%, whereas the HCO_3^- content increases with decreasing TDS values, where it exceeds 40% of the total anions at its lowest measured TDS value of less than 9000 mg/L.

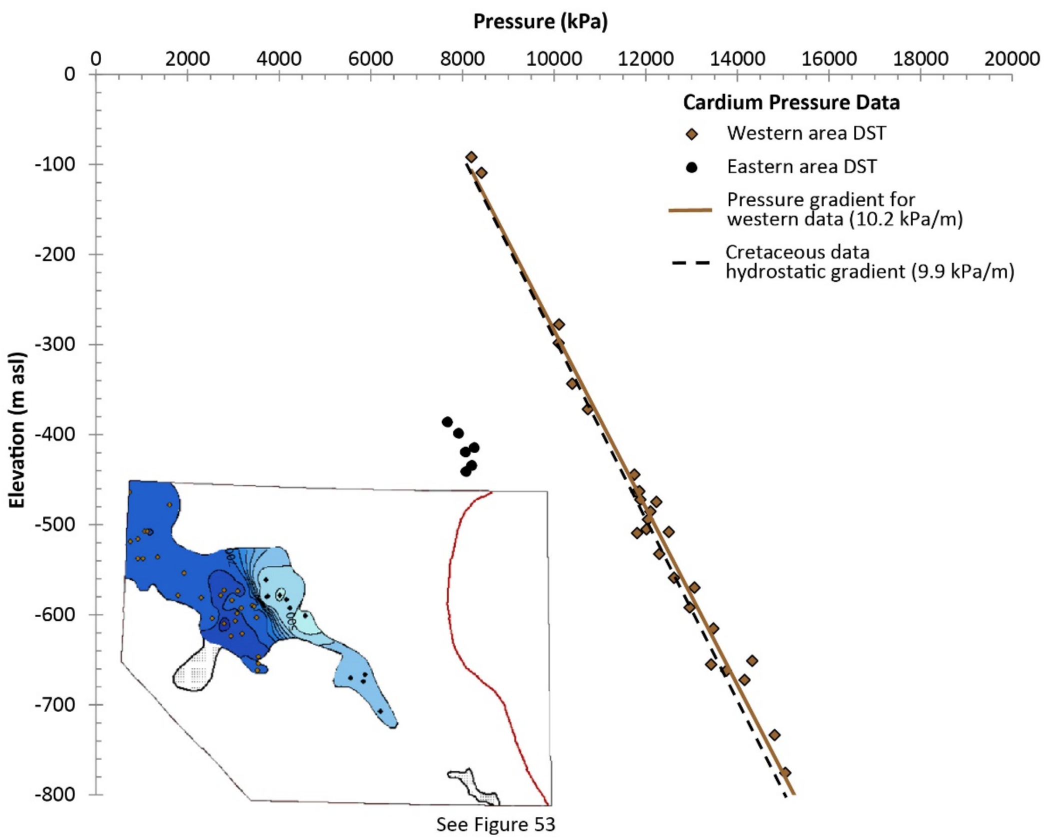

Figure 9. Pressure-elevation plot for the Cardium aquifer in the west-central Alberta study area with hydraulic head map shown as an inset. Abbreviation: DST, drillstem test.

5.1.3 Dunvegan Aquifer

5.1.3.1 Groundwater Flow

A hydraulic head map for the Dunvegan aquifer was not created because of the small spatial extent of the water-recovering DSTs and the insufficient amount of representative pressure data. However, hydraulic head values were calculated for the limited number of pressure data points, ranging from approximately 450 to 600 m asl. Plotting pressure versus elevation (Figure 10) shows that pressure data in the Dunvegan aquifer plot along a trend with a pressure gradient of 10.0 kPa/m, similar to the reference (hydrostatic) pressure gradient of 9.9 kPa/m for the Cretaceous succession.

5.1.3.2 Hydrochemistry

There was not enough data to create a map of the TDS distribution in the Dunvegan aquifer. The only sample left after culling is from well 100/02-27-066-25W5/0 and it has a TDS value of 11 333 mg/L. The main ions were Na^+ and Cl^- (Figure 114).

5.1.4 Viking Aquifer

5.1.4.1 Groundwater Flow

Hydraulic head in the Viking aquifer varies between 360 m asl in the northwestern and southeastern parts of the study area and 500 m asl in the central part of the study area (Figure 54). The contour pattern suggests divergent groundwater flow towards the northwest and southeast. The flow pattern in the Viking aquifer was analyzed using a pressure-elevation plot (Figure 11), which shows three different pressure trends within three respective areas of the study area.

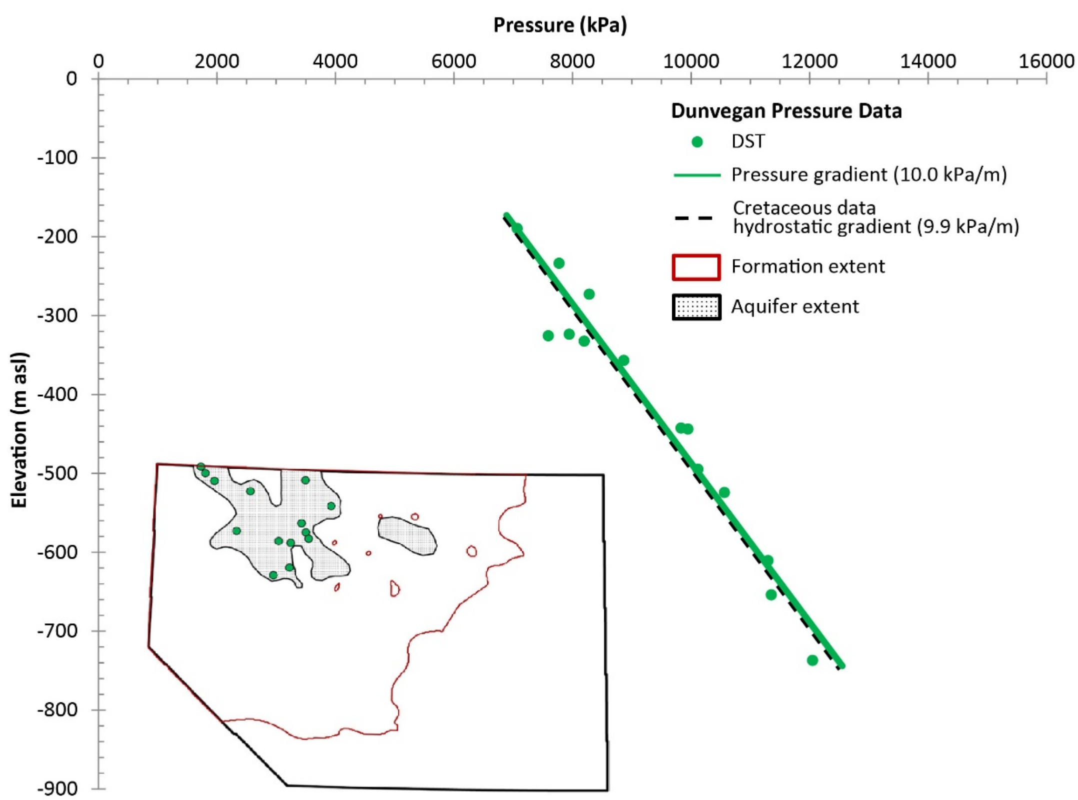

Figure 10. Pressure-elevation plot for the Dunvegan aquifer in the west-central Alberta study area with the location of pressure data shown as an inset map. Abbreviation: DST, drillstem test.

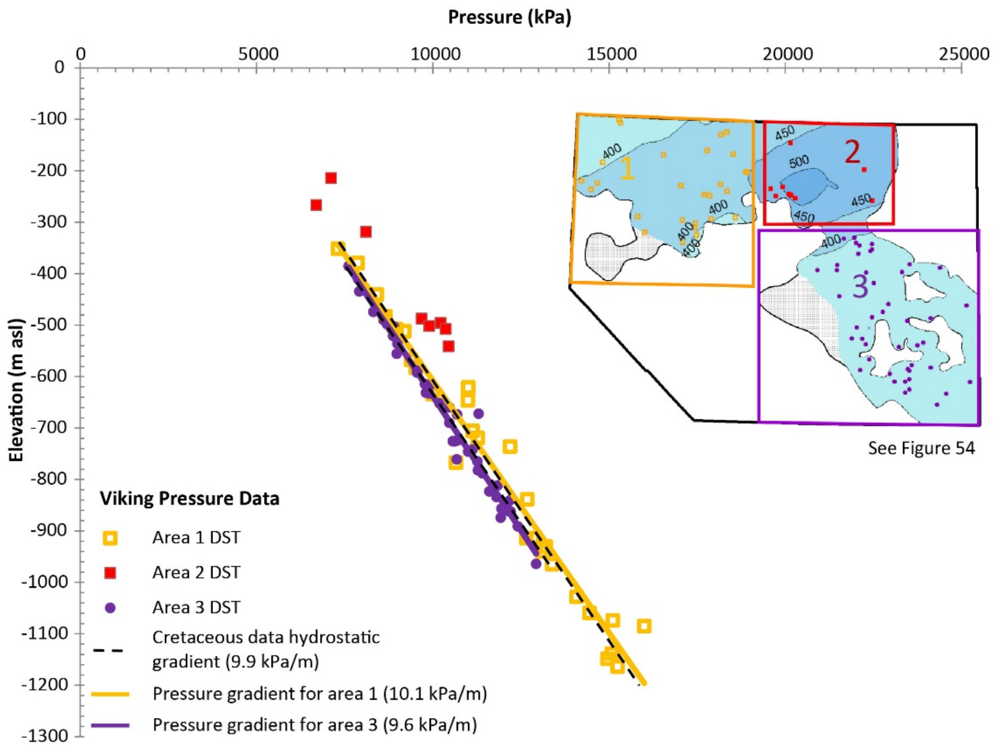

Figure 11. Pressure-elevation plot for the Viking aquifer in the west-central Alberta study area with the hydraulic head map shown as an inset. Abbreviation: DST, drillstem test.

Hydraulic head in area 1 (orange outline) shows two different flow directions. In the northern portion of area 1, groundwater flow is towards the northwest, whereas in the southern portion groundwater flows towards the south. The pressure-elevation plot for area 1 follows a trend with a pressure gradient of 10.1 kPa/m. The scatter of the data is the result of two opposite flow directions, and upward and downward components of flow. Thompson (1989) concluded that flow in the Peace River Formation (mapped together with the Viking Formation in the present study) follows decreasing ground surface elevations towards the Peace River valley and discharges where the formation outcrops at elevations below 350 m asl (Figure 2). Thompson's conclusion explains the northward-flow trend observed for a portion of the data in area 1, whereas the reversal of flow towards the gas-saturated deep basin appears to occur in a zone that transitions from flow dependent on local/regional topography to flow controlled by underpressuring in the deep basin (Bachu, 1999).

Data from area 2 (red outline) form a potentiometric mound. The potentiometric surface of this mound exceeds 500 m asl and corresponds to data plotting on a trend with a higher pressure gradient on the pressure-elevation plot (Figure 11). This potentiometric mound is discussed further in Section 5.4.1. The Viking aquifer in area 3 (purple outline) has a flat potentiometric surface of less than 400 m asl. Regional flow in this area is to the south towards the deep basin (Masters, 1979; Michael and Bachu, 2001; Bachu and Adams, 2003). Viking aquifer pressure data in this area plot on a trend with a subhydrostatic gradient of 9.6 kPa/m. The southward flow may be driven by underpressuring caused by erosional rebound as suggested by Bachu (1999). The density of Viking formation water results in no observable buoyancy effects on formation water flow in the Viking aquifer (Figure 95).

5.1.4.2 Hydrochemistry

The TDS values in the Viking aquifer range from 14 855 to over 28 000 mg/L (Figure 75). Examination of the Viking aquifer Piper plot (Figure 115) show that Na^+ and Cl^- are the major ionic components of

Viking formation water. Major ion plots for the Viking aquifer (Figure 137) show that Na^+ forms a strong linear (positive correlation) relationship with TDS values and has maximum concentrations exceeding 11 000 mg/L. Both K^+ and Mg^{2+} are minor components with highest measured values of 252 and 560 mg/L, respectively. The cationic percentage of Ca^{2+} has a positive association with TDS values and in places exceeds 10%. The anionic percentage of SO_4^{2-} is low with values below 6%, whereas the HCO_3^- content increases with decreasing TDS values. The maximum anionic percentage of HCO_3^- recorded was 28%.

5.1.5 Spirit River (Upper Mannville) Aquifer

5.1.5.1 Groundwater Flow

The hydraulic head map (Figure 55) and pressure-elevation plot (Figure 12) of the Spirit River aquifer revealed the presence of two pressure gradients. In the majority of the aquifer (area 1), groundwater flow is towards the northeast. On the pressure-elevation plot, data from this area forms a trend with a superhydrostatic pressure gradient of 11.5 kPa/m, indicating an upward component of flow, which may be the result of flow in the updip direction. Towards the southeastern portion of the Spirit River aquifer (area 2), the hydraulic head decreases with a change in flow direction towards the south. Data from this area correspond to the lower pressure data on the pressure-elevation plot (red data points, Figure 12). The flow direction may be the result of underpressuring caused by erosional rebound as suggested by Bachu (1999). Alternatively, this lower pressured system could be the result of interaction with the lower pressured Viking aquifer in this area (see Section 5.4). The density of the Spirit River formation water causes no observable buoyancy effects on groundwater flow in the Spirit River aquifer.

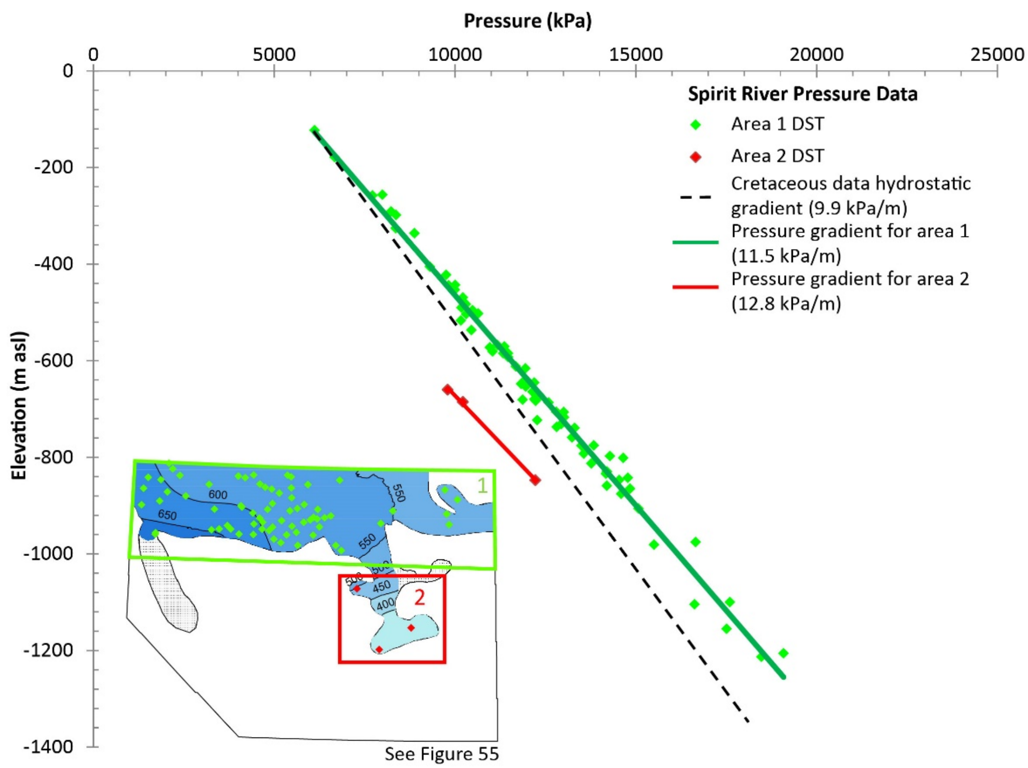

Figure 12. Pressure-elevation plot for the Spirit River aquifer in the west-central Alberta study area with the hydraulic head map shown as an inset. Abbreviation: DST, drillstem test.

5.1.5.2 Hydrochemistry

The TDS values in the Spirit River aquifer range from 10 965 to over 58 000 mg/L (Figure 76). Examination of the Piper plot for the Spirit River aquifer (Figure 116) revealed that Na^+ and Cl^- are the major ionic components of the water. Major ion plots for the Spirit River aquifer (Figure 138) show that Na^+ forms a strong linear (positive correlation) relationship with TDS values and reaches concentrations of over 26 000 mg/L. Both K^+ and Mg^{2+} also show positive relationships with TDS values, with maximum measured concentrations of 500 and 912 mg/L, respectively. The cationic percentage of Ca^{2+} appears more varied ranging from <1% to 20% of the total cations. Both HCO_3^- and SO_4 show a general decrease in anionic percentage with increasing TDS values, with the maximum anionic percentage of HCO_3^- reaching 34%, whereas the anionic percentage of SO_4^{2-} reaches a maximum of 15%.

5.1.6 Nikanassin–Lower Mannville Aquifer

5.1.6.1 Groundwater Flow

Pressure data from the Bluesky, Gething, Cadomin, and Nikanassin aquifers, which together comprise the Nikanassin–lower Mannville aquifer, were plotted versus elevation to analyze fluid flow within the Nikanassin–lower Mannville aquifer (Figure 13).

Little variation is observed between the hydraulic head maps for the Bluesky (Figure 56) and Cadomin aquifers (Figure 58), with the majority of hydraulic head values ranging between 600 and 700 m asl. Pressure data from these two aquifers plot on a slightly subhydrostatic gradient of 9.4 kPa/m (Figure 13). This gradient is near the Cretaceous data hydrostatic gradient (9.9 kPa/m), which indicates sluggish flow between the Bluesky and Cadomin aquifers. A hydraulic head map of the Nikanassin aquifer was not created due to an insufficient amount of representative pressure data. Some of the data from the Nikanassin aquifer plot on the same gradient as the Bluesky and Cadomin aquifers, implying a potential for vertical communication whereas other data from the Nikanassin aquifer plot at a slightly lower pressure trend. The water driving force (WDF) map for the Cadomin aquifer (Figure 98) suggests potential buoyancy effects in the western portion of the Cadomin aquifer that may result in flow at an angle to the head vector.

The Gething aquifer extent appears discontinuous and hydraulic head is more variable ranging from less than 450 m asl to greater than 750 m asl (Figure 57). On the pressure-elevation plot (Figure 13), data from the Gething aquifer show a higher degree of scatter than those from the other aquifers, with some data points overlapping the data from the Bluesky and Cadomin aquifers, indicating potential for hydraulic communication between aquifers in these areas. The scatter observed in the Gething aquifer data may be caused by a channelized system where pressure regimes are discontinuous. The Gething aquifer pressure data were evaluated in more detail (Figure 14). The majority of Gething aquifer data fall near either the light blue trend line (area 1or the dark blue trend line (area 2). Both trends show a slightly subhydrostatic gradient (9.4 kPa/m), indicative of a downward component of flow.

Towards the east, more complexity is observed with four other clusters of data (areas 3 to 6). The data from these areas were further evaluated in relation to neighbouring formations (see Section 5.4). The WDF map for the Gething aquifer suggests that buoyancy does not have an impact on groundwater flow (Figure 97).

5.1.6.2 Hydrochemistry

The TDS values in the Gething aquifer vary from less than 18 000 mg/L in the western portion, to more than 78 000 mg/L in the eastern portion of the aquifer (Figure 77). The TDS values in the Cadomin aquifer range from less than 33 000 mg/L to greater than 68 000 mg/L (Figure 78).

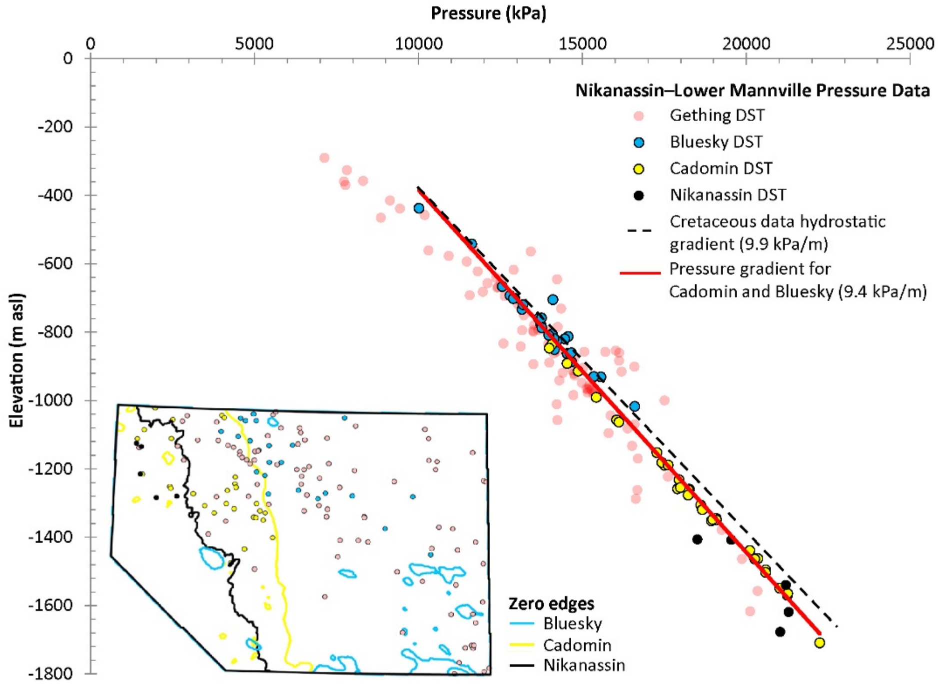

Figure 13. Pressure-elevation plot for the Nikanassin–lower Mannville aquifer in the west-central Alberta study area. The inset map shows the location of the data in relation to the zero edges of the formations. Abbreviation: DST, drillstem test.

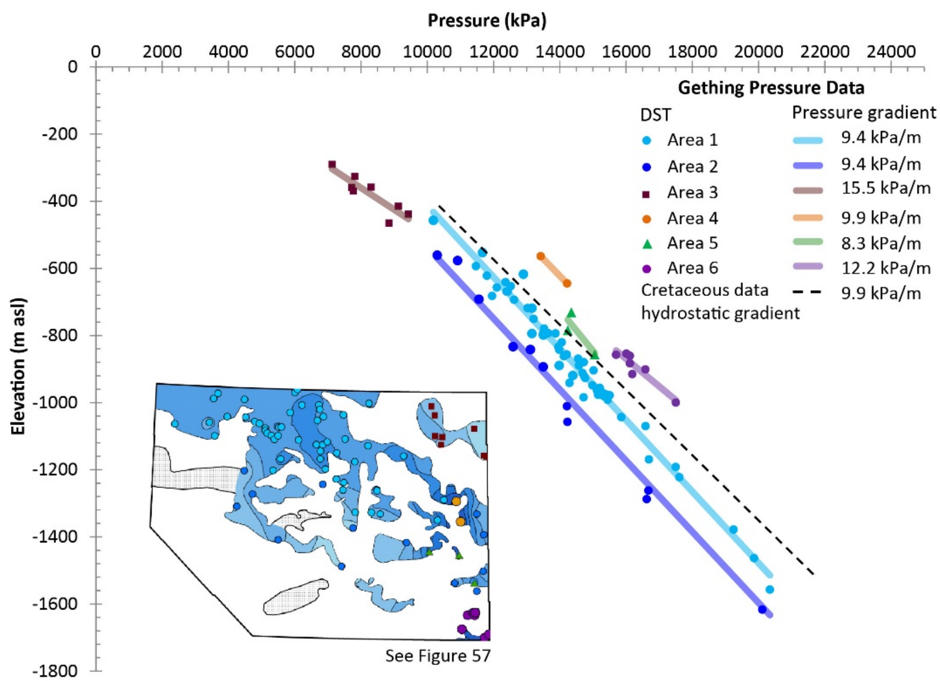

Figure 14. Pressure-elevation plot for the Gething aquifer in the west-central Alberta study area with the hydraulic head map shown as an inset. Abbreviation: DST, drillstem test.

Examination of the Piper plots for the Bluesky, Gething, and Cadomin aquifers (Figures 117–119) revealed that Na^+ and Cl^- are the major ionic components of the water. The major ion plots for the data from Bluesky, Gething, Cadomin, and Nikanassin aquifers (Figure 139) show that Na^+ forms a strong linear (positive correlation) relationship with TDS values and reaches concentrations above 32 000 mg/L. Both K^+ and Mg^{2+} are minor components with highest measured values of 933 and 620 mg/L, respectively. The cationic percentage of Ca^{2+} appears variable and ranges from <1% to 9%. The anionic percentage of SO_4^{2-} is low with values of less than 4%. A general increase is observed in the anionic percentage of HCO_3^- with decreasing TDS values. The maximum anionic percentage of HCO_3^- recorded was 28%.

5.2 Mississippian–Jurassic Aquifers

5.2.1 Groundwater Flow

Pressure data from the Mississippian–Jurassic aquifers were plotted against elevation (Figure 15) and used to create hydraulic head maps (Figures 59–65) for each aquifer in order to evaluate flow in the Mississippian to Jurassic succession.

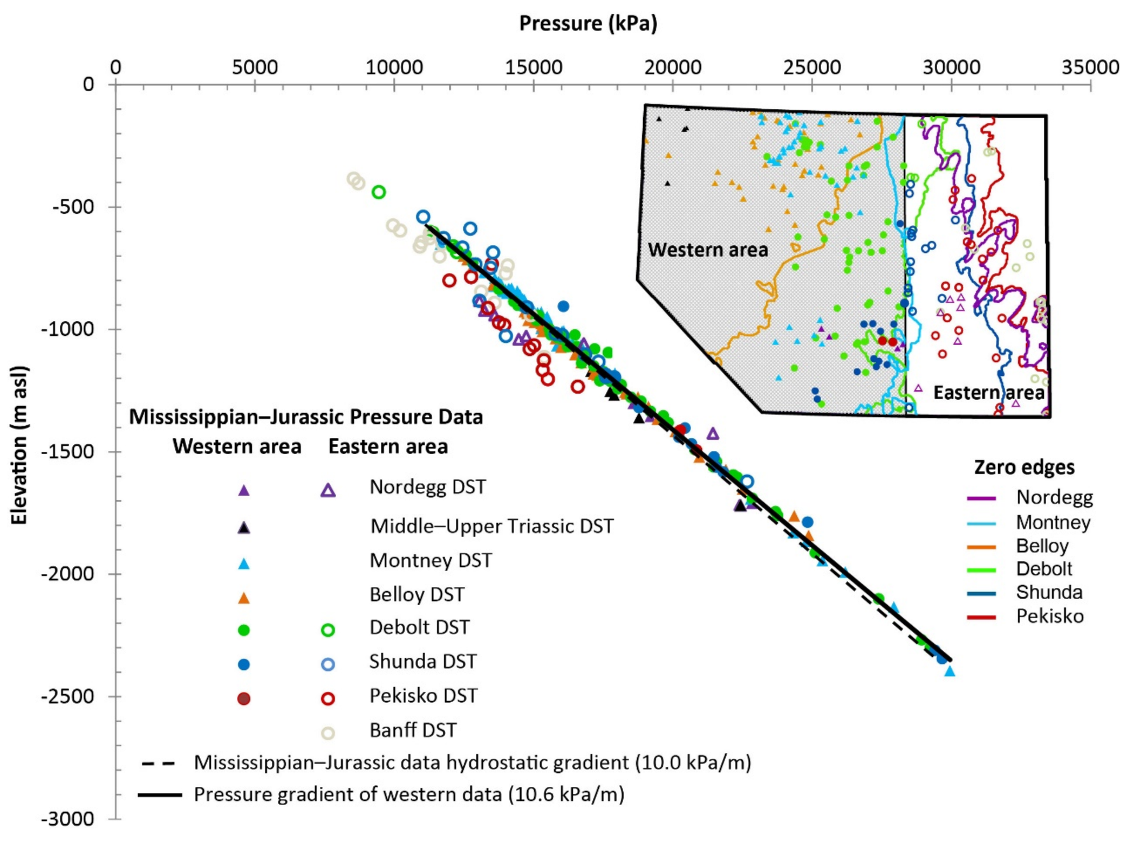

Figure 15. Pressure-elevation plot for the Mississippian–Jurassic aquifers in the west-central Alberta study area. The inset map shows the location of the data in relation to the zero edges of the formations/member.

Flow patterns of the Montney, Belloy, and Debolt aquifers (Figures 60–62), whose mapped extents overlap and occupy the western part of the study area, are similar and show a northeastward groundwater flow direction with hydraulic head values ranging between 526 m asl in the Debolt aquifer and 707 m asl in the Belloy aquifer. The pressure-elevation plot (Figure 15) shows that pressure data from the Montney, Belloy, and Debolt aquifers combined with some pressure data from the Shunda and Pekisko aquifers found in the western portion of the study area, plot along a trend line with a pressure gradient of 10.6 kPa/m. A very limited aquifer extent of the Middle–Upper Triassic succession was delineated in the northwestern part of the study area (Figure 38). In contrast, water-recovering DSTs were not found in the overlying Nordegg Member and underlying Montney Formation in this area, suggesting that these units act as aquitards in the northwestern part of the study area isolating the Middle–Upper Triassic aquifer. The limited aquifer extent of the Middle–Upper Triassic succession did not allow for a hydraulic head map to be created.

Flow patterns of the Nordegg, Shunda, Pekisko, and Banff aquifers (Figures 59, 63–65), whose mapped extents mainly occupy the eastern part of the study area, also suggest a northeastward groundwater flow direction towards the zero edges of the formations/member. The pressure-elevation plot (Figure 15) shows that pressure data from the Nordegg, Shunda, and Pekisko aquifers in the eastern area, as well as most of the data from the Banff aquifer, plot along a lower pressure trend. These data from the eastern part of the study area were evaluated in greater detail and are further discussed in Section 5.4.

5.2.2 Hydrochemistry

The TDS concentrations throughout the Mississippian–Jurassic aquifers range between a low of 24 339 mg/L in the Nordegg aquifer to a high of 174 813 mg/L found in the Debolt aquifer (Figures 79–85). The horizontal distribution of TDS concentrations shows a general trend of decreasing values from west to east. Examination of the Piper plots of the Mississippian–Jurassic aquifer data (Figures 120–127) revealed that Na^+ and Cl^- are the major ionic components of the water. The major ion plots (Figure 140) show that Na^+ forms a strong linear (positive correlation) relationship with TDS values and reaches concentrations up to 64 000 mg/L. Both K^+ and Mg^{2+} also show a positive relationship with TDS values, and reach maximum concentrations of 3714 and 2379 mg/L, respectively. The cationic percentage of Ca^{2+} shows an increase with increasing TDS values, with values up to 18%. Both HCO_3^- and SO_4^{2-} increase with decreasing TDS values but remain low, making up less than 7% of the anions.

5.3 Cambrian–Devonian Aquifers

5.3.1 Groundwater Flow

The presence/absence of Leduc reefs appears to have a significant influence on the hydrogeological characteristics of the entire Cambrian–Devonian succession. Where the Leduc reefs are present in the western portion of the study area, similar hydrogeological characteristics are observed throughout the entire succession, and pressure-elevation data plot on a continuous superhydrostatic gradient of 11.9 kPa/m (Figure 16), indicative of an upward component of flow. The hydraulic head maps for the individual aquifers (Figures 66–72) indicate updip flow towards the east. In the eastern portion, where the Leduc reefs are replaced by thick shales deposited during the Late Devonian, data from the Wabamun, Blue Ridge, and Nisku aquifers show a lower pressure trend than in the western portion of the study area where the Leduc reefs are present. The hydraulic head values in these aquifers decrease to less than 500 m asl, whereas the deeper Devonian (Swan Hills, Elk Point) and Cambrian aquifers maintain hydraulic head values over 750 m asl. This suggests a clear distinction in hydrogeological properties of aquifers above and below the shales deposited during the Late Devonian in the eastern part of the study area.

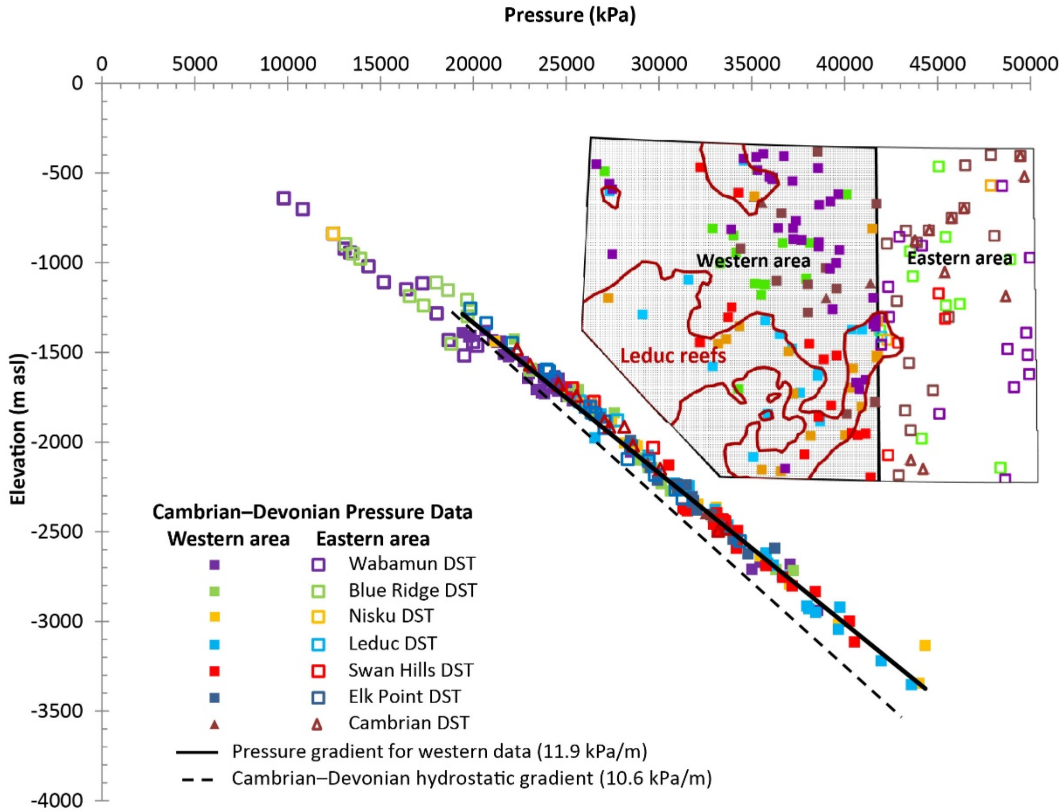

Figure 16. Pressure-elevation plot for the Cambrian–Devonian aquifers in the west-central Alberta study area. The inset map shows the location of the data and the extent of the Leduc Formation (reefs) in the study area. Abbreviation: DST, drillstem test.

The WDF analysis (Figures 106–111) suggests that density-related buoyancy forces are having a significant effect on fluid flow in the Upper Devonian succession in the western portion of the study area and the Swan Hills, Elk Point, and Cambrian aquifers throughout the entire study area. This effect results in sluggish updip flow, or even flow reversal in the downdip direction.

Density-related buoyancy forces do not appear to have a strong influence on flow in the eastern portion of the study area for the Wabamun, Blue Ridge, and Nisku aquifers.

5.3.2 Hydrochemistry

High TDS concentrations of more than 200 000 mg/L are observed in all the Devonian aquifers in most of the western portion of the study area (Wabamun, Blue Ridge, Nisku, Leduc, Swan Hills, Elk Point), as well as in the Cambrian aquifer (Figures 86–92). The TDS values in the Wabamun (Figure 86) and Blue Ridge (Figure 87) aquifers show a large decrease from over 250 000 mg/L in the west to under 150 000 mg/L in the east. In the Nisku aquifer, TDS values decrease from 240 000 mg/L in the west to 180 000 mg/L in the east (Figure 88). The Leduc (Figure 89) and Swan Hills (Figure 90) aquifers did not have data on the far eastern edge of the study area but also showed a general decrease in TDS values from west to east. The TDS values in the Elk Point (Figure 91) and Cambrian (Figure 92) aquifers remain over 200 000 mg/L in the eastern portion of the study.

Examination of the Piper plots (Figures 128–134) revealed that Na^+ and Cl^- are the major ionic components of the water in the Cambrian–Devonian aquifers. An increase in the Ca^{2+} component is noted within these aquifers.

The major ion plots for the Cambrian–Devonian aquifers (Figure 141) show that Na^+ forms a strong linear (positive correlation) relationship with TDS values and has concentrations up to 100 000 mg/L. Both K^+ and Mg^{2+} show an increase in concentration with increasing TDS values, with concentrations up to 4742 and 8228 mg/L, respectively. The cationic percentage of Ca^{2+} shows an increase with increasing TDS values, with values up to 38%. Both HCO_3^- and SO_4^{2-} are minor components with anionic percentages below 5%.

5.4 Cross-Formational Flow

This section focuses on the cross-formational flow, interpreted from detailed pressure-elevation plots and the analysis of hydraulic head and TDS maps. Understanding cross-formational flow allows aquitard strength and aquifer connectivity to be inferred, which is important for both water-sourcing and water-disposal activities. Cross-formational flow was analyzed between the Viking and Spirit River aquifers in the entire study area, and throughout the Cretaceous to Cambrian aquifers focusing on the northeastern and southeastern portions of the study area (Figure 17).

5.4.1 Cross-Formational Flow Between the Viking and Spirit River Aquifers

The cross-formational flow between the Viking and Spirit River aquifers was analyzed by plotting pressure versus elevation, and looking into the correlation between the location of pressure data and the thickness of the Joli Fou aquitard (Figure 18). The pressure-elevation plot shows that data from the Viking and Spirit River aquifers plot along two distinct pressure trends, suggesting that the intervening Joli Fou aquitard is an effective barrier to vertical flow on a regional scale. The majority of the Viking aquifer data plot along a trend with pressure gradient of 9.8 kPa/m, whereas the majority of the Spirit River aquifer data plot along a trend with a higher pressure gradient of 11.7 kPa/m. However, the pressure-elevation plot also shows some scatter of pressure data, which may suggest that vertical hydraulic communication between the aquifers is possible in some areas.

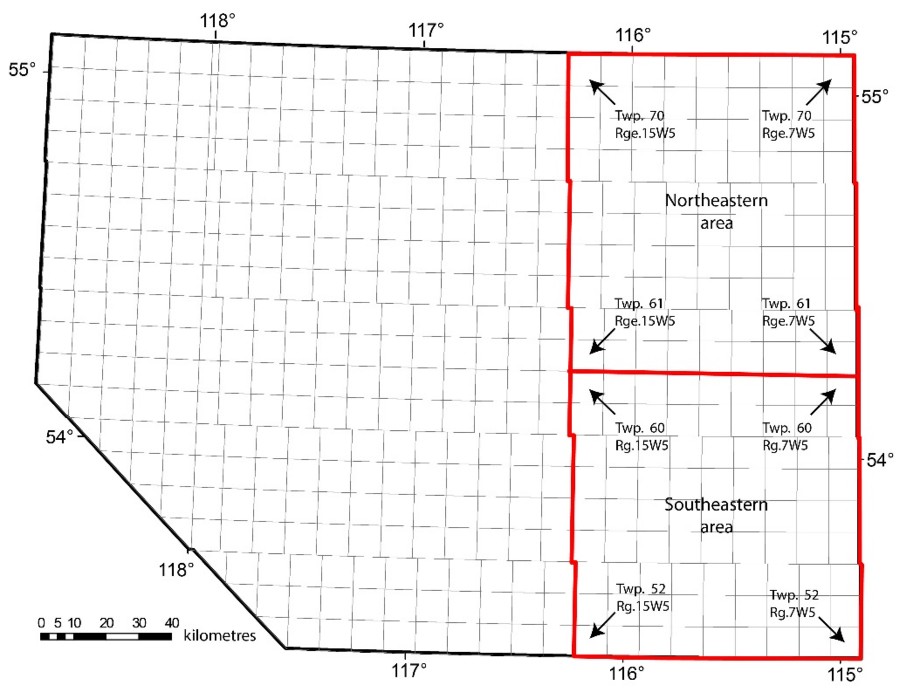

Figure 17. Focus areas (in the west-central Alberta study area) for cross-formational flow analysis of Cambrian to Cretaceous aquifers.

a)

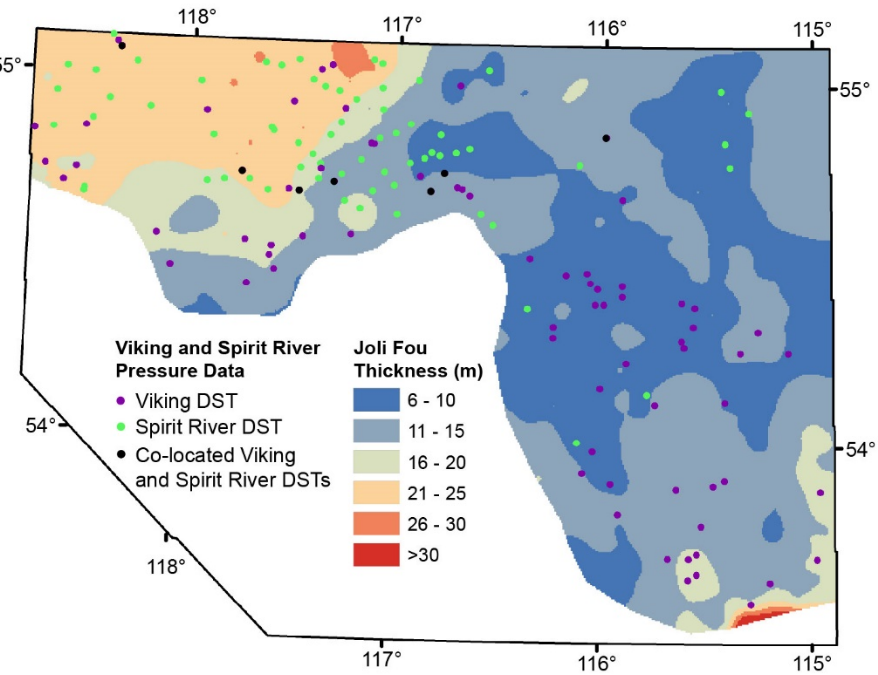

b)

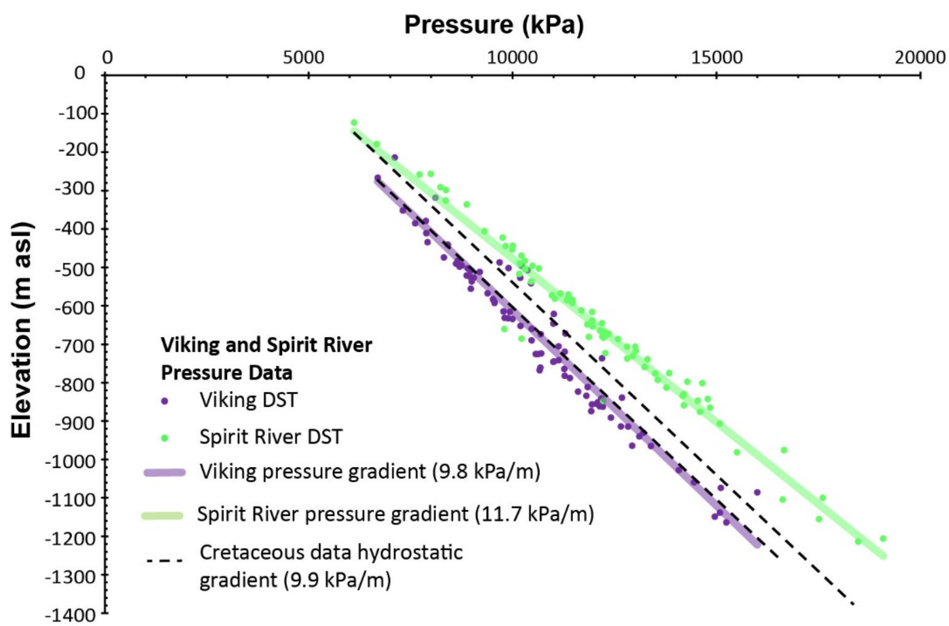

Figure 18. a) Joli Fou aquitard thickness with locations of pressure data for Spirit River and Viking aquifers in the west-central Alberta study area. b) Pressure-elevation plot for the Spirit River and Viking aquifers. Abbreviation: DST, drillstem test.

Hydraulic communication between the Viking and Spirit River aquifers was further analyzed by examining pressure-elevation plots for specific areas (Figure 19). These plots show that the Joli Fou acts as a strong aquitard in the northwestern part of the study area (Figure 19a), where in places it exceeds 25 m in thickness. In the north-central part (Figure 19b), the Joli Fou aquitard weakens. In this area, a potentiometric mound in the Viking aquifer was observed, and more scatter was observed on the pressure-elevation plot. Viking and Spirit River aquifer data from this area plot on the same trend with a pressure gradient of 12.4 kPa/m, suggesting hydraulic communication between the aquifers is possible.

The Joli Fou aquitard continues to thin towards the east, where in places it can be less than 10 m thick. The pressure-elevation plot of data from the northeastern area (Figure 19c) suggests hydraulic communication between the Viking and Spirit River aquifers, with data plotting on a trend with a pressure gradient of 12.5 kPa/m.

There are not many Spirit River aquifer data in the southeastern part of the study area, with no data at all in the farthest southeastern corner where the Joli Fou aquitard begins to thicken again (Figure 19d). As a result, hydraulic communication was difficult to interpret in this area. However, the three Spirit River aquifer data points fall on the same trend as the Viking aquifer data with a pressure gradient of 9.6 kPa/m, suggesting hydraulic communication.

Other studies suggest that in areas where the Joli Fou aquitard is absent, such as south of the west-central Alberta study area, vertical flow communication between the Viking and Spirit River aquifers may be possible (Rostron, 1995).

Salinity values in the Viking and Spirit River aquifers throughout the majority of the study area are similar, ranging between 13 000 and 30 000 mg/L (Figures 75 and 76), which may also support the idea of vertical hydraulic communication. Higher salinity is observed in the eastern part of the Spirit River aquifer with values greater than 58 000 mg\L. In this area, no Viking aquifer data are present.

5.4.2 Cross-Formational Flow in the Northeastern Focus Area

In the northeastern focus area, several Mississippian and Jurassic formations subcrop below Lower Cretaceous strata at the sub-Cretaceous unconformity creating hydrogeological complexity and allowing for the possibility of cross-formational flow between aquifers. The cross-formational flow throughout the Cretaceous (Gething) and Mississippian (Debolt, Shunda, Pekisko, Banff) aquifers was analyzed and numerous pressure gradients were identified and are described below.

Data from the Gething, Shunda, and Pekisko aquifers (Figure 20) located near the Fernie Formation zero edge (data points outlined in green) plot on a superhydrostatic gradient of 10.7 kPa/m, slightly higher than the reference hydrostatic gradient (10.0 kPa/m) calculated for Mississippian aquifers. The similar pressure trends between aquifers suggest hydraulic communication through the thinning Fernie aquitard down to the Pekisko aquifer. However, examination of TDS values in this area shows that the Gething aquifer has TDS values of <60 000 mg/L (Figure 77), whereas the TDS values for the Mississippian aquifers range from 80 354 to 117 062 mg/L (Figures 82–85), suggesting that the similar pressure trends may not be related to communication.

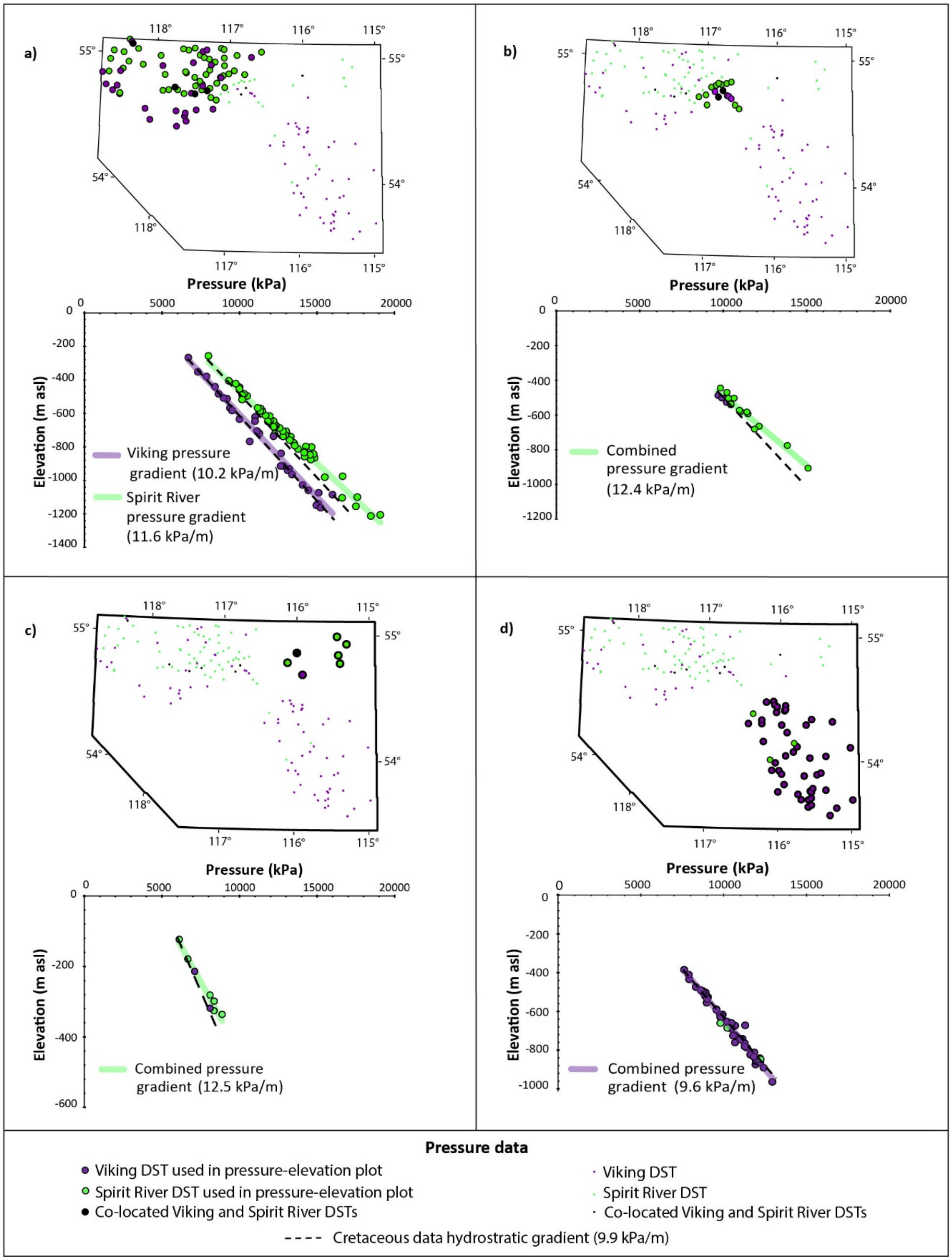

Figure 19. Pressure-elevation plots for the Viking and Spirit River aquifers in the a) northwestern portion of the west-central Alberta study area, b) north-central portion of the study area, c) northeastern portion of the study area, and d) southeastern portion of the study area. Abbreviation: DST, drillstem test.

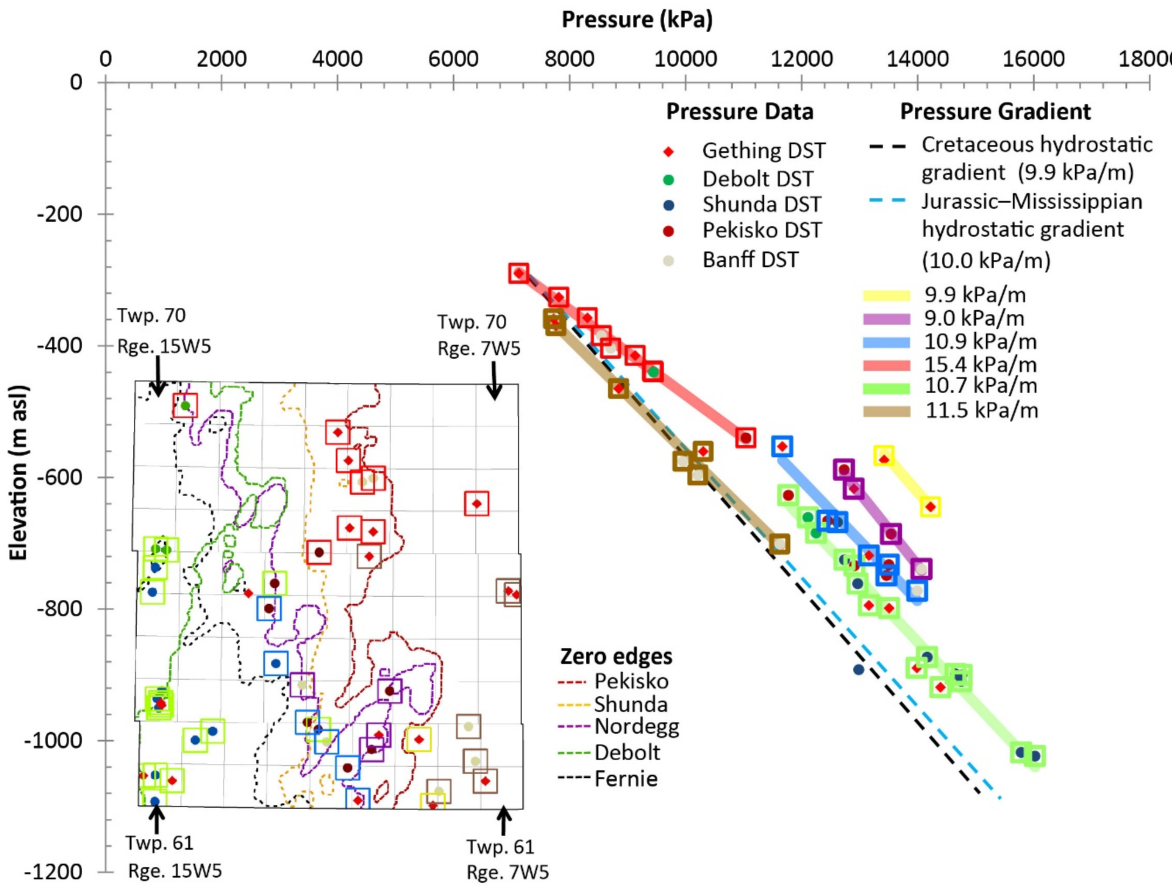

Figure 20. Pressure-elevation plot for the Mississippian (Banff, Pekisko, Shunda, Debolt) and Lower Cretaceous (Gething) aquifers in the northeastern focus area (west-central Alberta study area). The inset map shows the location of the data in relation to the zero edges of the formations/member. The colour of the square outline indicates which gradient the data plots on. Abbreviation: DST, drillstem test.

Another pressure gradient is noted in the data from the Gething, Debolt, and Banff aquifers (Figure 20, data points outlined in red) in locations where the Fernie and Nordegg aquitards are absent (i.e., where the Gething aquifer directly overlies the subcropping Debolt or Banff aquifers). These data plot on a superhydrostatic gradient of 15.4 kPa/m suggesting hydraulic communication. Furthermore, in locations where the Gething aquifer directly overlies the Banff aquifer, salinity in both aquifers is similar (~60 000 mg/L). Unfortunately, due to a lack of data in the Gething aquifer, salinity could not be compared in places where the Gething aquifer overlies the Debolt aquifer. However, the Debolt aquifer salinity in this area is greater than 100 000 mg/L (Figure 82). Farther south, where the Gething aquifer directly overlies the Banff aquifer, data from the Gething and Banff aquifers fall on another superhydrostatic gradient of 11.5 kPa/m (Figure 20, data points outlined in brown). Although the Gething and Banff aquifers appear to be in communication in this area, the gradient is at a slightly lower pressure, unique from the gradient formed by tests found to the north, suggesting a different flow system. Another superhydrostatic gradient (10.9 kPa/m) is formed by data from the Gething, Shunda, Pekisko, and Banff aquifers (Figure 20, data points outlined in blue). These data points are in close proximity to the Nordegg Member's zero edge. Salinity in the Mississippian aquifers in this area has decreased to ~60 000 mg/L, similar to what is observed in the Gething aquifer. The salinity and pressure trends in this area suggest that mixing is taking place across the sub-Cretaceous unconformity. Farther east, anomalously high pressure data from the Gething and Pekisko aquifers form two separate subhydrostatic gradients (Figure 20, data points outlined in yellow and purple), indicating downward vertical flow. Salinity in these aquifers in this area is also similar, suggesting communication across the sub-Cretaceous unconformity between these aquifers. The origin of these anomalously high pressures is unknown.

On the pressure-elevation plot of data from the Cambrian–Devonian aquifers in the northeastern focus area, two flow systems have been identified (Figure 21). The majority of the data from the Blue Ridge, Nisku, Swan Hills, and Elk Point aquifers plot on a superhydrostatic gradient of 11.2 kPa/m (brown trend line). Some data from the Blue Ridge and Nisku aquifers (east of the dashed blue line on the inset map in Figure 21) along with the Wabamun aquifer data form another superhydrostatic gradient of 13.0 kPa/m (blue trend line).

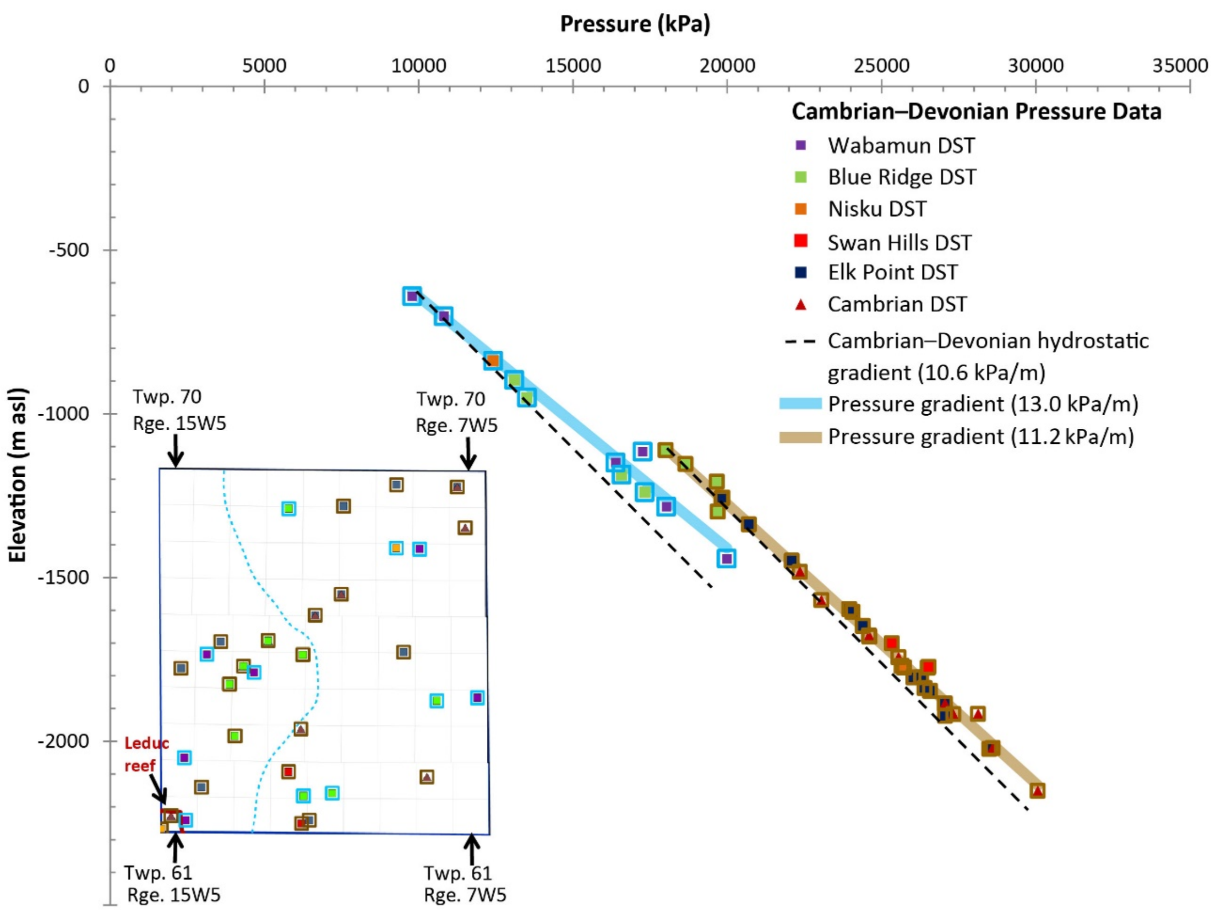

Figure 21. Pressure-elevation plot for the Cambrian and Devonian aquifers in the northeastern focus area (west-central Alberta study area). The inset map shows the location of the data; the dashed blue line denotes the separation of data from the Blue Ridge aquifer plotting on the blue gradient (east of the dashed line) and the brown gradient (west of the dashed line). The colour of the square outline indicates which gradient the data plots on. Abbreviation: DST, drillstem test.

The transition of the Blue Ridge and Nisku aquifers to a lower pressure similar to that seen in the Wabamun aquifer may be related to the increasing distance from a Leduc reef in the southwestern corner of the focus area. Close to the Leduc reef (west of the dashed blue line, Figure 21), the Blue Ridge and Nisku aquifers plot with a similar trend to the underlying aquifers. Farther away from the reef (east of the dashed blue line), the Blue Ridge and Nisku aquifers plot at lower pressures similar to that of the Wabamun aquifer. Both gradients suggest upward cross-formational flow from deeper to shallower aquifers (Leduc to Blue Ridge and Nisku to Wabamun). Examination of the individual potentiometric surface maps for these aquifers show eastward flow in the updip direction.

5.4.3 Cross-Formational Flow in the Southeastern Focus Area

As previously shown in Section 5.2, the pressure regime of Mississippian–Jurassic aquifers across the eastern part of the west-central Alberta study area differs from that in the western part. The southeastern focus area was examined in greater detail to assess its potential for cross-formational flow within the Mississippian–Cretaceous interval. Several flow systems were defined for the Mississippian–Cretaceous interval in the southeastern focus area.

The majority of the data from the Gething, Shunda, Pekisko, and Banff aquifers fall on a subhydrostatic gradient of 8.4 kPa/m (Figure 22, data points outlined in red), suggesting communication between these aquifers with downward flow. Throughout the eastern portion of the focus area, TDS values in the Gething and Banff aquifers appear similar, ranging from ~28 000 to 80 000 mg/L (Figures 77 and 85) supporting the interpretation of communication across the sub-Cretaceous unconformity. Many pressure data from the Gething aquifer (data points outlined in green) plot on a superhydrostatic gradient of 14.9 kPa/m suggesting upward flow. The cause of these higher pressures is unknown. Throughout the western portion of the focus area, pressures from the Gething, Nordegg, and Shunda aquifers (data outlined in blue) plot on a superhydrostatic gradient of 12.2 kPa/m indicating upward flow between these aquifers. However, further evaluation of salinity data in this area revealed that salinities in the Gething and Nordegg aquifers appear to be lower than in the Mississippian aquifers, suggesting that the similar pressure trends may not be related to communication.

Data from the Blue Ridge, Nisku, Leduc, Swan Hills, Elk Point, and Cambrian aquifers from the western portion of the focus area plot on a superhydrostatic gradient of 11.1 kPa/m (Figure 23, data points outlined in brown). The placement of the Blue Ridge and Nisku data points on this gradient suggests communication throughout the entire interval from the Blue Ridge aquifer to the Cambrian aquifer, which is likely due to the presence of Leduc reefs in the western portion of the study area. Farther east, the Blue Ridge aquifer data plot with the Wabamun aquifer data on a superhydrostatic gradient of 11.3 kPa/m (Figure 23, data points outlined in blue), indicating a clear separation of these aquifers from the Swan Hills to Cambrian aquifers in this area. This is due to the presence of the Devonian Woodbend and Waterways shale aquitards in this area, separating the Wabamun, Blue Ridge, and Nisku aquifers from the Swan Hills, Elk Point, and Cambrian aquifers, creating two flow systems.

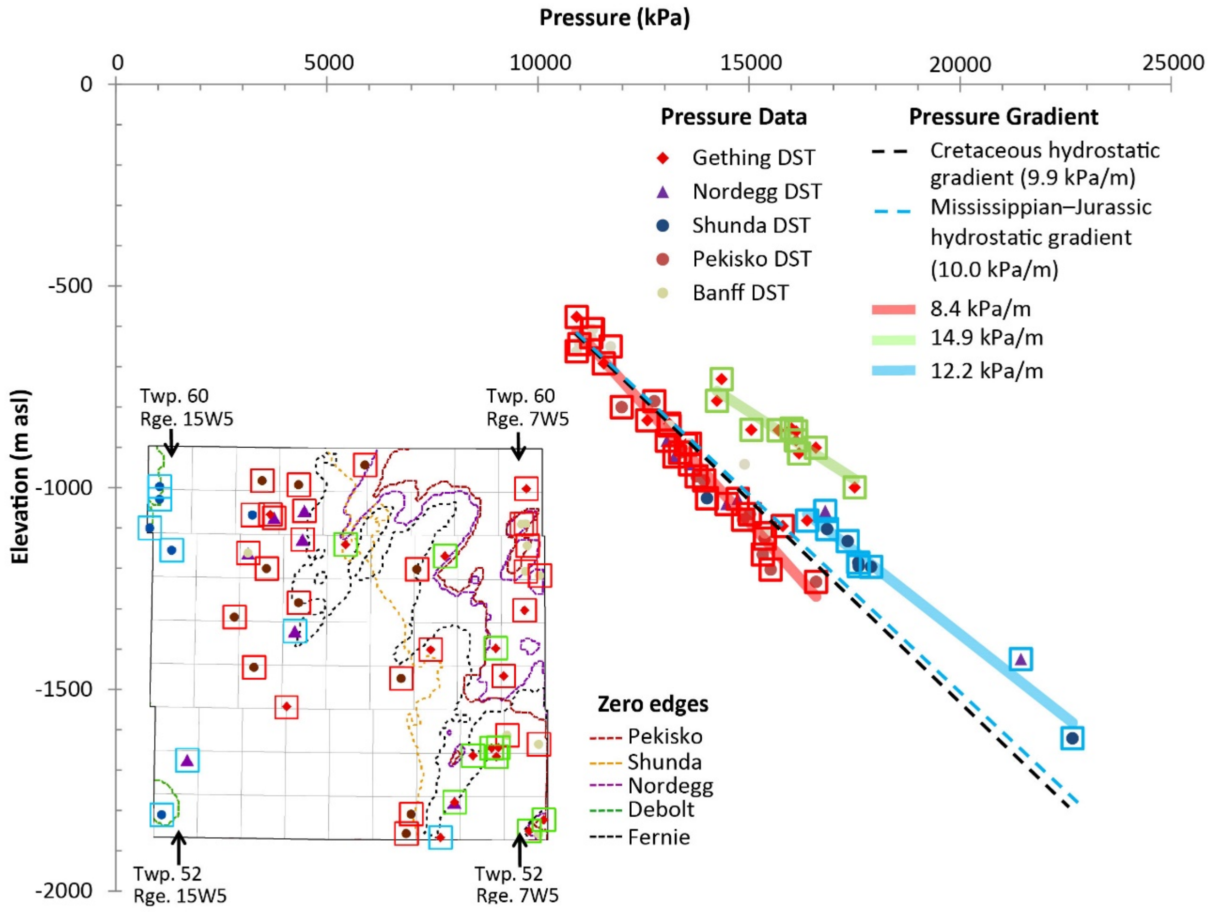

Figure 22. Pressure-elevation plot for the Gething to Banff aquifers in the southeastern focus area (west-central Alberta). The inset map shows the location of the data in relation to the zero edges of the formations/member. The colour of the square outline indicates which gradient the data plot on. Abbreviation: DST, drillstem test.

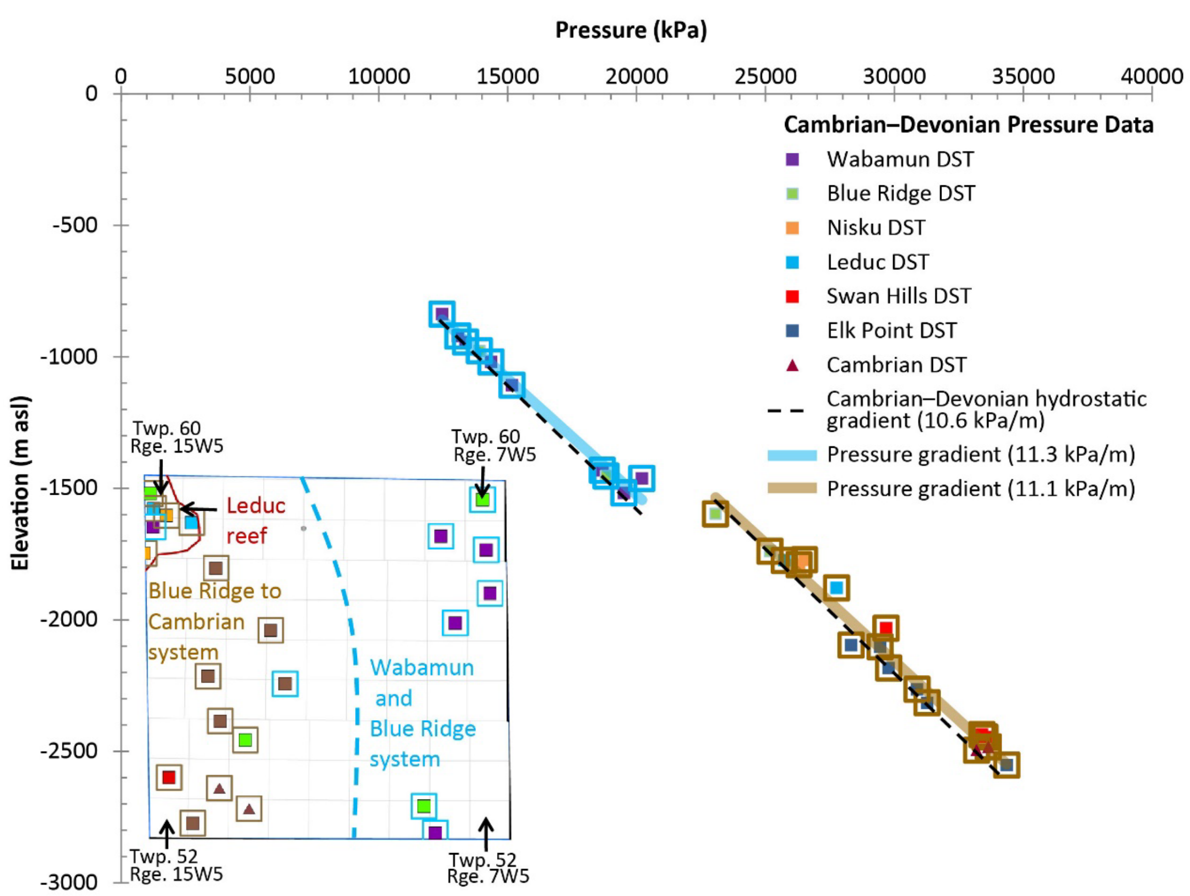

Figure 23. Pressure-elevation plot for the Cambrian–Devonian aquifers in the southeastern focus area (west-central Alberta). The inset map shows the location of the data. The colour of the square outline indicates which gradient the data plot on. Abbreviation: DST, drillstem test.

6 Summary and Conclusions

This study evaluated the hydrogeological attributes and regional flow of 24 aquifers in an area of west-central Alberta, from the near-surface bedrock down to the Precambrian basement.

Groundwater flow in the Cretaceous aquifers is mainly influenced by surface topography and the location of formation subcrops, which are underneath Quaternary sediments north of the study area. The ionic compositions of Cretaceous waters are mainly dominated by Na^+ and Cl^-, but may contain significant HCO_3^- and Ca^{2+} in waters with lower total dissolved solids values. Cross-formational flow analyses of the Viking and Spirit River aquifers showed that in areas where the intervening Joli Fou aquitard thins, communication between the two aquifers may occur. Generally, buoyancy has no effect on the groundwater flow direction and magnitude within the Cretaceous aquifers, however, there are some areas within the Cadomin aquifer where buoyancy can play a role, and care should be taken when interpreting groundwater flow direction and magnitude in these areas.

The Mississippian–Jurassic aquifers share similar hydrogeological properties and generally show the potential for updip groundwater flow from west to east, which is consistent with the expected flow that follows decreasing basinal elevation towards the low hydraulic heads found in the Devonian Grosmont Formation, which acts as a basin-scale drain (Hitchon, 1969; Anfort et al., 2001). Mixing of formation waters associated with cross-formational flow occurs in the eastern part of the study area, where Mississippian–Jurassic aquifers subcrop at the sub-Cretaceous unconformity. The highest salinity values are observed in the western portion of the study area and gradually decrease towards the east. Waters within Mississippian–Jurassic aquifers are dominated by Na^+ and Cl^-.

Groundwater flow in the Devonian aquifers is generally in the updip direction in the eastern portion of the study area, where the potentiometric surfaces of the Upper Devonian Wabamun, Blue Ridge, and Nisku aquifers are similar to the potentiometric surface of the Mississippian–Jurassic aquifers. This resemblance of hydrogeological characteristics of the Mississippian–Jurassic aquifers and the Upper Devonian aquifers in the eastern part of the study area may be a result of decreased effectiveness of the Exshaw confining unit in the area. Leduc reefs, which are present in the western part of the study area, provide a permeable conduit that allows for vertical hydraulic communication between the aquifers in the Devonian–Cambrian interval. In the eastern portion of the study area, where the reefs are replaced by Devonian shales, two separate flow systems are observed. In the western part of the study area, the high salinities in the succession cause density to have a large influence on the flow of water. The composition of waters from the Cambrian–Devonian aquifers is mainly dominated by Na^+ and Cl^-, although high Ca^{2+} content is observed in waters with high total dissolved solids values, with Ca^{2+} accounting for up to 38% of the total cations.

Hydraulic head and salinity maps as well as pressure-elevation plots created in this study help gain a better understanding of the groundwater flow systems within west-central Alberta. The water recovery maps made as part of this study were used to delineate the aquifer portions of mapped formations. The water driving force maps identify regions within an aquifer where density-driven flow needs to be taken into consideration. In addition, schematic hydrogeological cross-sections were created to summarize the hydrogeological attributes and groundwater flow interpretations in the west-central Alberta study area (Figures 24–27).

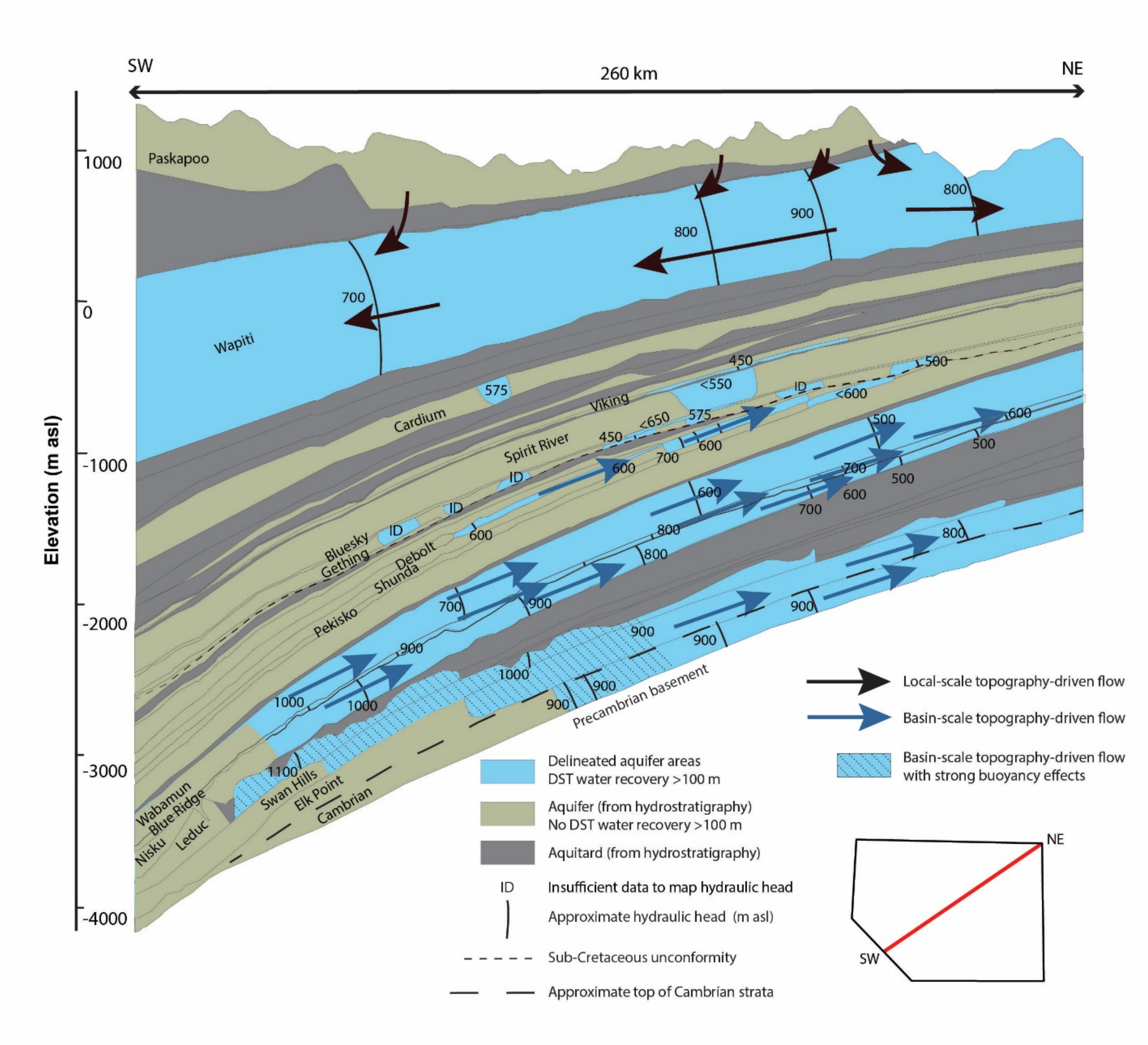

Figure 24. Schematic southwest (SW)–northeast (NE) hydrogeological cross-section depicting the distribution of hydraulic head in the west-central Alberta study area. Abbreviation: DST, drillstem test.

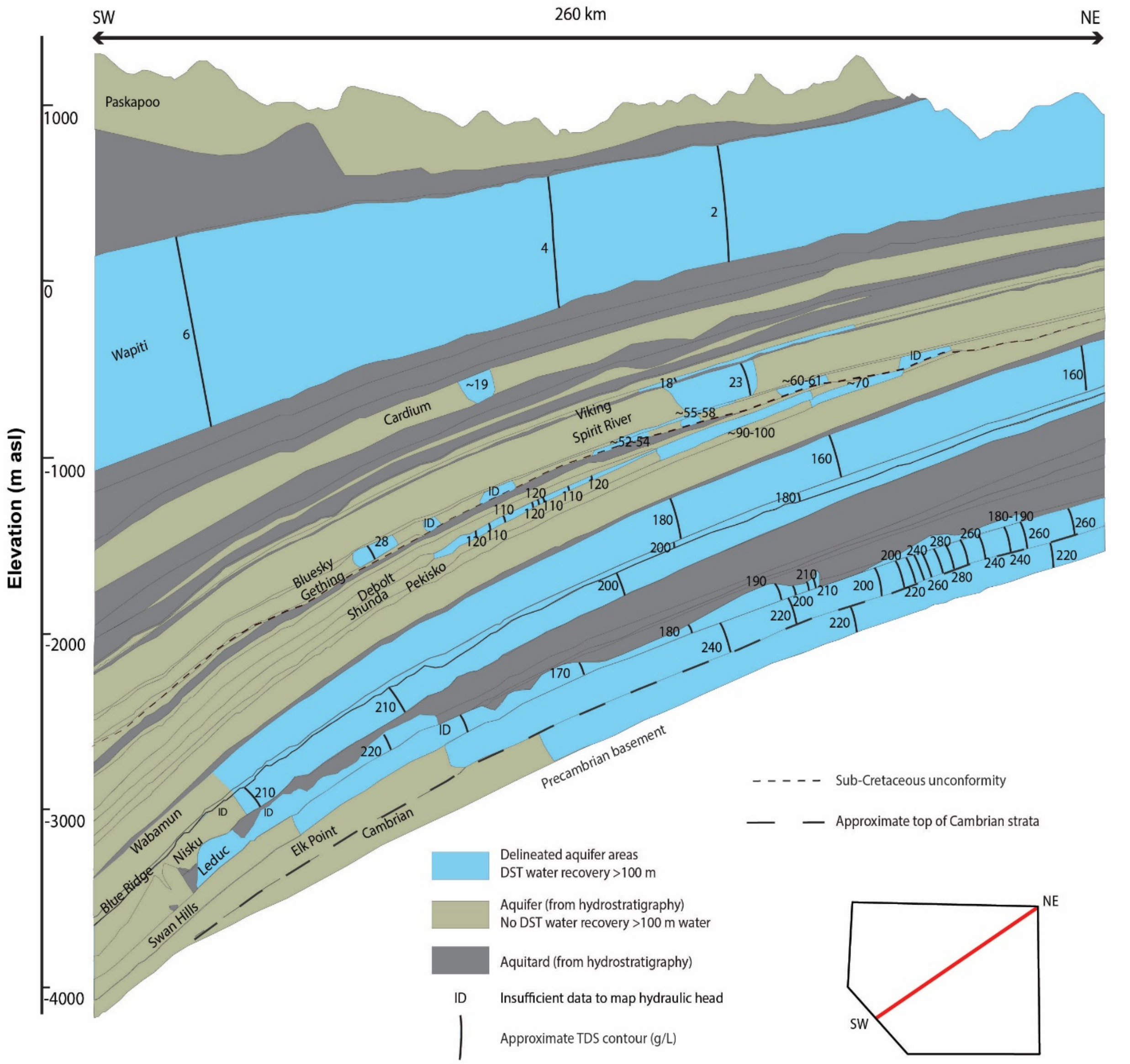

Figure 25. Schematic southwest (SW)–northeast (NE) hydrogeological cross-section depicting the distribution of total dissolved solids (TDS) in the west-central Alberta study area. Abbreviation: DST, drillstem test.

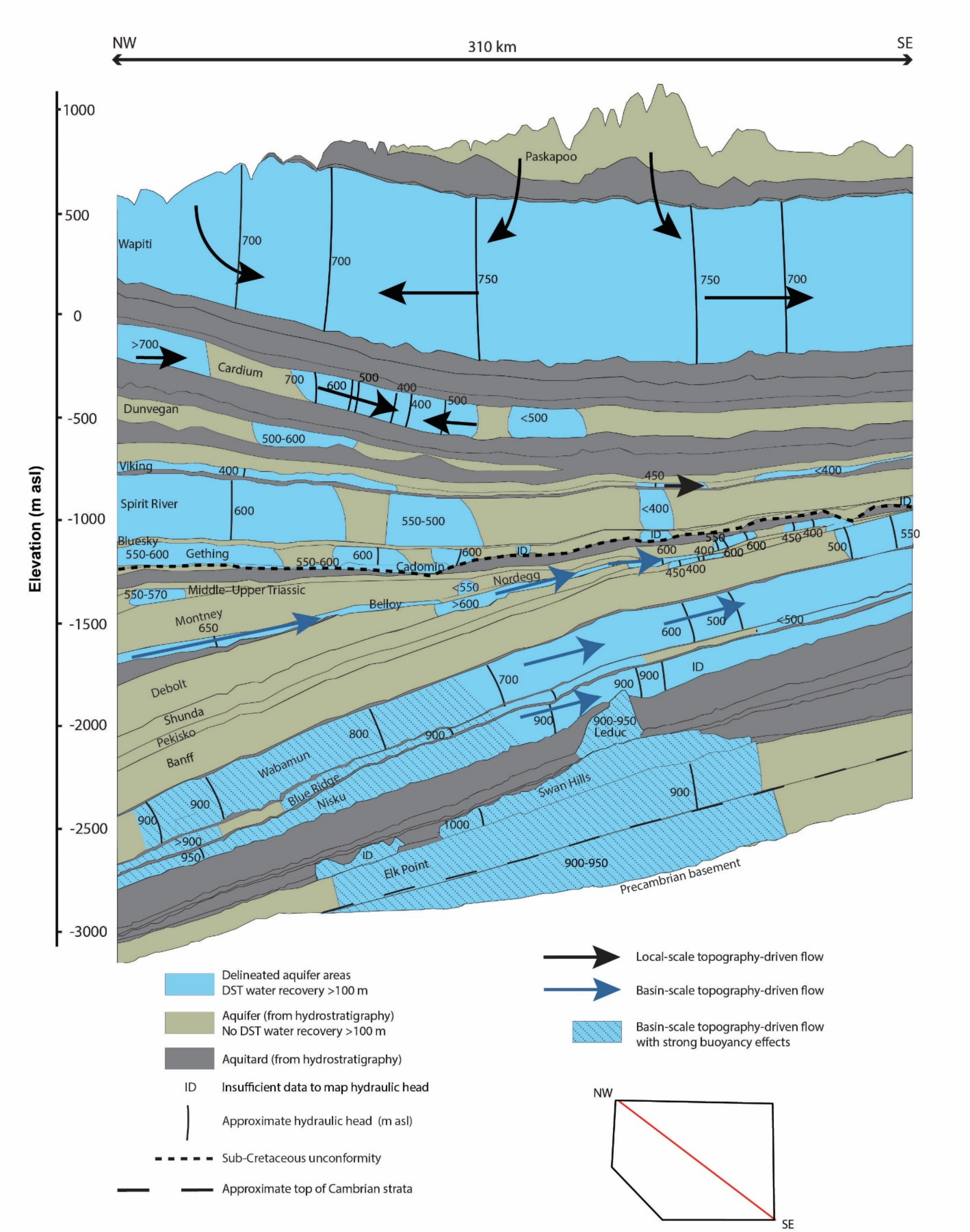

Figure 26. Schematic northwest (NW)–southeast (SE) cross-section depicting the distribution of hydraulic head in the west-central Alberta study area. Abbreviation: DST, drillstem test.

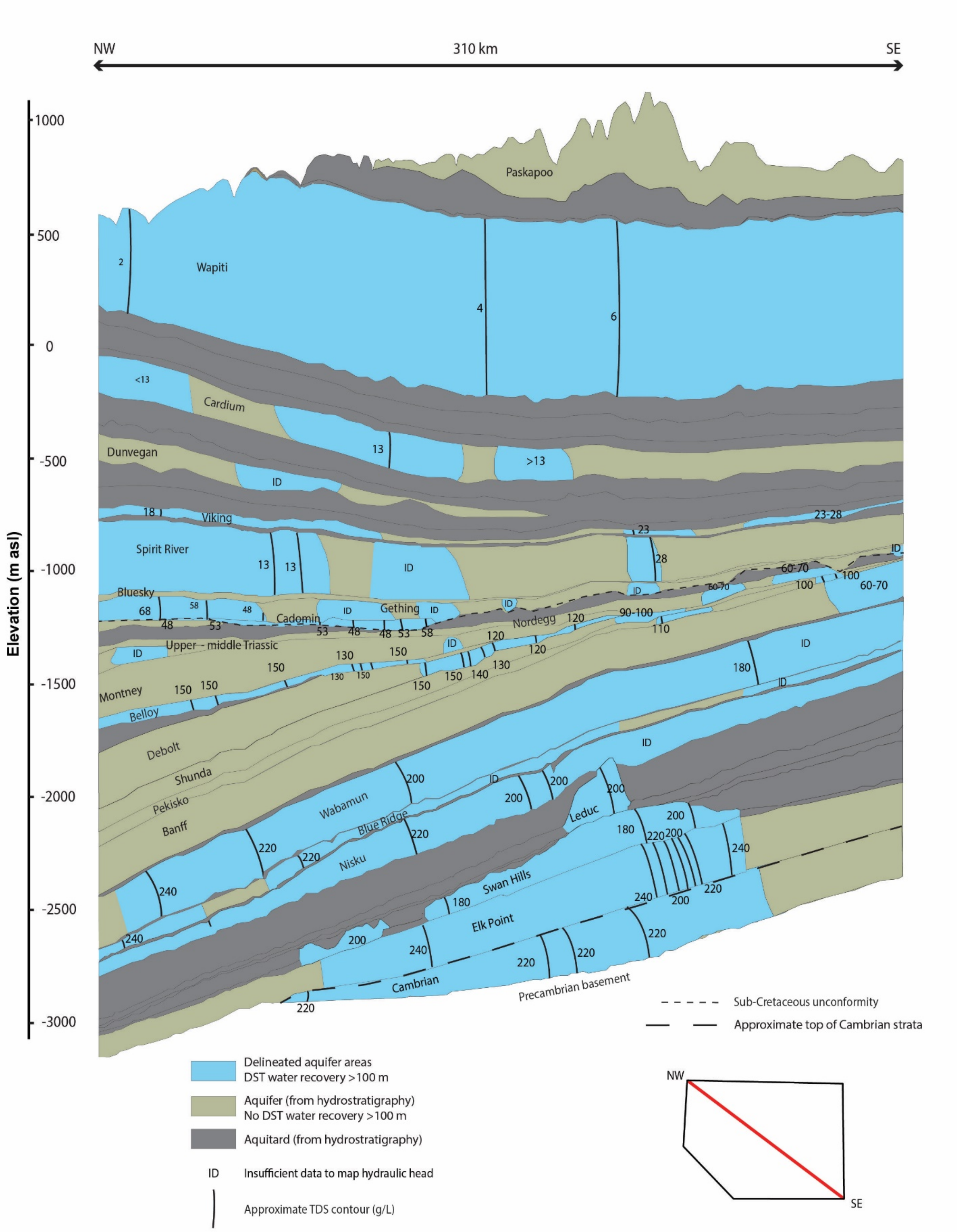

Figure 27. Schematic northwest (NW)-southeast (SE) hydrogeological cross-section depicting the distribution of total dissolved solids (TDS) in the west-central Alberta study area. Abbreviation: DST, drillstem test.

7 References

Alberta Environment and Parks (2013): Alberta Water Well Information Database; URL <https://www.alberta.ca/alberta-water-well-information-database-overview.aspx> [March 2017].

Alberta Environment and Parks (2015): Provincial DEM; Altalis Ltd., 25 m cell, Esri grid format, URL <http://www.altalis.com/products/terrain/dem.html> [February 2016].

Alberta Geological Survey (2019a): 3D Provincial Geological Framework Model of Alberta, version 2; Alberta Energy Regulator / Alberta Geological Survey, AER/AGS Model 2018-02.

Alberta Geological Survey (2019b): Alberta Table of Formations; Alberta Energy Regulator / Alberta Geological Survey, URL <https://ags.aer.ca/publications/Table_of_Formations_2019.html#summary> [December 2019].

Alberta Government (2014): Our water, our future: a plan for action; URL <https://open.alberta.ca/publications/9781460118900> [December 2019].

Alessi, D.S., Zolfaghari, A., Kletke, S., Gehman, J., Allen, D.M. and Goss, G.G. (2017): Comparative analysis of hydraulic fracturing wastewater practices in unconventional shale development: water sourcing, treatment, and disposal practices; Canadian Water Resources Journal, v. 42, p. 105–121.

Anfort, S.J. (1998): Regional-scale hydrogeology of Lower Cretaceous to Middle Devonian aquifers in southeastern Alberta; M.Sc. thesis, University of Calgary, 160 p.

Anfort, S.J., Bachu, S. and Bentley, L.R. (2001): Regional-scale hydrogeology of the Upper Devonian-Lower Cretaceous sedimentary succession, south-central Alberta basin, Canada; AAPG Bulletin, v. 85, p. 637–660.

Babakhani, M., MacCormack, K.E., Playter, T.L., Corlett, H., Hathway, B. and Peterson, J.T. (2019): 3D geological model of west-central Alberta (dataset, multiple files); Alberta Energy Regulator / Alberta Geological Survey, AER/AGS Model 2019-03, URL <https://ags.aer.ca/data-maps-models/MOD_2019_03.html> [January 2020].

Bachu, S. (1995): Synthesis and model of formation-water flow, Alberta Basin, Canada; AAPG Bulletin, v. 79, p. 1159–1178.

Bachu, S. (1999): Flow systems in the Alberta Basin: patterns, types and driving mechanisms; Bulletin of Canadian Petroleum Geology, v. 47, p. 455–474.

Bachu, S. and Adams, J.J. (2003): Sequestration of CO_2 in geological media in response to climate change: capacity of deep saline aquifers to sequester CO_2 in solution; Energy and Conversion Management, v. 44, p. 3151–3175.

Bachu, S. and Michael, K. (2002): Flow of variable-density formation water in deep sloping aquifers: minimizing the error in representation and analysis when using hydraulic-head distributions; Journal of Hydrology, v. 259, p. 49–65.

Brinsky, J. (in press a): Distribution of hydraulic head in the Cardium hydrostratigraphic unit; Alberta Energy Regulator / Alberta Geological Survey, AER /AGS Map 545, scale 1:1 750 000.

Brinsky, J. (in press b): Distribution of total dissolved solids in the Cardium hydrostratigraphic unit; Alberta Energy Regulator / Alberta Geological Survey, AER /AGS Map 544, scale 1:1 750 000.

Chierici, G.L. (1994): Principles of Petroleum Reservoir Engineering; Springer-Verlag Berlin Heidelberg GmbH, 407 p.

Corlett, H.J., Playter, T.L., Babakhani, M., Hathway, B., Peterson, J.T. and MacCormack, K.E. (2019): Regional stratigraphic correlation and 3D geological modelling of west-central Alberta; Alberta

Energy Regulator / Alberta Geological Survey, AER/AGS Open File Report 2019-04, 53 p., URL <https://ags.aer.ca/publications/OFR_2019_04.html> [January 2020].

Dawson, F.M., Evans, C.G., Marsh, R. and Richardson, R. (1994): Uppermost Cretaceous and Tertiary strata of the Western Canada Sedimentary Basin; *in* Geological atlas of the Western Canada Sedimentary Basin, G.D. Mossop and I. Shetsen (comp.), Canadian Society of Petroleum Geologists and Alberta Research Council, URL <https://ags.aer.ca/atlas-the-western-canada-sedimentary-basin/chapter-24-uppermost-cretaceous-and-tertiary-strata> [December 2019].

Edwards, D.E., Barclay, J.E., Gibson, D.W., Kvill, G.E. and Halton, E. (1994): Triassic strata of the Western Canada Sedimentary Basin; *in* Geological atlas of the Western Canada Sedimentary Basin, G.D. Mossop and I. Shetsen (comp.), Canadian Society of Petroleum Geologists and Alberta Research Council, URL <https://ags.aer.ca/atlas-the-western-canada-sedimentary-basin/chapter-16-triassic-strata> [April 2019].

Hitchon, B. (1969): Fluid flow in the Western Canada Sedimentary Basin: 1. effect of topography; Water Resources Research, v. 5, p. 186–195.

Hitchon, B. (1990): Hydrochemistry of the Peace River Arch area, Alberta and British Columbia; prepared for the Alberta Research Council, 81 p., URL <https://ags.aer.ca/publications/OFR_1990_18.html> [November 2018].

Hitchon, B. (1996): Rapid evaluation of the hydrochemistry of a sedimentary basin using only "standard" formation water analyses: example from the Canadian portion of the Williston Basin; Applied Geochemistry, v. 11, p. 789–795.

Hitchon, B. and Brulotte, M. (1994): Culling criteria for "standard" formation water analyses; Applied Geochemistry, v. 9, no. 6, p. 637–645.

Hitchon, B. Sauveplane, C.M., Bachu, S., Koster, E.M. and Lytviak, A.T. (1989): Hydrogeology of the Swan Hills area, Alberta: evaluation for deep waste injection; Alberta Research Council, Alberta Geological Survey, Bulletin 58, 85 p., URL <https://ags.aer.ca/publications/BUL_058.html> [May 2017].

Hitchon, B., Bachu, S. and Underschultz, J.R. (1990): Regional subsurface hydrogeology, Peace River Arch area, Alberta and British Columbia; Bulletin of Canadian Petroleum Geology, v. 38A, p. 196–217.

IHS Markit (2019): AccuMap™; IHS Markit, URL <https://ihsmarkit.com/products/oil-gas-tools-accumap.html> [September 2019].

Jensen, G.K.S., Rostron, B., Palombi, D. and Melnik, A. (2013): Saskatchewan Phanerozoic Fluids and Petroleum Systems Project: hydrogeological mapping framework; *in* Summary of Investigations 2013, v. 1, Saskatchewan Geological Survey, Saskatchewan Ministry of the Economy, Miscellaneous Report 2013-4.1, Paper a-5, 10 p.

Masters, J.A. (1979): Deep basin gas trap, western Canada; AAPG Bulletin, v. 63, no. 2, p. 152–181.

Michael, K. (2002): Flow of formation water in the Alberta Basin adjacent to the Rocky Mountains thrust and fold belt, west-central Alberta, Canada; Ph.D. thesis, University of Alberta, 332 p.

Michael, K. and Bachu, S. (2001): Fluids and pressure distributions in the foreland-basin succession in the west-central part of the Alberta Basin, Canada: evidence for permeability barriers and hydrocarbon generation and migration; AAPG Bulletin, v. 85, no. 7, p. 1231–1252.

Michael, K. and Buschkuehle, M. (2008): Subsurface characterization of the acid-gas injection operations in the Peace River Arch area; Energy Resources Conservation Board, ERCB/AGS Special Report 90, 186 p., URL <https://ags.aer.ca/publication/spe-090> [November 2020].

Nakevska, N. and Singh, A. (2018): Distribution of total dissolved solids in the Wapiti / Belly River hydrostratigraphic unit; Alberta Energy Regulator/ Alberta Geological Survey, AER/AGS Map 542, scale 1:1 750 000, URL <https://ags.aer.ca/publications/MAP_542.html> [January 2021].

Palombi, D.D. (2008): Regional hydrogeological characterisation of the northeastern margin in the Williston Basin; M.Sc. thesis, University of Alberta, 196 p.

Prior, G.J., Hathway, B., Glombick, P.M., Pană, D.I., Banks, C.J., Hay, D.C., Schneider, C.L., Grobe, M., Elgr, R. and Weiss, J.A. (2013): Bedrock geology of Alberta; Alberta Energy Regulator, AER/AGS Map 600, scale 1:1 000 000, URL <https://ags.aer.ca/publication/map-600> [January 2021].

Reid, H.W. (2011): Practical drillstem test interpretation; unpublished course notes, 308 p.

Rostron, B.J. (1995): Cross-formational fluid flow in Upper Devonian to Lower Cretaceous strata, west-central Alberta, Canada; Ph.D. thesis, University of Alberta, 201 p.

Singh, A. and Nakevska, N. (2018): Distribution of hydraulic head in the Wapiti / Belly River hydrostratigraphic unit; Alberta Energy Regulator / Alberta Geological Survey, AER/AGS Map 543, scale 1:1 750 000, URL <https://ags.aer.ca/publications/MAP_543.html> [January 2019].

Singh, A., Palombi, D., Nakevska, N., Jensen, G. and Rostron, B. (2017): An efficient approach for characterizing basin-scale hydrodynamics; Marine and Petroleum Geology, v. 84, p. 332–340.

Smerdon, B.D., Klassen, J. and Gardner, W.P. (2019): Hydrogeological characterization of the Upper Cretaceous–Quaternary units in the Fox Creek area, west-central Alberta; Alberta Energy Regulator / Alberta Geological Survey, AER/AGS Report 98, 35 p., URL <https://ags.aer.ca/publications/REP_98.html> [January 2020].

Thompson, M.J. (1989): Gas fields, formation-fluid flow and hydrochemistry in Early Cretaceous formations, Peace River Region, N.W. Alberta, Canada; M.Sc. thesis, University of Alberta, 160 p.

Appendix 1 – Hydrogeological Maps

1.1 Location of Water-Recovering Drillstem Tests and Delineated Aquifers

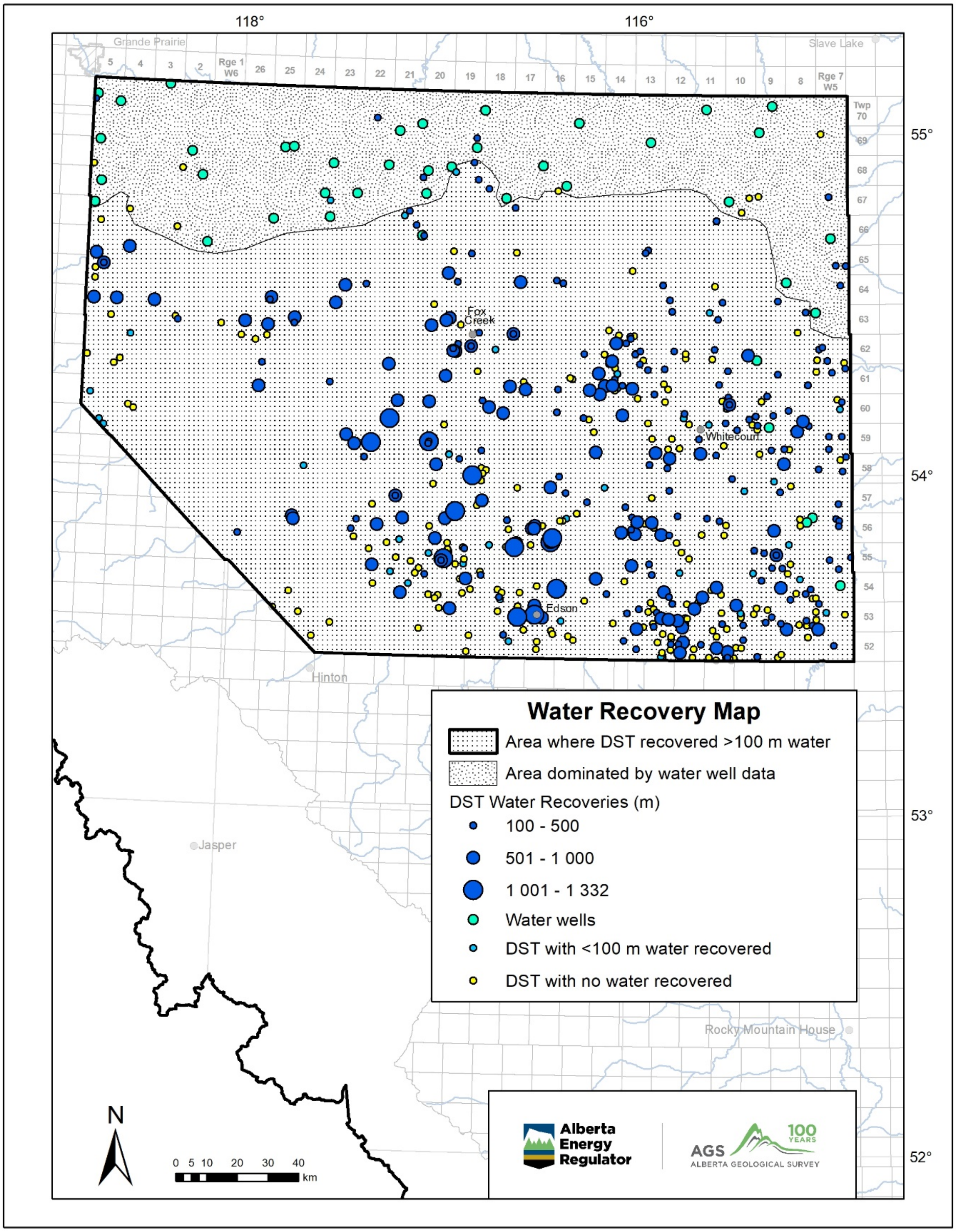

Figure 28. Water recoveries from drillstem tests (DSTs) in the Wapiti aquifer, west-central Alberta study area, and location of water wells.

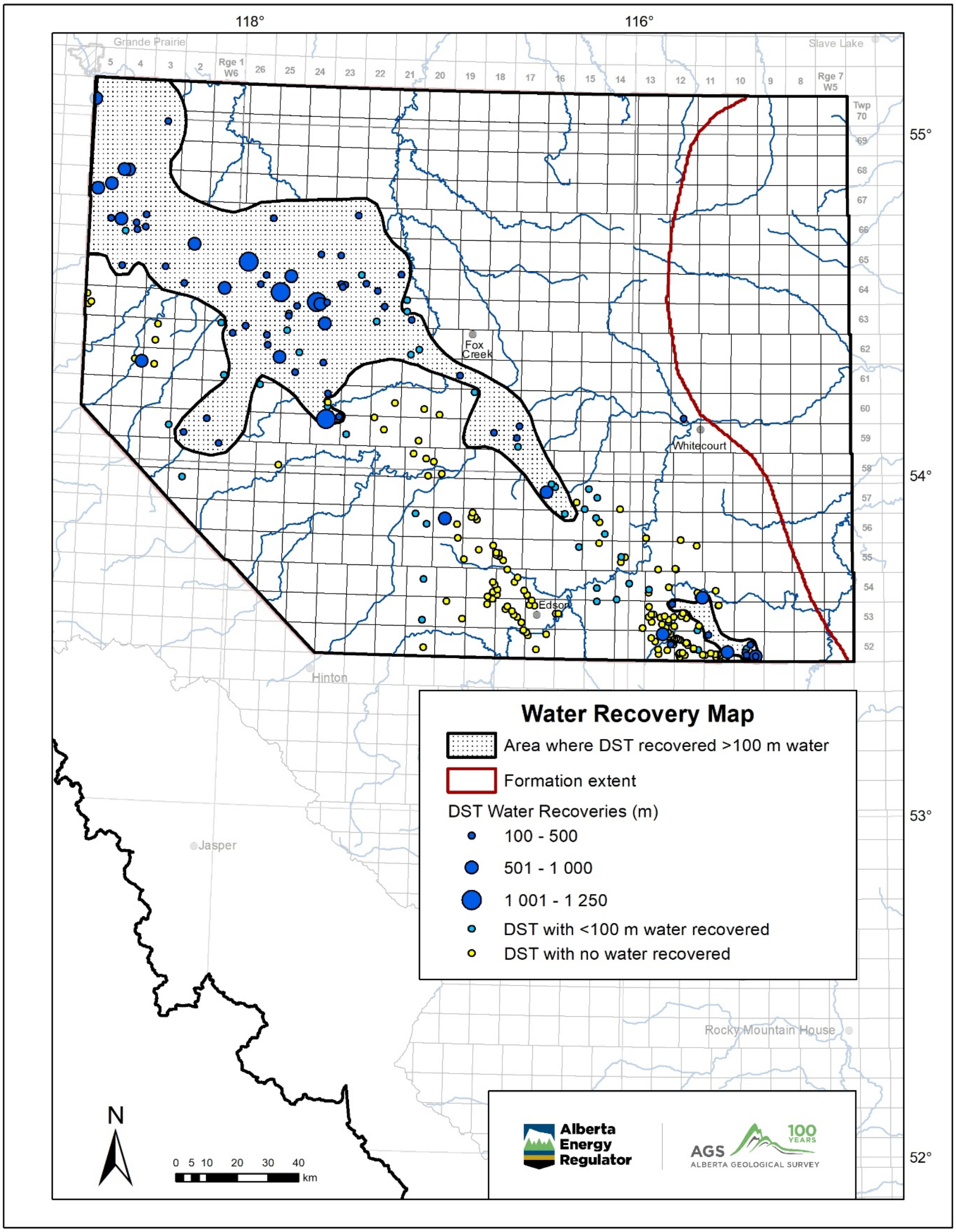

Figure 29. Water recoveries from drillstem tests (DSTs) in the Cardium aquifer, west-central Alberta study area.

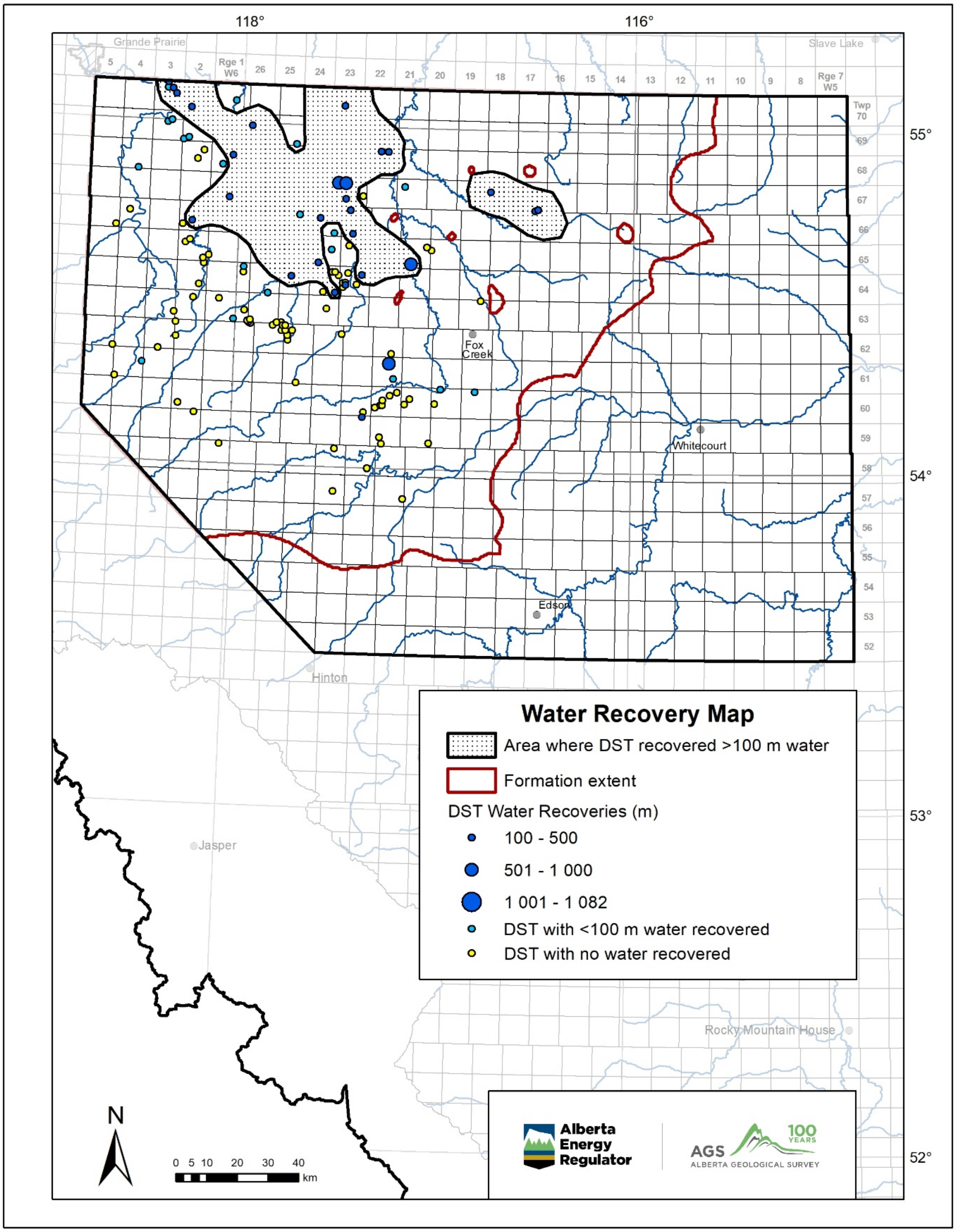

Figure 30. Water recoveries from drillstem tests (DSTs) in the Dunvegan aquifer, west-central Alberta study area.

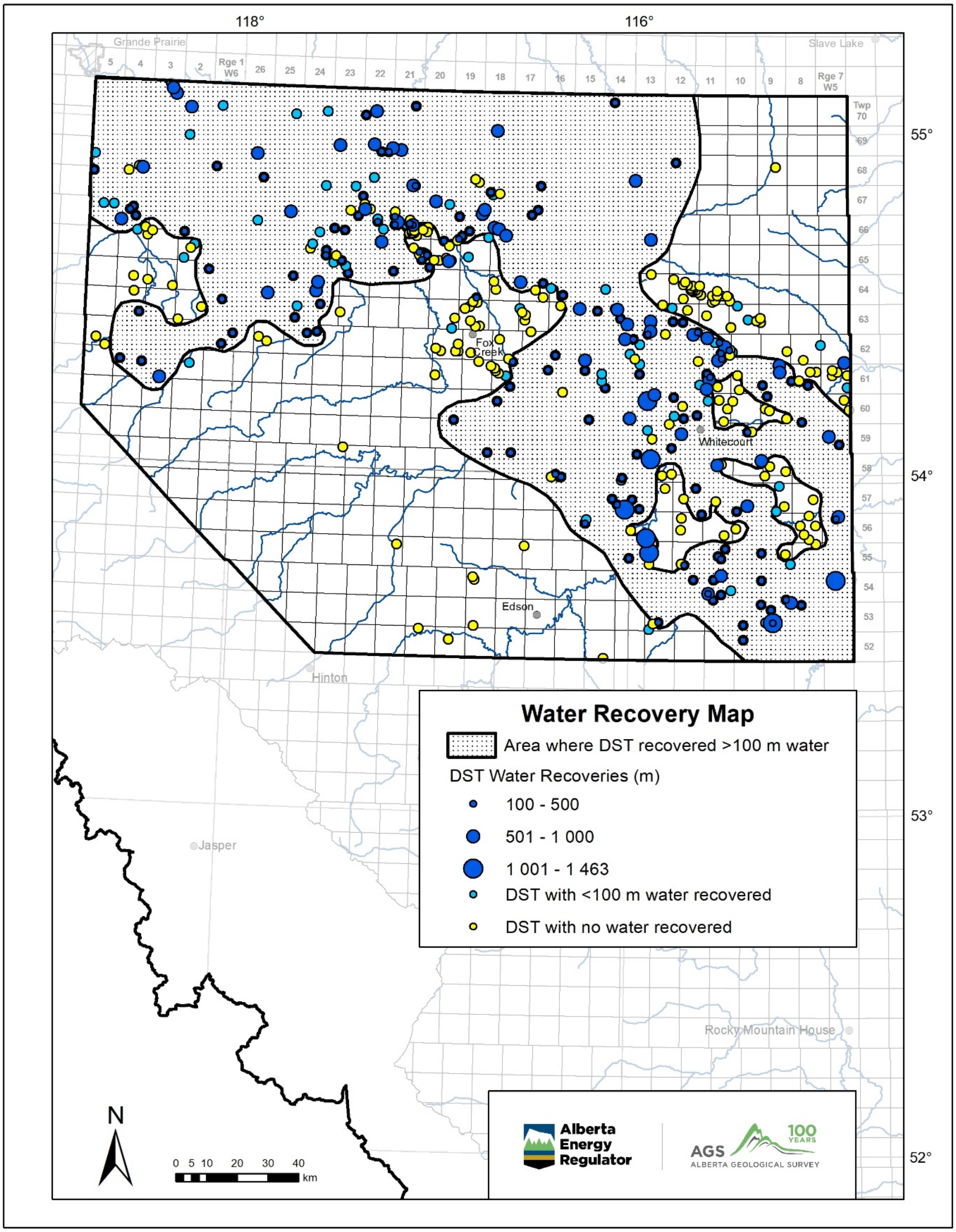

Figure 31. Water recoveries from drillstem tests (DSTs) in the Viking aquifer, west-central Alberta study area.

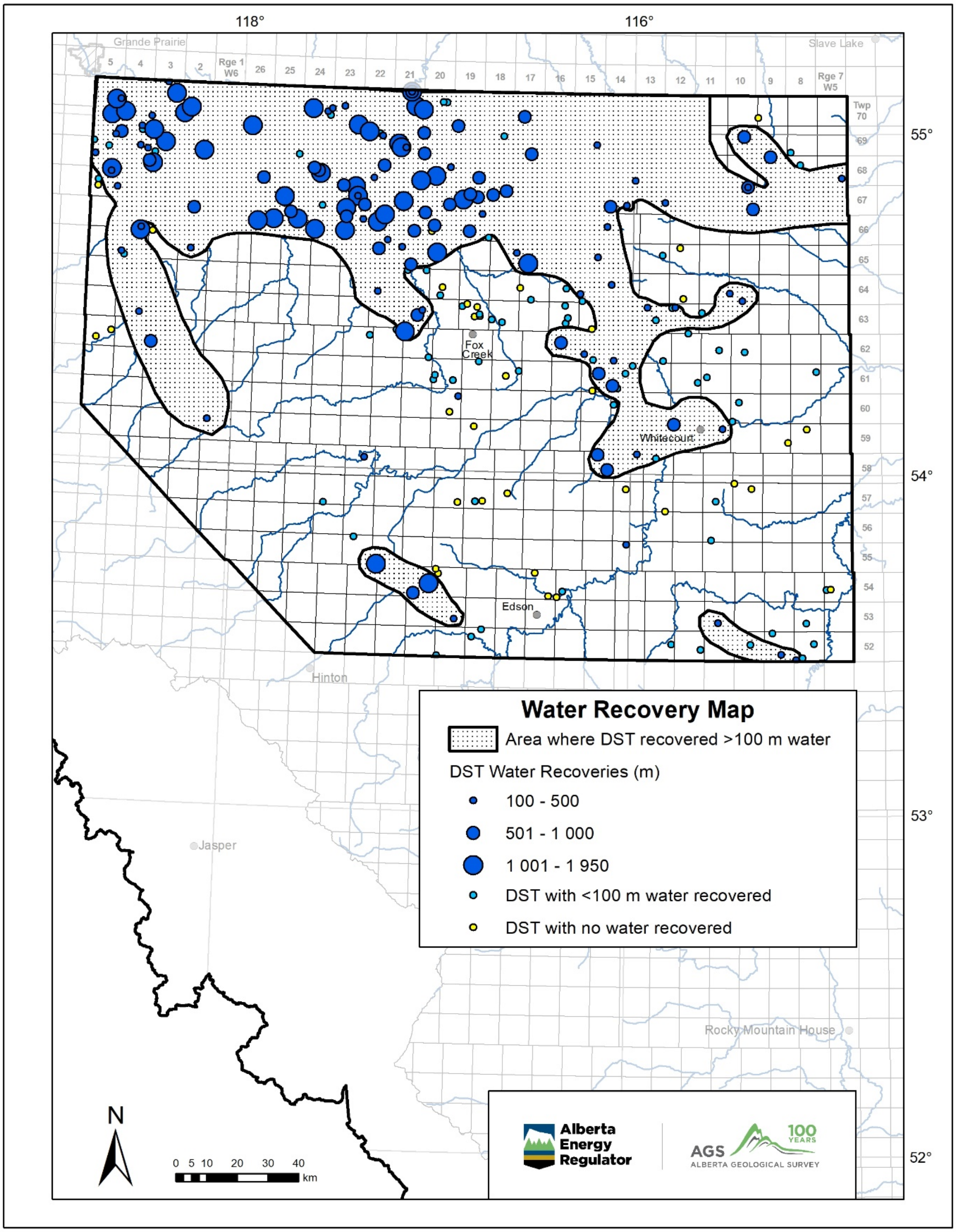

Figure 32. Water recoveries from drillstem tests (DSTs) in the Spirit River aquifer, west-central Alberta study area.

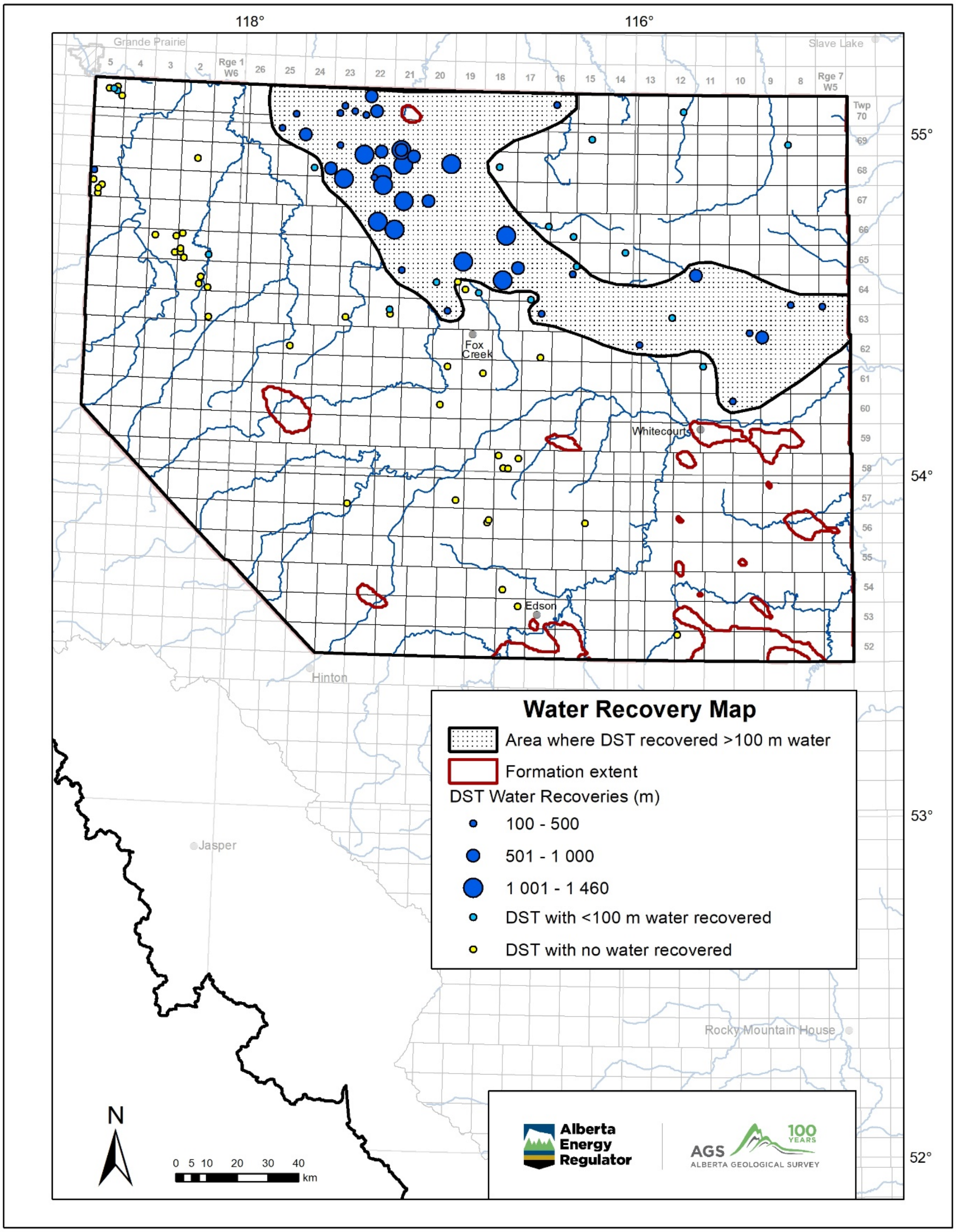

Figure 33. Water recoveries from drillstem tests (DSTs) in the Bluesky aquifer, west-central Alberta study area.

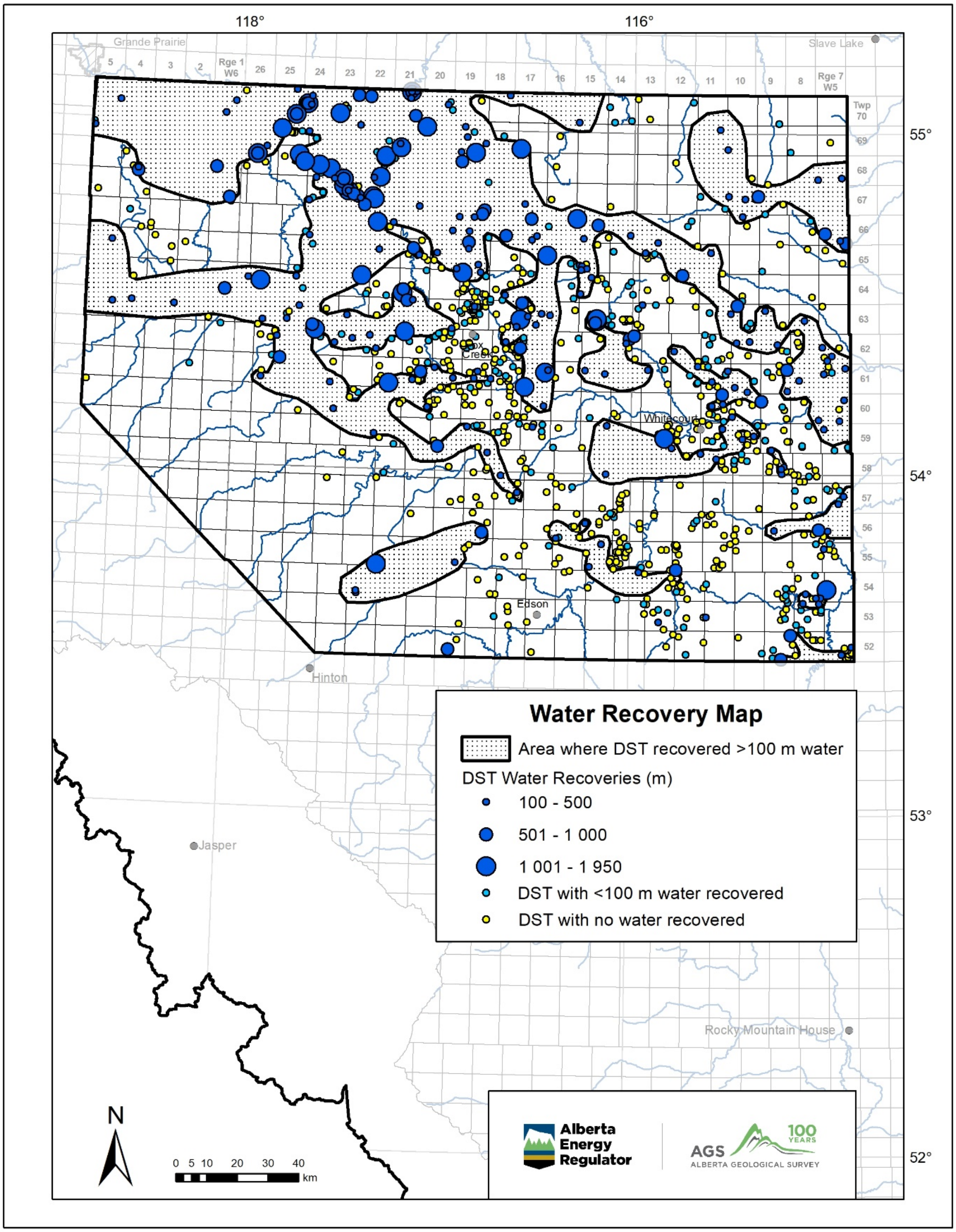

Figure 34. Water recoveries from drillstem tests (DSTs) in the Gething aquifer, west-central Alberta study area.

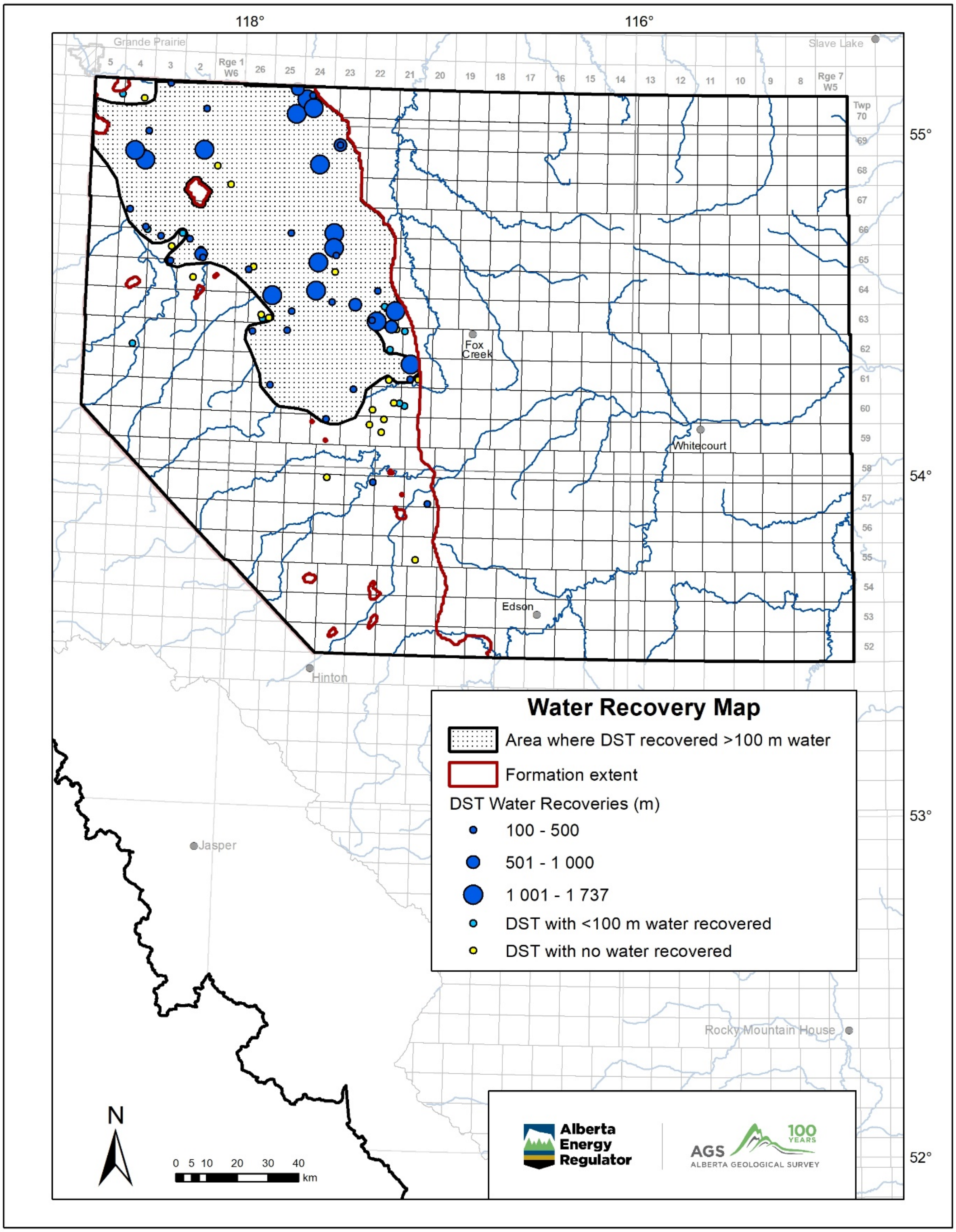

Figure 35. Water recoveries from drillstem tests (DSTs) in the Cadomin aquifer, west-central Alberta study area.

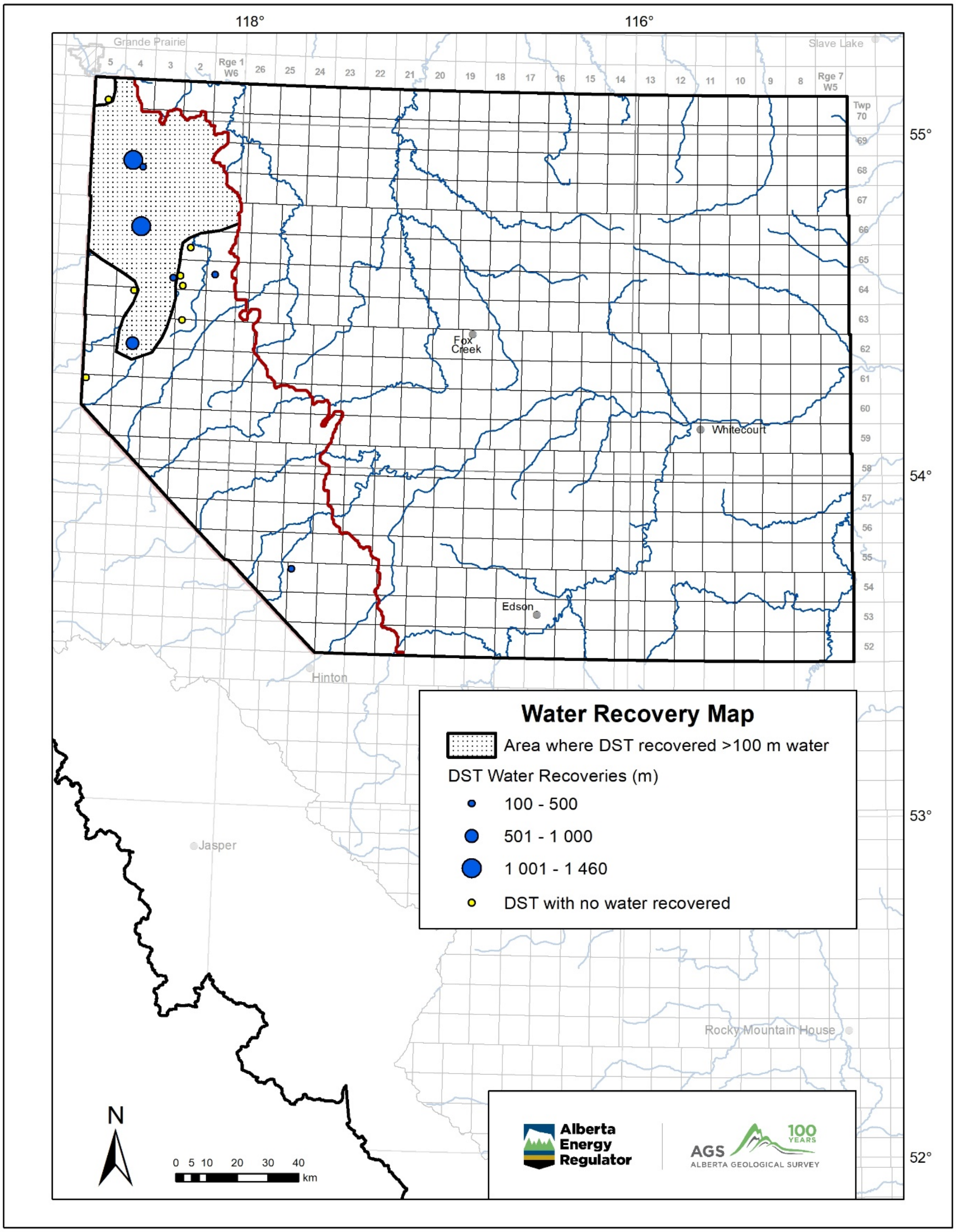

Figure 36. Water recoveries from drillstem tests (DSTs) in the Nikanassin aquifer, west-central Alberta study area.

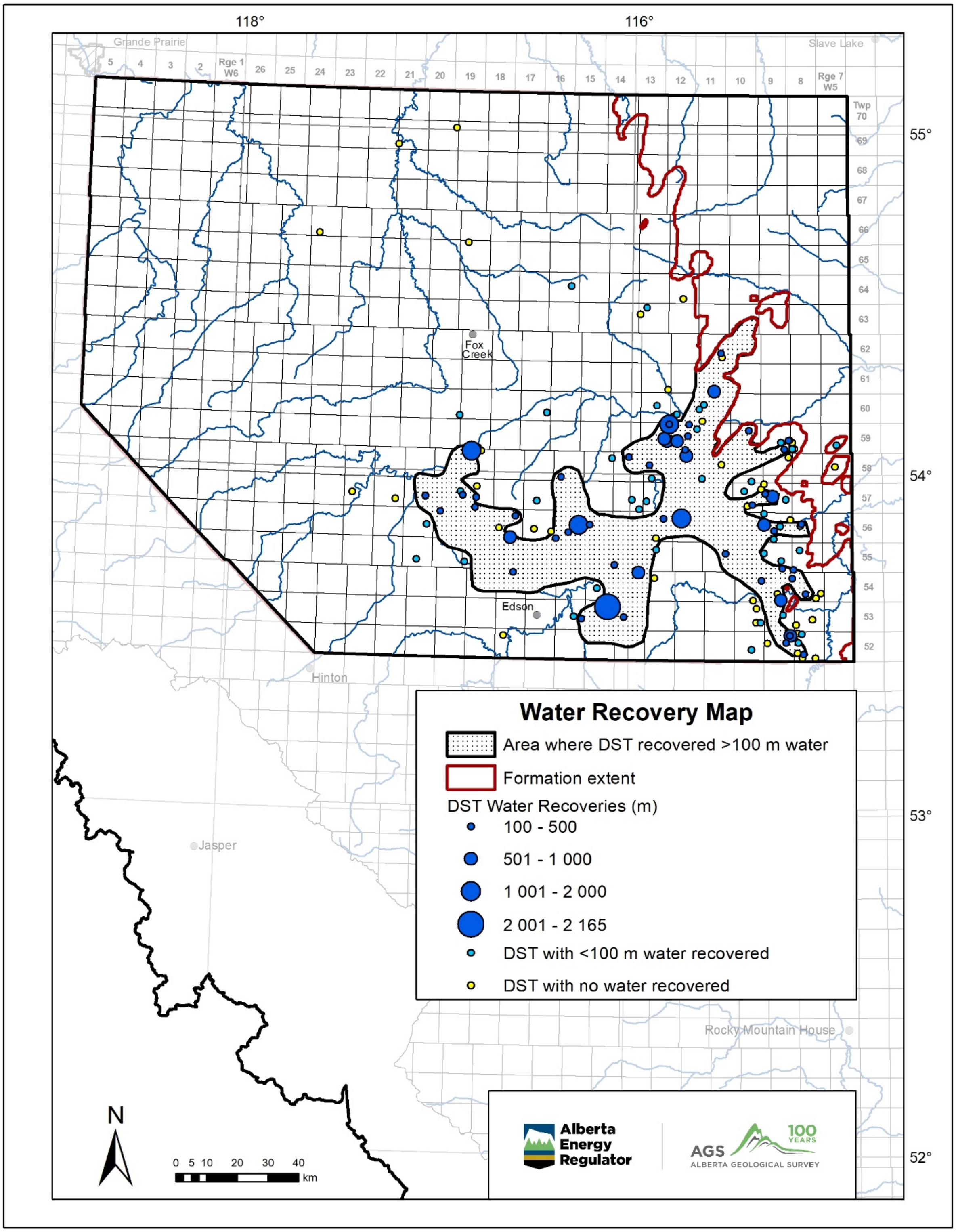

Figure 37. Water recoveries from drillstem tests (DSTs) in the Nordegg aquifer, west-central Alberta study area.

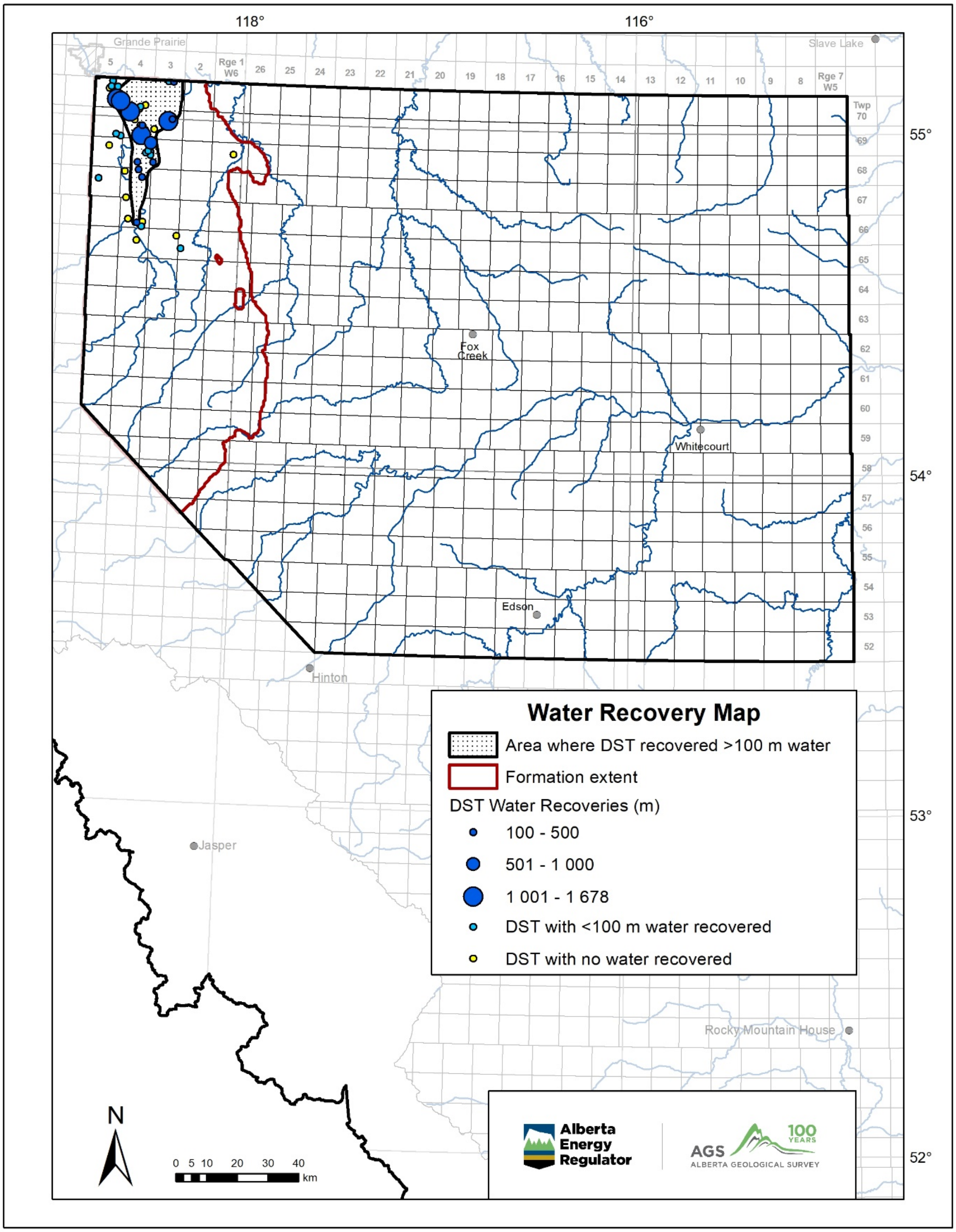

Figure 38. Water recoveries from drillstem tests (DSTs) in the Middle–Upper Triassic aquifer, west-central Alberta study area.

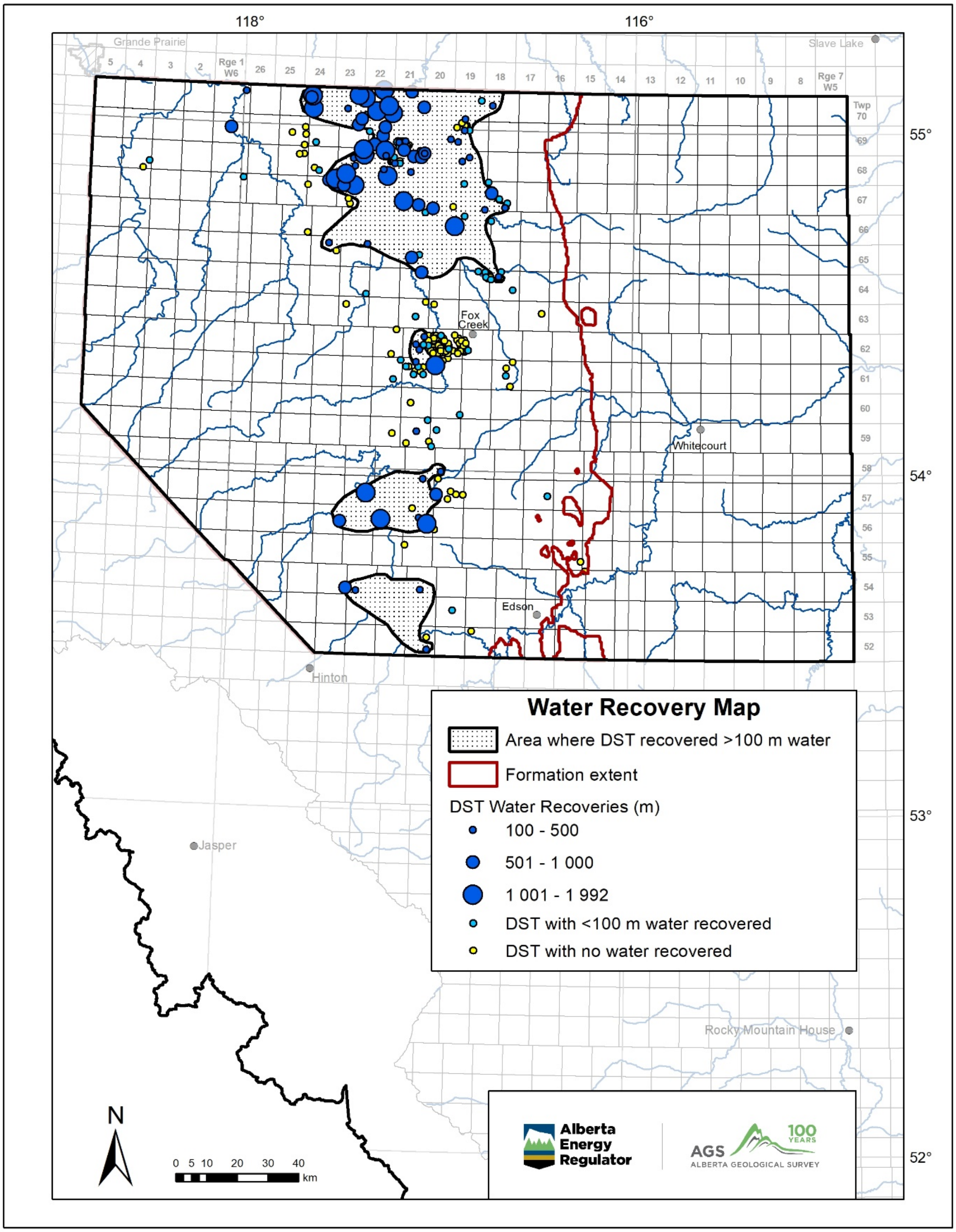

Figure 39. Water recoveries from drillstem tests (DSTs) in the Montney aquifer, west-central Alberta study area.

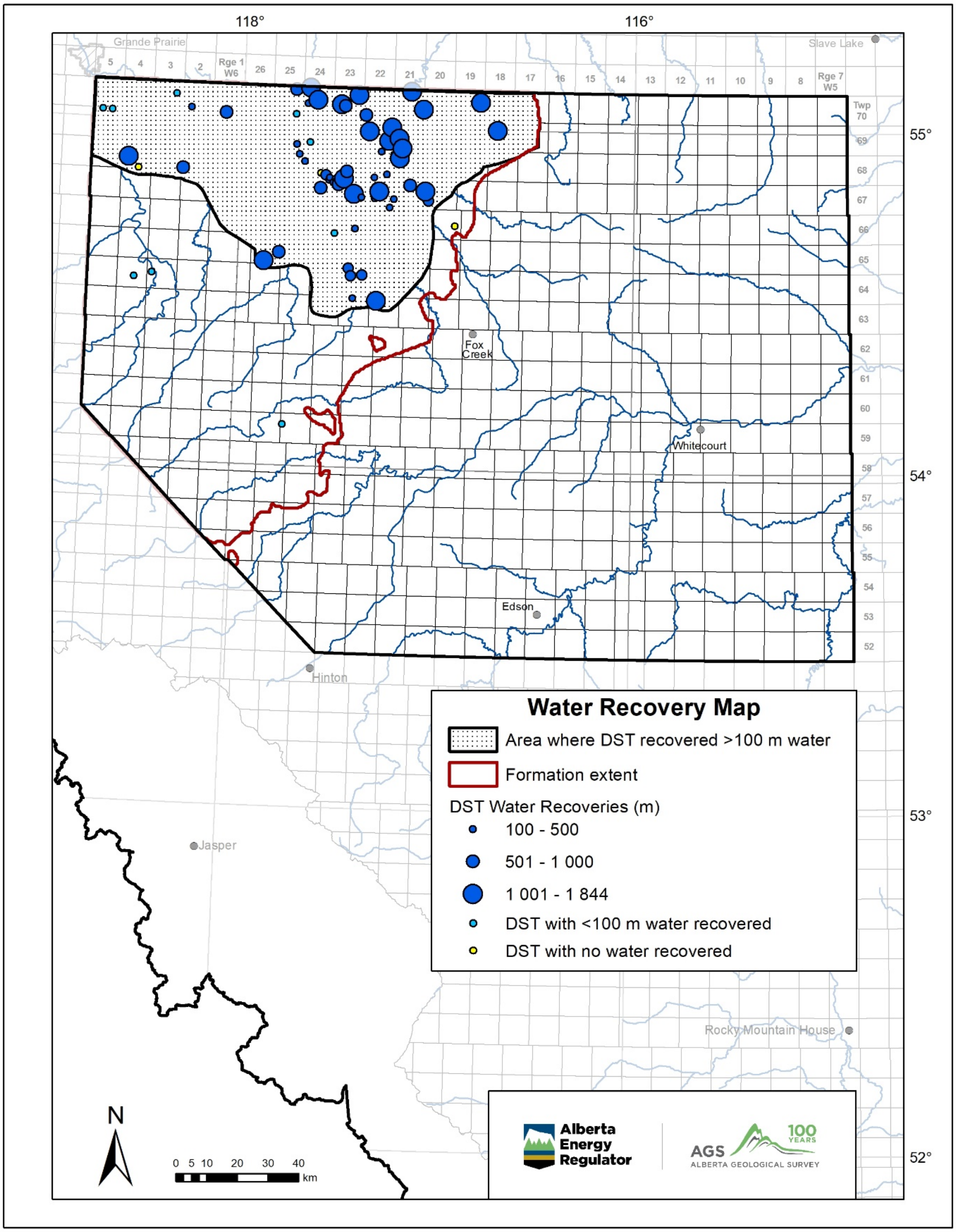

Figure 40. Water recoveries from drillstem tests (DSTs) in the Belloy aquifer, west-central Alberta study area.

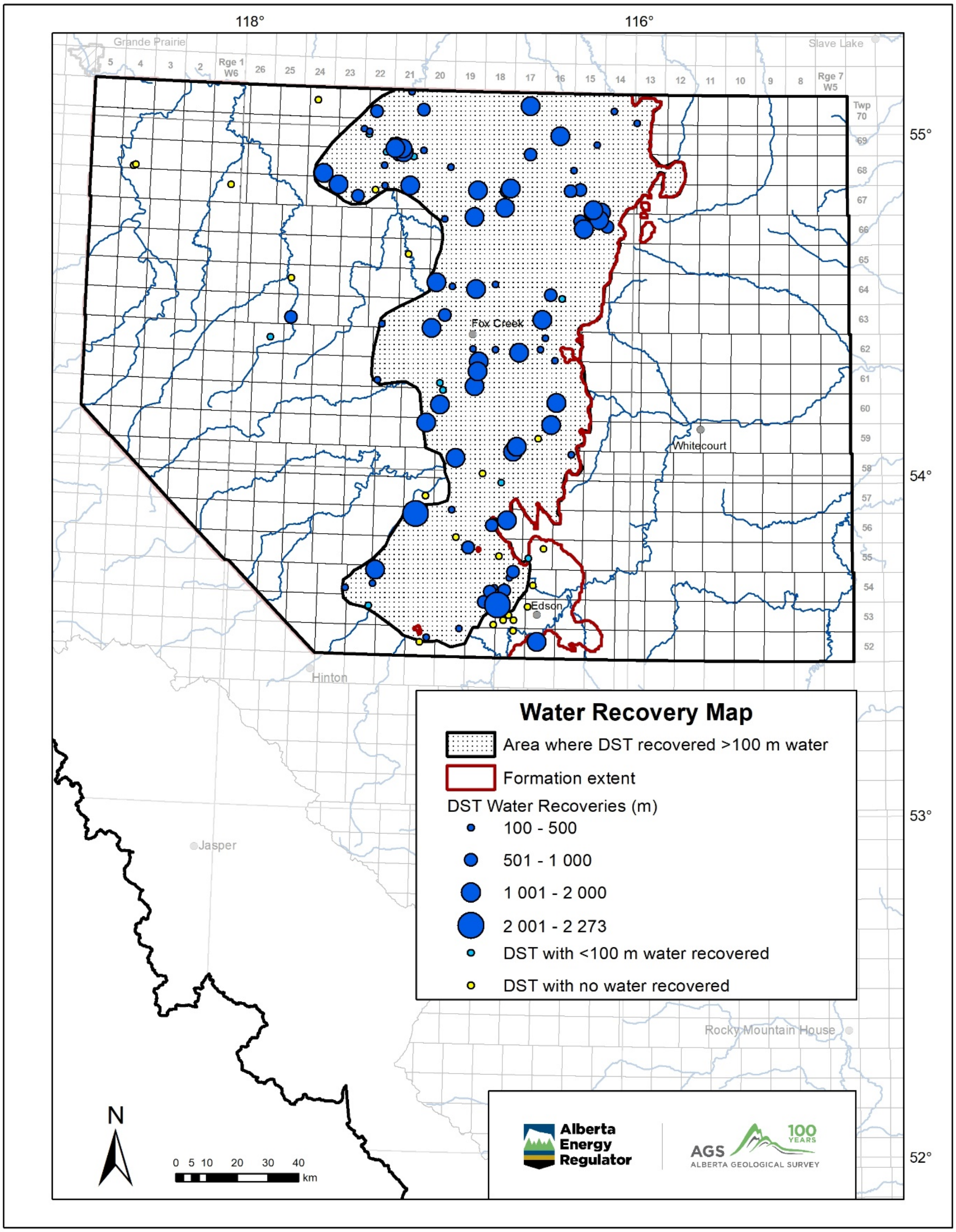

Figure 41. Water recoveries from drillstem tests (DSTs) in the Debolt aquifer, west-central Alberta study area.

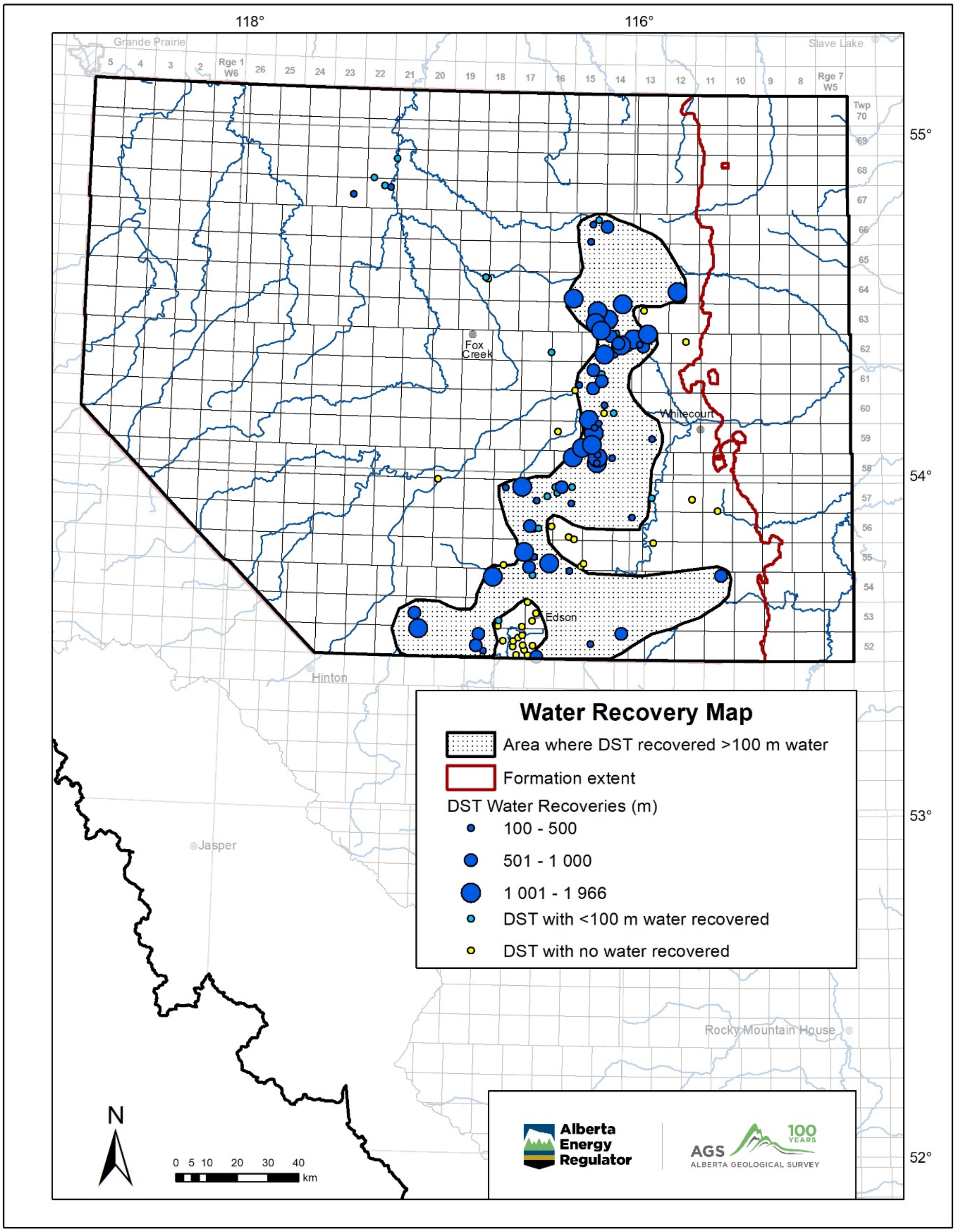

Figure 42. Water recoveries from drillstem tests (DSTs) in the Shunda aquifer, west-central Alberta study area.

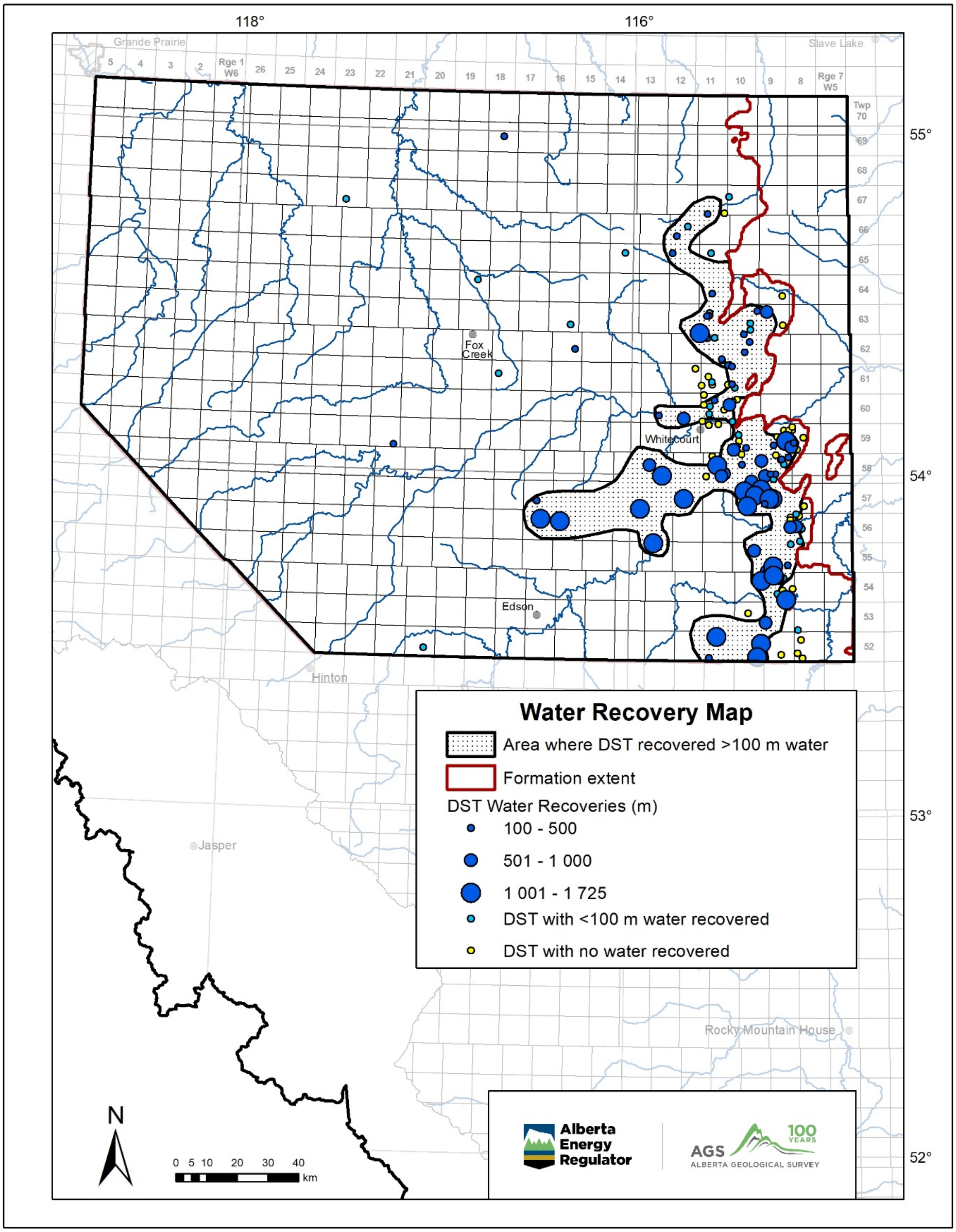

Figure 43. Water recoveries from drillstem tests (DSTs) in the Pekisko aquifer, west-central Alberta study area.

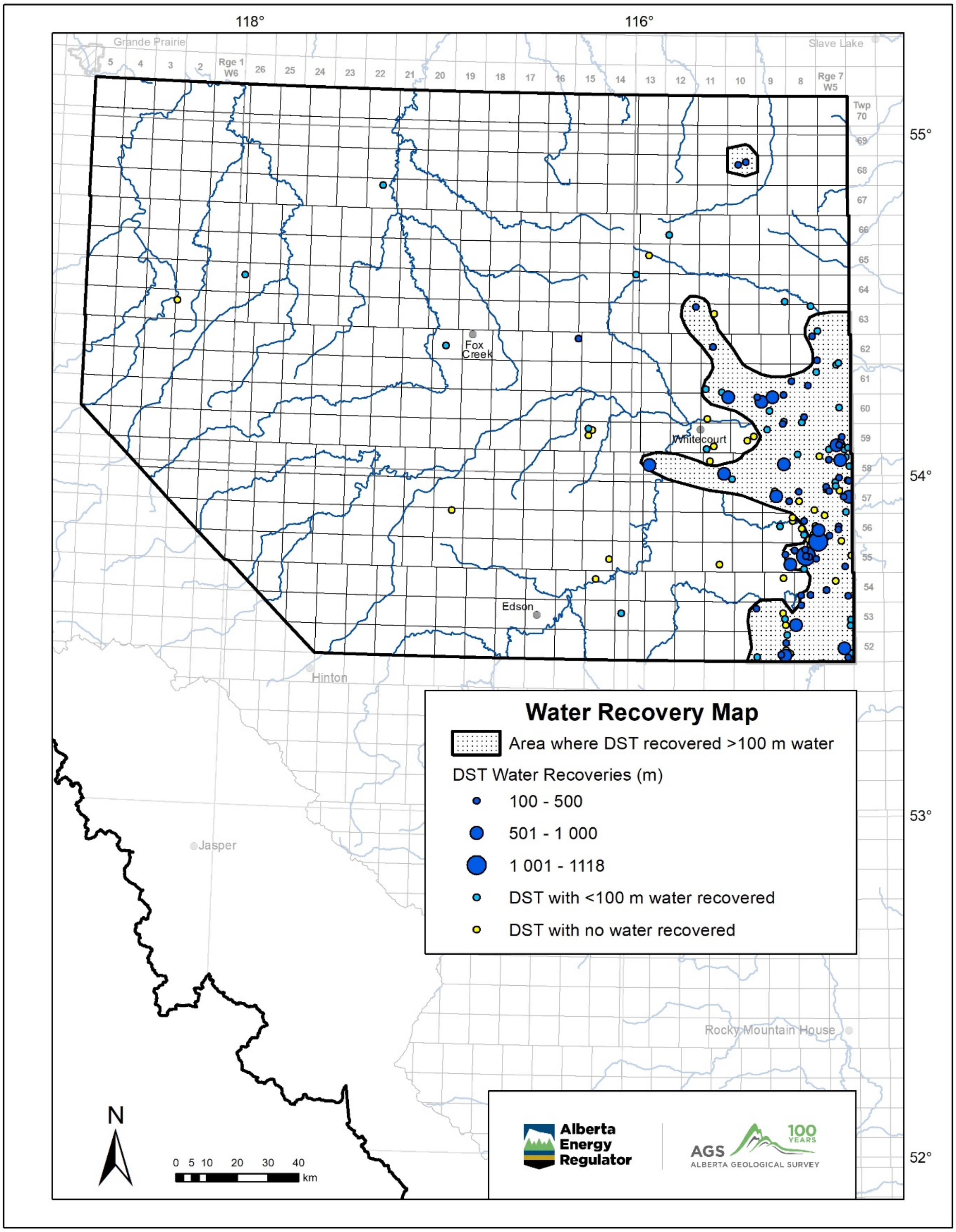

Figure 44. Water recoveries from drillstem tests (DSTs) in the Banff aquifer, west-central Alberta study area.

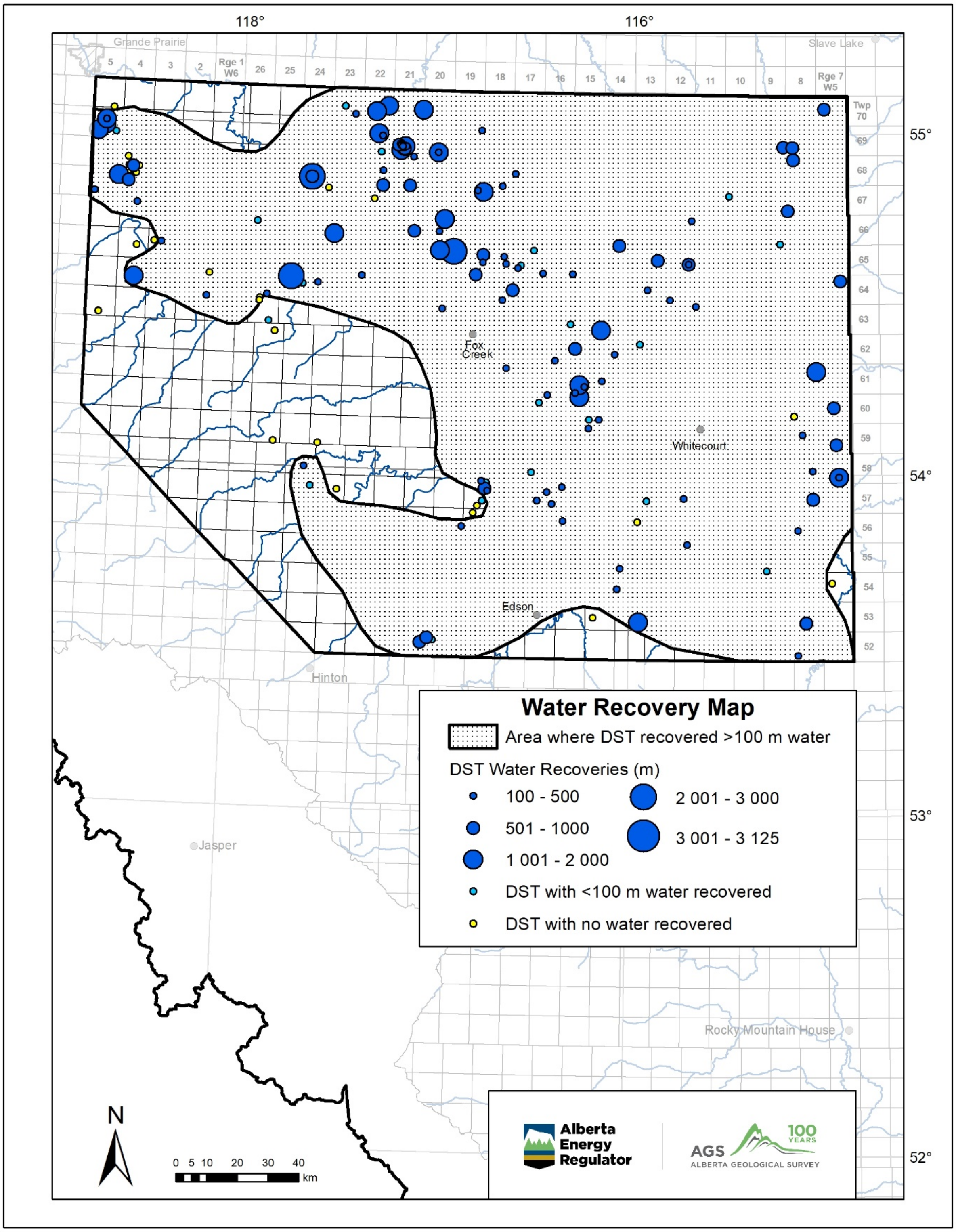

Figure 45. Water recoveries from drillstem tests (DSTs) in the Wabamun aquifer, west-central Alberta study area.

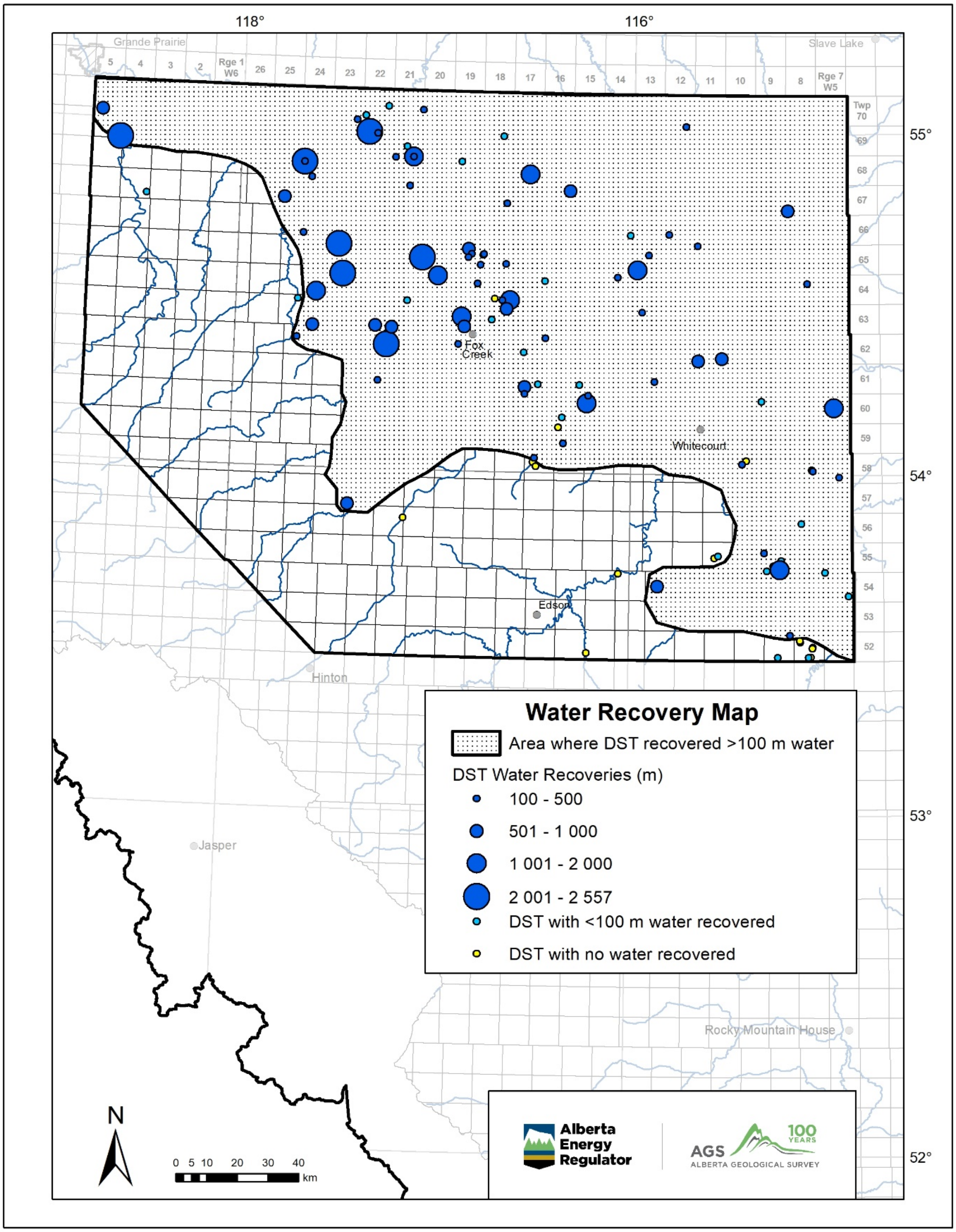

Figure 46. Water recoveries from drillstem tests (DSTs) in the Blue Ridge aquifer, west-central Alberta study area.

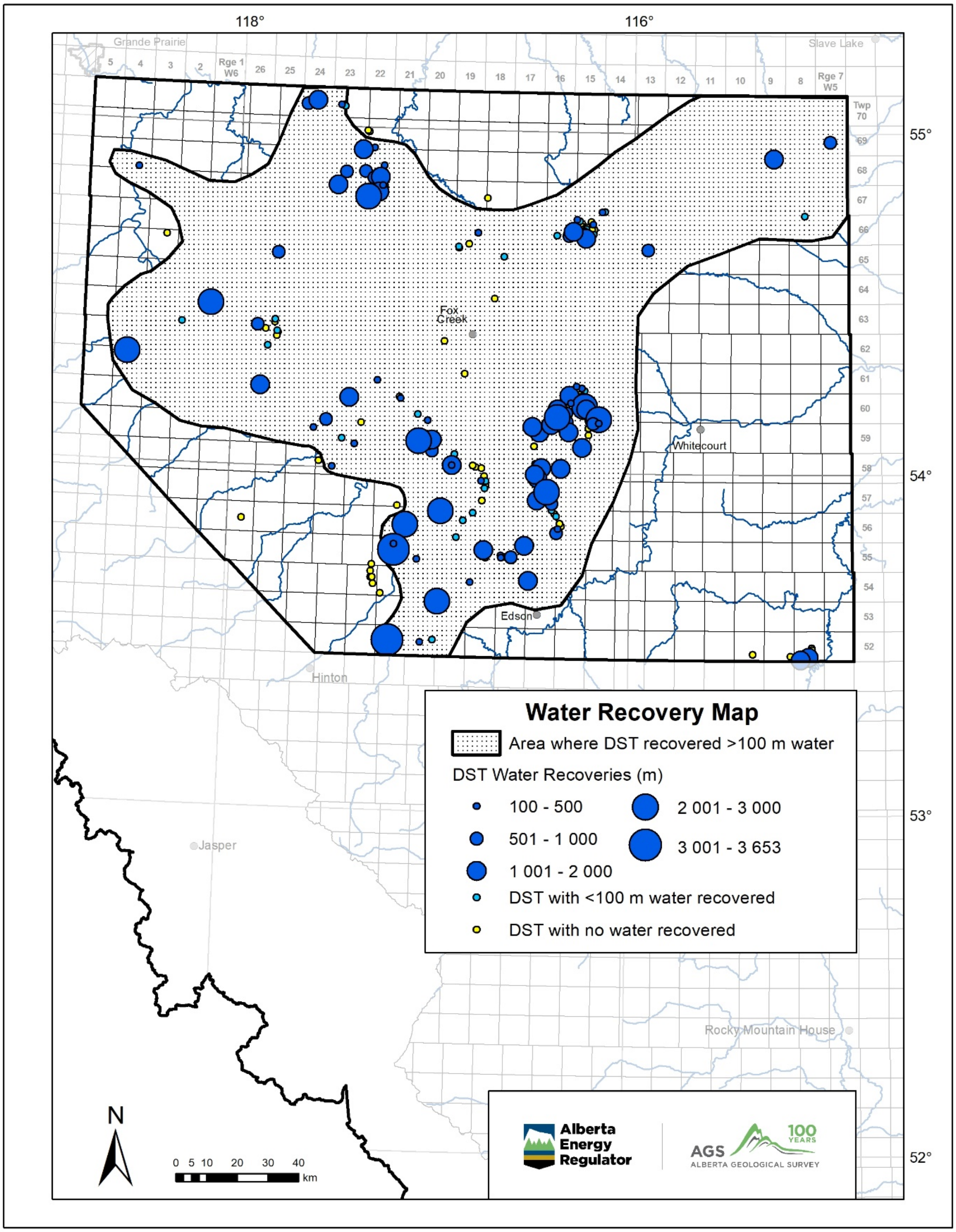

Figure 47. Water recoveries from drillstem tests (DSTs) in the Nisku aquifer, west-central Alberta study area.

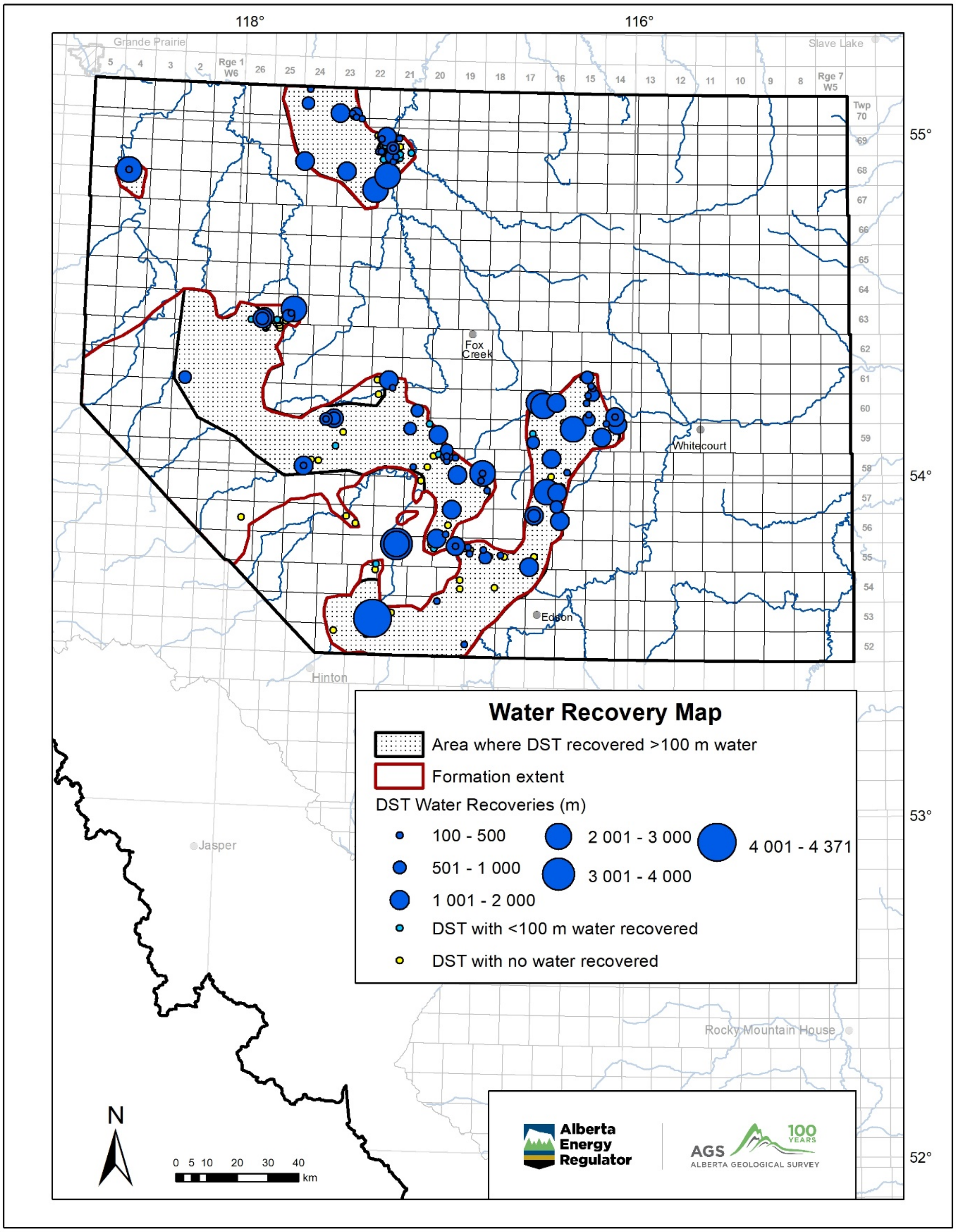

Figure 48. Water recoveries from drillstem tests (DSTs) in the Leduc aquifer, west-central Alberta study area.

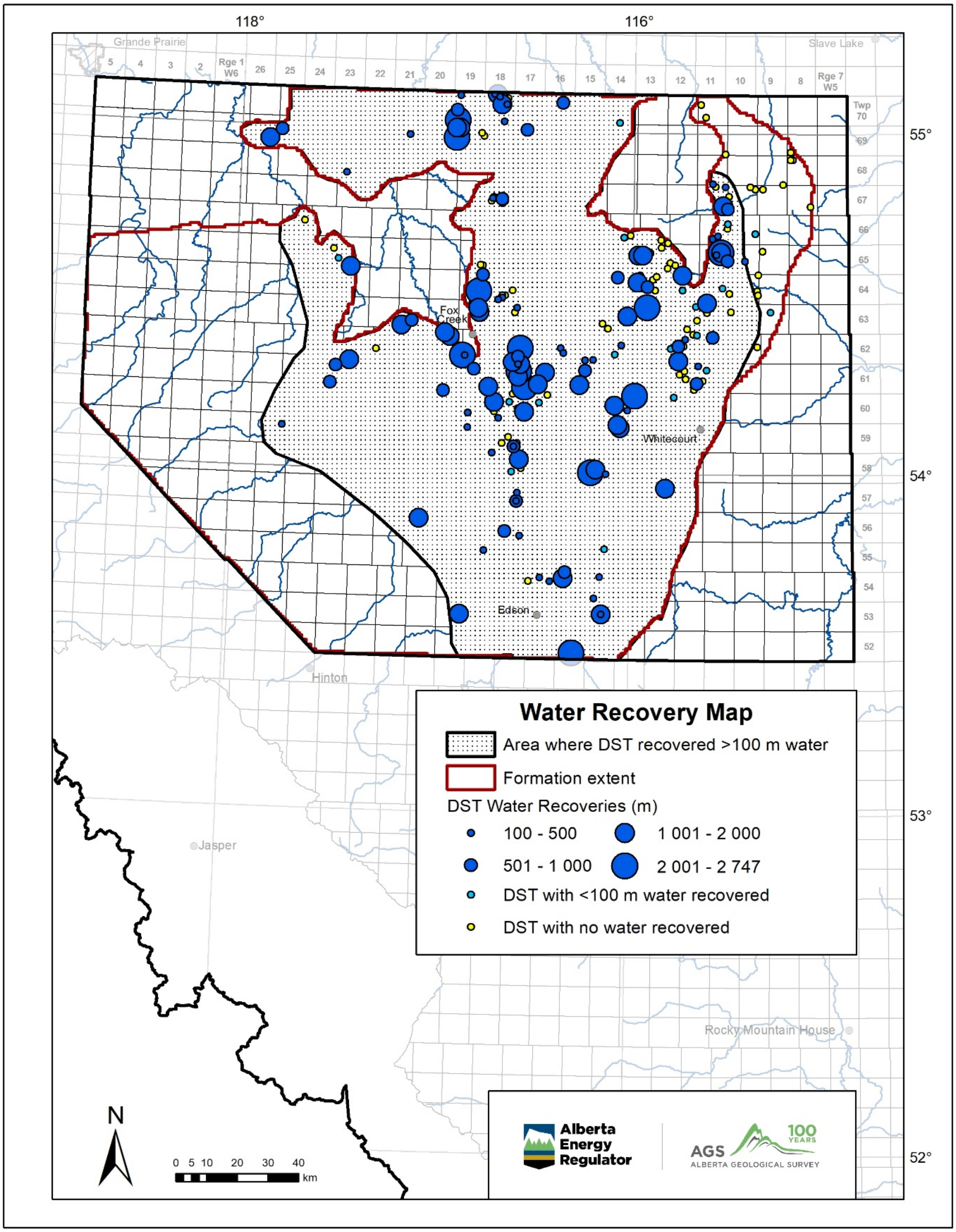

Figure 49. Water recoveries from drillstem tests (DSTs) in the Swan Hills aquifer, west-central Alberta study area.

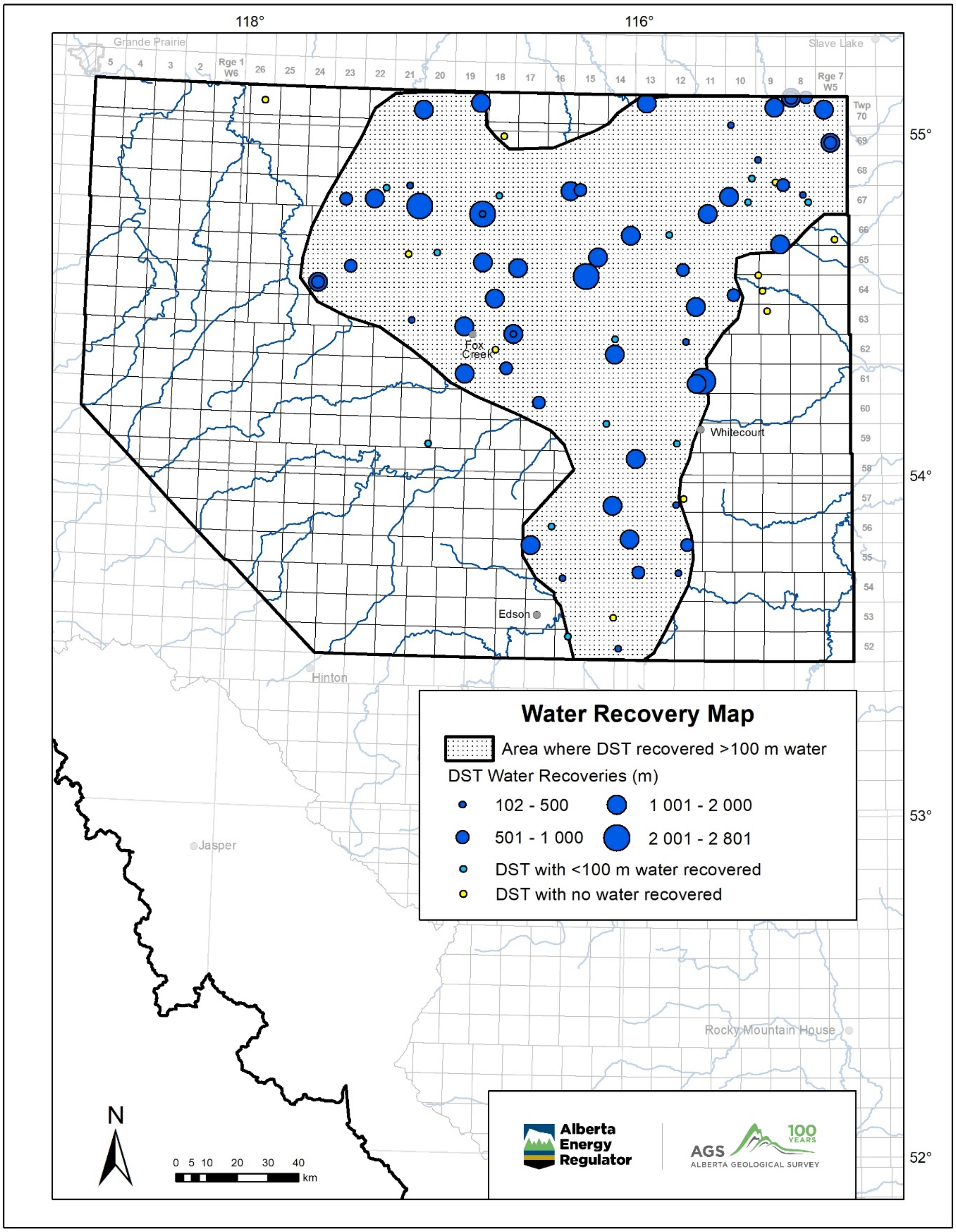

Figure 50. Water recoveries from drillstem tests (DSTs) in the Elk Point aquifer, west-central Alberta study area.

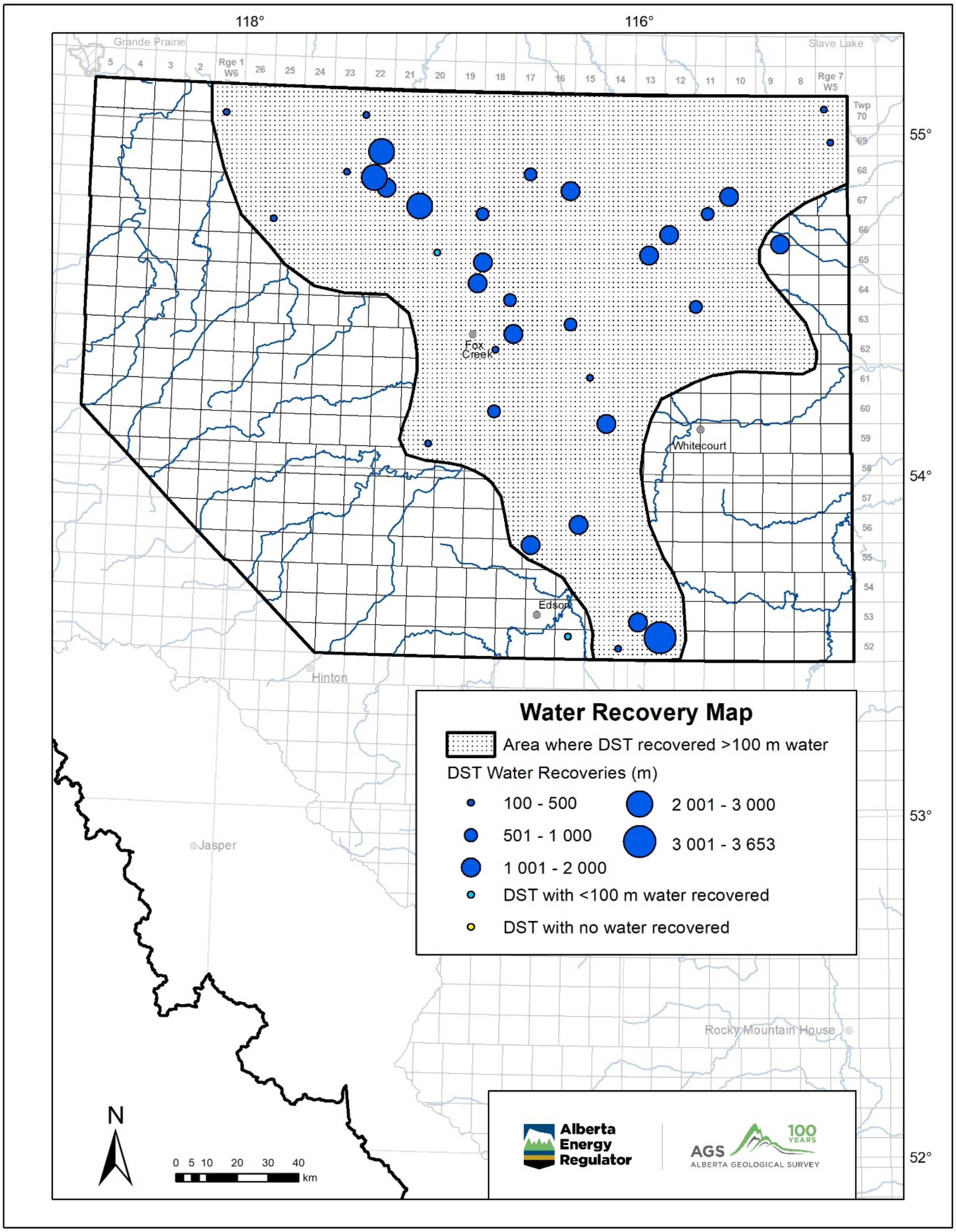

Figure 51. Water recoveries from drillstem tests (DSTs) in the Cambrian aquifer, west-central Alberta study area.

1.2 Hydraulic Head Maps

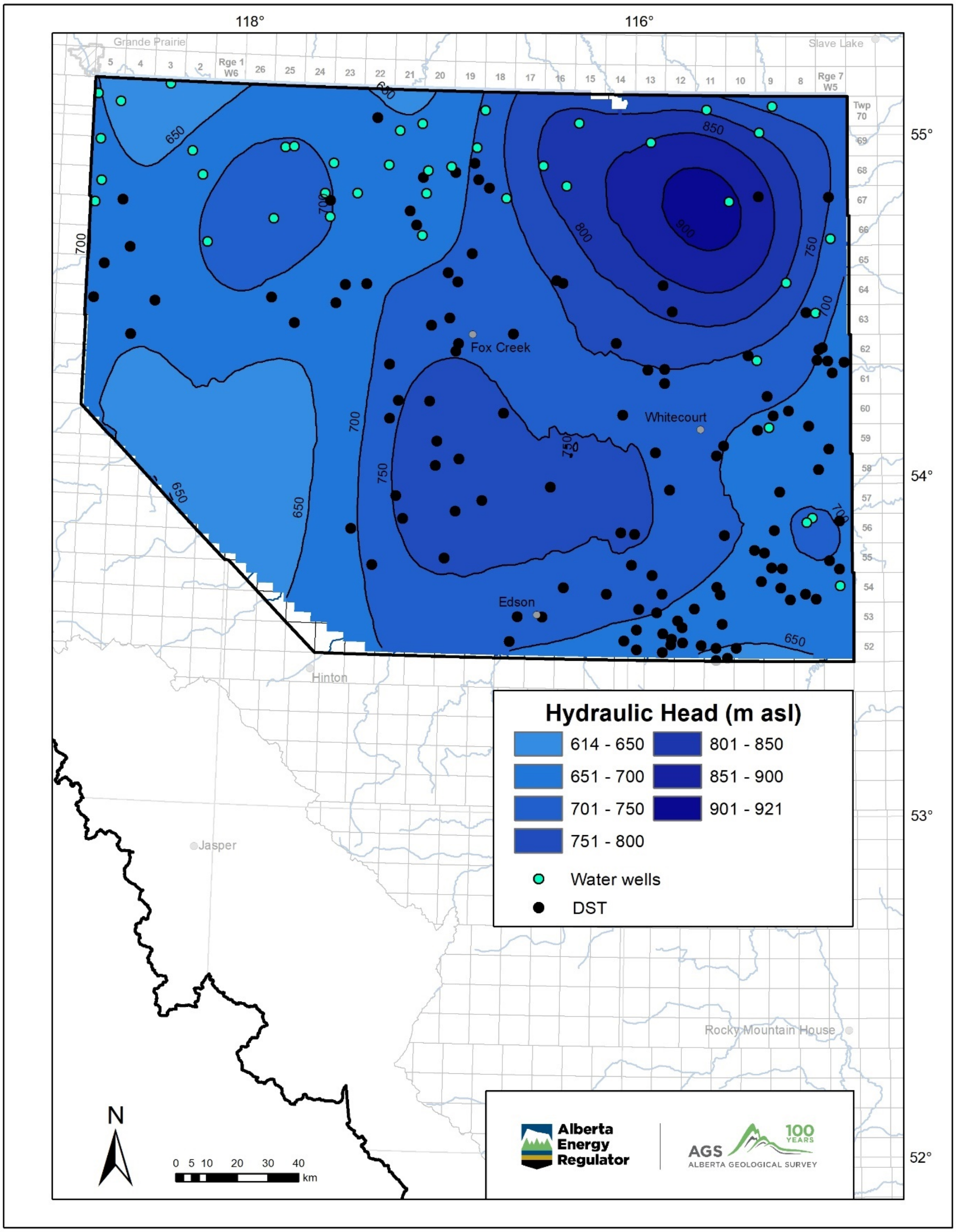

Figure 52. Hydraulic head distribution in the Wapiti aquifer, west-central Alberta study area (extracted from Singh and Nakevska, 2017). Abbreviation: DST, drillstem test.

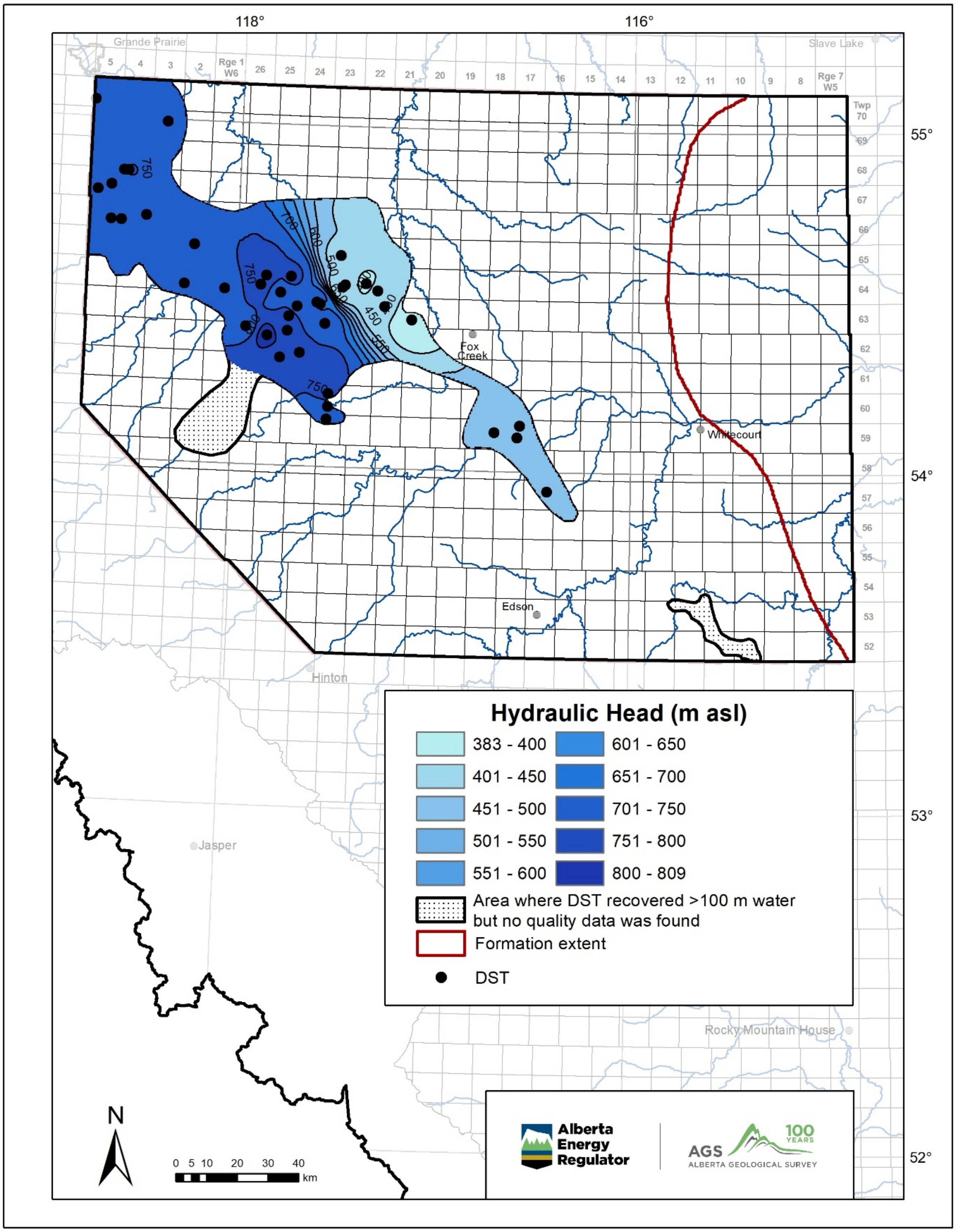

Figure 53. Hydraulic head distribution in the Cardium aquifer, west-central Alberta study area. Abbreviation: DST, drillstem test.

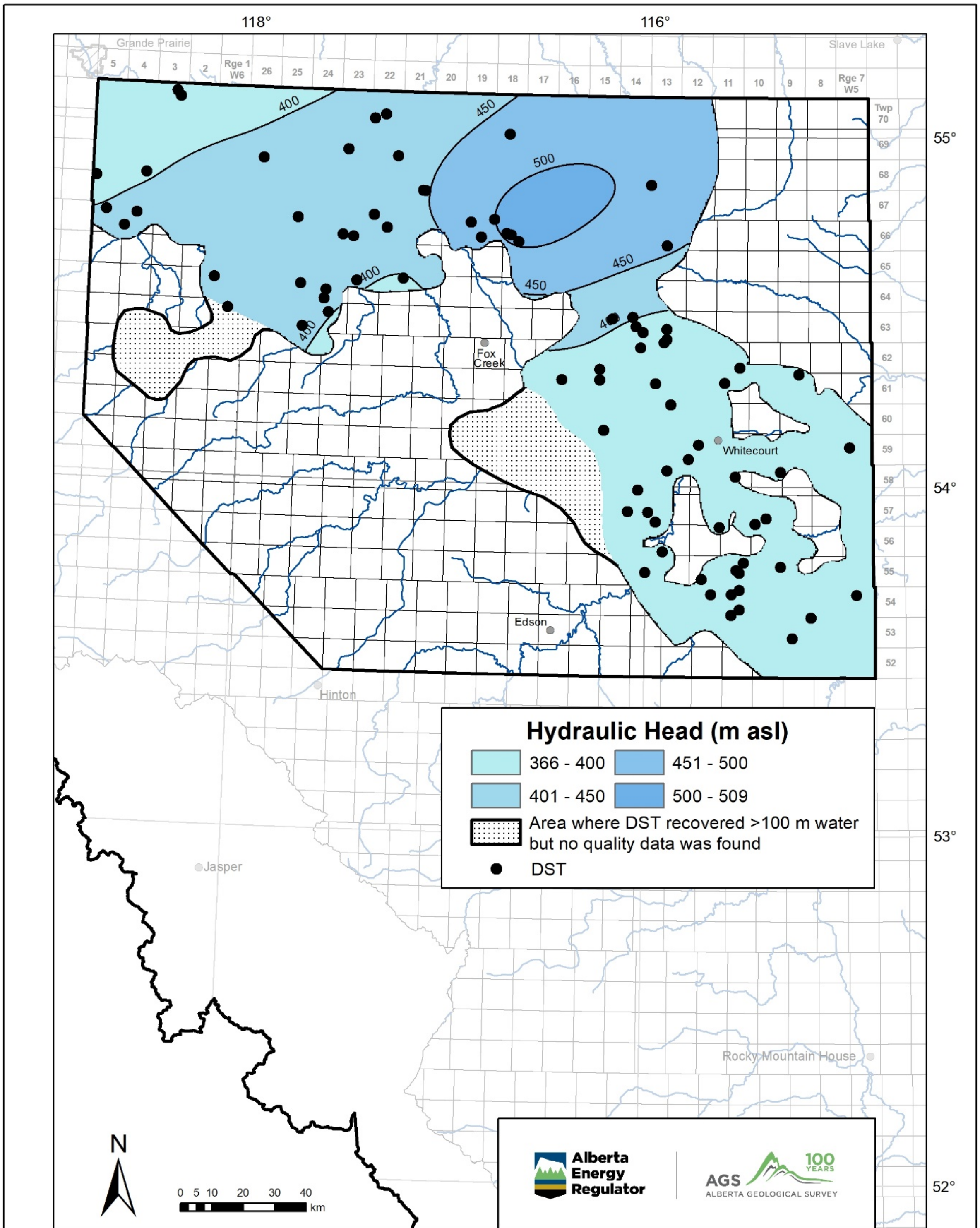

Figure 54. Hydraulic head distribution in the Viking aquifer, west-central Alberta study area. Abbreviation: DST, drillstem test.

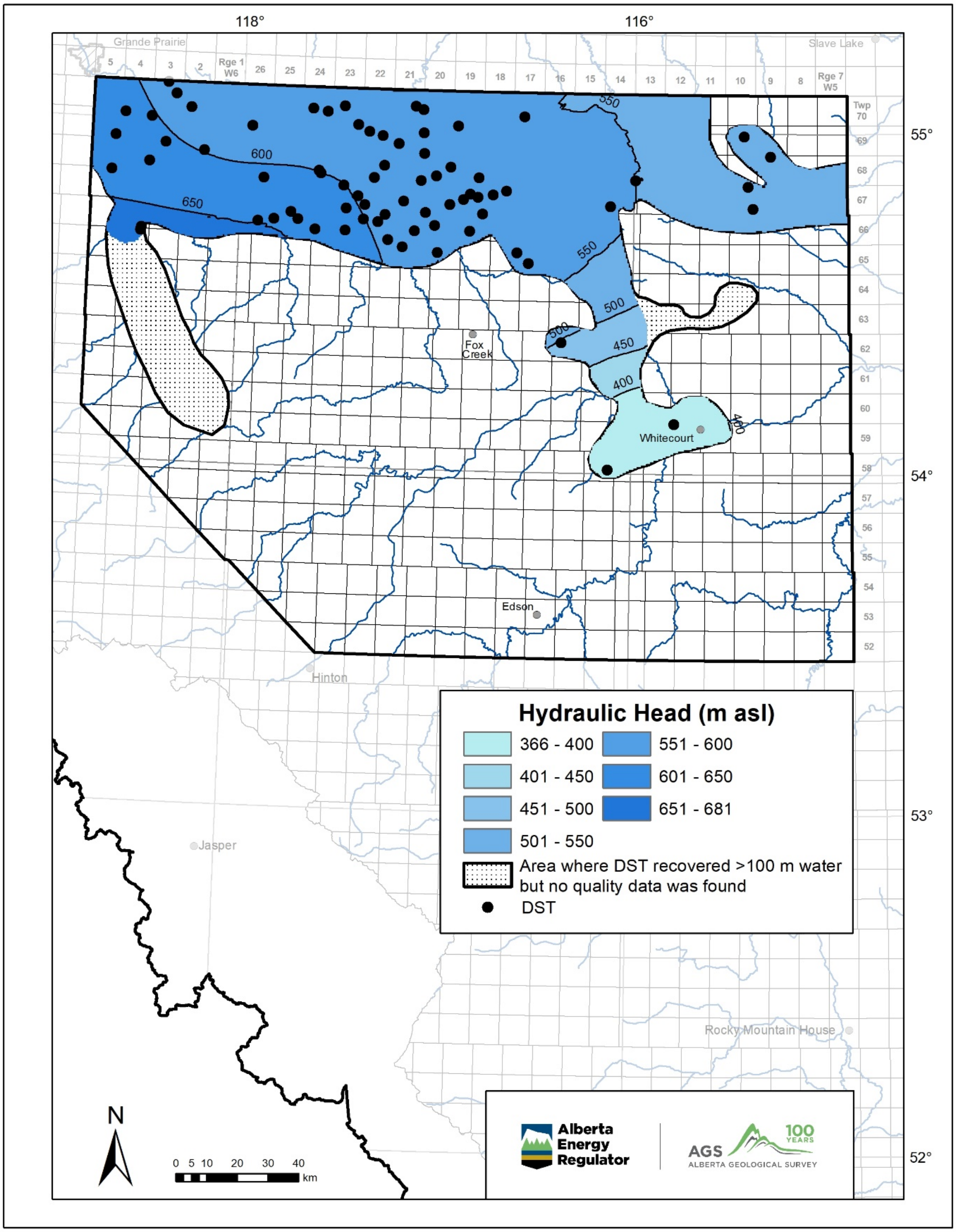

Figure 55. Hydraulic head distribution in the Spirit River aquifer, west-central Alberta study area. Abbreviation: DST, drillstem test.

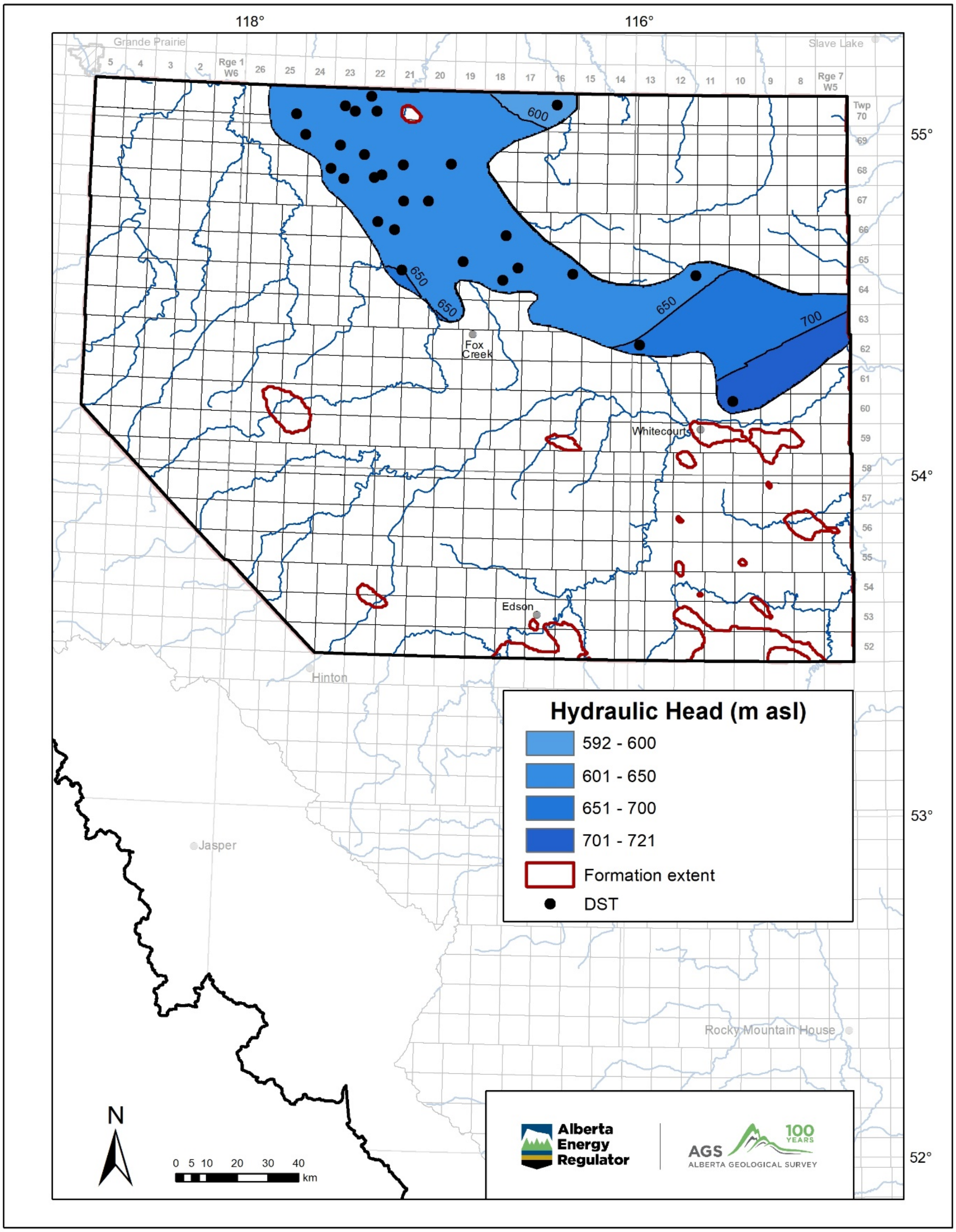

Figure 56. Hydraulic head distribution in the Bluesky aquifer, west-central Alberta study area. Abbreviation: DST, drillstem test.

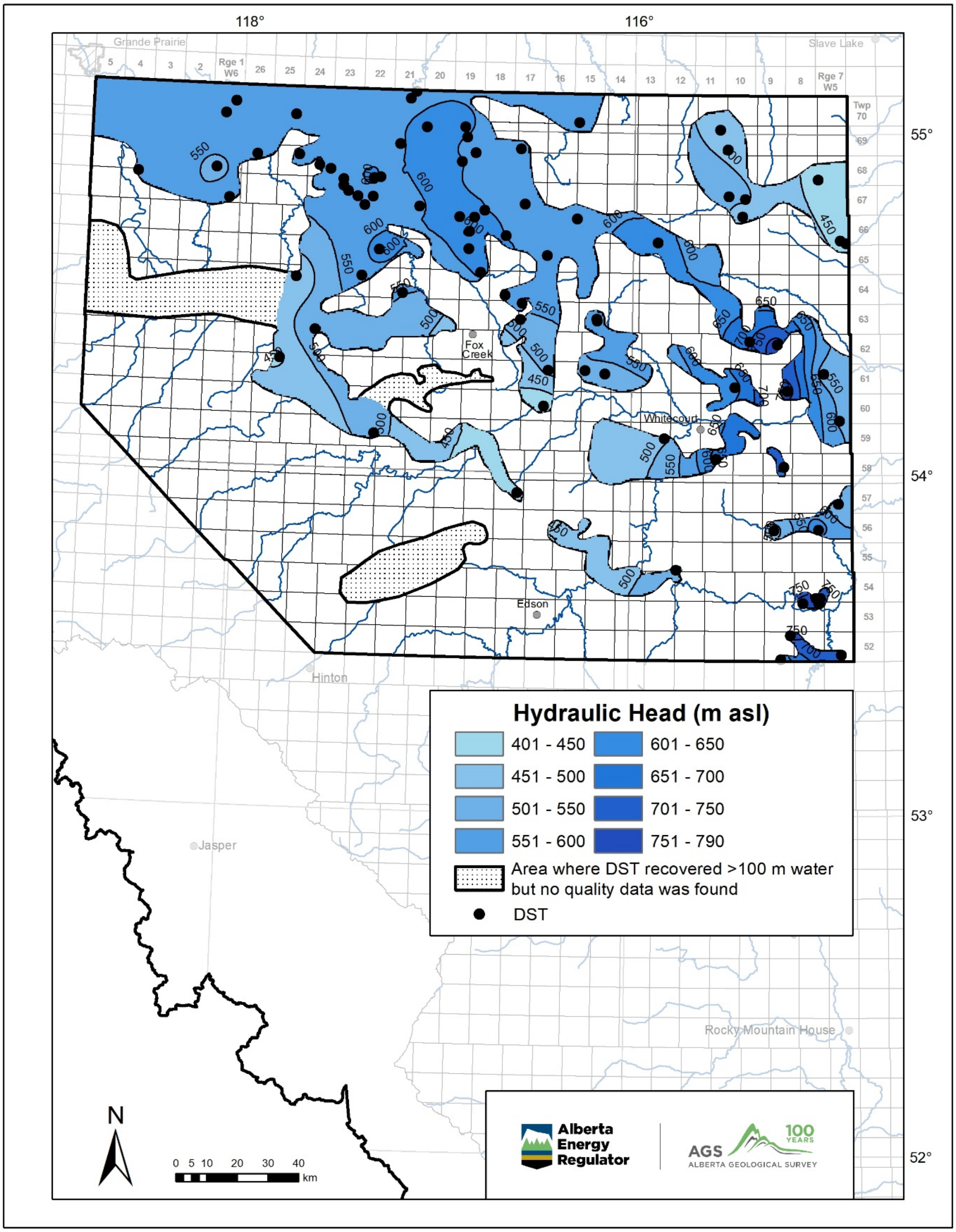

Figure 57. Hydraulic head distribution in the Gething aquifer, west-central Alberta study area. Abbreviation: DST, drillstem test.

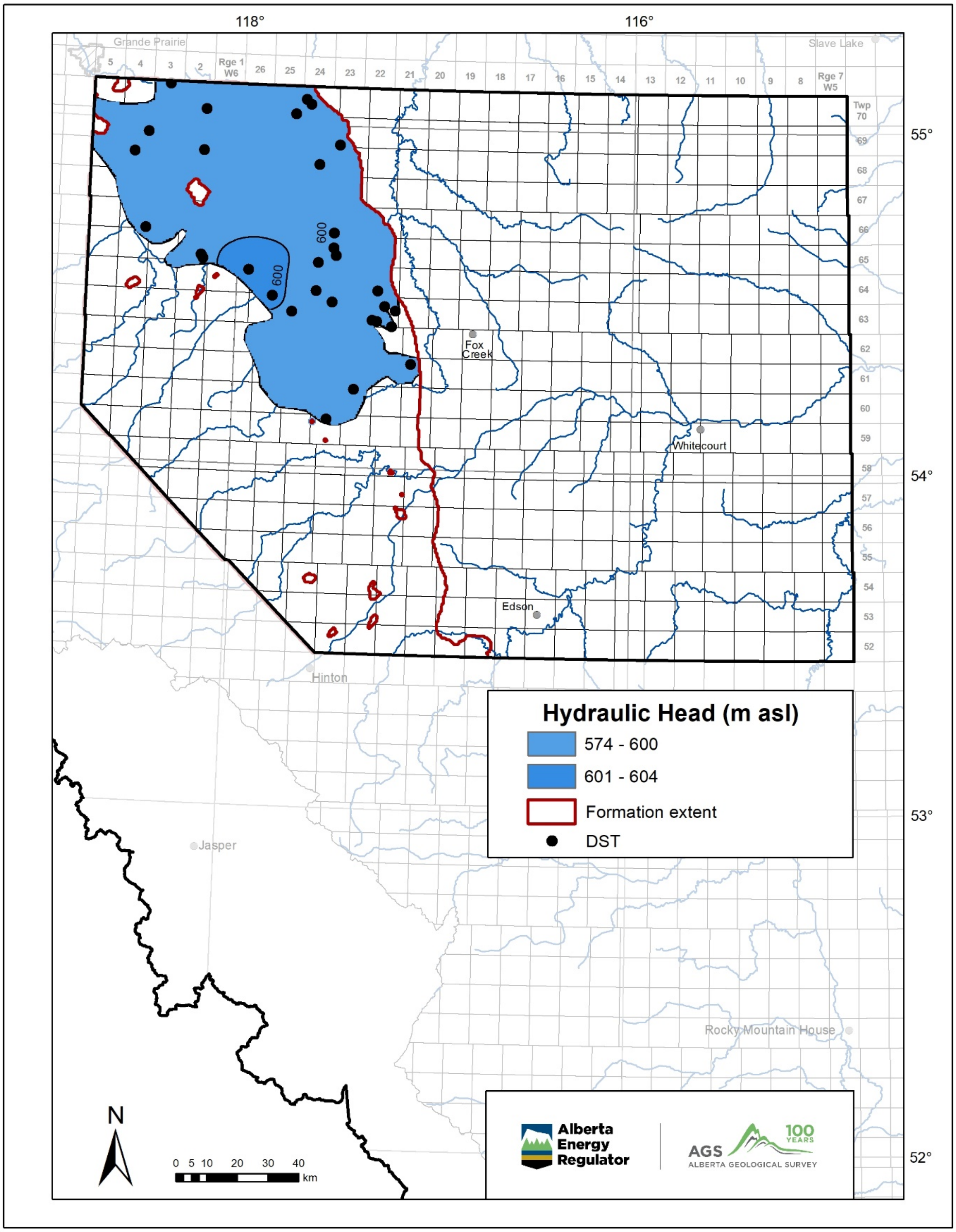

Figure 58. Hydraulic head distribution in the Cadomin aquifer, west-central Alberta study area. Abbreviation: DST, drillstem test.

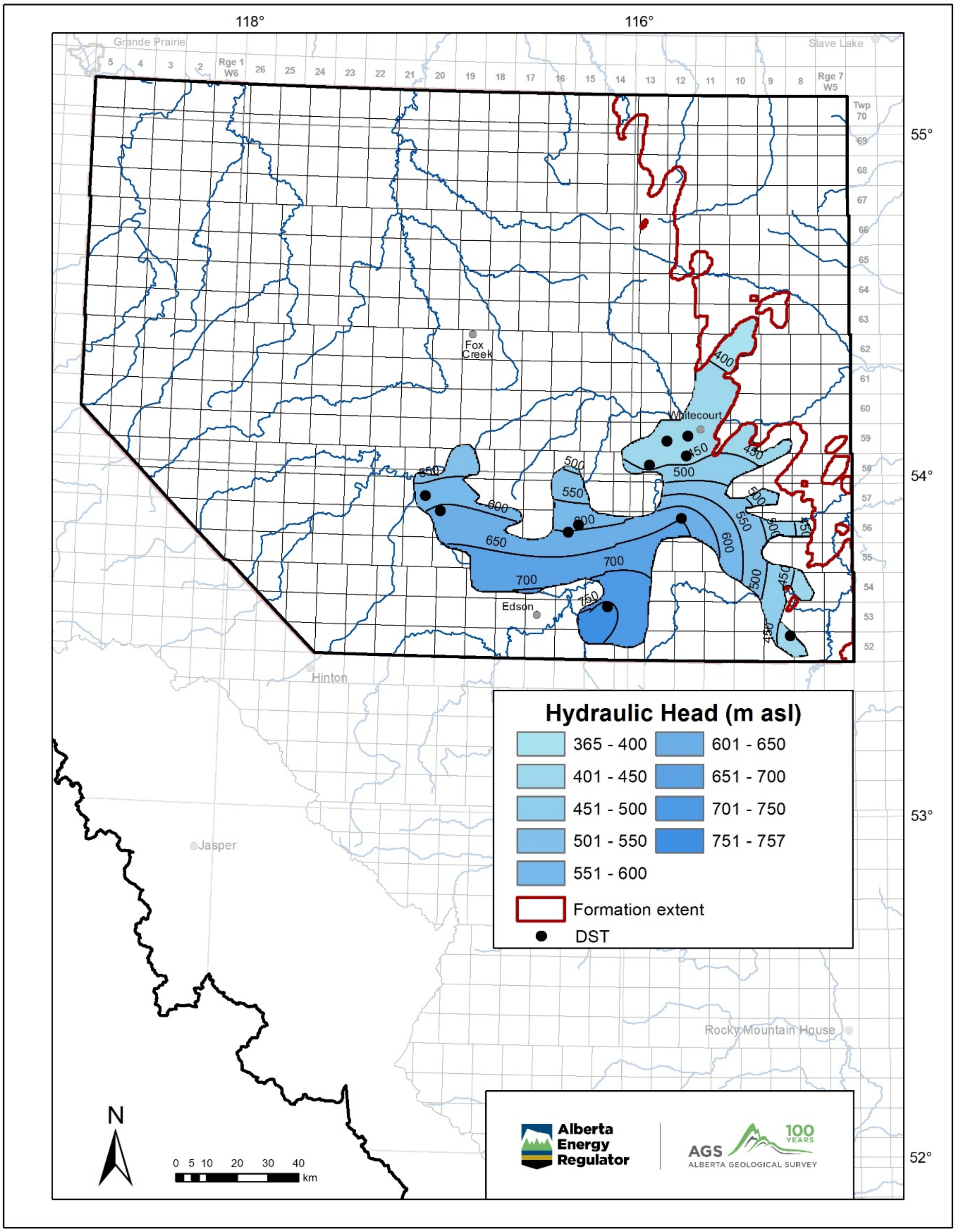

Figure 59. Hydraulic head distribution in the Nordegg aquifer, west-central Alberta study area. Abbreviation: DST, drillstem test.

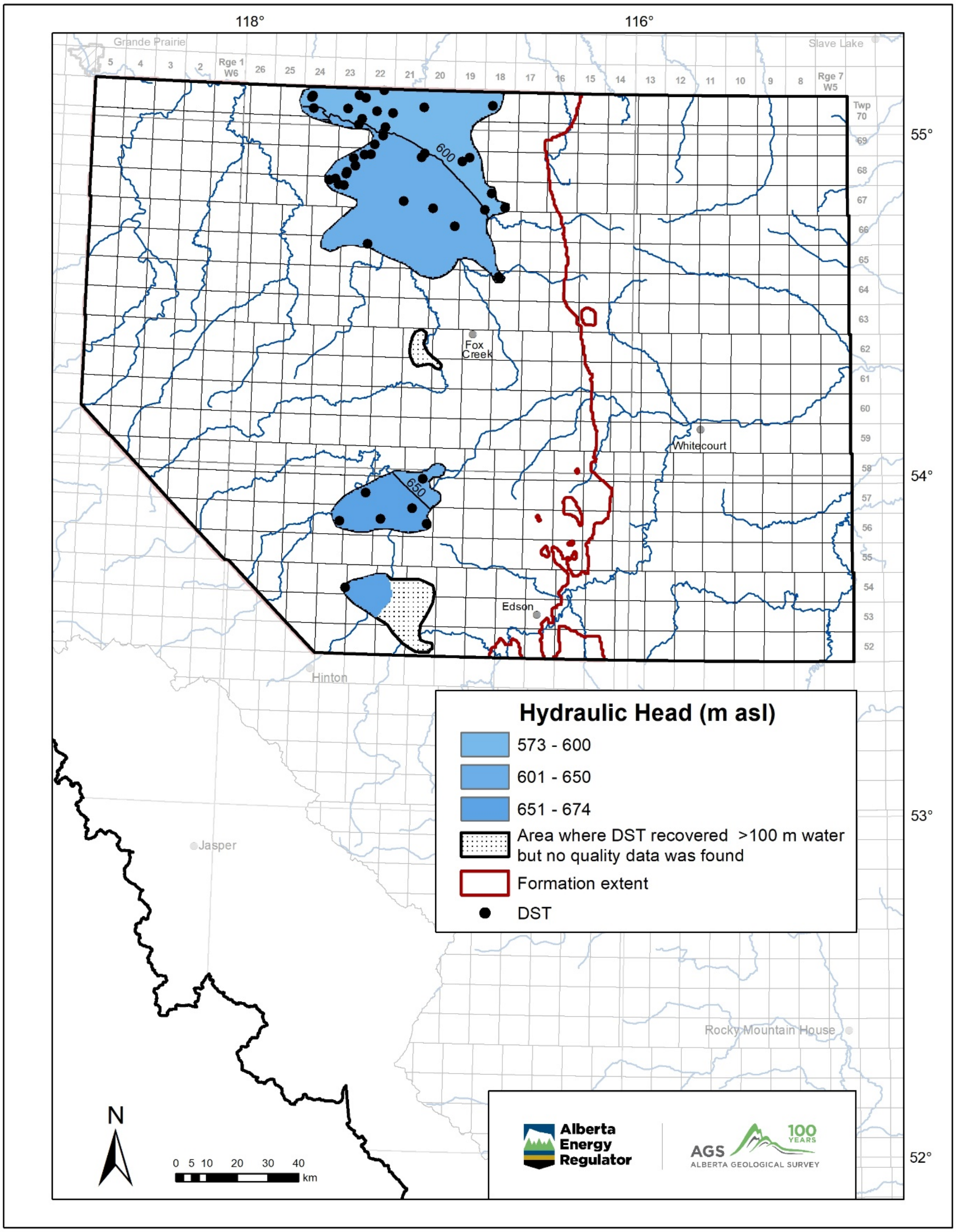

Figure 60. Hydraulic head distribution in the Montney aquifer, west-central Alberta study area. Abbreviation: DST, drillstem test.

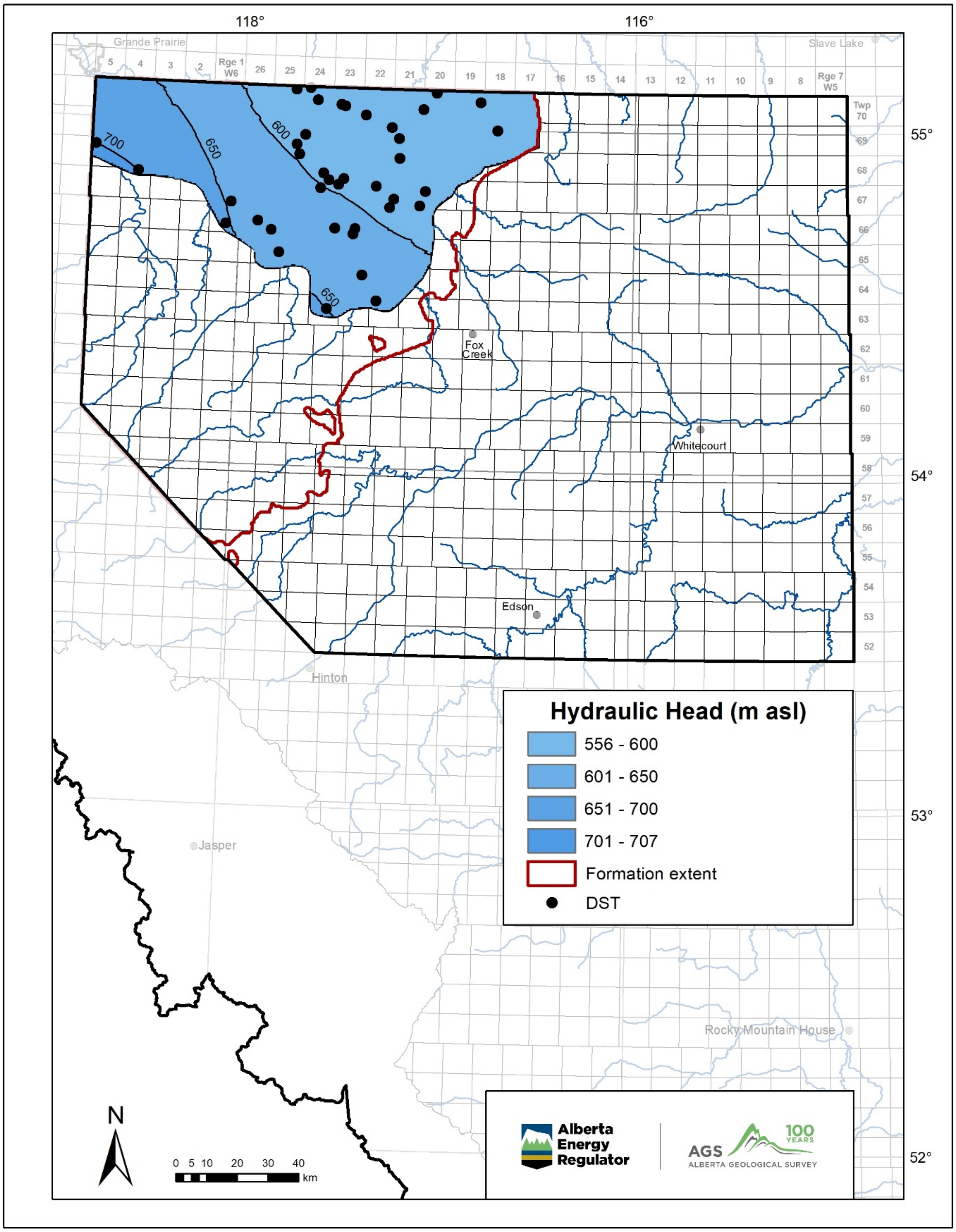

Figure 61. Hydraulic head distribution in the Belloy aquifer, west-central Alberta study area. Abbreviation: DST, drillstem test.

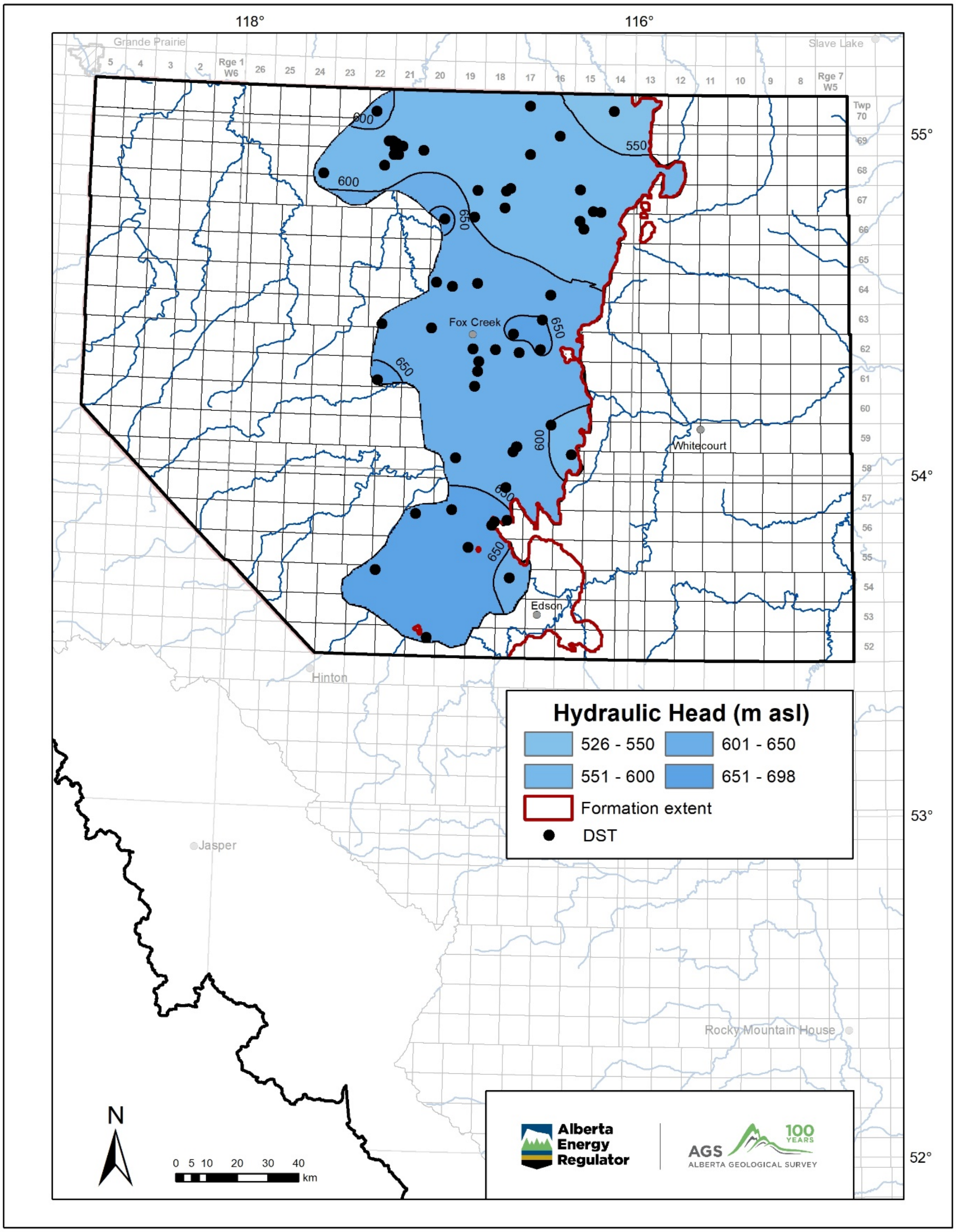

Figure 62. Hydraulic head distribution in the Debolt aquifer, west-central Alberta study area. Abbreviation: DST, drillstem test.

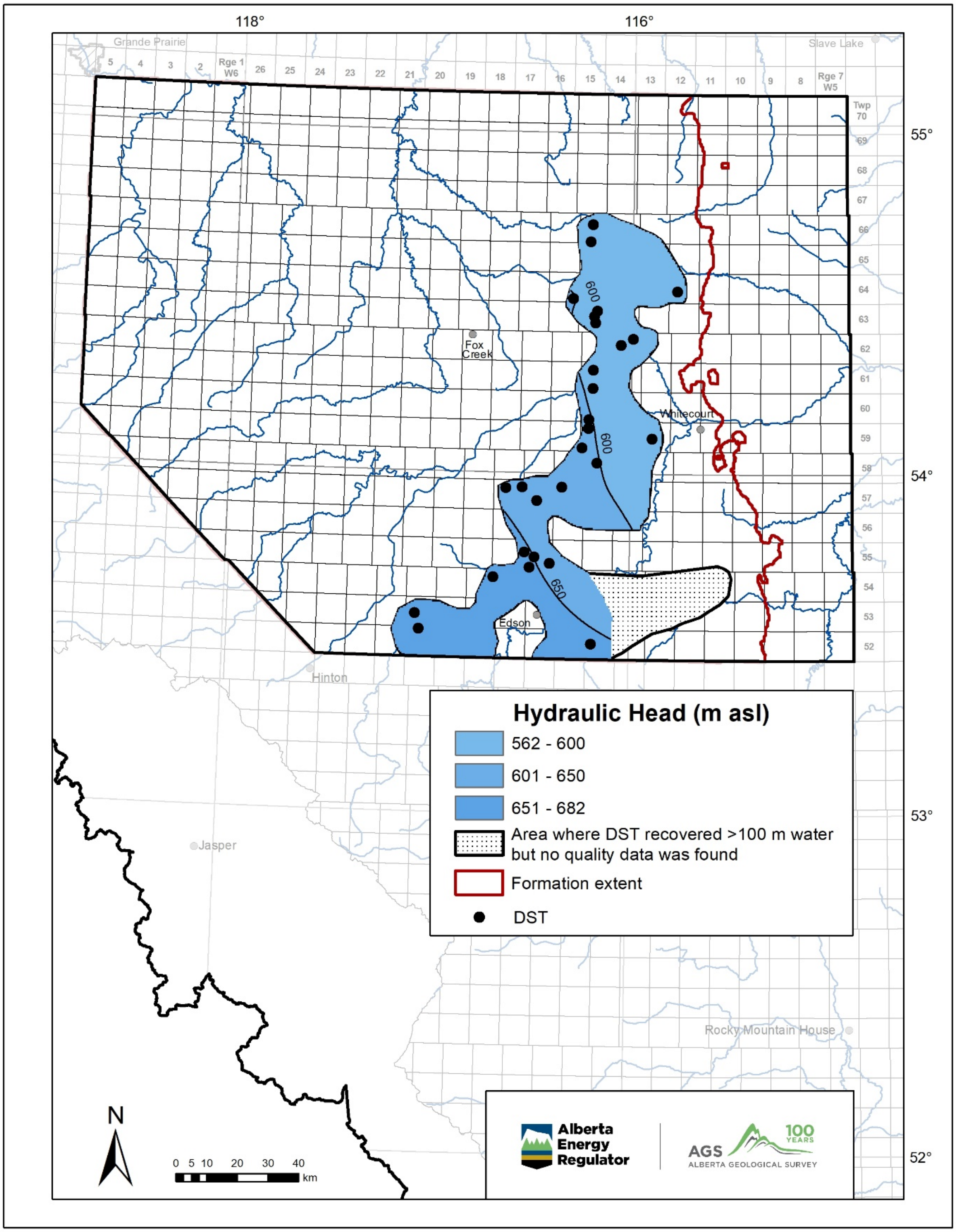

Figure 63. Hydraulic head distribution in the Shunda aquifer, west-central Alberta study area. Abbreviation: DST, drillstem test.

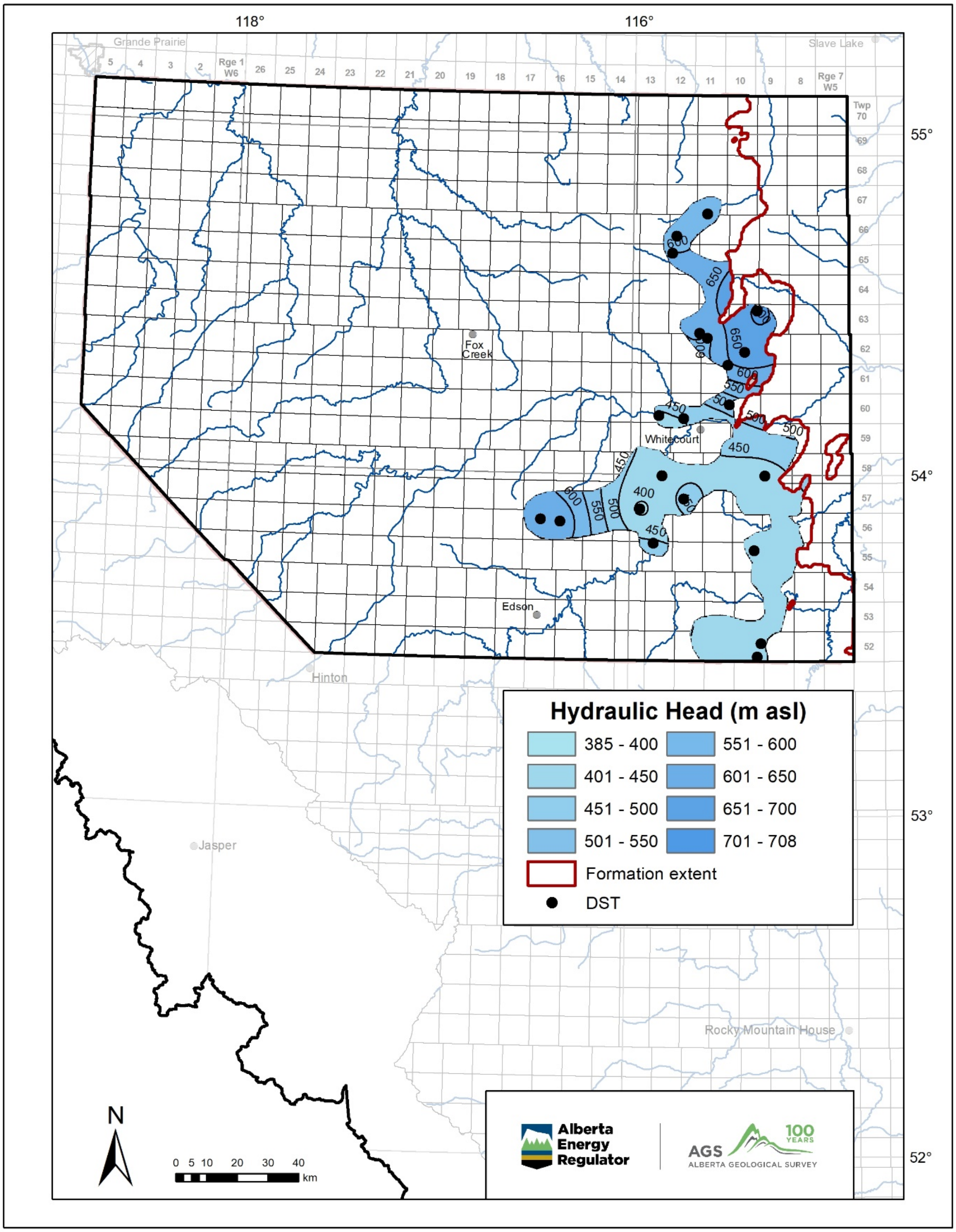

Figure 64. Hydraulic head distribution in the Pekisko aquifer, west-central Alberta study area. Abbreviation: DST, drillstem test.

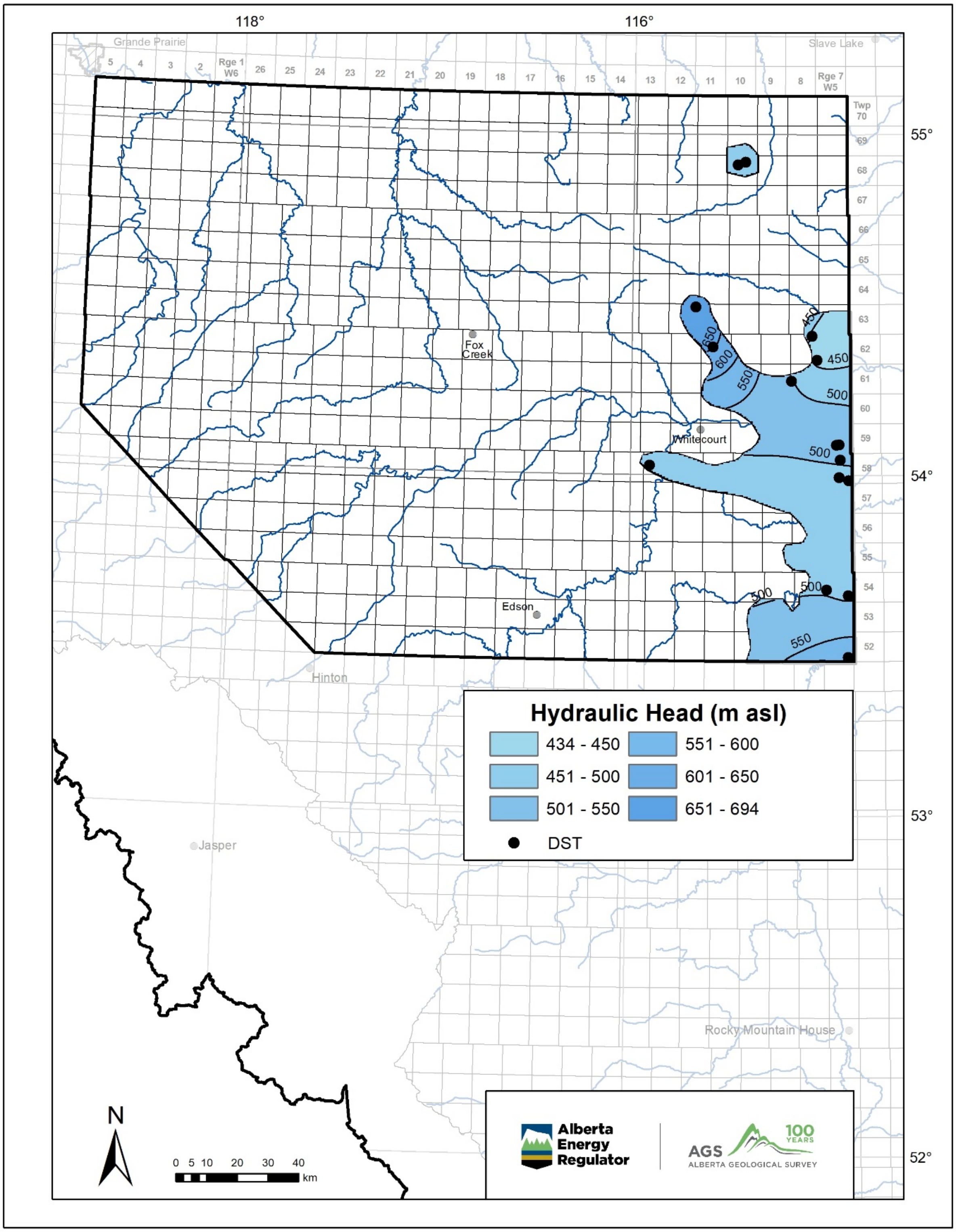

Figure 65. Hydraulic head distribution in the Banff aquifer, west-central Alberta study area. Abbreviation: DST, drillstem test.

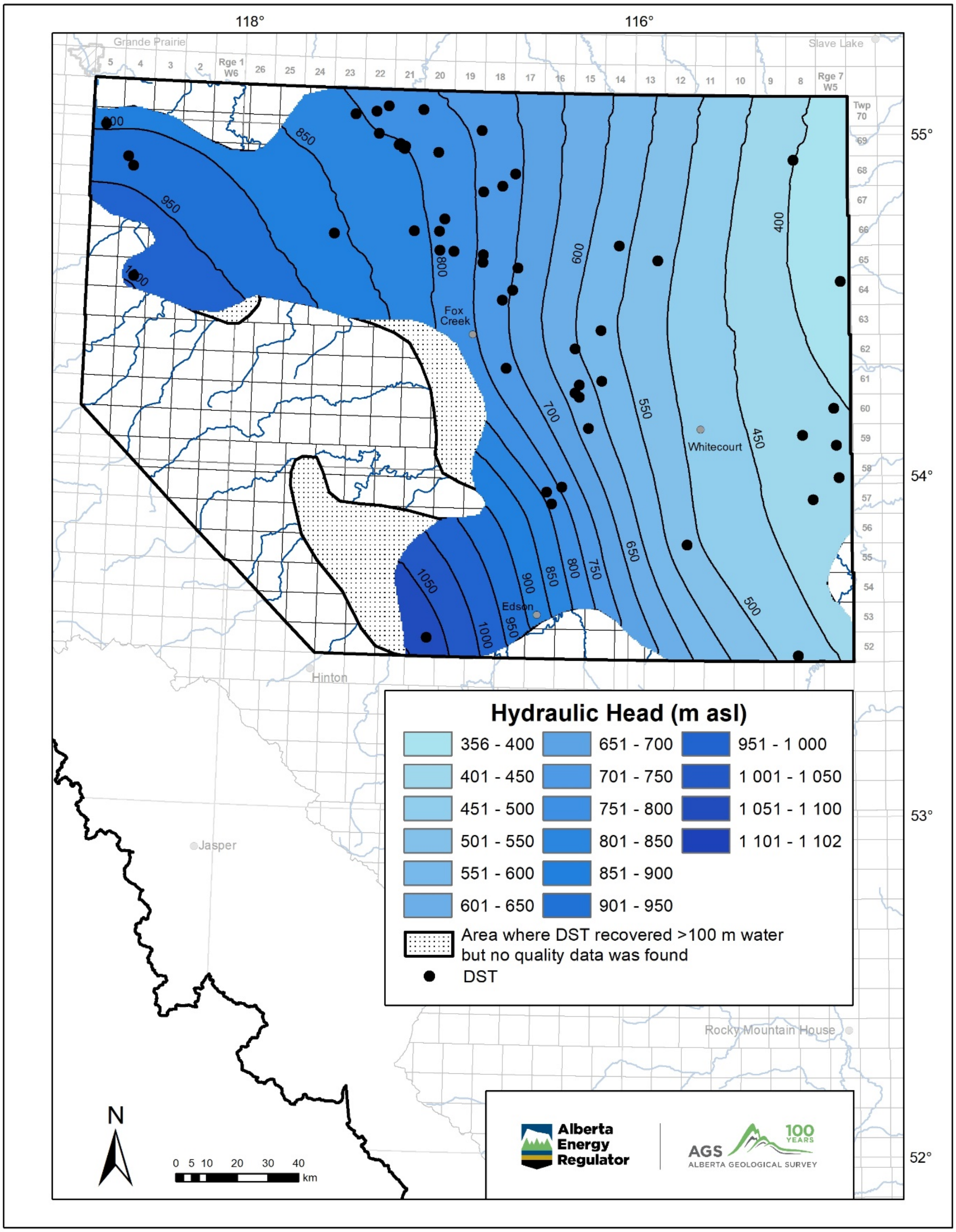

Figure 66. Hydraulic head distribution in the Wabamun aquifer, west-central Alberta study area. Abbreviation: DST, drillstem test.

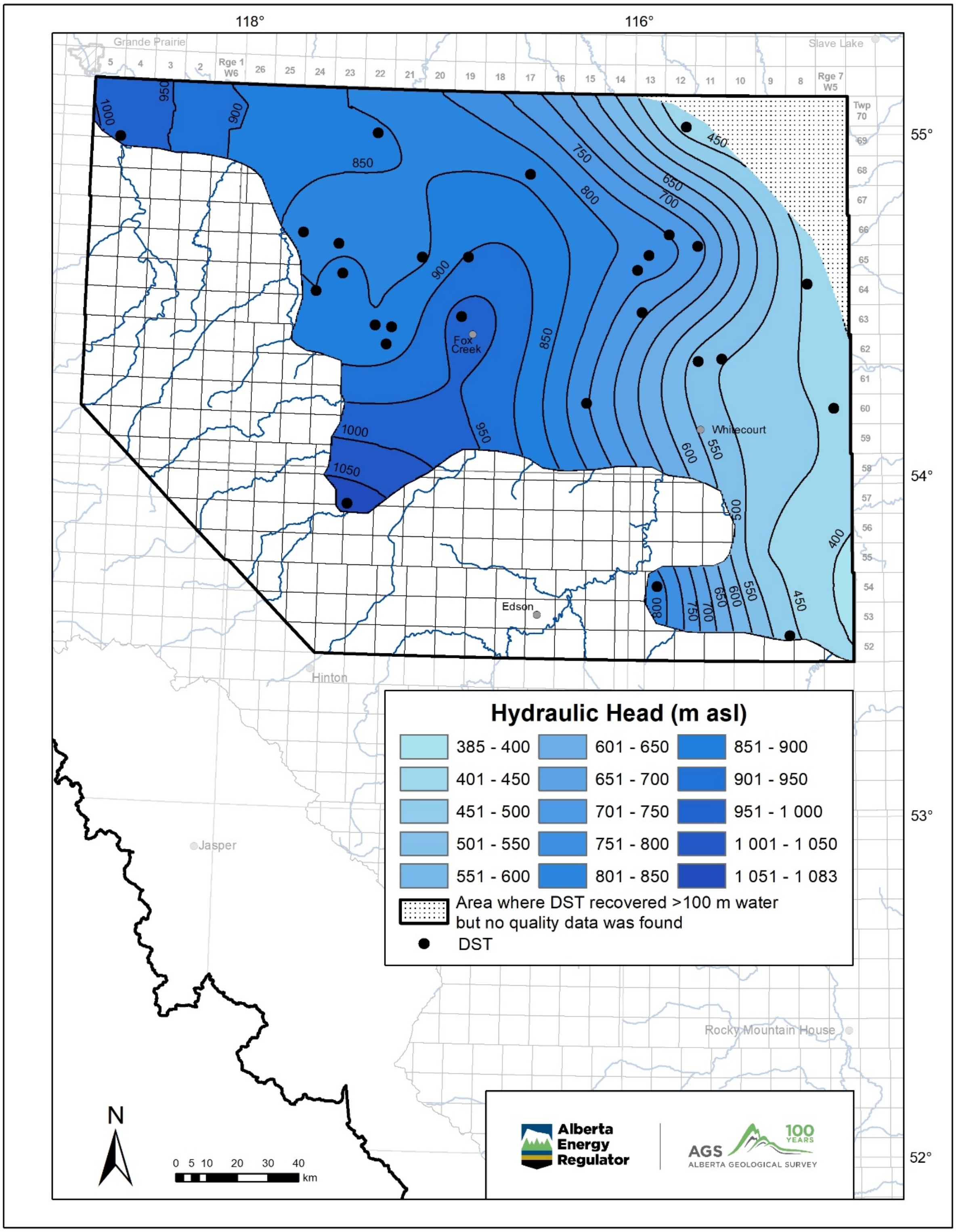

Figure 67. Hydraulic head distribution in the Blue Ridge aquifer, west-central Alberta study area. Abbreviation: DST, drillstem test.

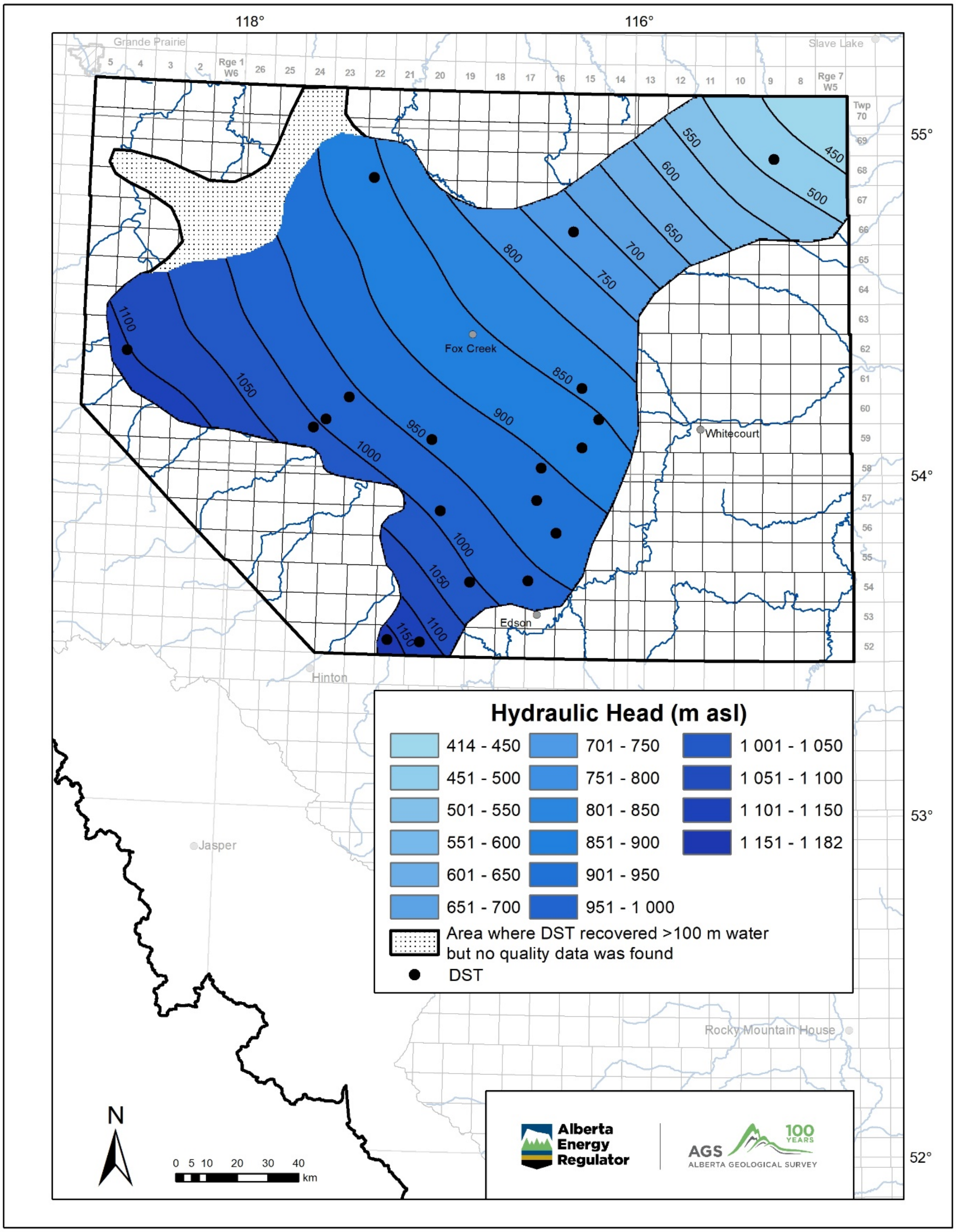

Figure 68. Hydraulic head distribution in the Nisku aquifer, west-central Alberta study area. Abbreviation: DST, drillstem test.

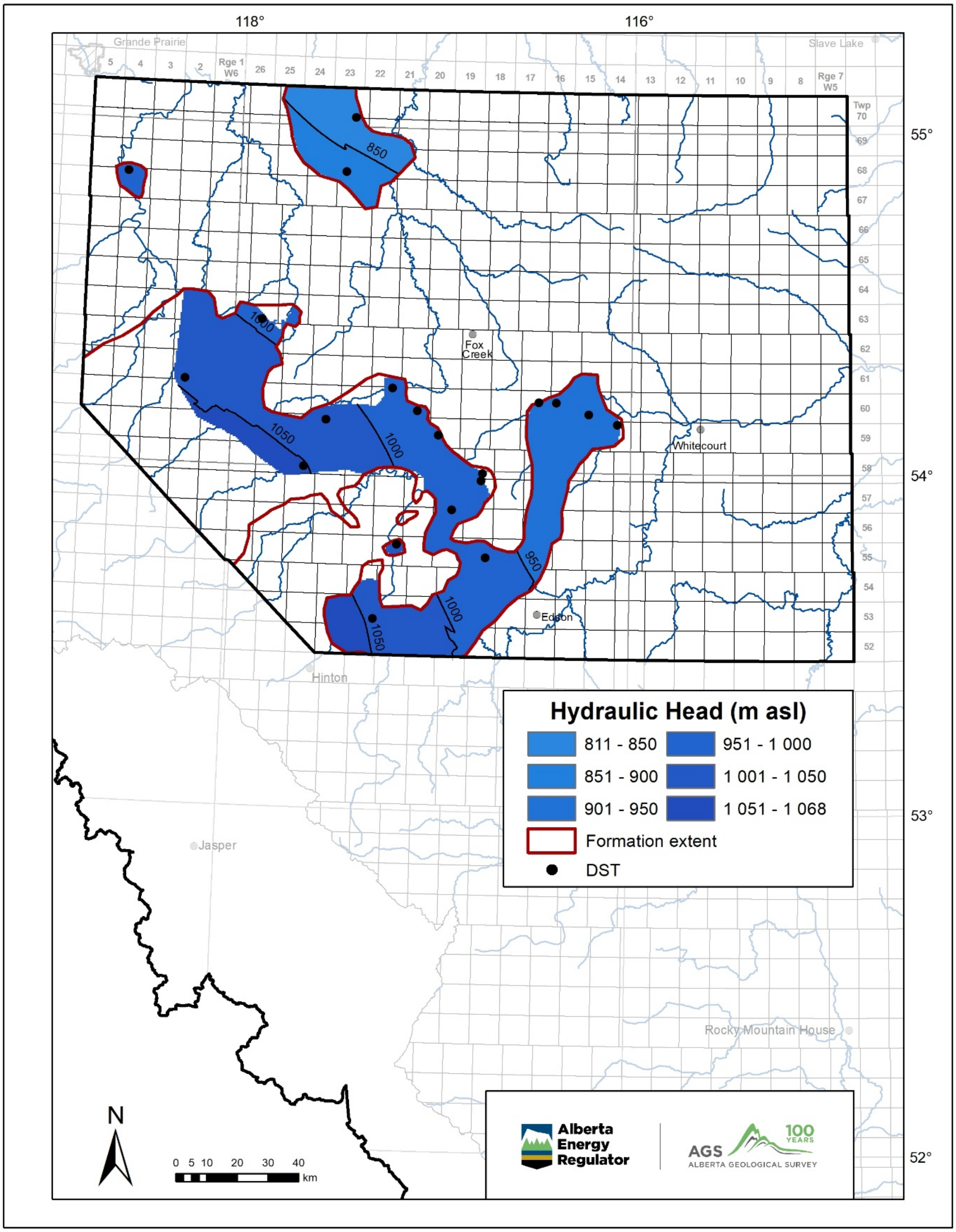

Figure 69. Hydraulic head distribution in the Leduc aquifer, west-central Alberta study area. Abbreviation: DST, drillstem test.

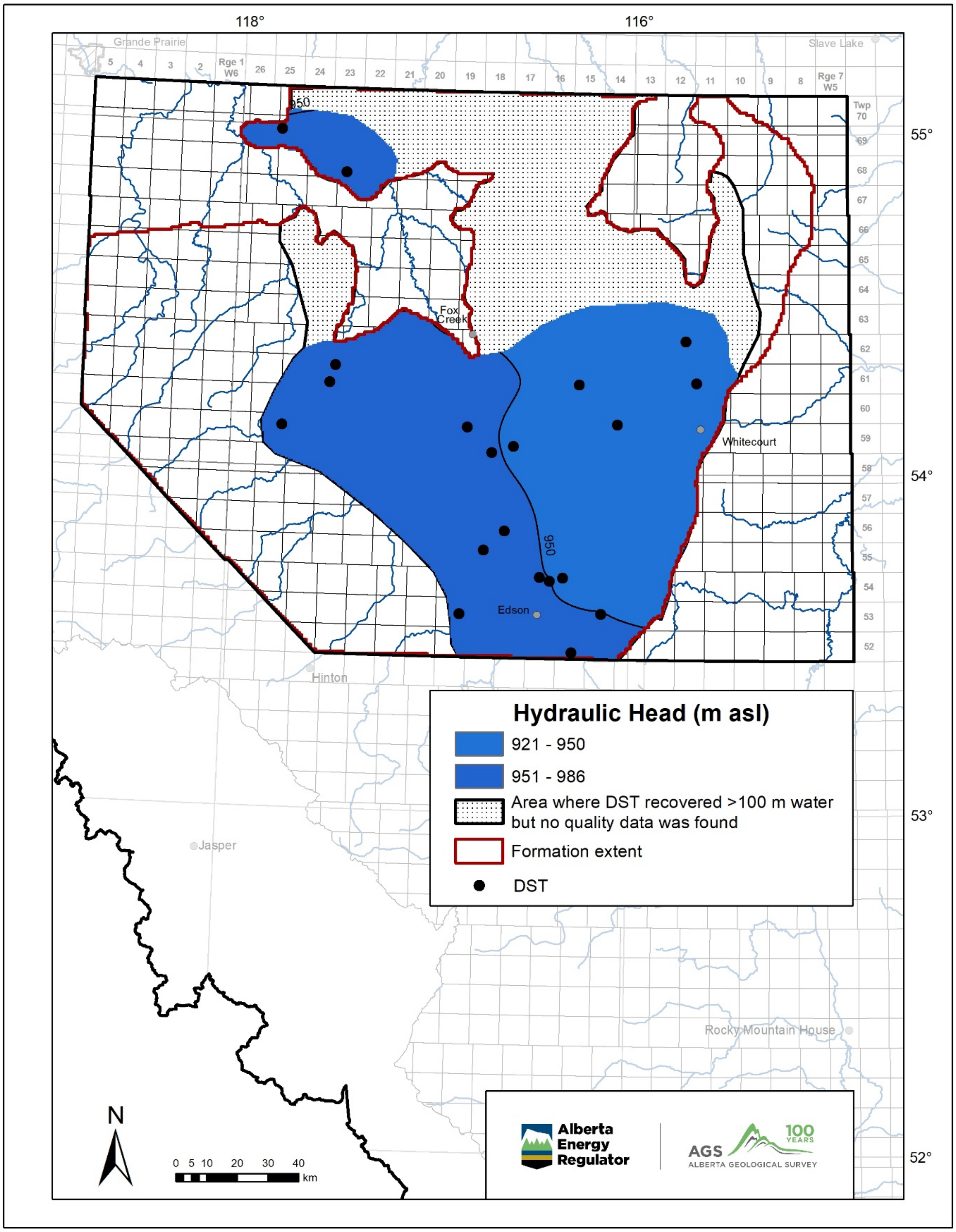

Figure 70. Hydraulic head distribution in the Swan Hills aquifer, west-central Alberta study area. Abbreviation: DST, drillstem test.

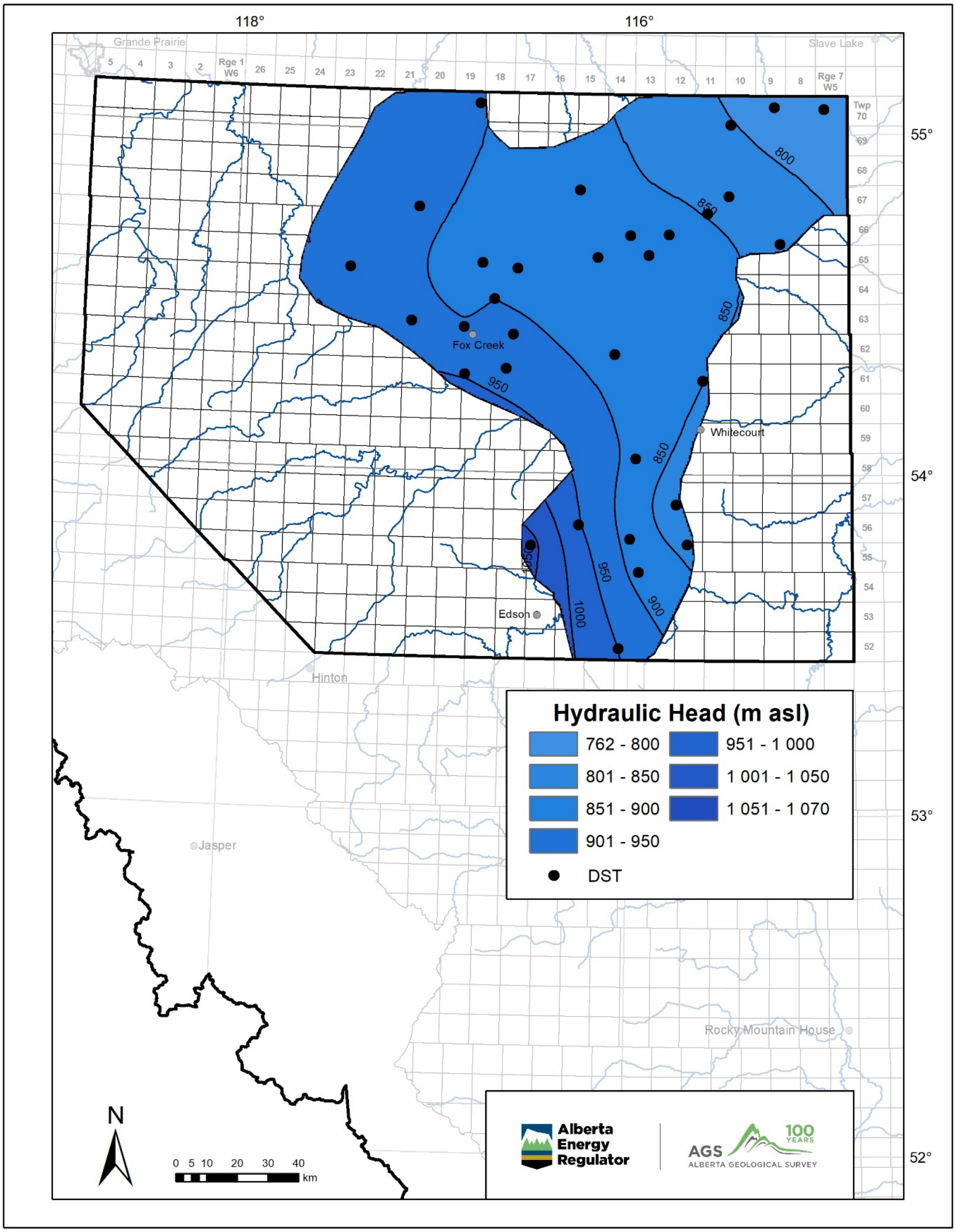

Figure 71. Hydraulic head distribution in the Elk Point aquifer, west-central Alberta study area. Abbreviation: DST, drillstem test.

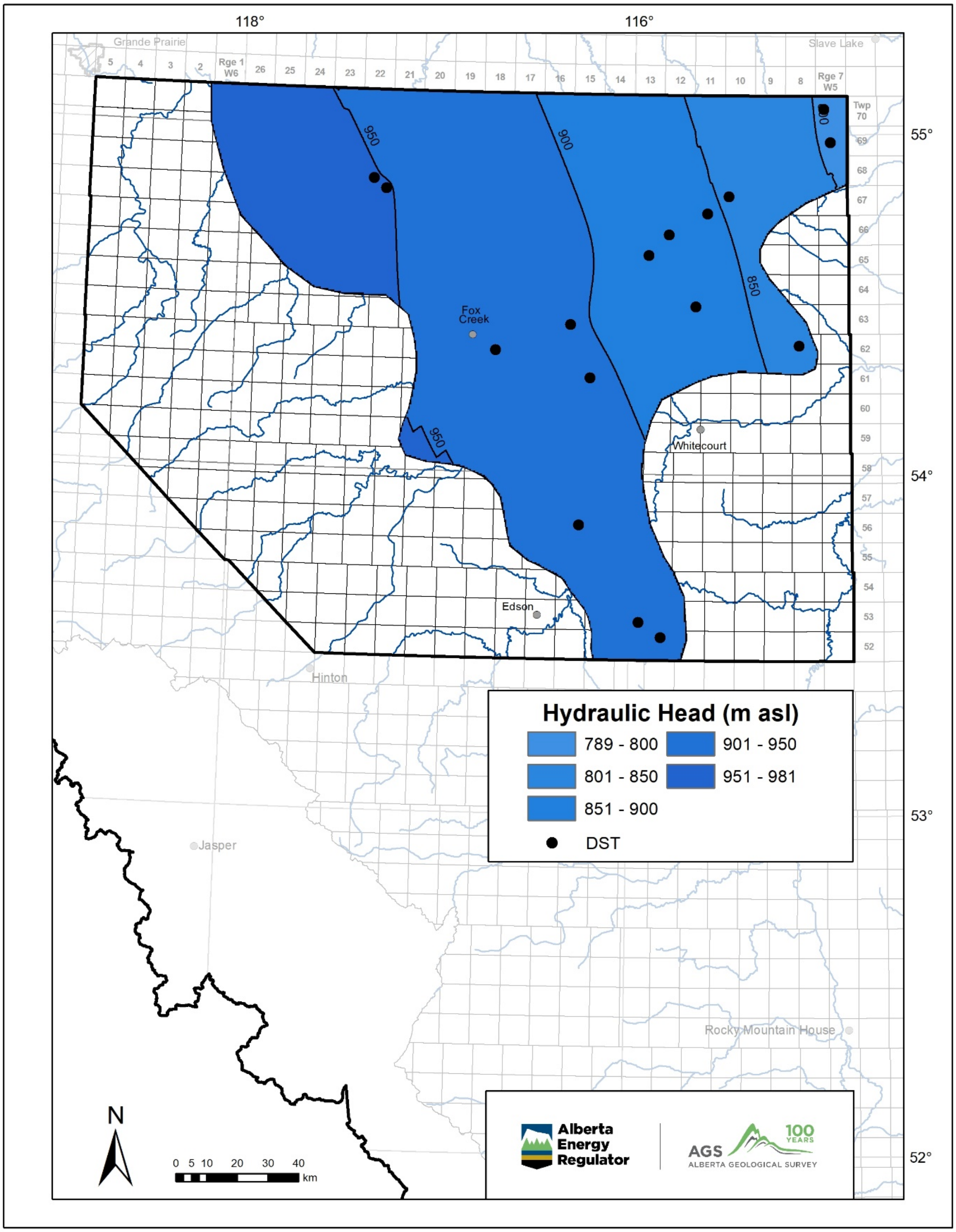

Figure 72. Hydraulic head distribution in the Cambrian aquifer, west-central Alberta study area. Abbreviation: DST, drillstem test.

1.3 Total Dissolved Solids Maps

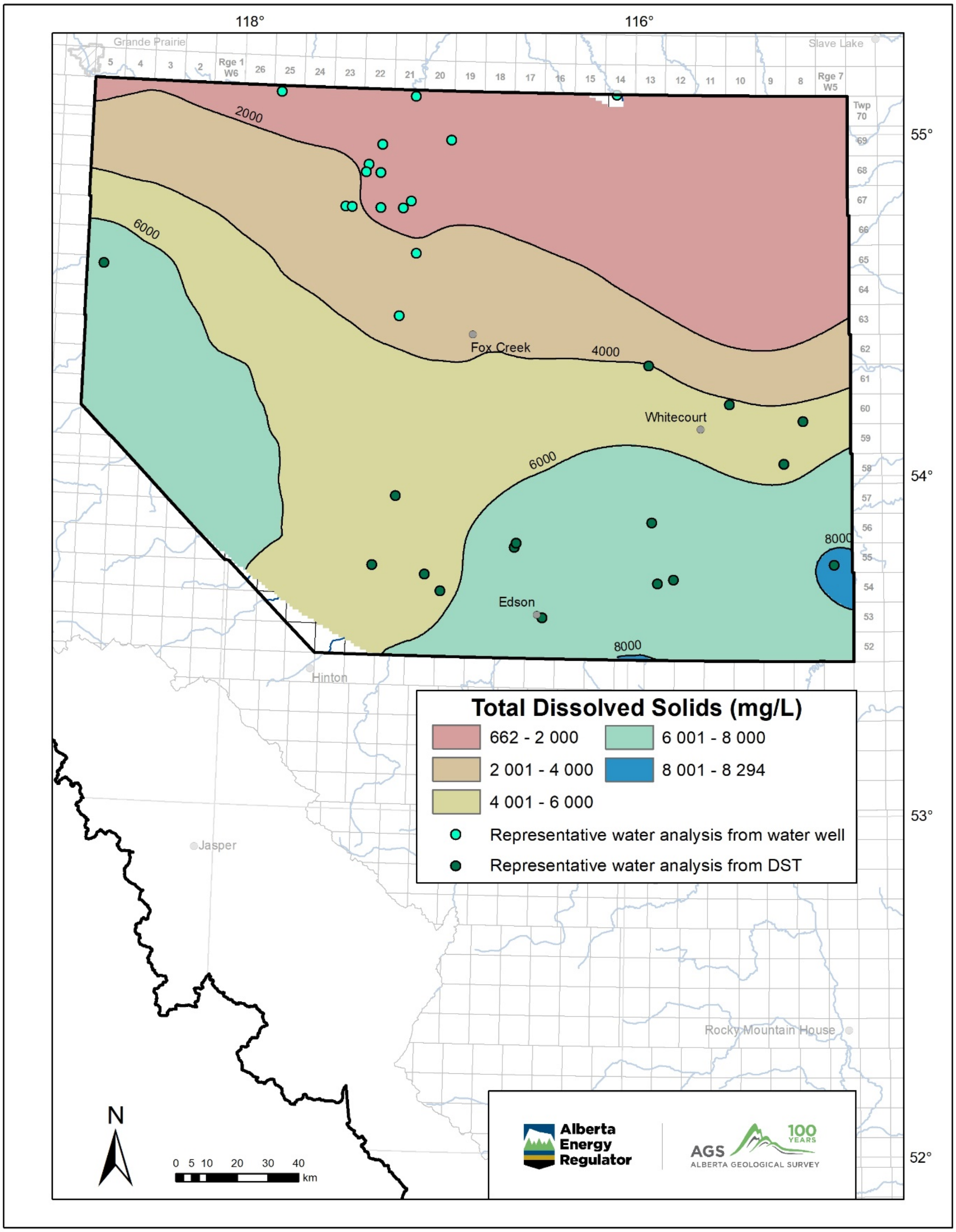

Figure 73. Distribution of total dissolved solids (TDS) in the Wapiti aquifer, west-central Alberta study area (extracted from Nakevska and Singh, 2017). Abbreviation: DST, drillstem test.

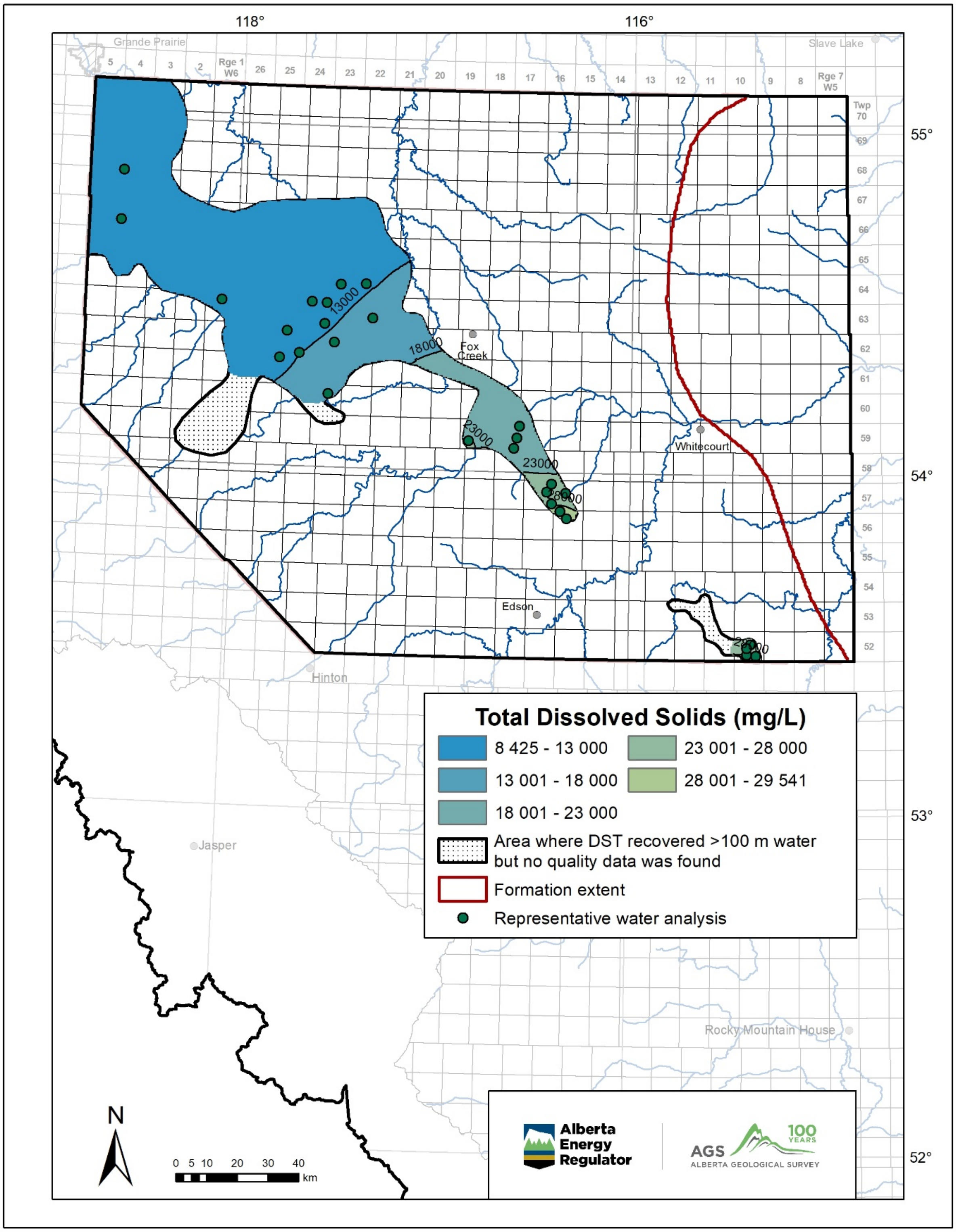

Figure 74. Distribution of total dissolved solids (TDS) in the Cardium aquifer, west-central Alberta study area. Abbreviation: DST, drillstem test.

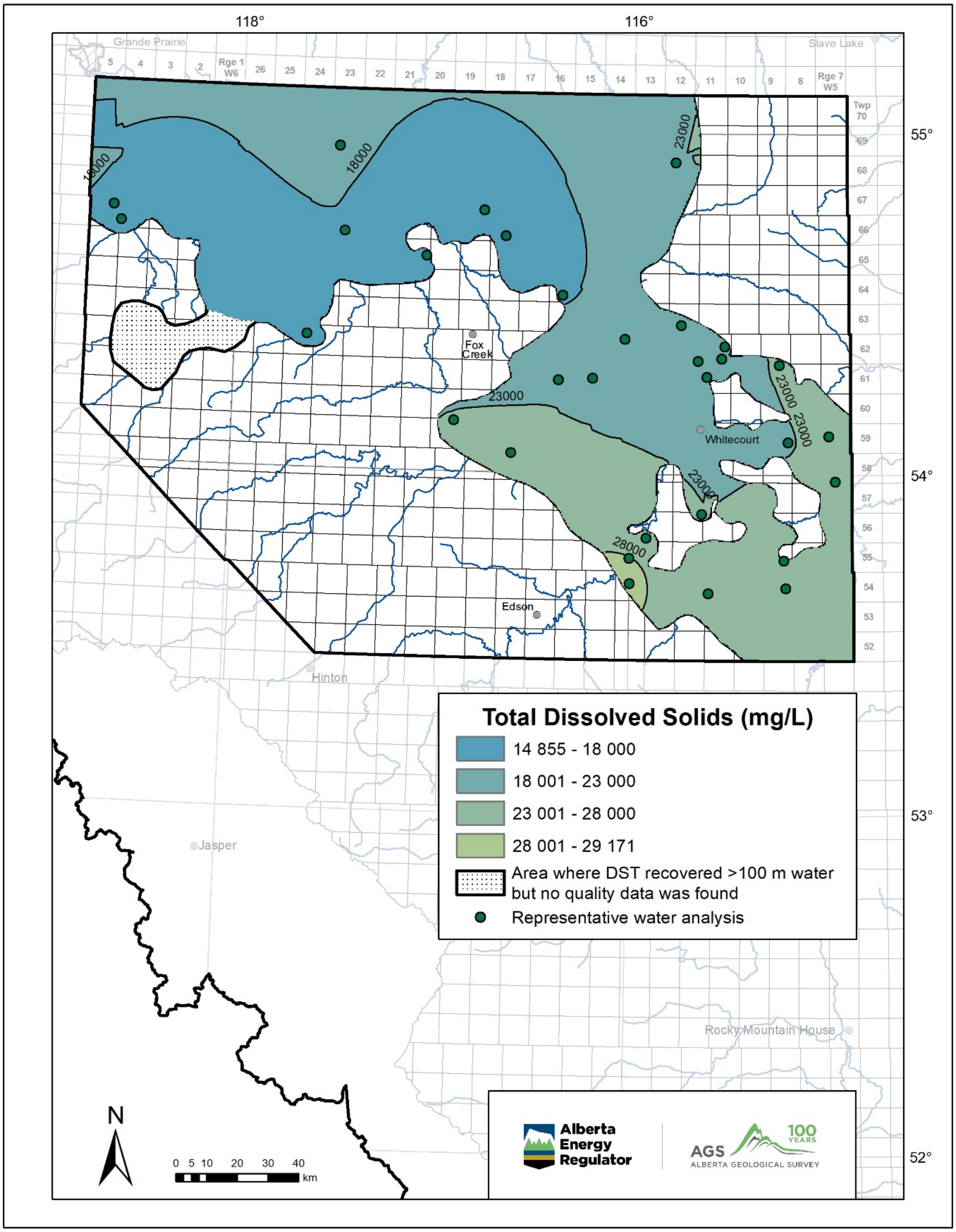

Figure 75. Distribution of total dissolved solids (TDS) in the Viking aquifer, west-central Alberta study area. Abbreviation: DST, drillstem test.

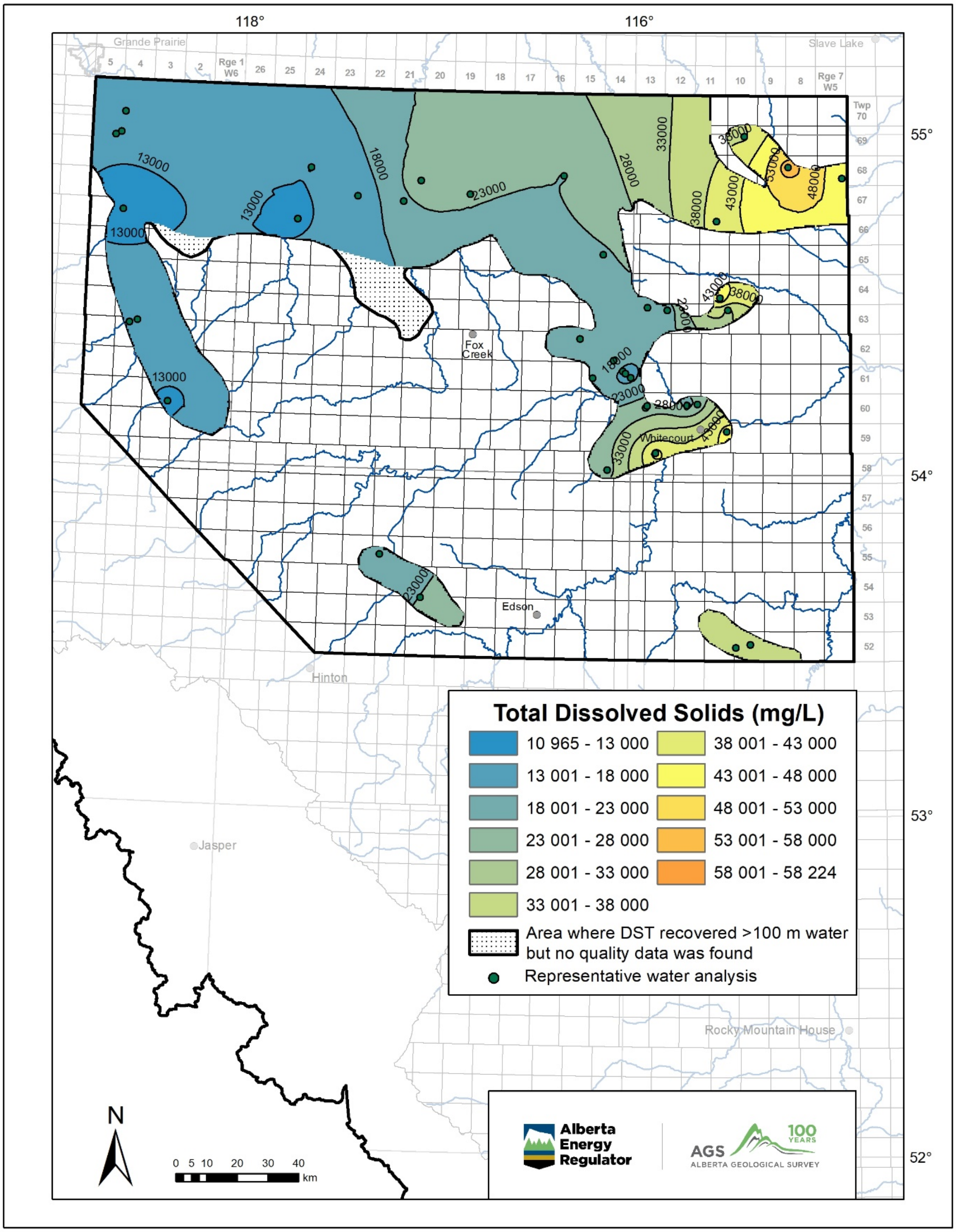

Figure 76. Distribution of total dissolved solids (TDS) in the Spirit River aquifer, west-central Alberta study area. Abbreviation: DST, drillstem test.

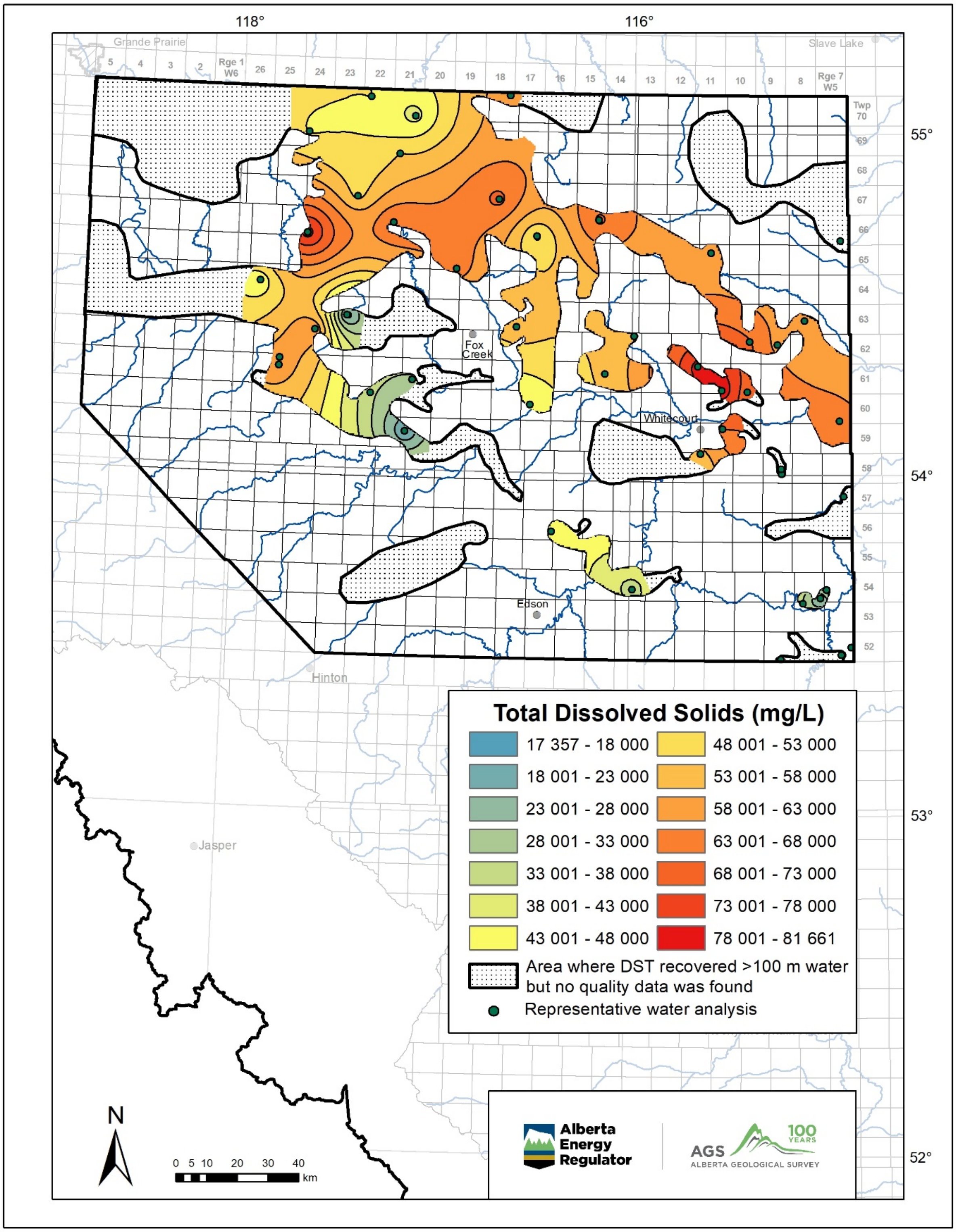

Figure 77. Distribution of total dissolved solids (TDS) in the Gething aquifer, west-central Alberta study area. Abbreviation: DST, drillstem test.

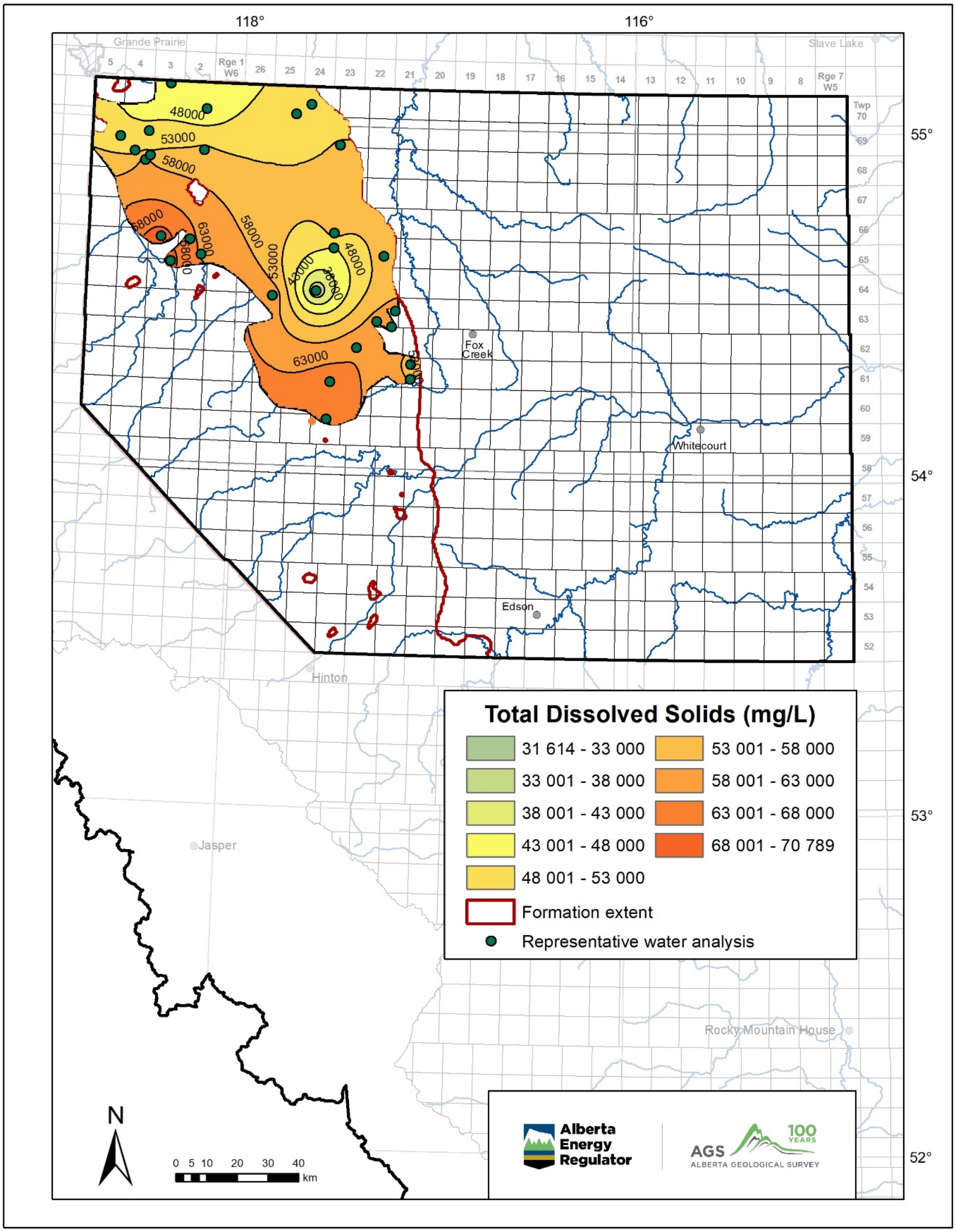

Figure 78. Distribution of total dissolved solids (TDS) in the Cadomin aquifer, west-central Alberta study area.

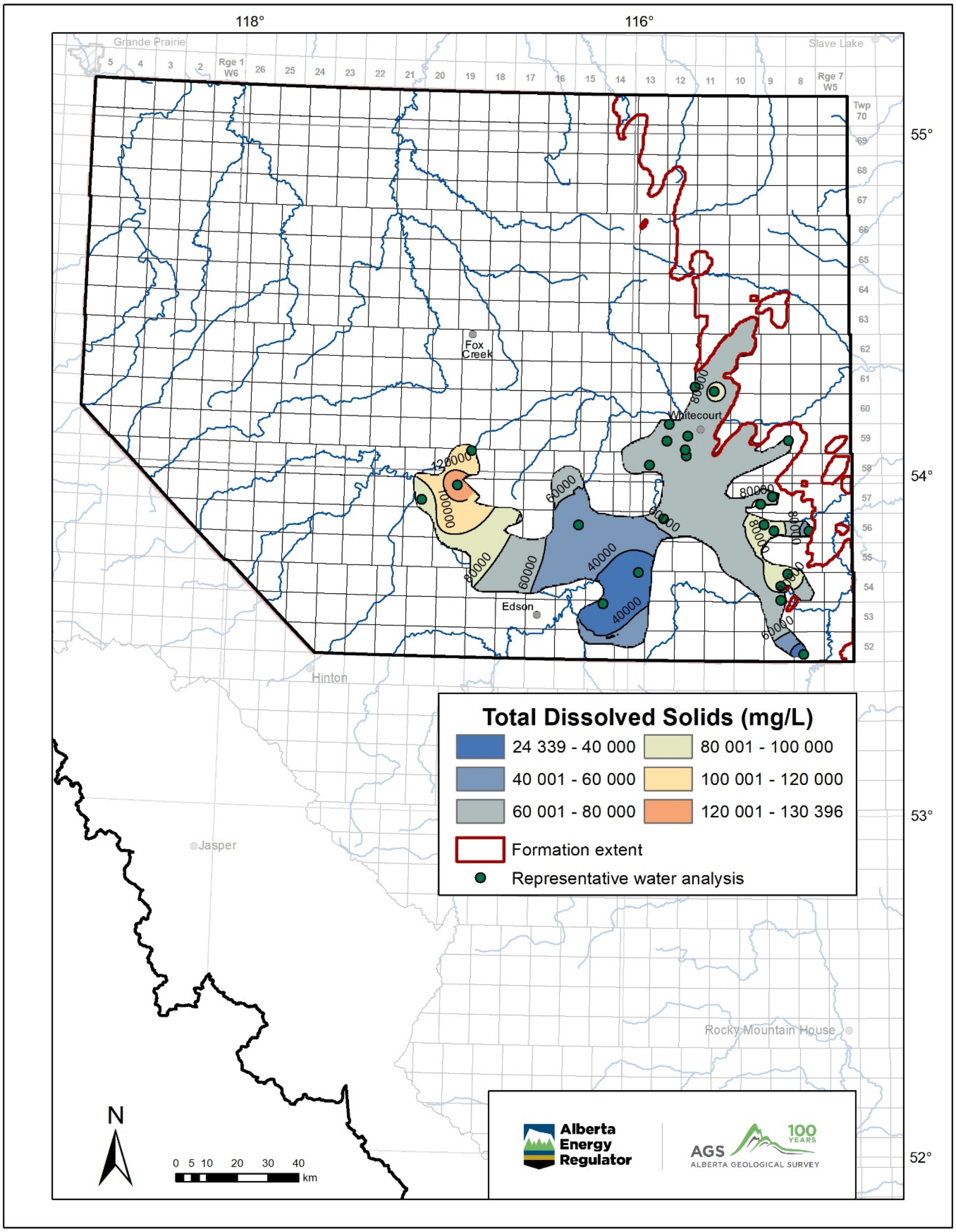

Figure 79. Distribution of total dissolved solids (TDS) in the Nordegg aquifer, west-central Alberta study area.

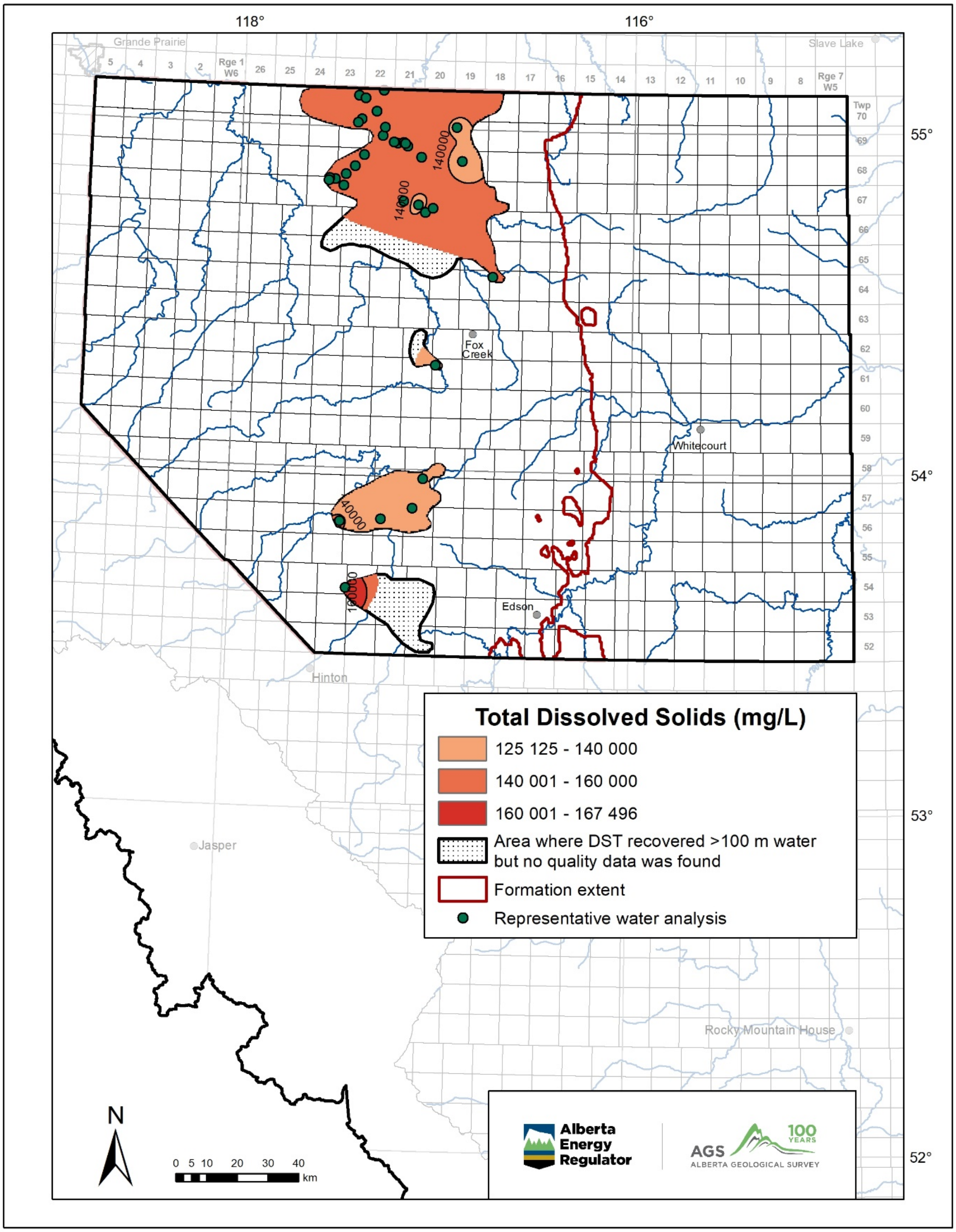

Figure 80. Distribution of total dissolved solids (TDS) in the Montney aquifer, west-central Alberta study area. Abbreviation: DST, drillstem test.

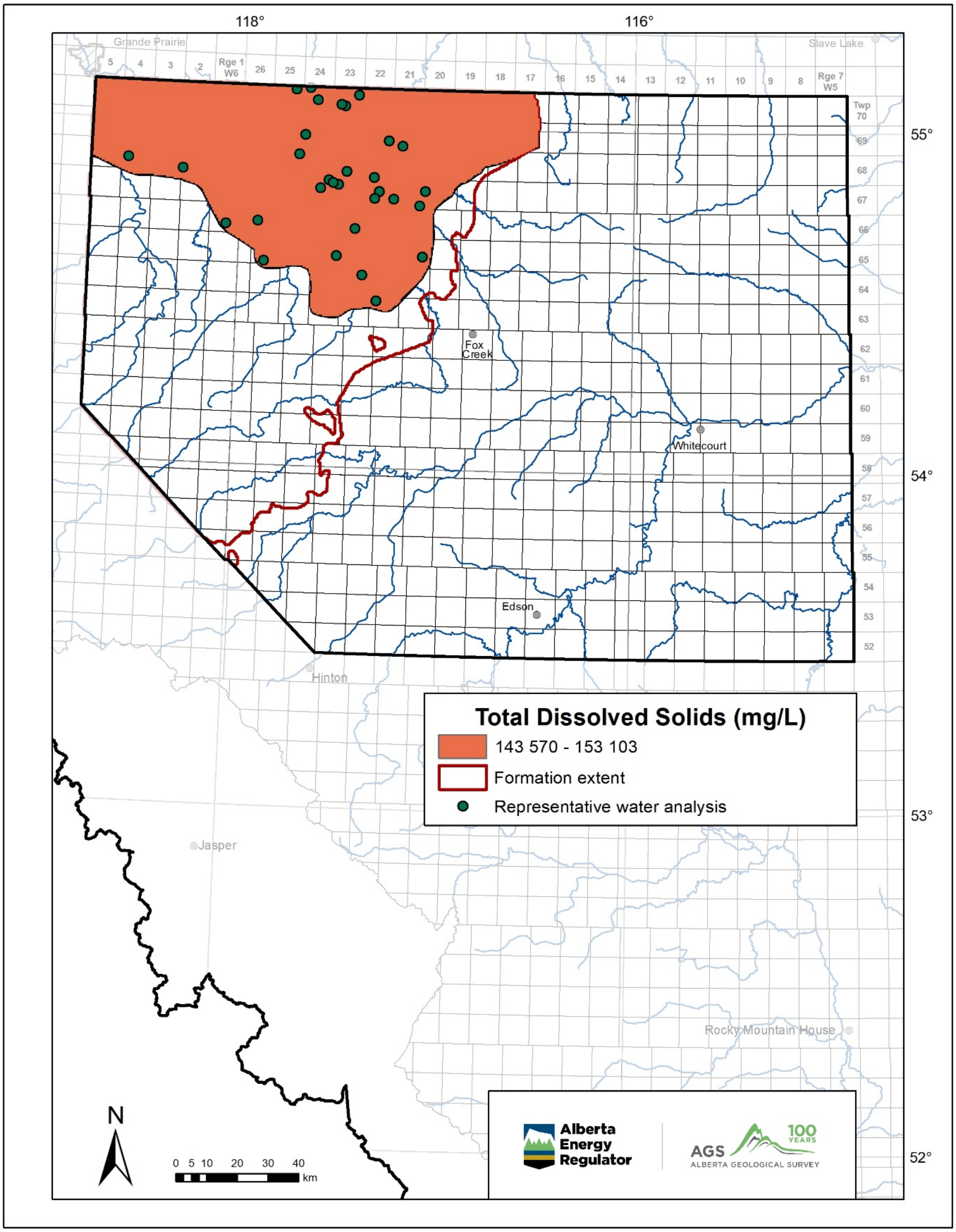

Figure 81. Distribution of total dissolved solids (TDS) in the Belloy aquifer, west-central Alberta study area.

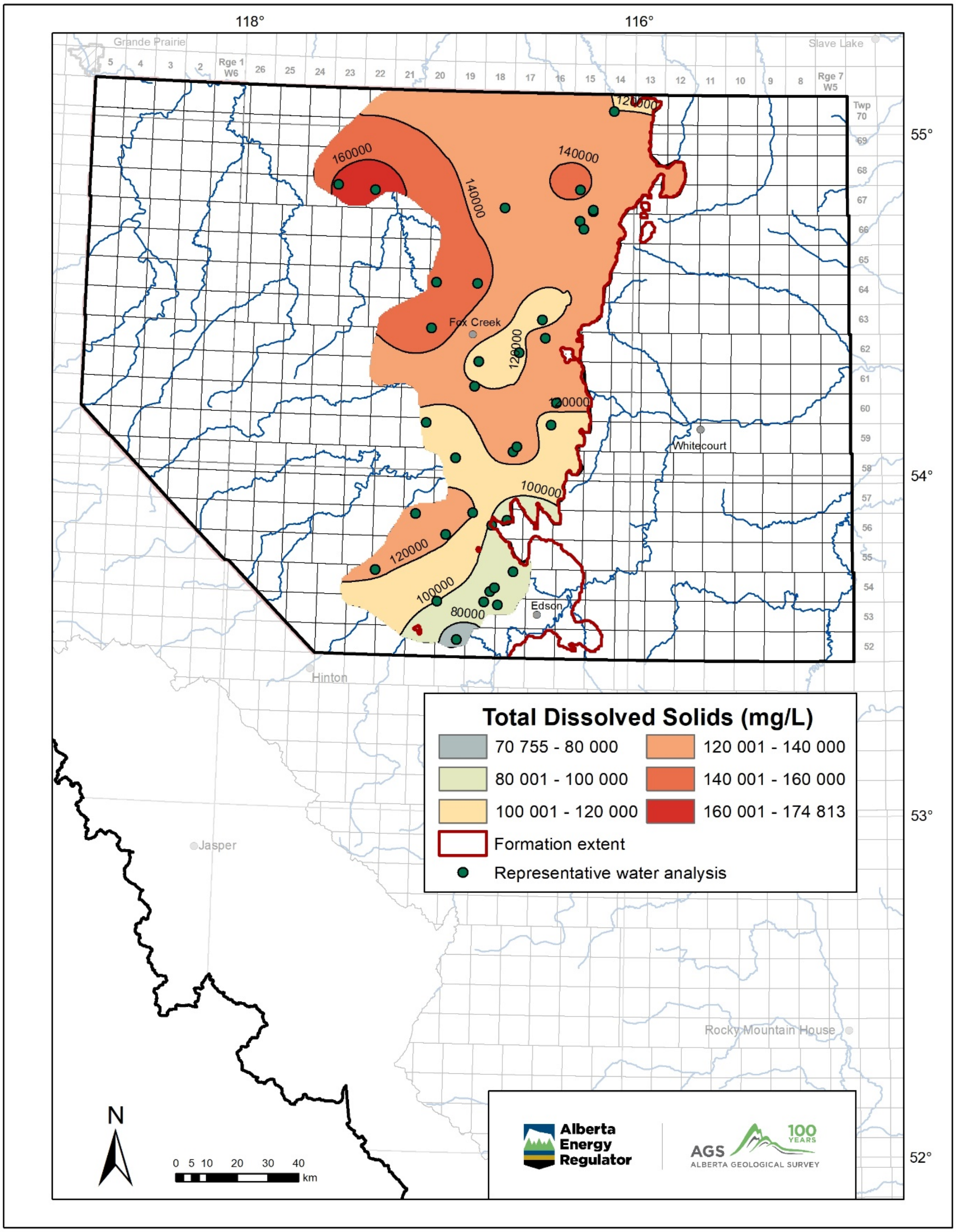

Figure 82. Distribution of total dissolved solids (TDS) in the Debolt aquifer, west-central Alberta study area.

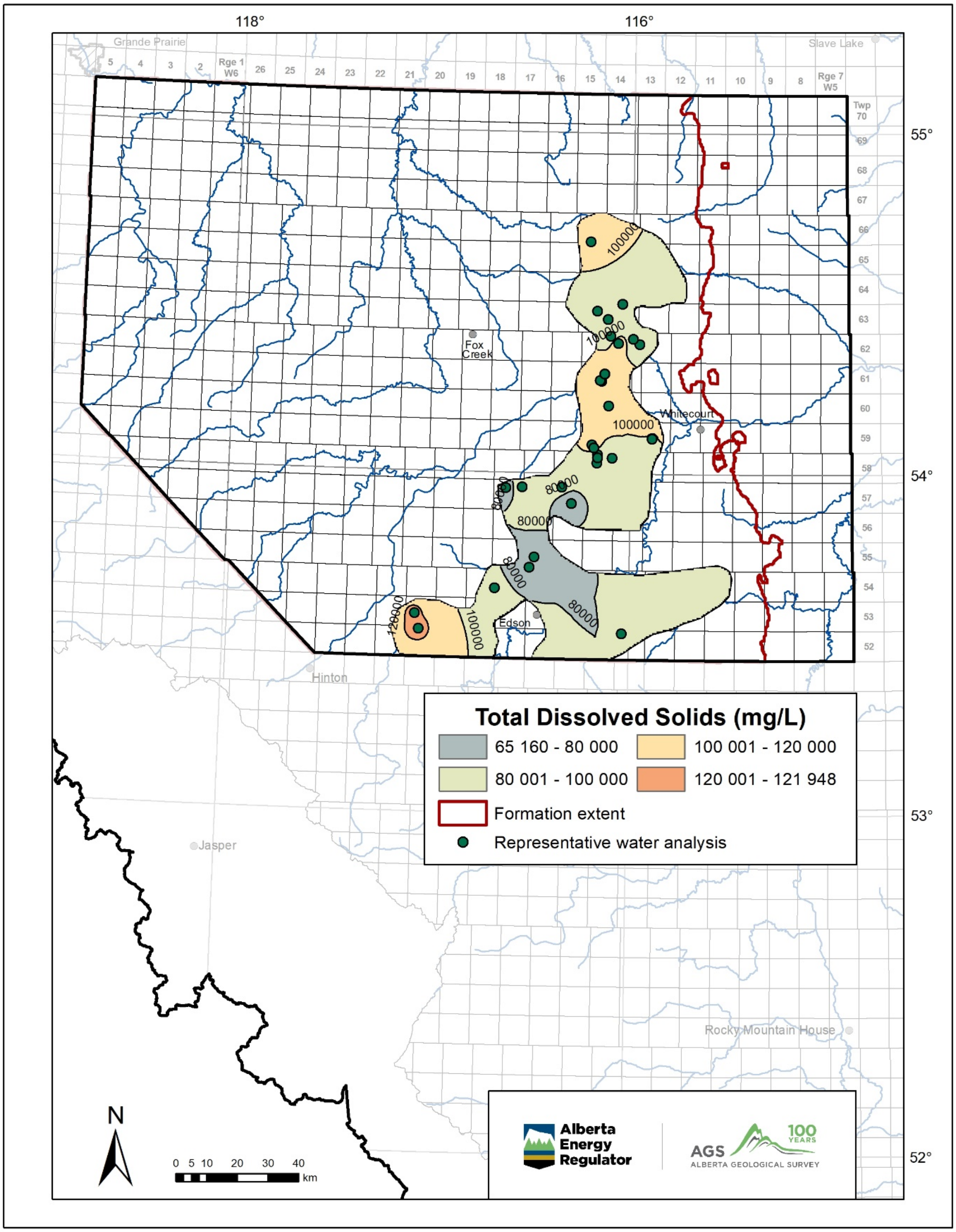

Figure 83. Distribution of total dissolved solids (TDS) in the Shunda aquifer, west-central Alberta study area.

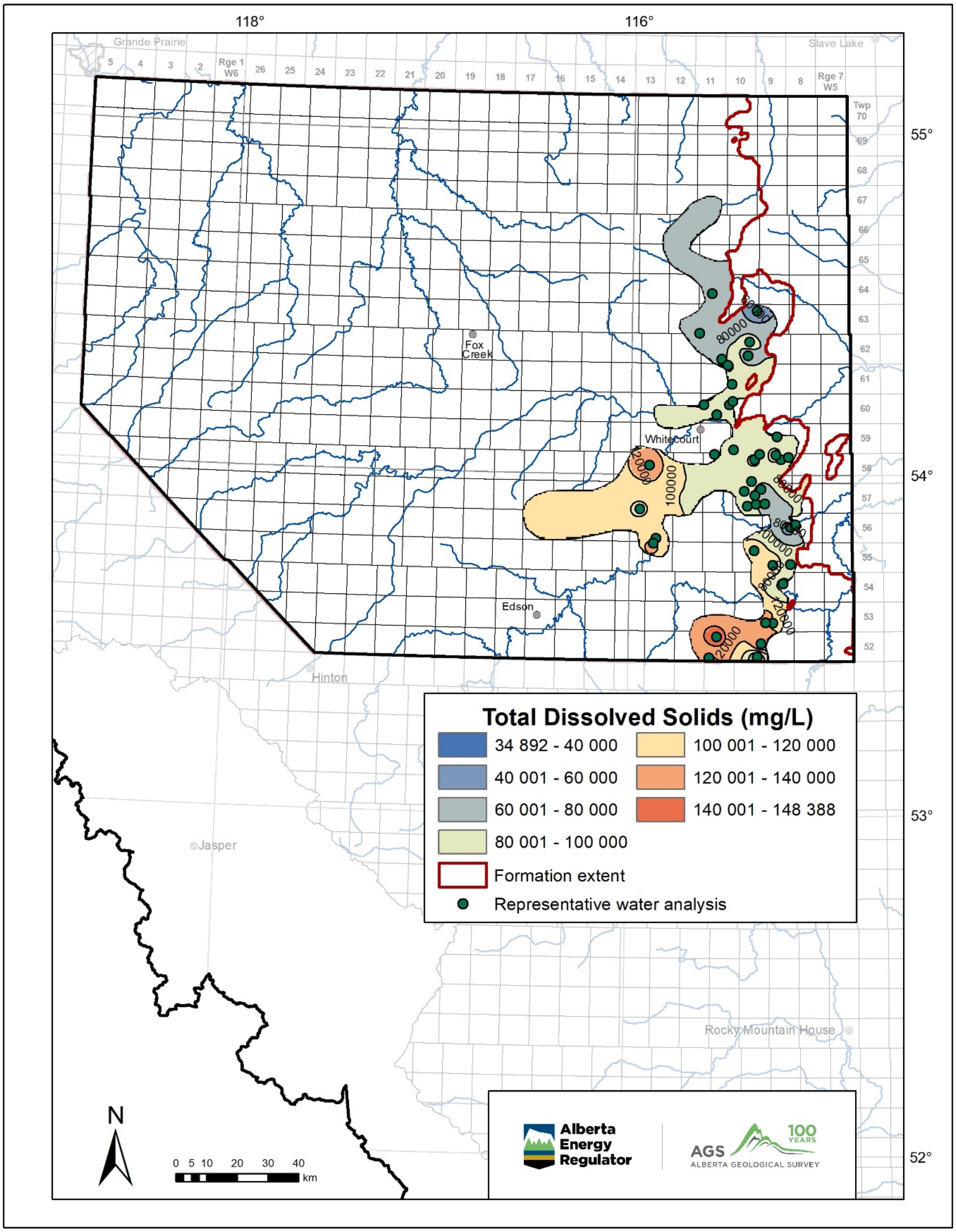

Figure 84. Distribution of total dissolved solids (TDS) in the Pekisko aquifer, west-central Alberta study area.

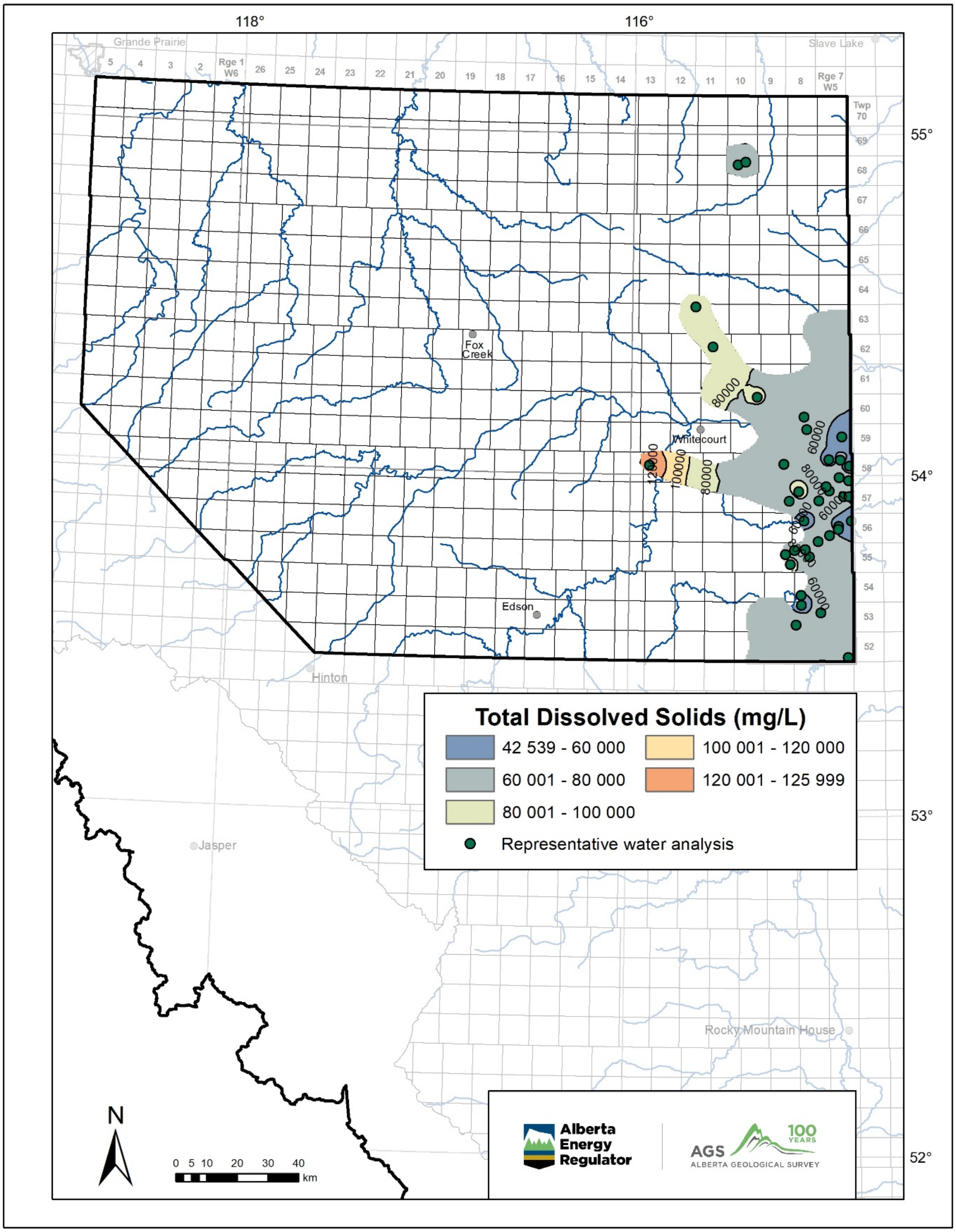

Figure 85. Distribution of total dissolved solids (TDS) in the Banff aquifer, west-central Alberta study area.

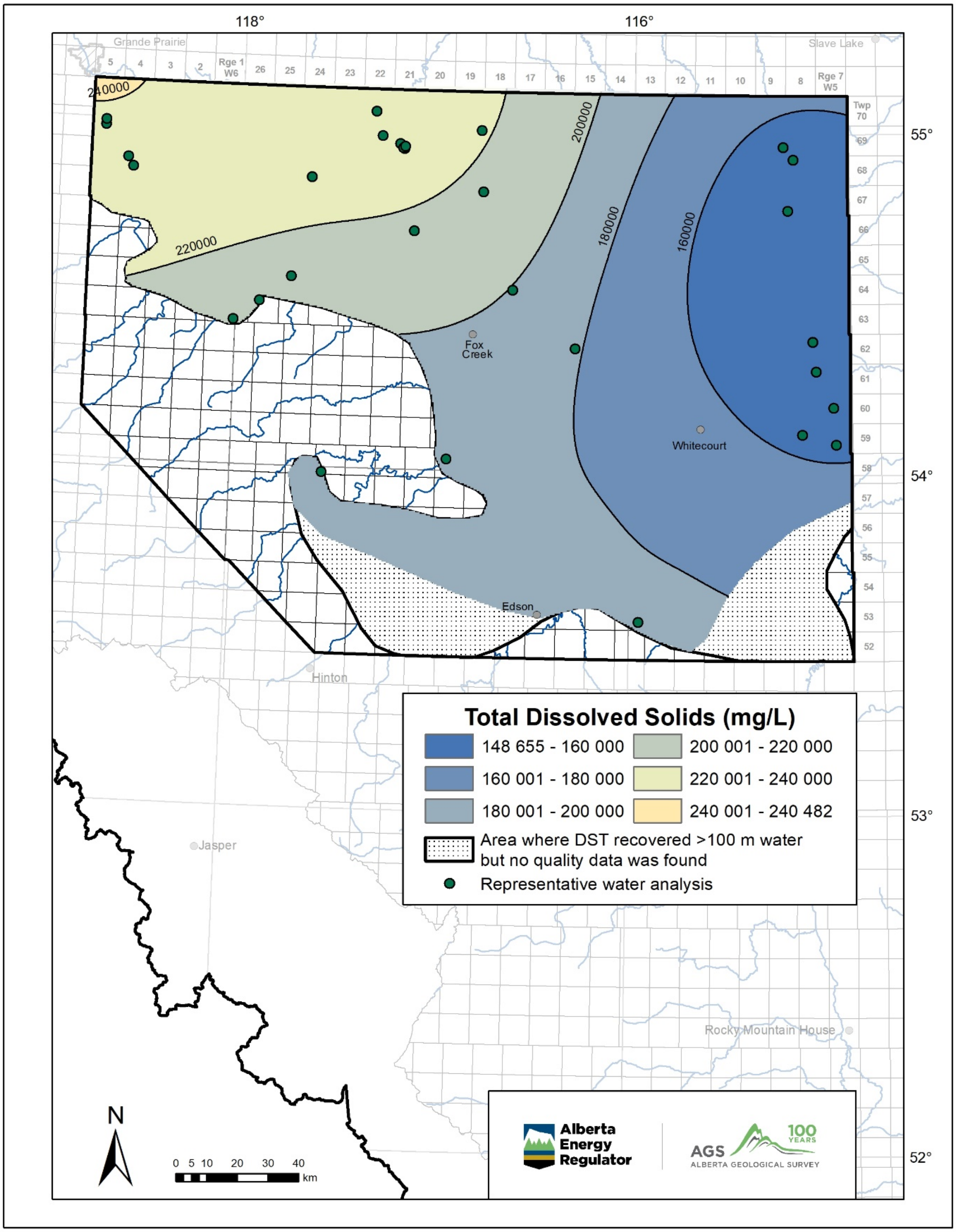

Figure 86. Distribution of total dissolved solids (TDS) in the Wabamun aquifer, west-central Alberta study area. Abbreviation: DST, drillstem test.

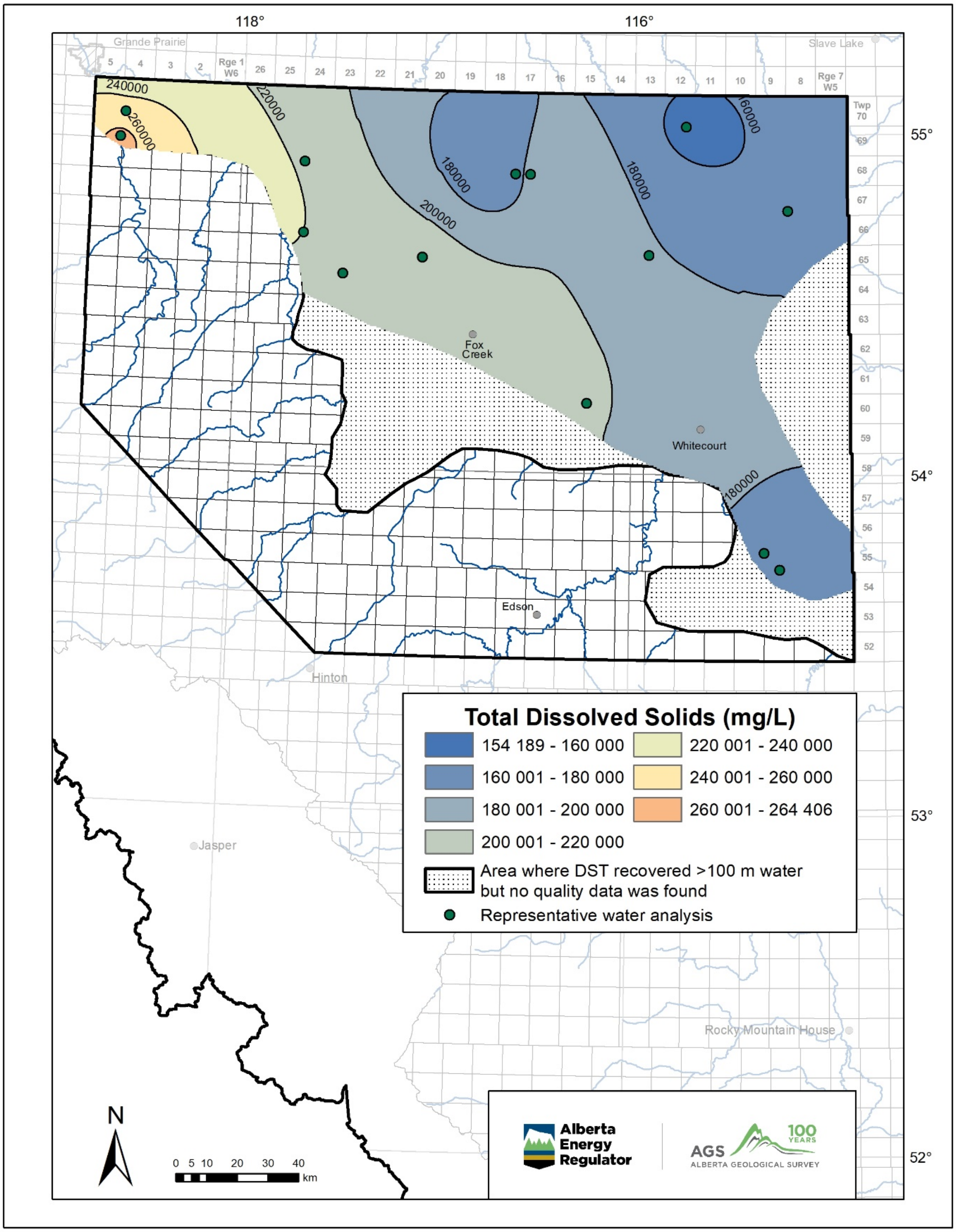

Figure 87. Distribution of total dissolved solids (TDS) in the Blue Ridge aquifer, west-central Alberta study area. Abbreviation: DST, drillstem test.

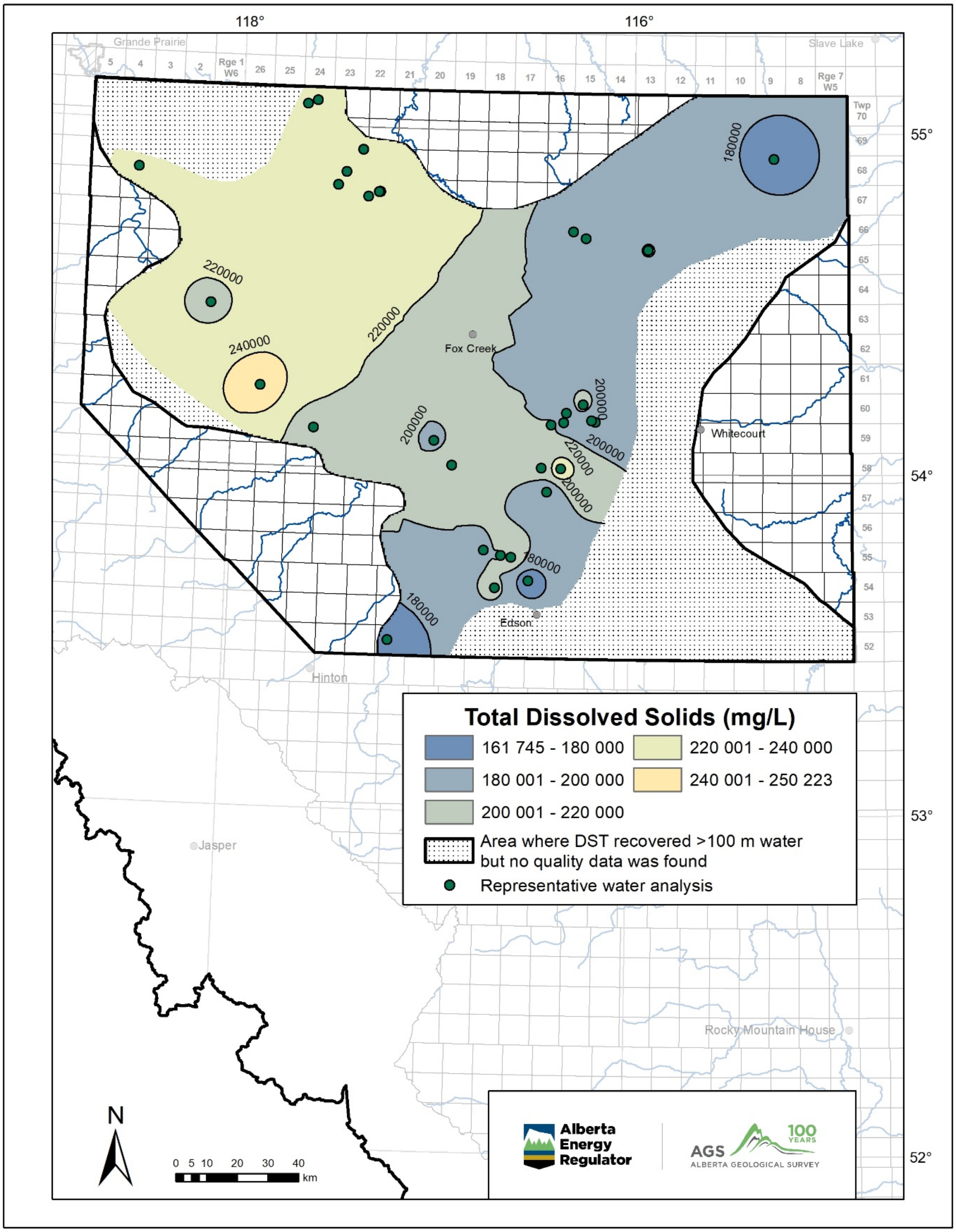

Figure 88. Distribution of total dissolved solids (TDS) in the Nisku aquifer, west-central Alberta study area. Abbreviation: DST, drillstem test.

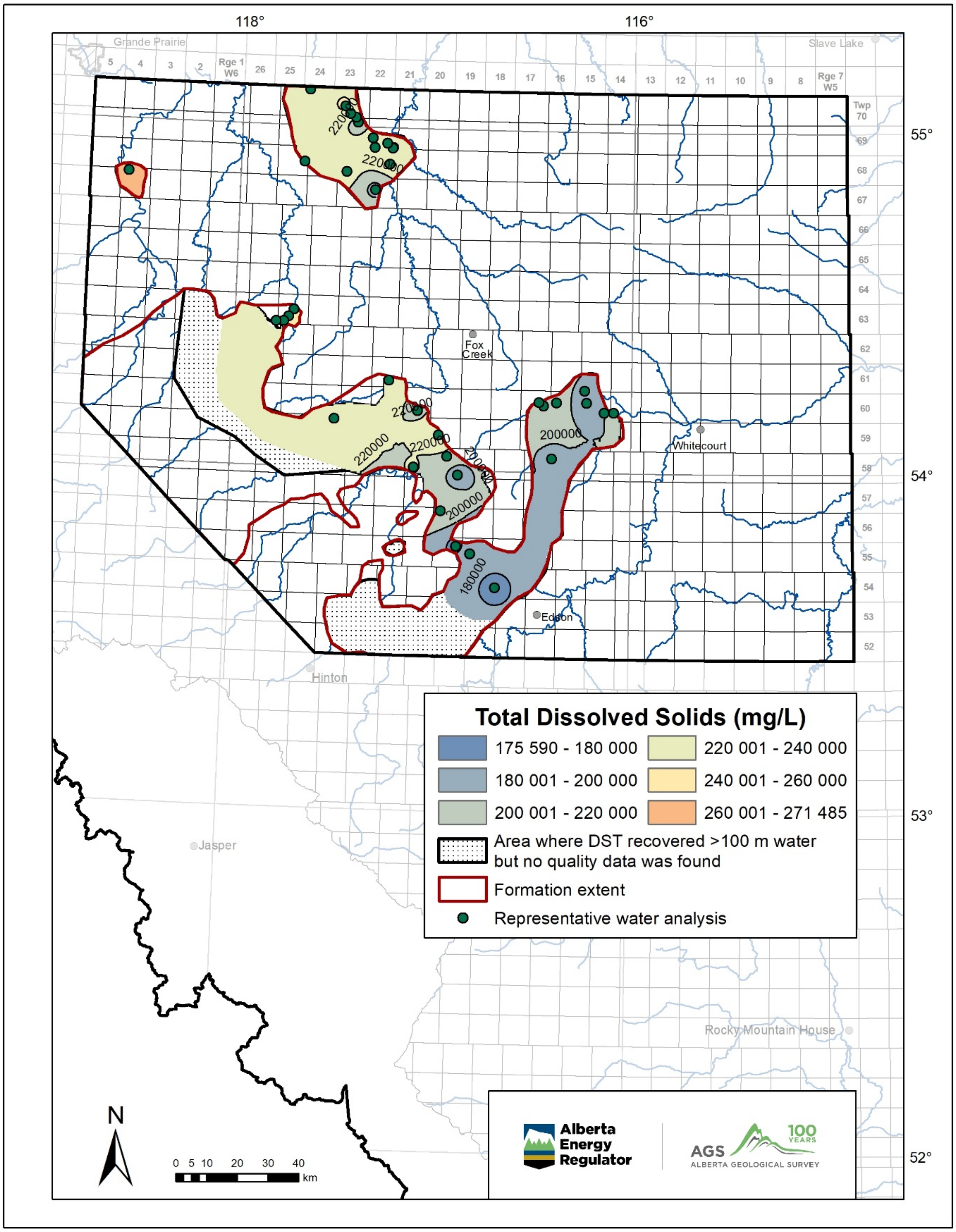

Figure 89. Distribution of total dissolved solids (TDS) in the Leduc aquifer, west-central Alberta study area. Abbreviation: DST, drillstem test.

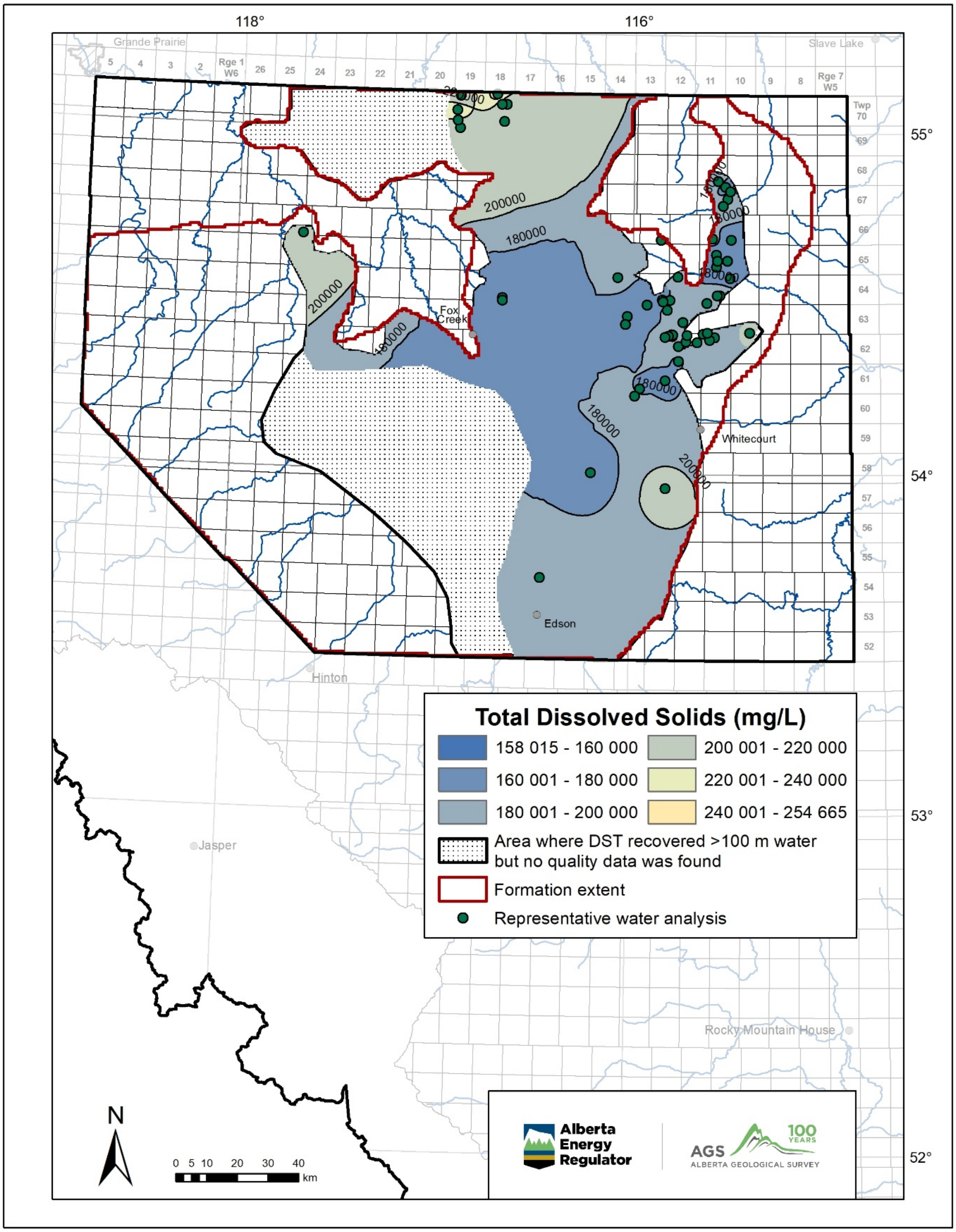

Figure 90. Distribution of total dissolved solids (TDS) in the Swan Hills aquifer, west-central Alberta study area. Abbreviation: DST, drillstem test.

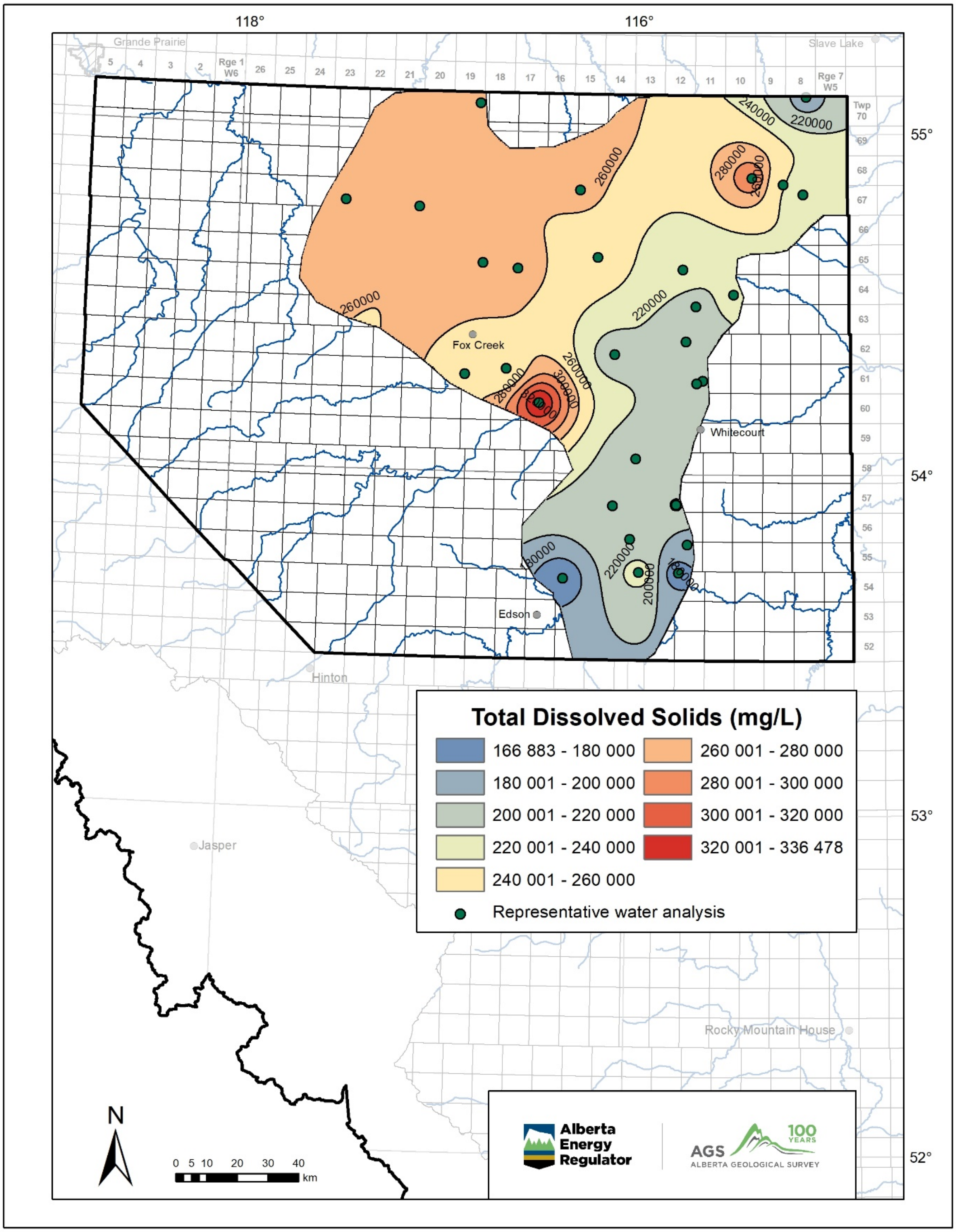

Figure 91. Distribution of total dissolved solids (TDS) in the Elk Point aquifer, west-central Alberta study area.

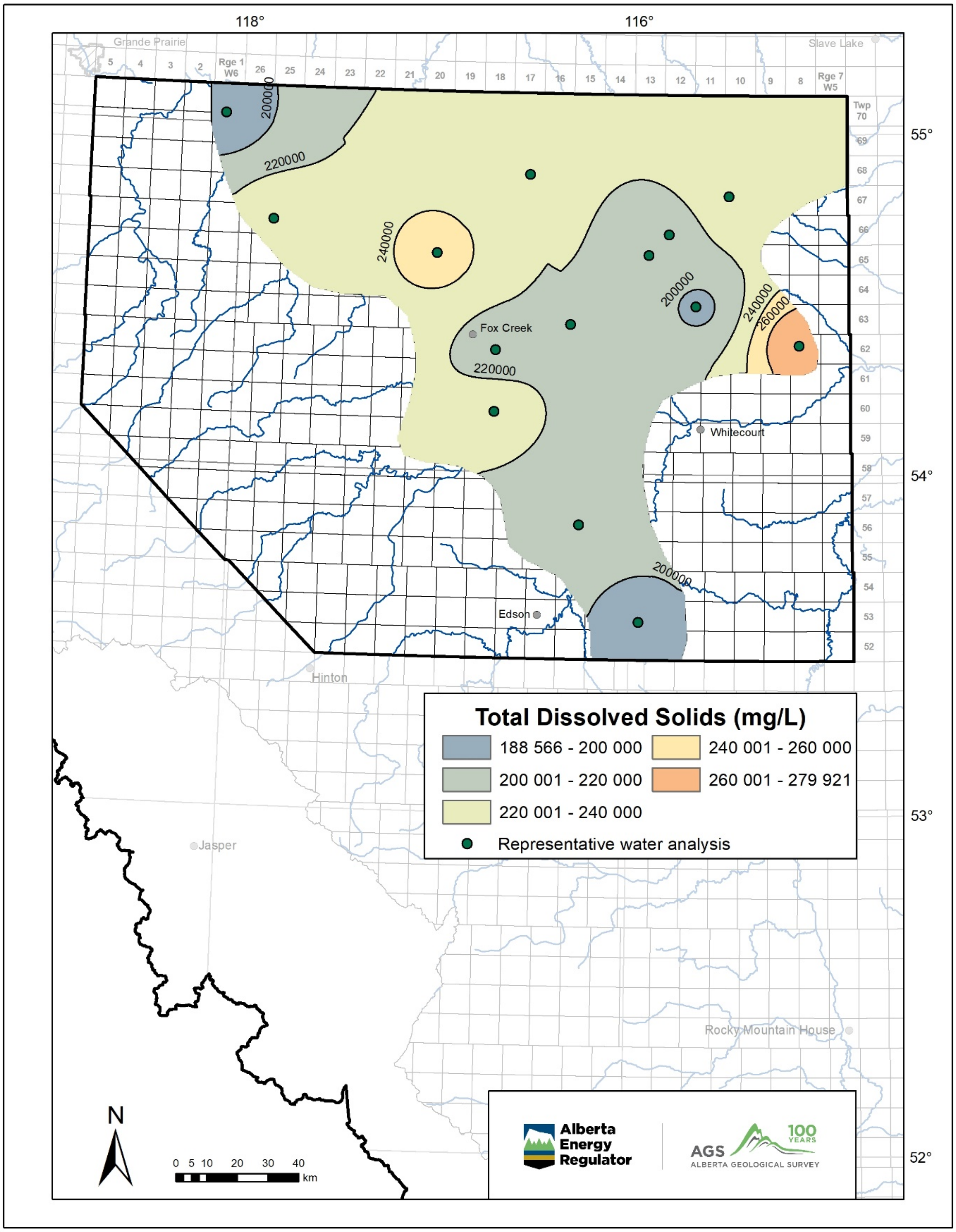

Figure 92. Distribution of total dissolved solids (TDS) in the Cambrian aquifer, west-central Alberta study area.

1.4 Water Driving Force Maps

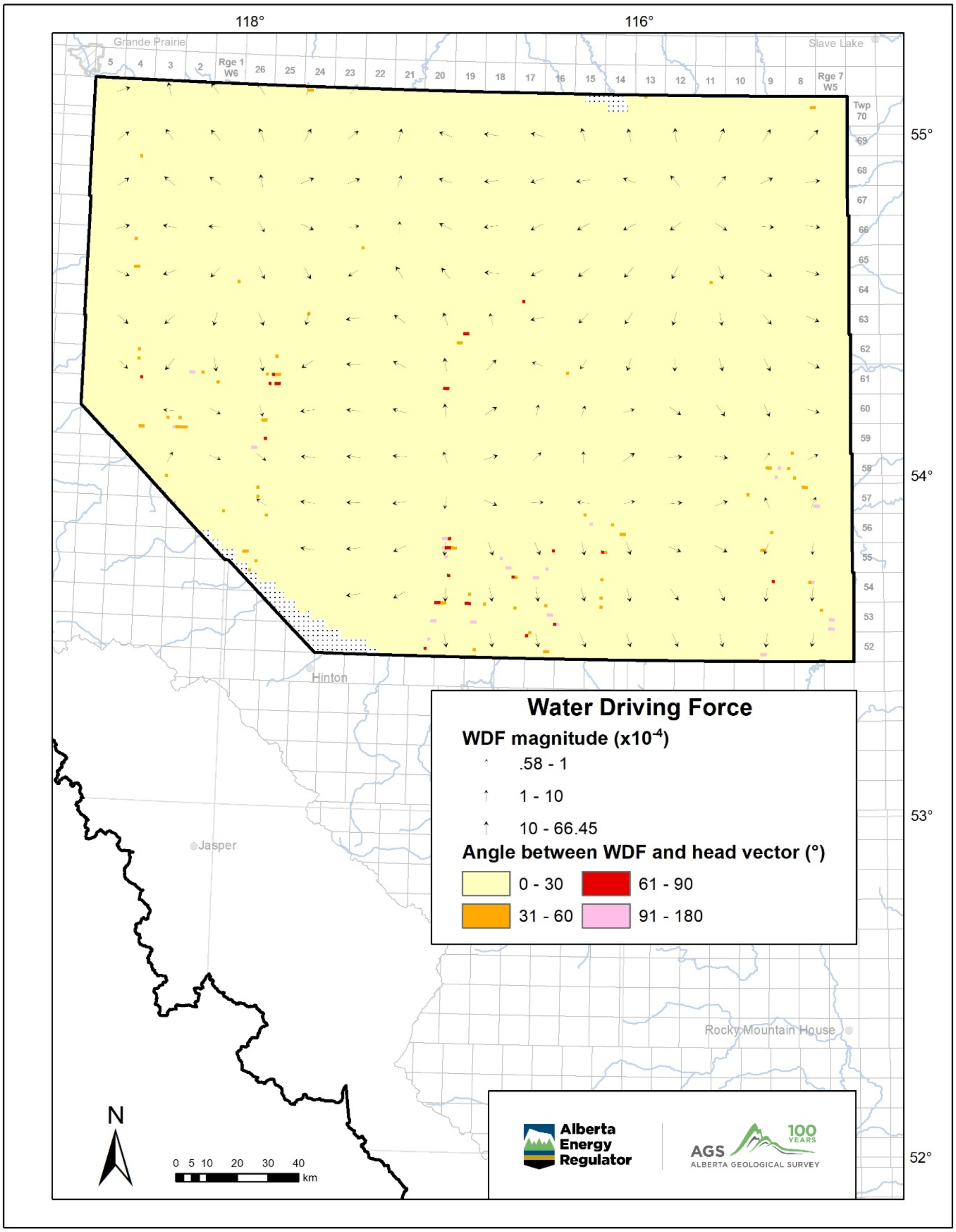

Figure 93. Water driving force (WDF) map for the Wapiti aquifer, west-central Alberta study area (extracted from Nakevska and Singh, 2017).

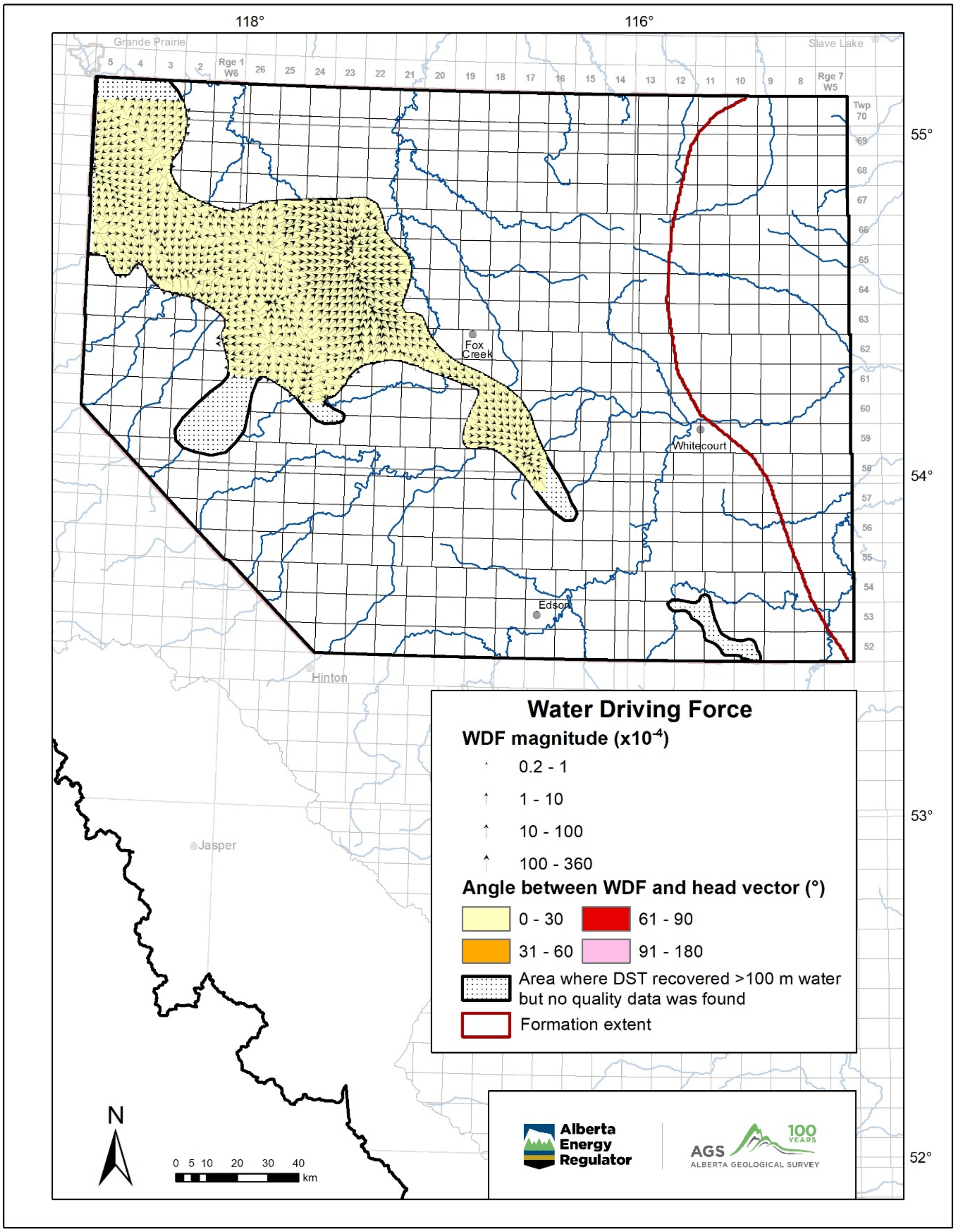

Figure 94. Water driving force (WDF) map for the Cardium aquifer, west-central Alberta study area. Abbreviation: DST, drillstem test.

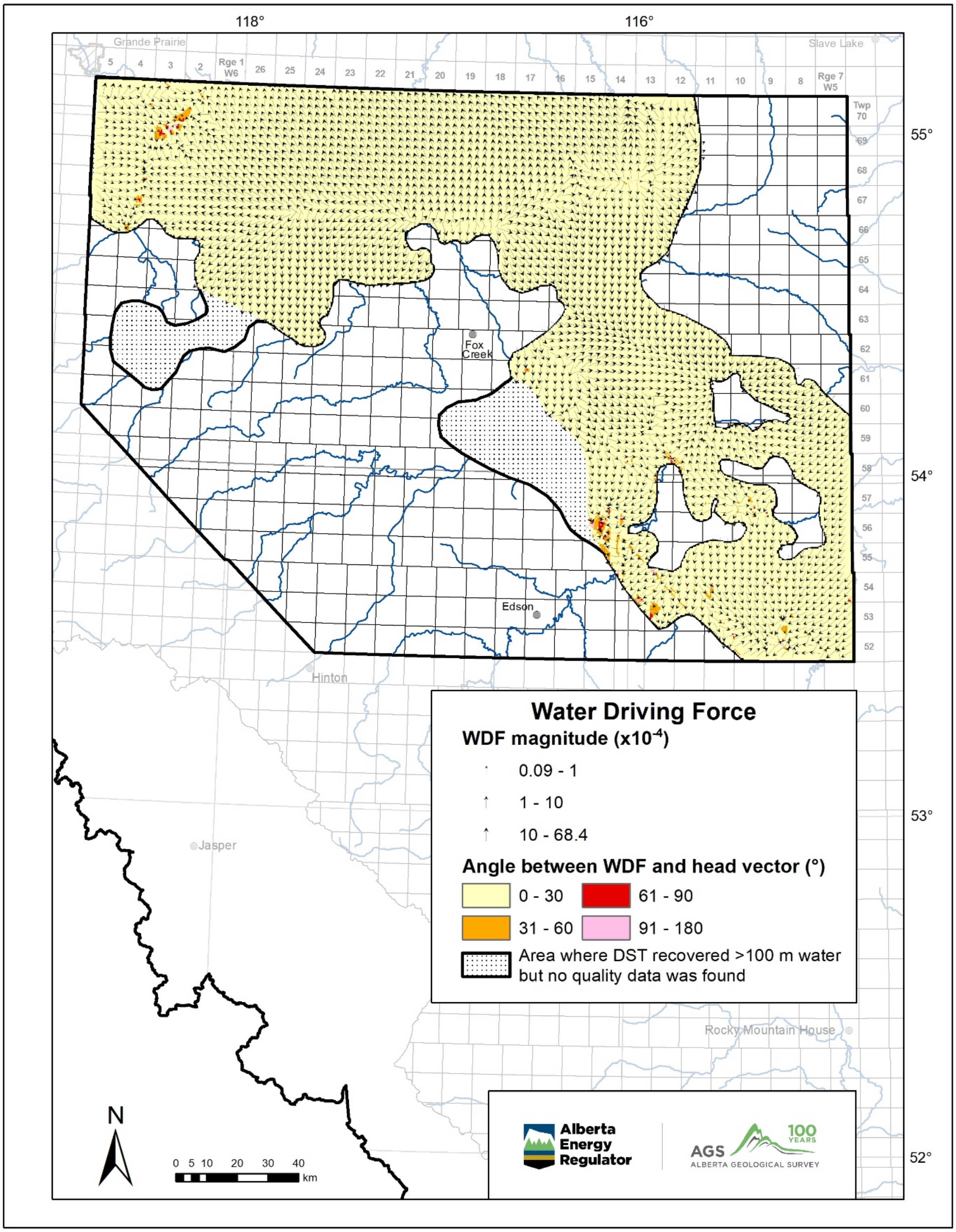

Figure 95. Water driving force (WDF) map for the Viking aquifer, west-central Alberta study area. Abbreviation: DST, drillstem test.

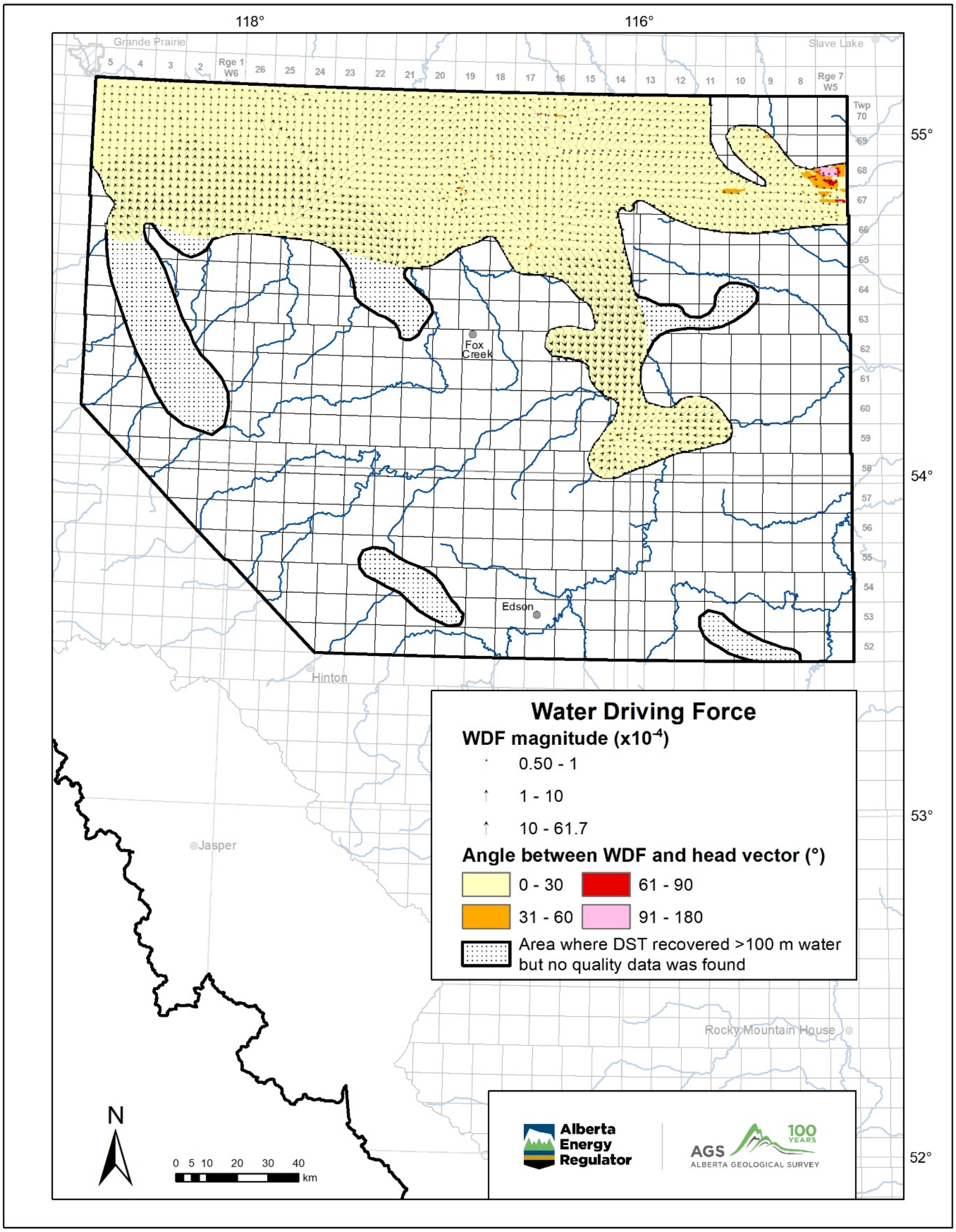

Figure 96. Water driving force (WDF) map for the Spirit River aquifer, west-central Alberta study area. Abbreviation: DST, drillstem test.

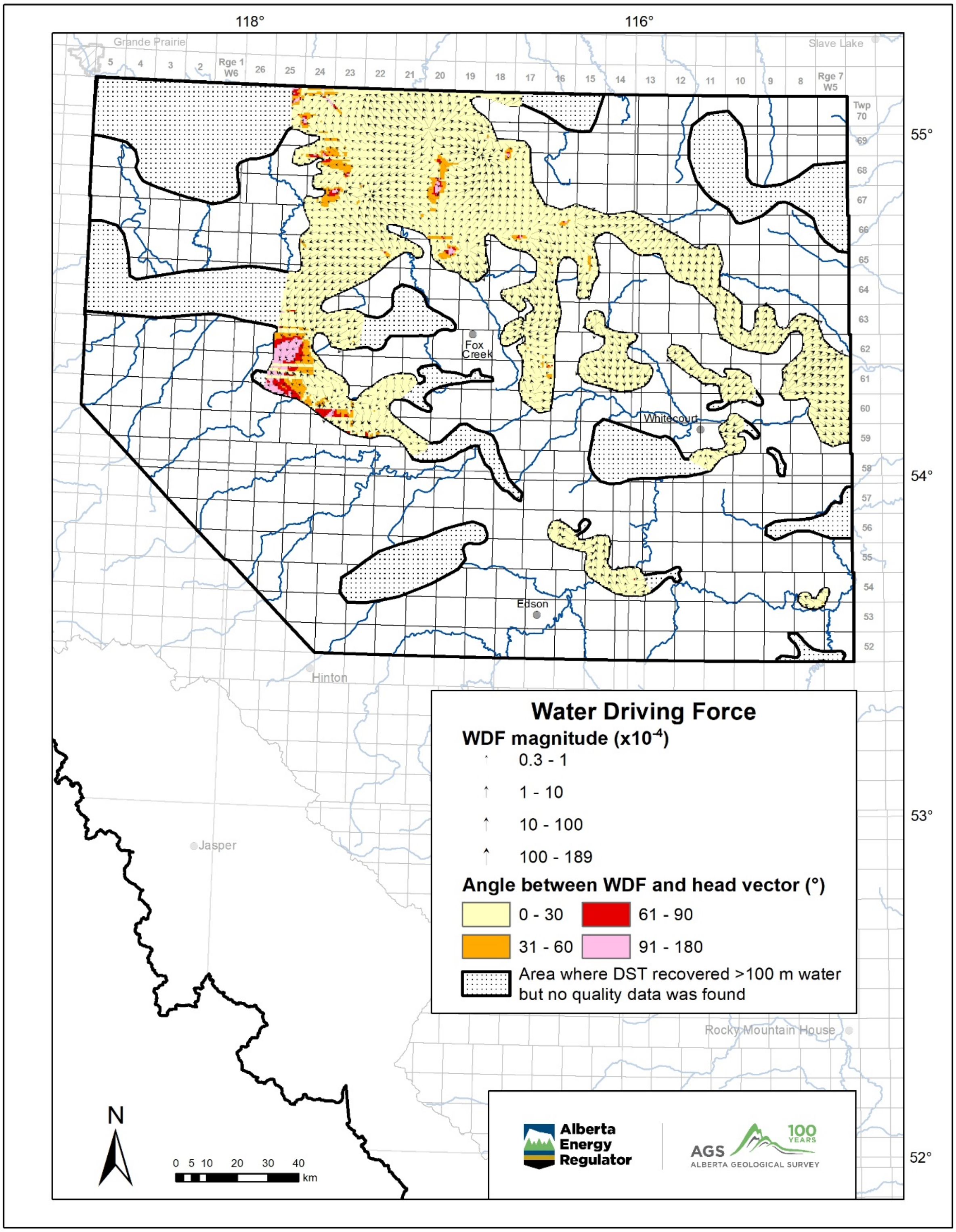

Figure 97. Water driving force (WDF) map for the Gething aquifer, west-central Alberta study area. Abbreviation: DST, drillstem test.

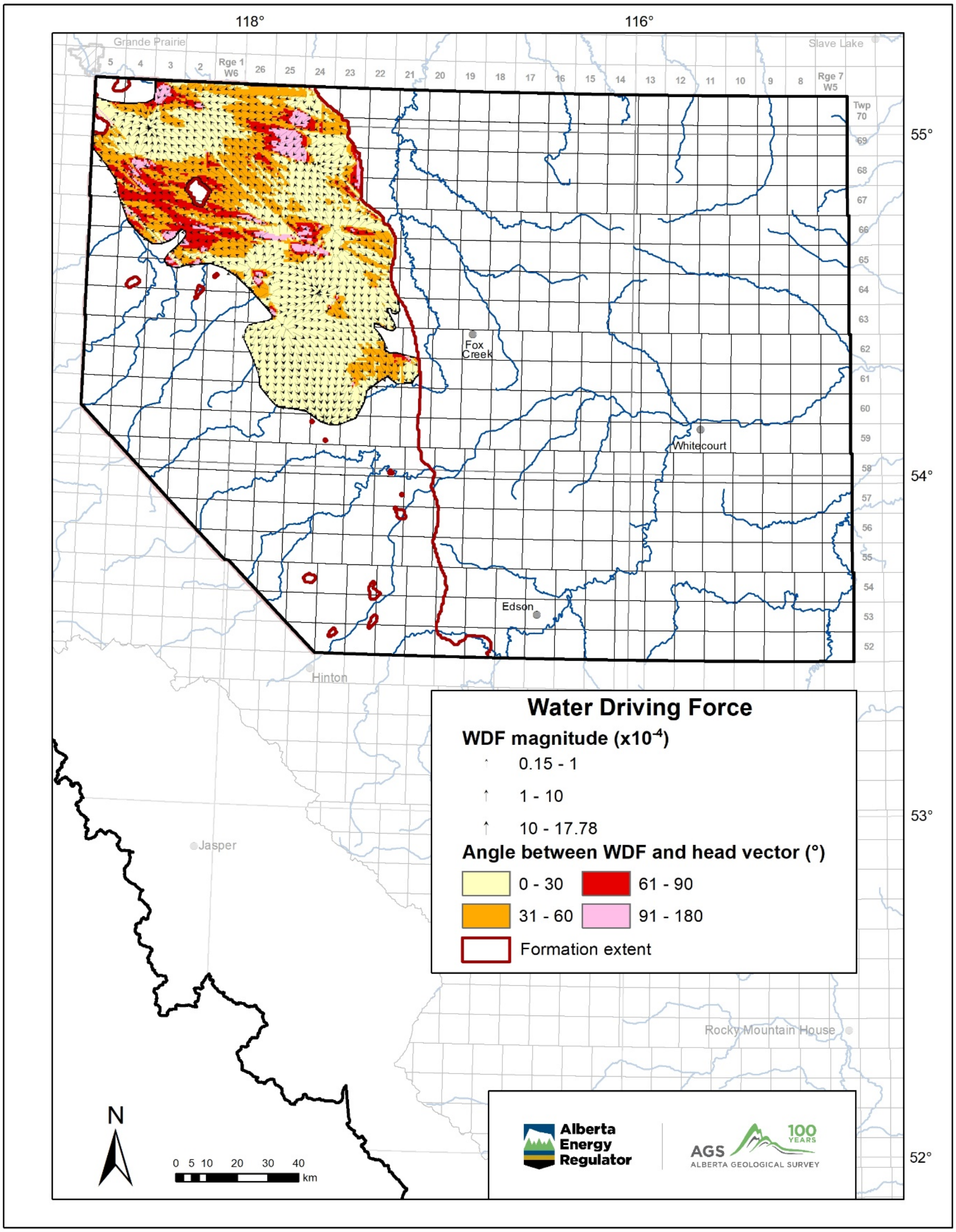

Figure 98. Water driving force (WDF) map for the Cadomin aquifer, west-central Alberta study area.

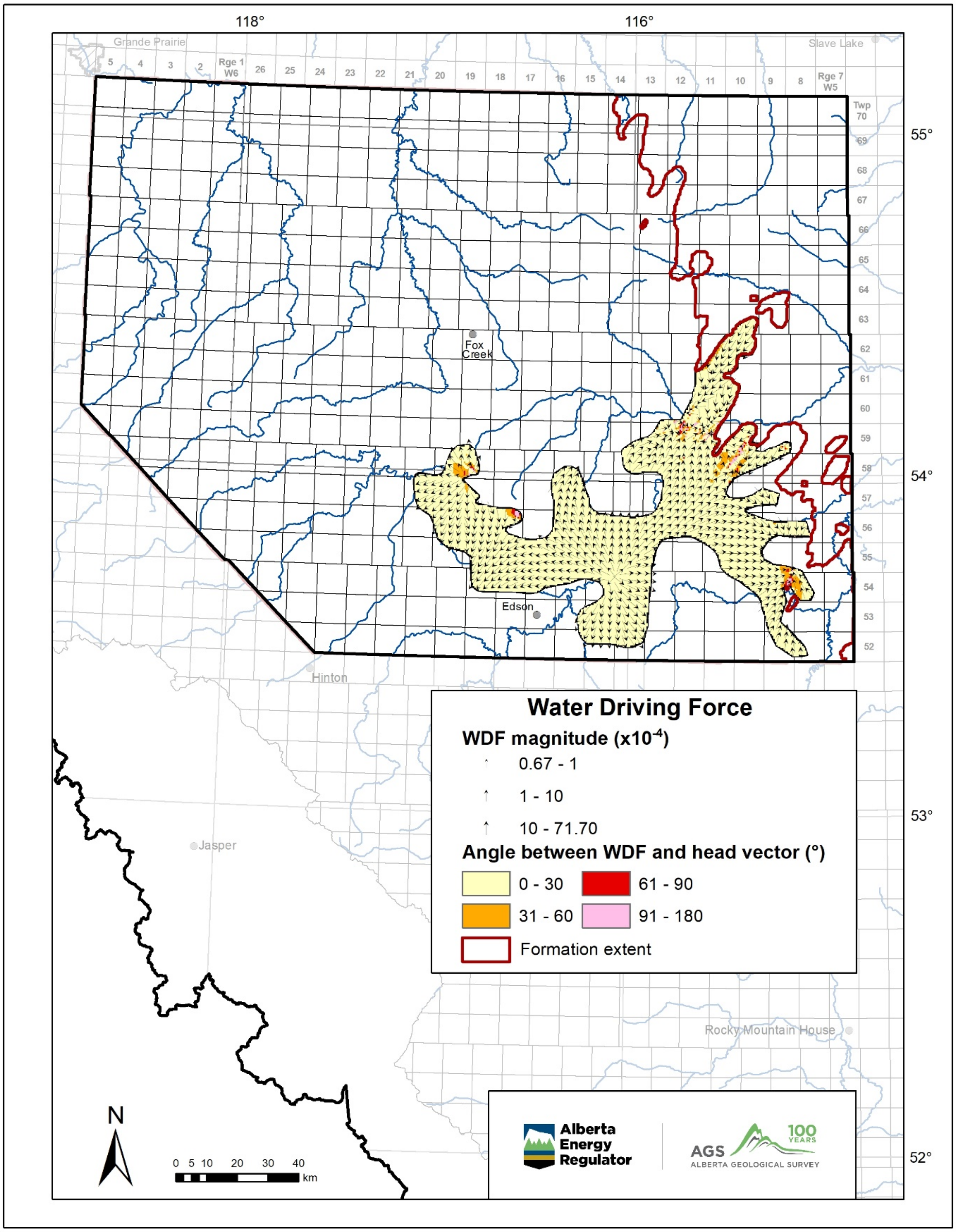

Figure 99. Water driving force (WDF) map for the Nordegg aquifer, west-central Alberta study area.

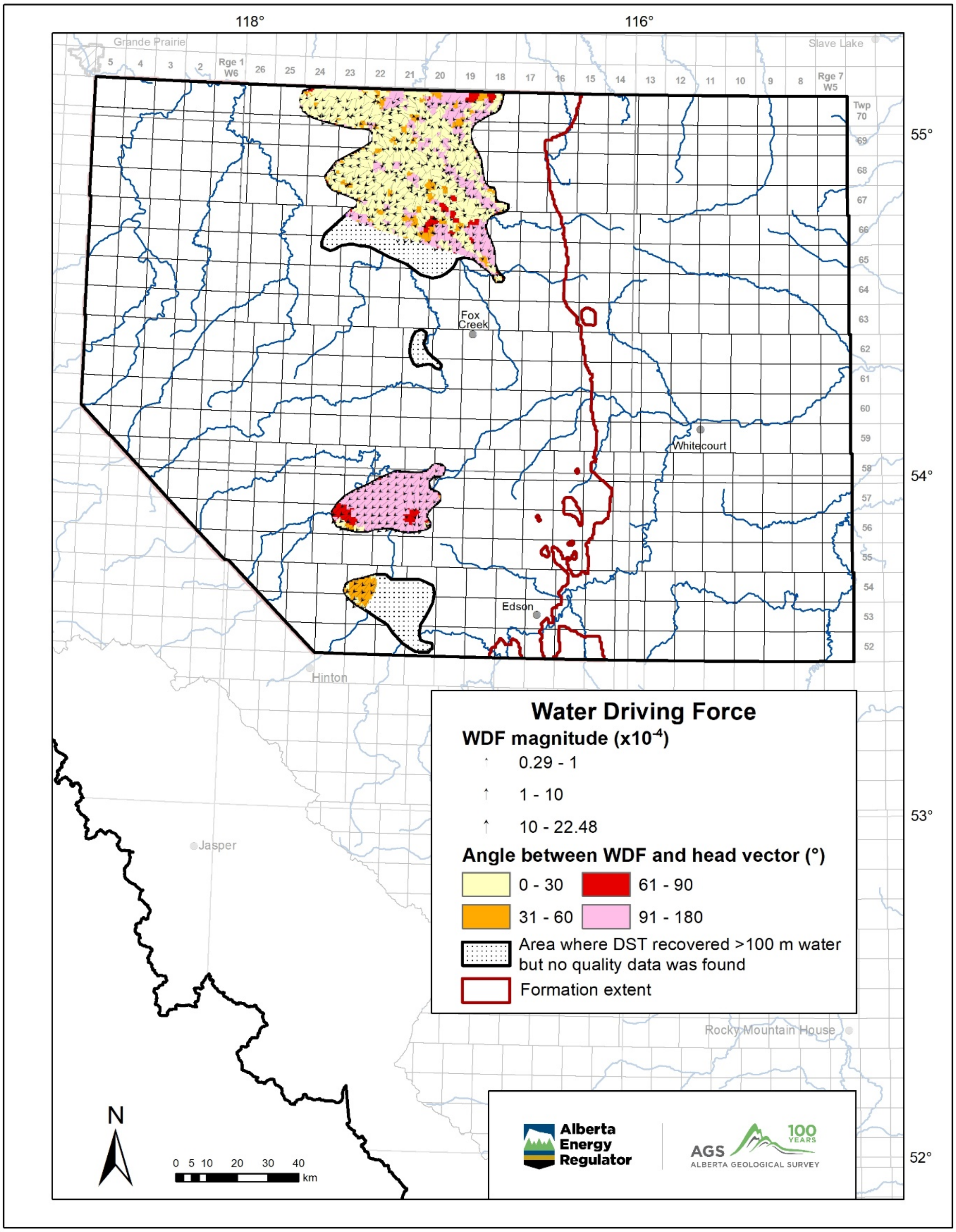

Figure 100. Water driving force (WDF) map for the Montney aquifer, west-central Alberta study area. Abbreviation: DST, drillstem test.

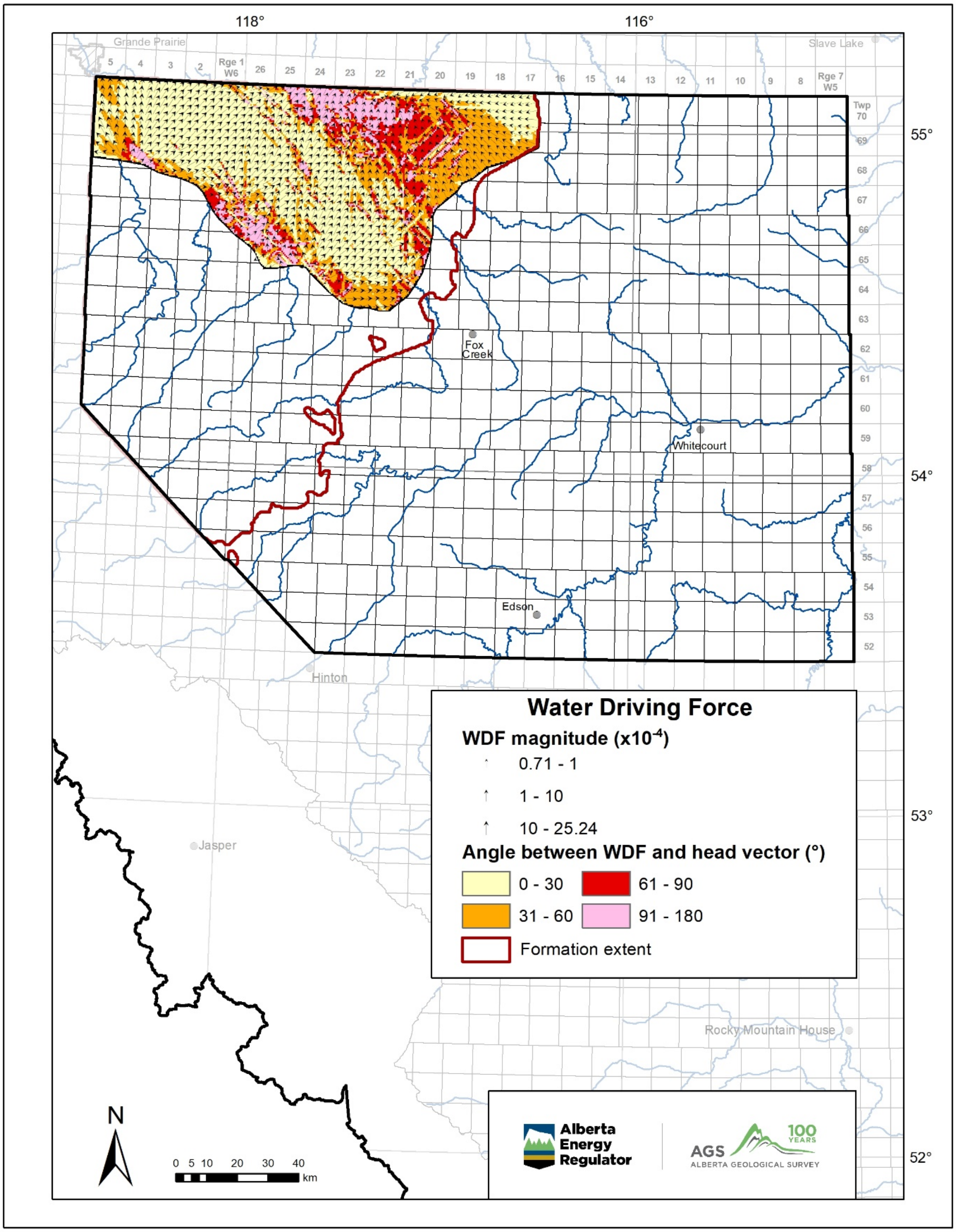

Figure 101. Water driving force (WDF) map for the Belloy aquifer, west-central Alberta study area.

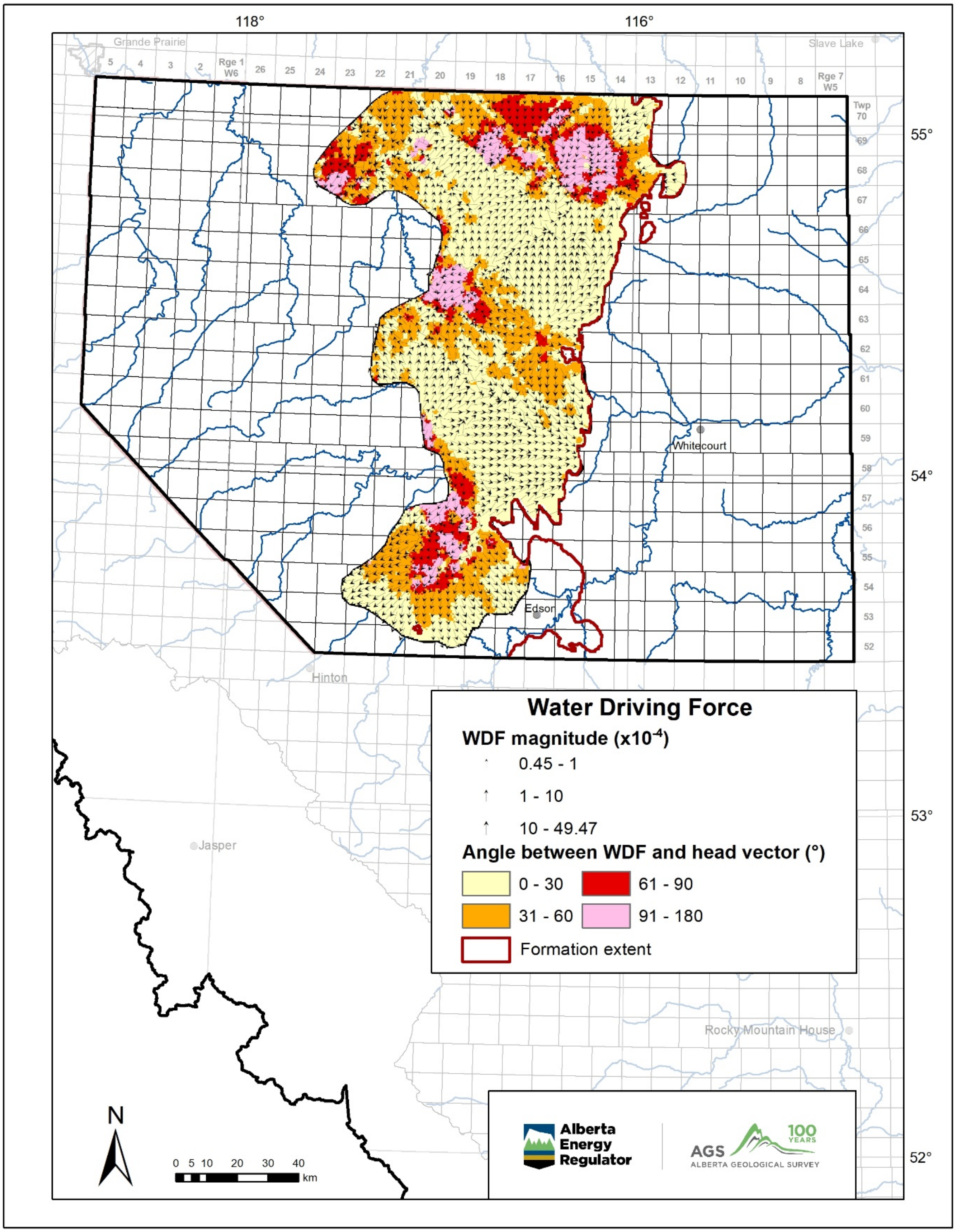

Figure 102. Water driving force (WDF) map for the Debolt aquifer, west-central Alberta study area.

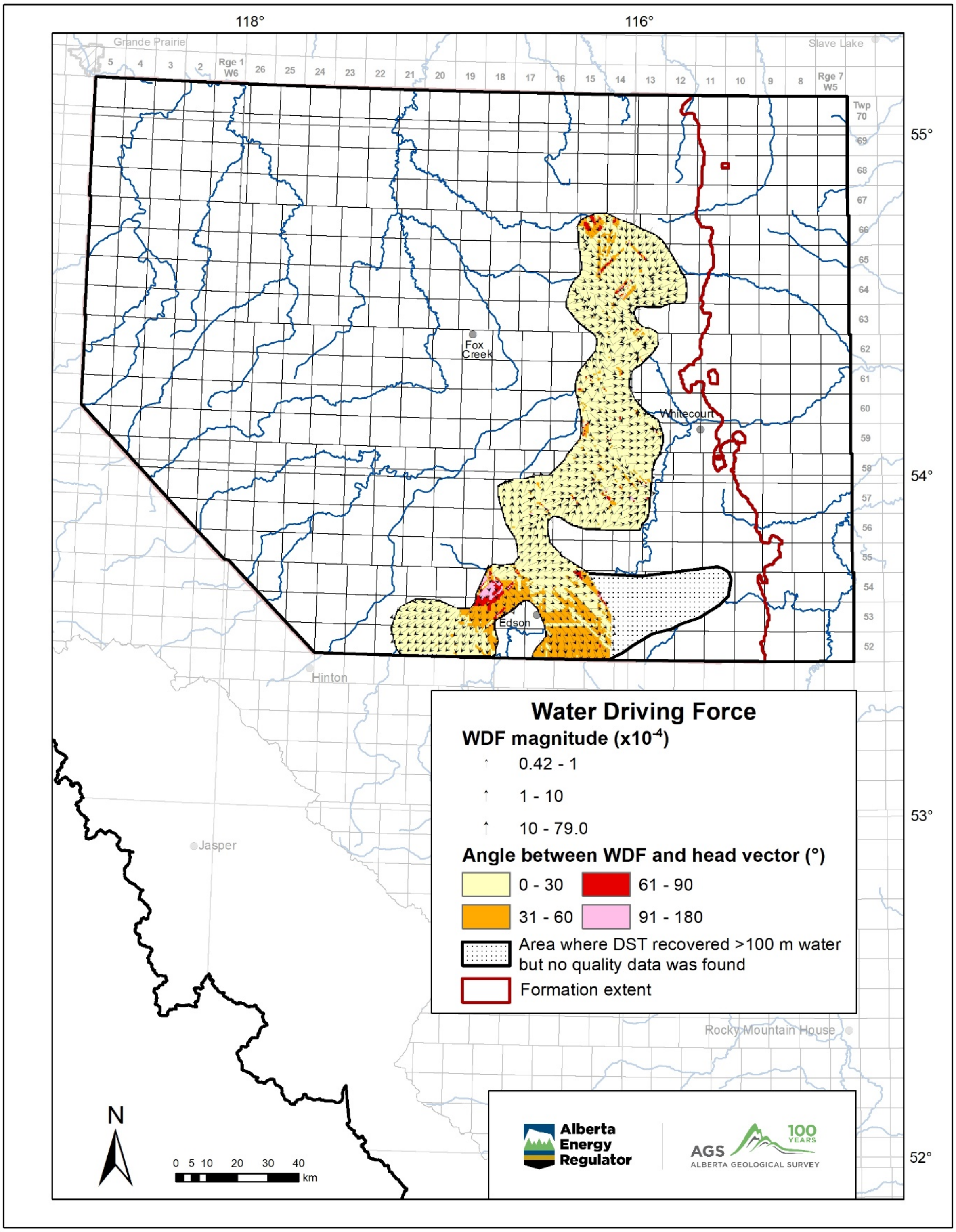

Figure 103. Water driving force (WDF) map for the Shunda aquifer, west-central Alberta study area. Abbreviation: DST, drillstem test.

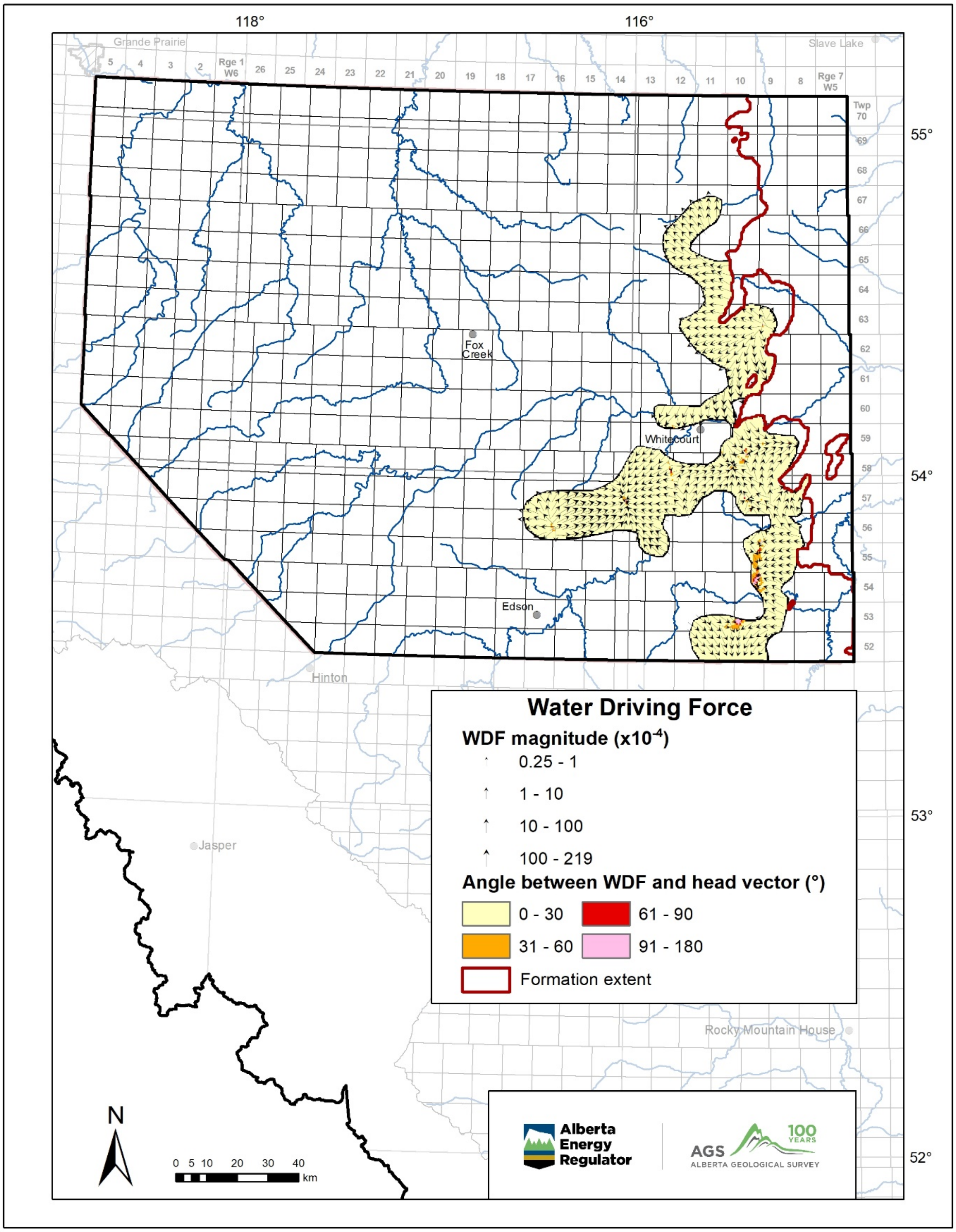

Figure 104. Water driving force (WDF) map for the Pekisko aquifer, west-central Alberta study area.

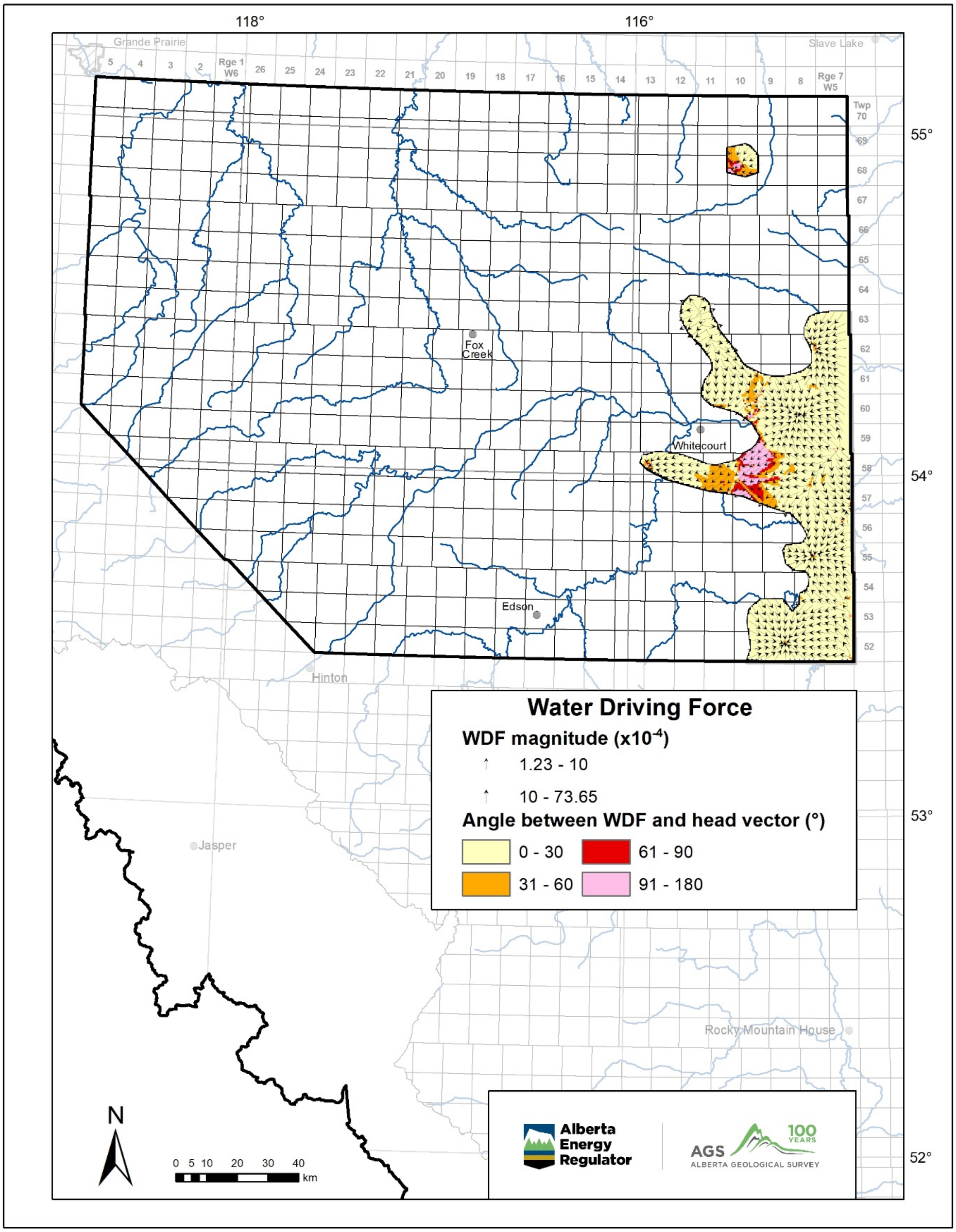

Figure 105. Water driving force (WDF) map for the Banff aquifer, west-central Alberta study area.

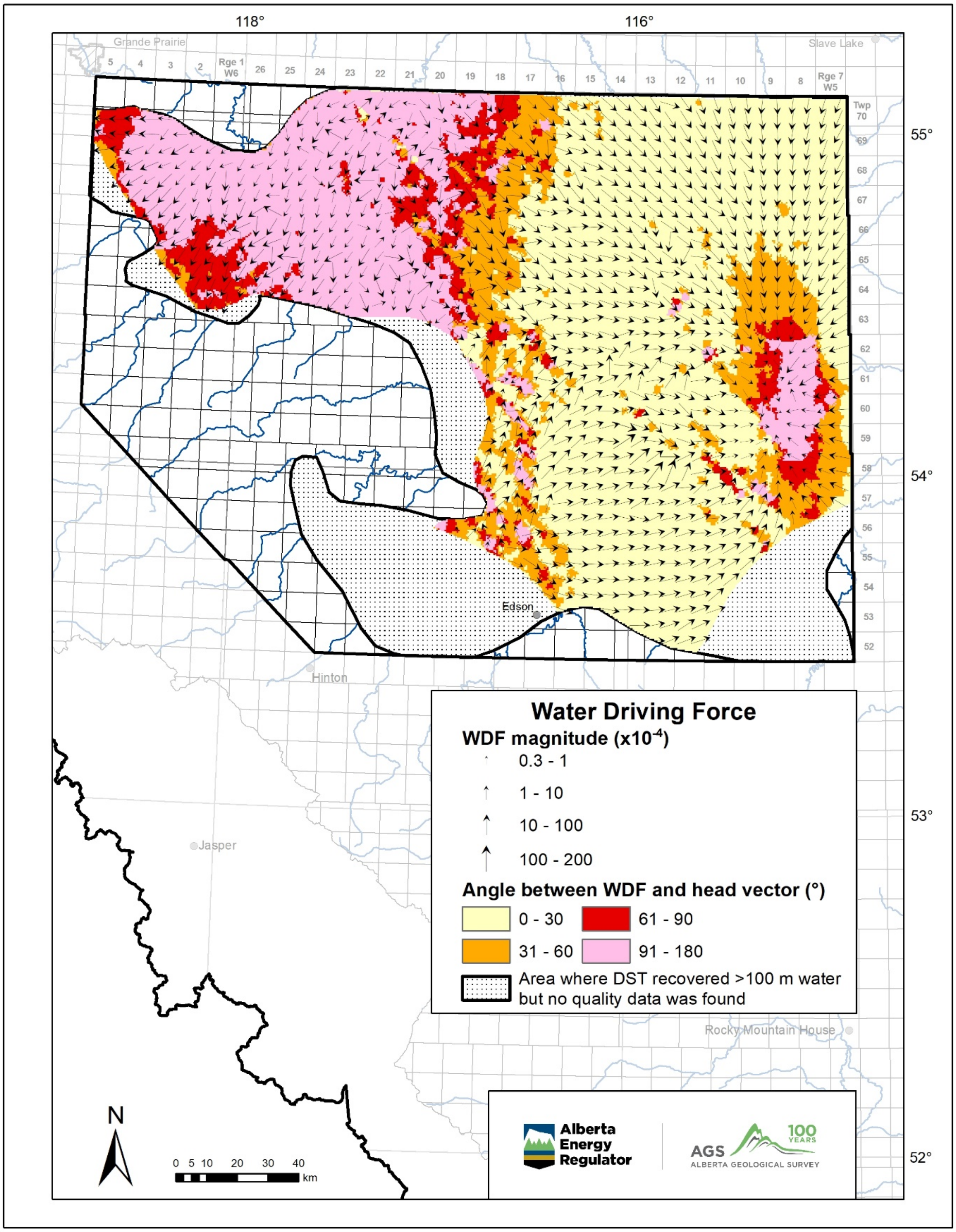

Figure 106. Water driving force (WDF) map for the Wabamun aquifer, west-central Alberta study area. Abbreviation: DST, drillstem test.

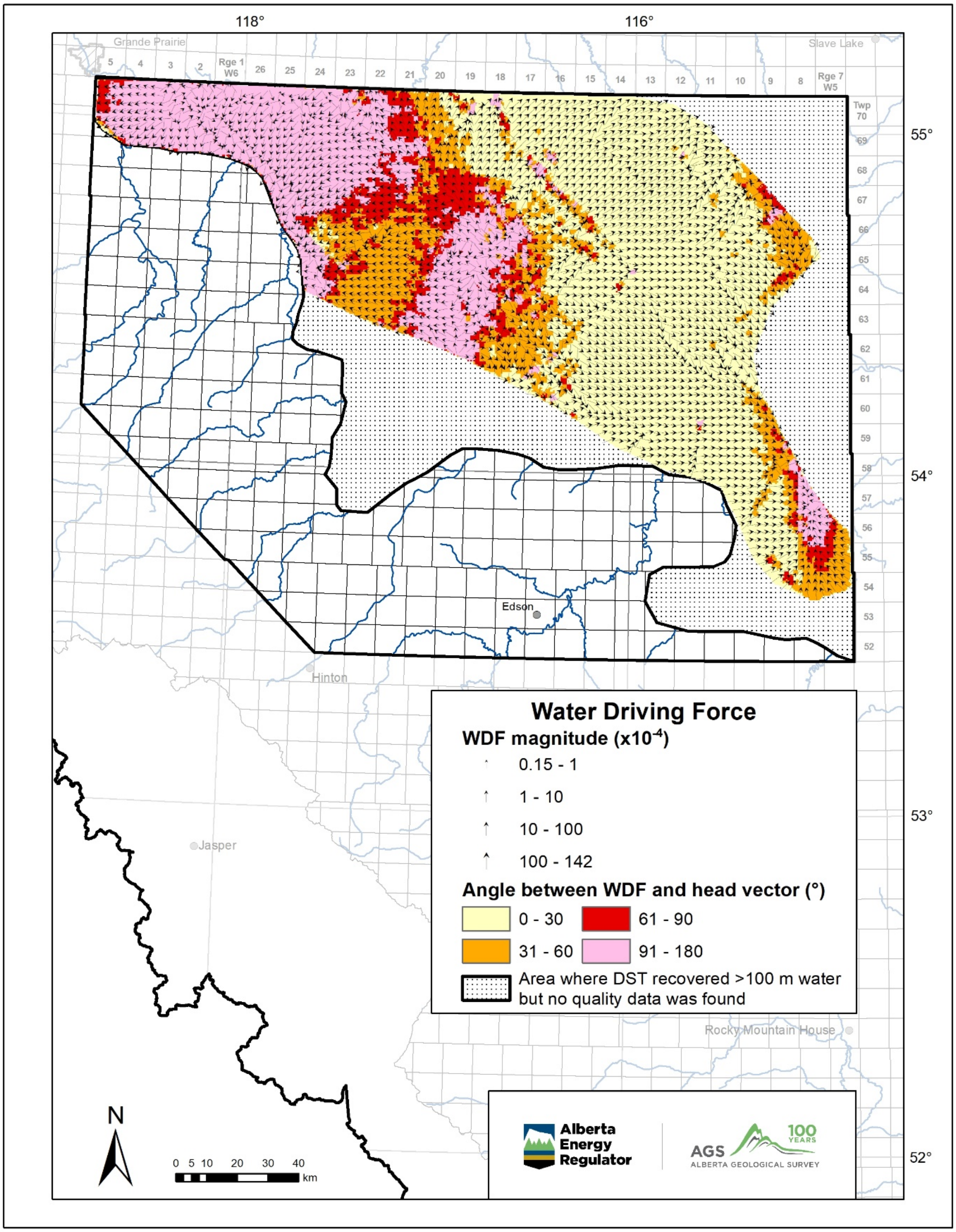

Figure 107. Water driving force (WDF) map for the Blue Ridge aquifer, west-central Alberta study area. Abbreviation: DST, drillstem test.

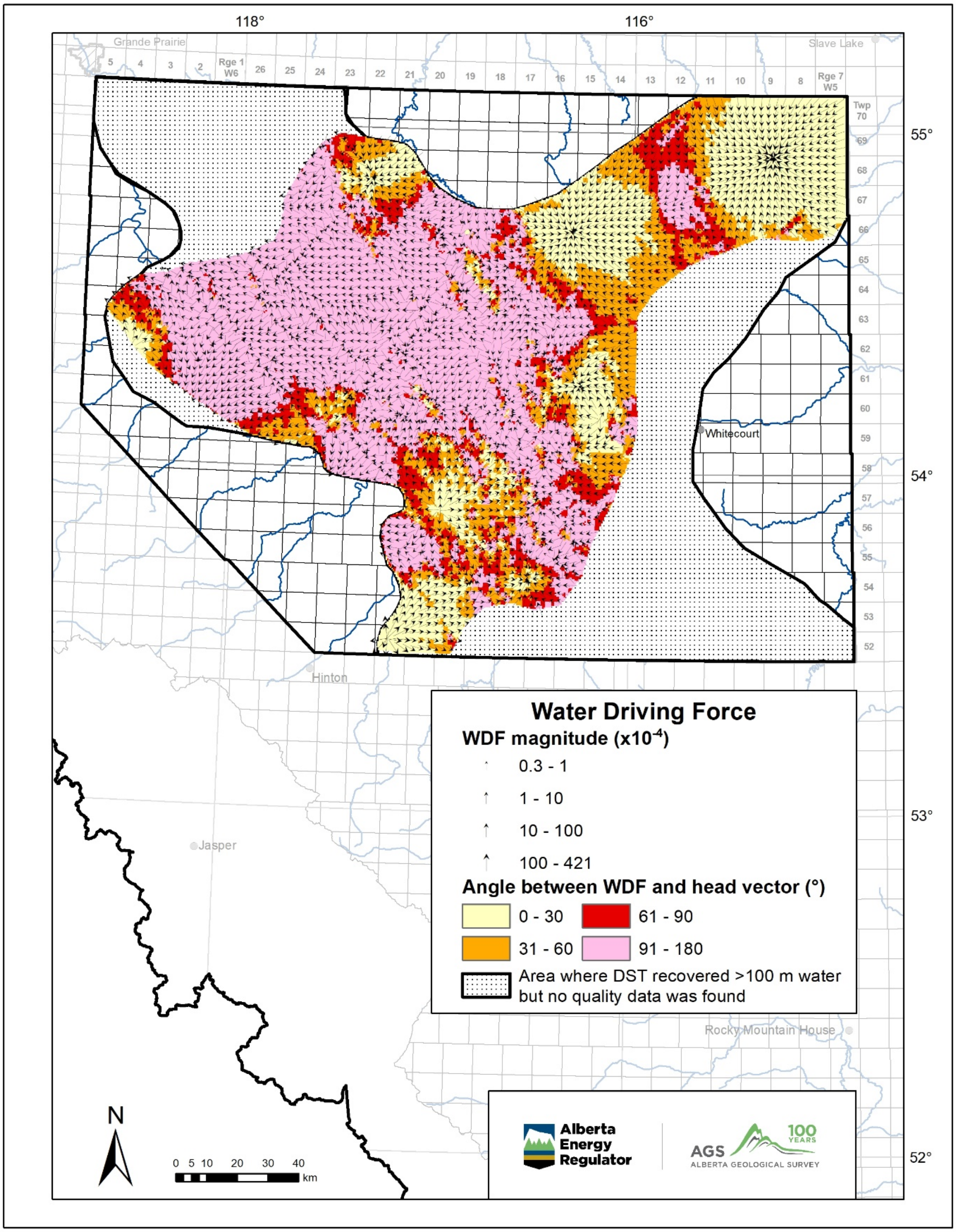

Figure 108. Water driving force (WDF) map for the Nisku aquifer, west-central Alberta study area. Abbreviation: DST, drillstem test.

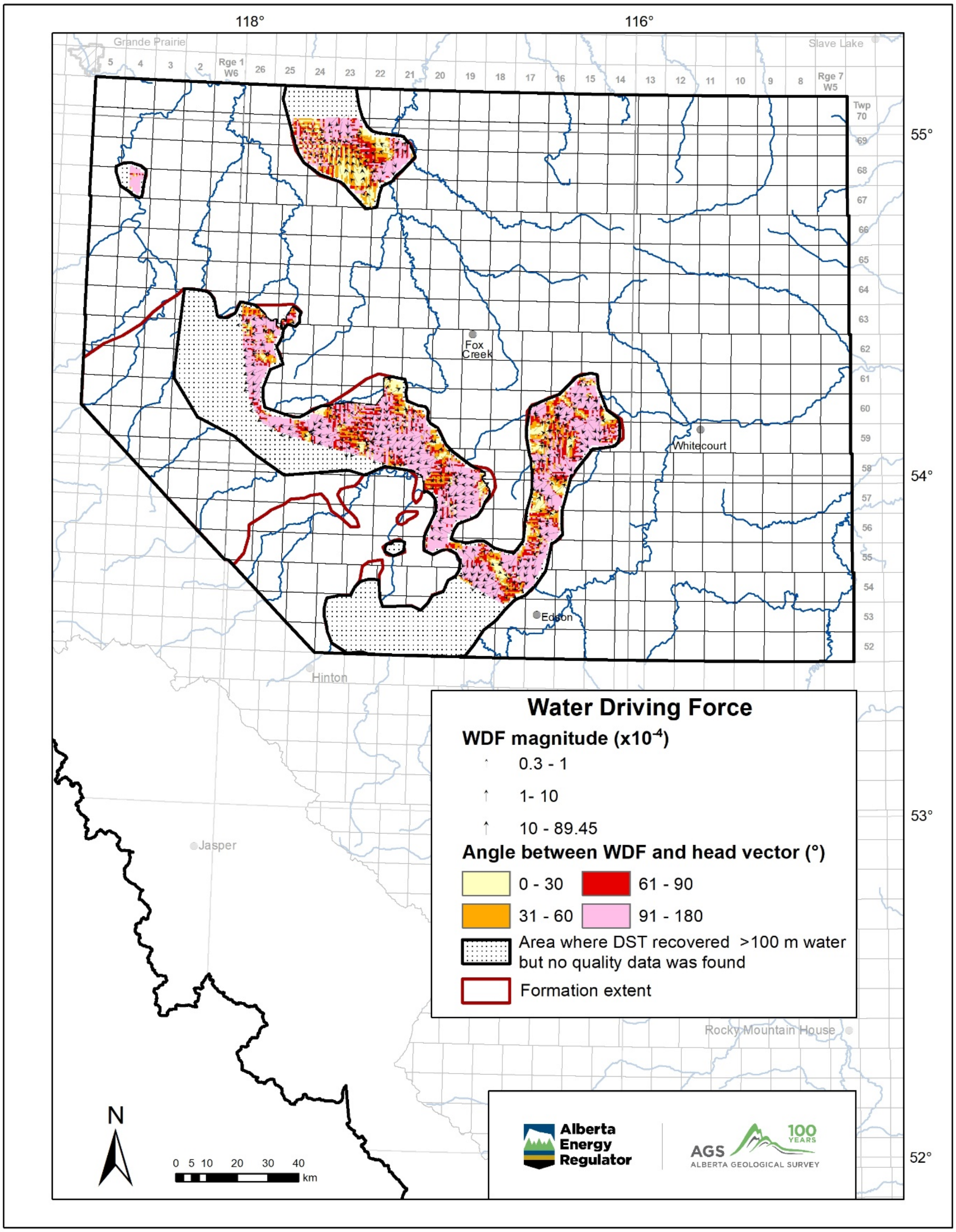

Figure 109. Water driving force (WDF) map for the Leduc aquifer, west-central Alberta study area. Abbreviation: DST, drillstem test.

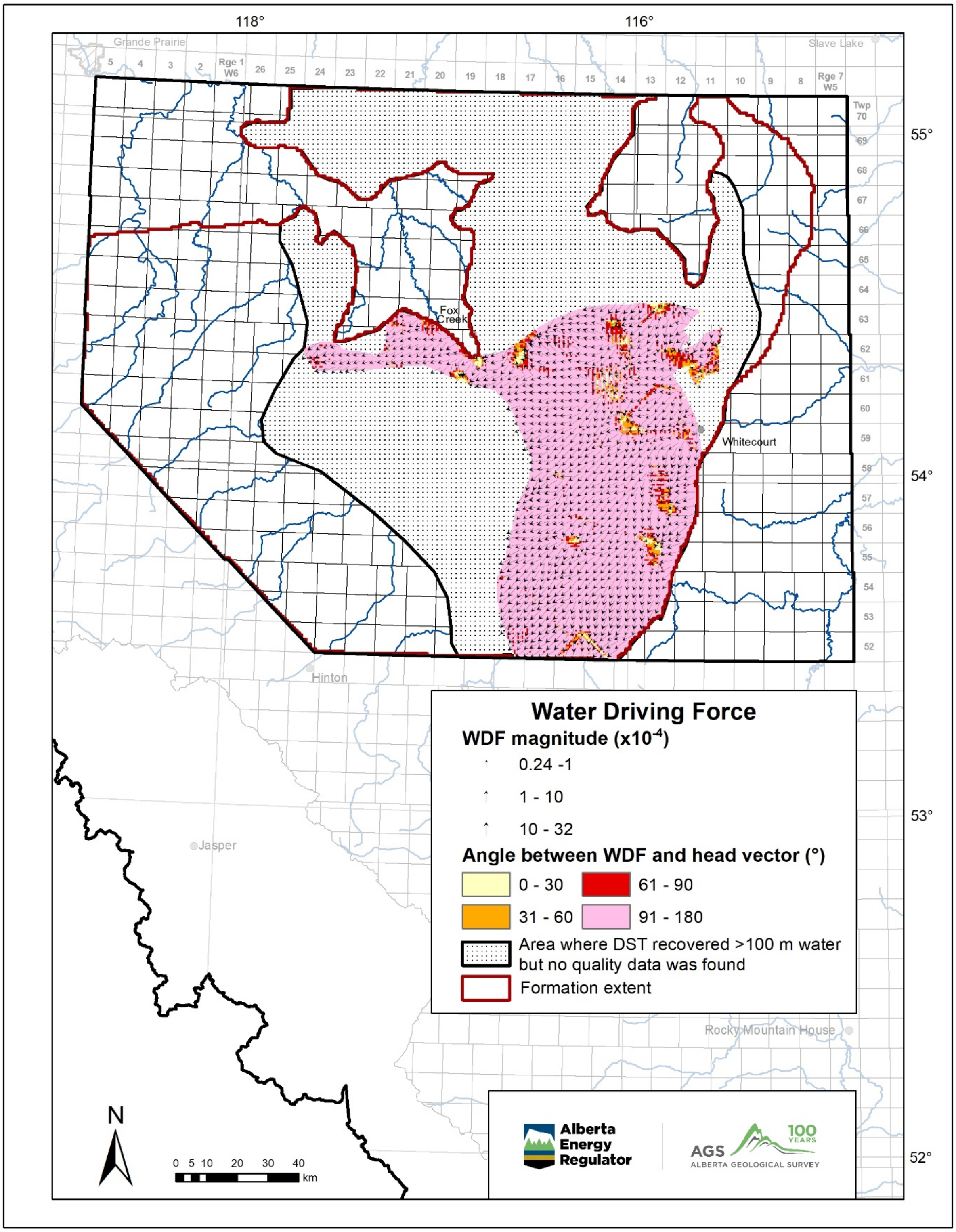

Figure 110. Water driving force (WDF) map for the Swan Hills aquifer, west-central Alberta study area. Abbreviation: DST, drillstem test.

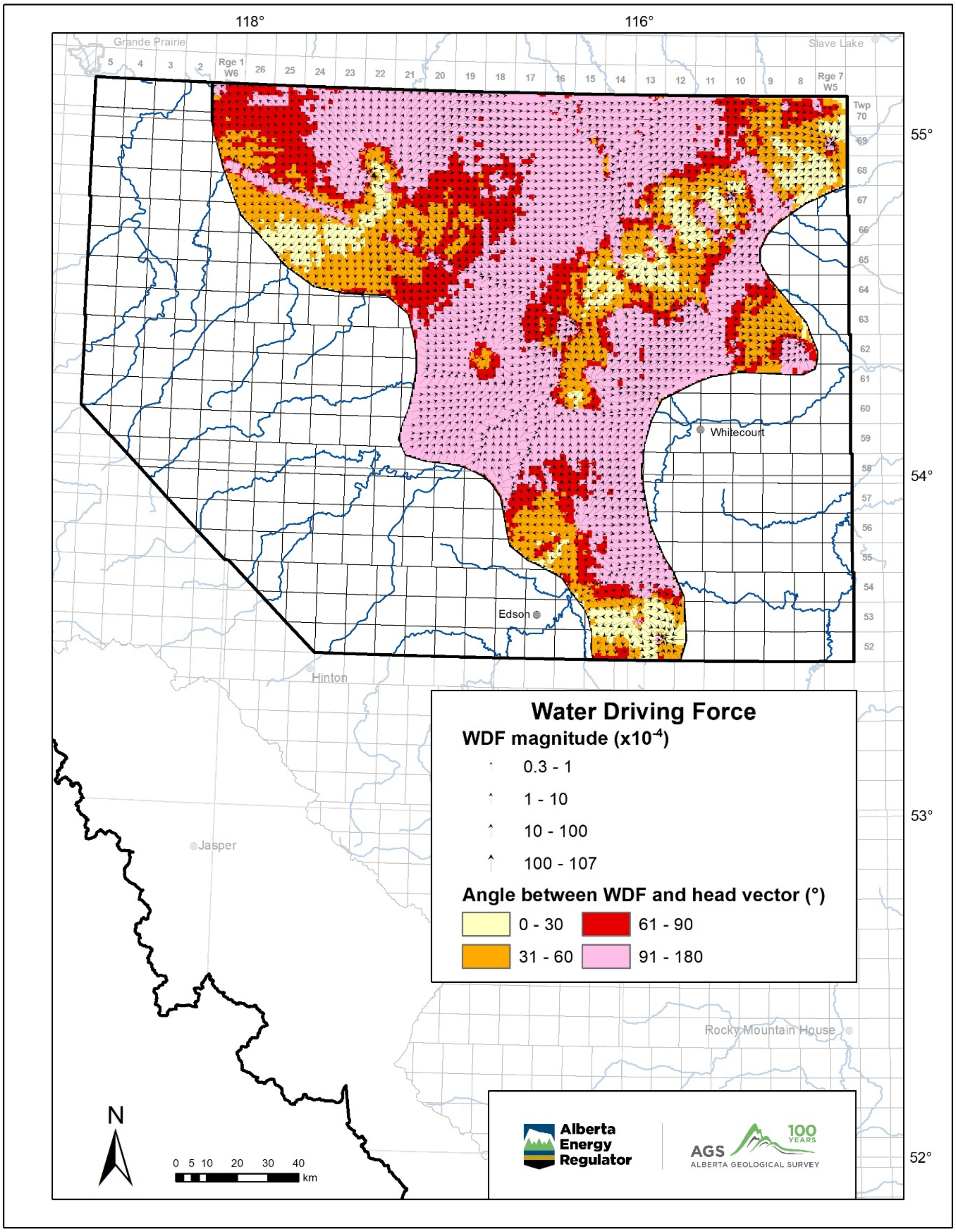

Figure 111. Water driving force (WDF) map for the Cambrian aquifer, west-central Alberta study area.

Appendix 2 – Water Chemistry Plots

2.1 Piper Plots

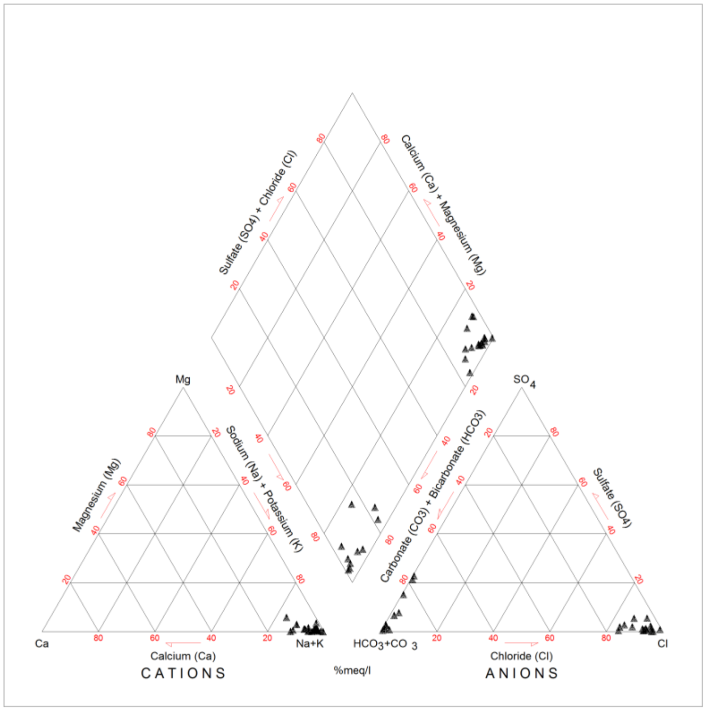

Figure 112. Piper plot for the Wapiti aquifer, west-central Alberta study area. Abbreviation: meq, milliequivalent.

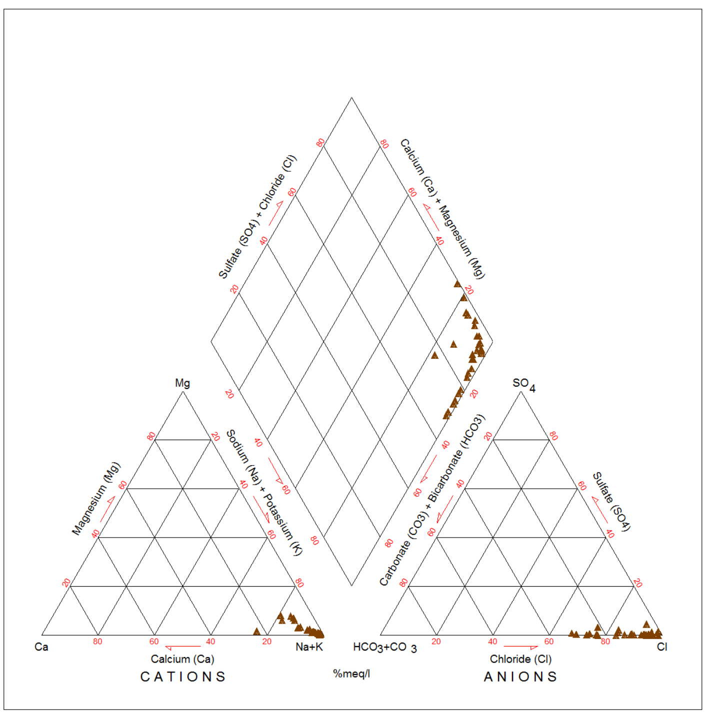

Figure 113. Piper plot for the Cardium aquifer, west-central Alberta study area. Abbreviation: meq, milliequivalent.

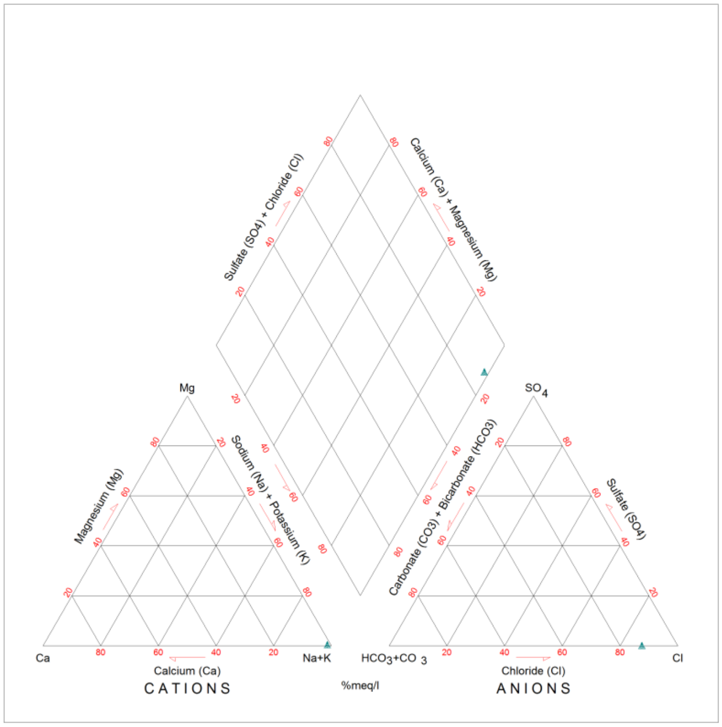

Figure 114. Piper plot for the Dunvegan aquifer, west-central Alberta study area. Abbreviation: meq, milliequivalent.

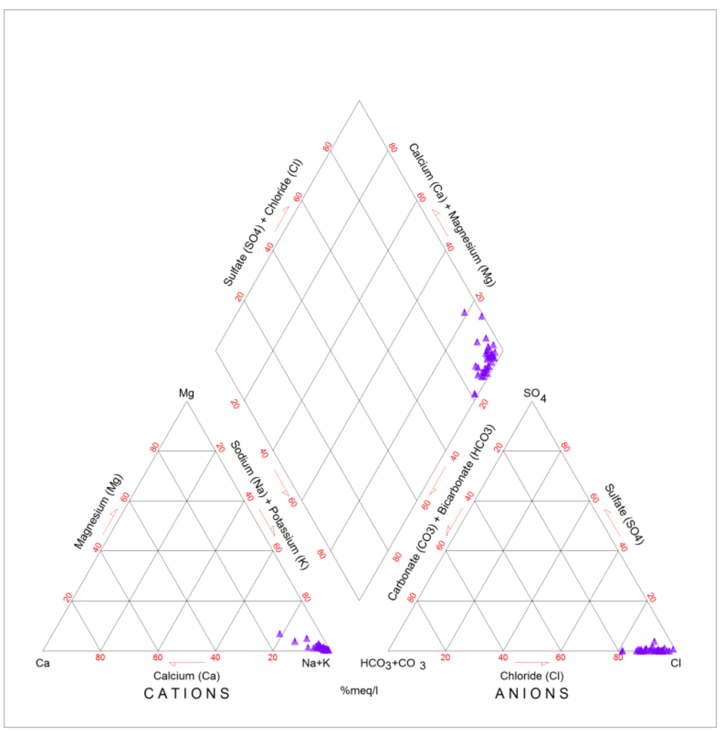

Figure 115. Piper plot for the Viking aquifer, west-central Alberta study area. Abbreviation: meq, milliequivalent.

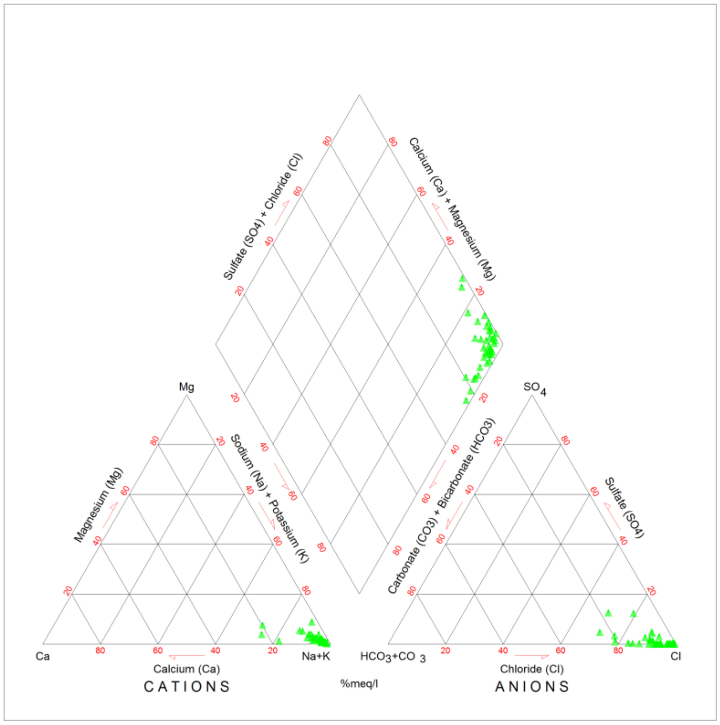

Figure 116. Piper plot for the Spirit River aquifer, west-central Alberta study area. Abbreviation: meq, milliequivalent.

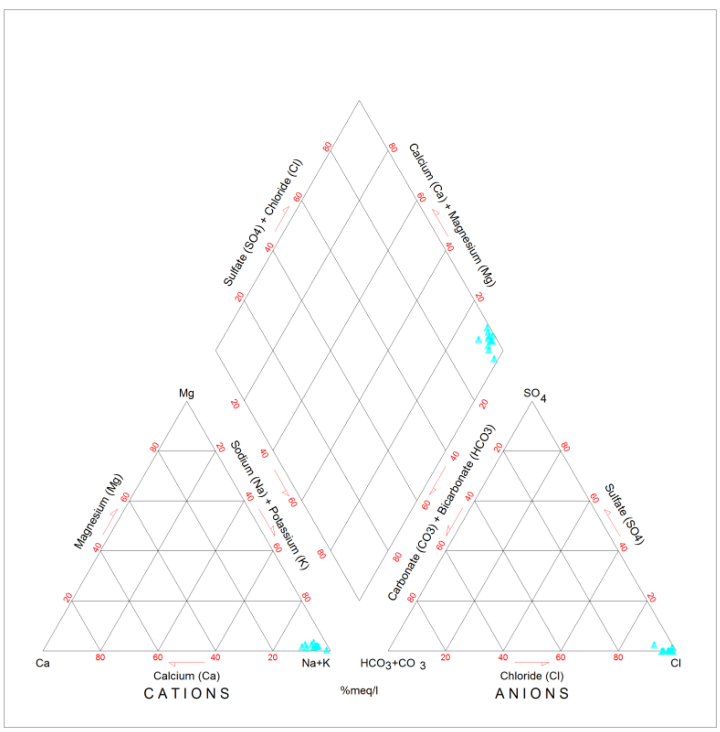

Figure 117. Piper plot for the Bluesky aquifer, west-central Alberta study area. Abbreviation: meq, milliequivalent.

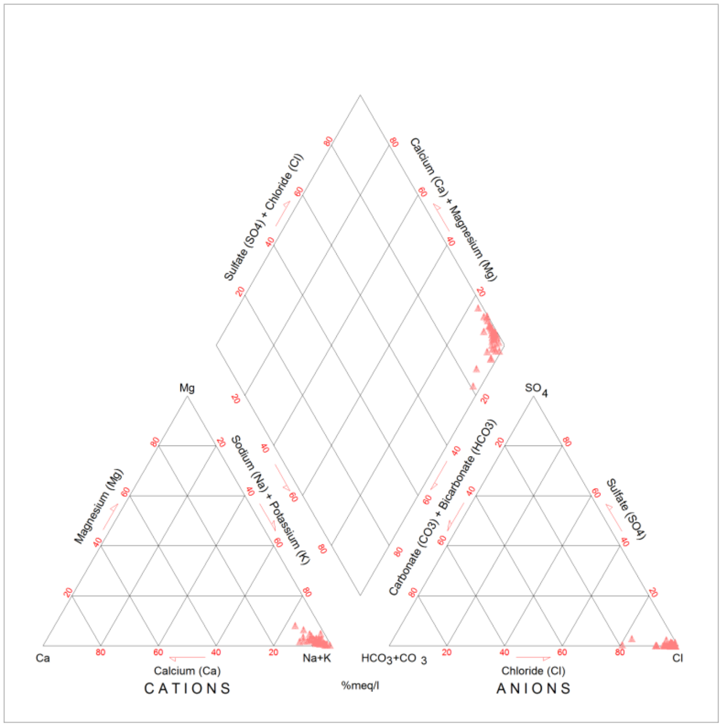

Figure 118. Piper plot for the Gething aquifer, west-central Alberta study area. Abbreviation: meq, milliequivalent.

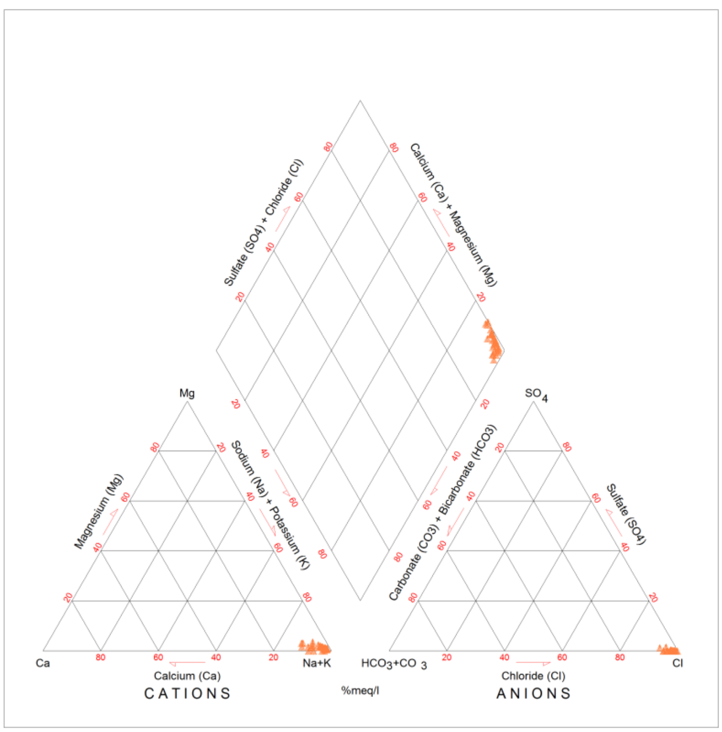

Figure 119. Piper plot for the Cadomin aquifer, west-central Alberta study area. Abbreviation: meq, milliequivalent.

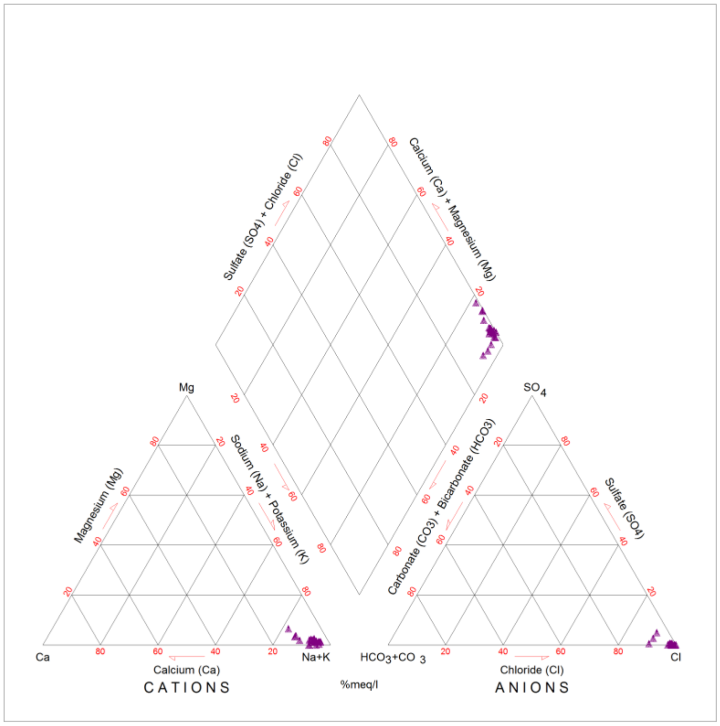

Figure 120. Piper plot for the Nordegg aquifer, west-central Alberta study area. Abbreviation: meq, milliequivalent.

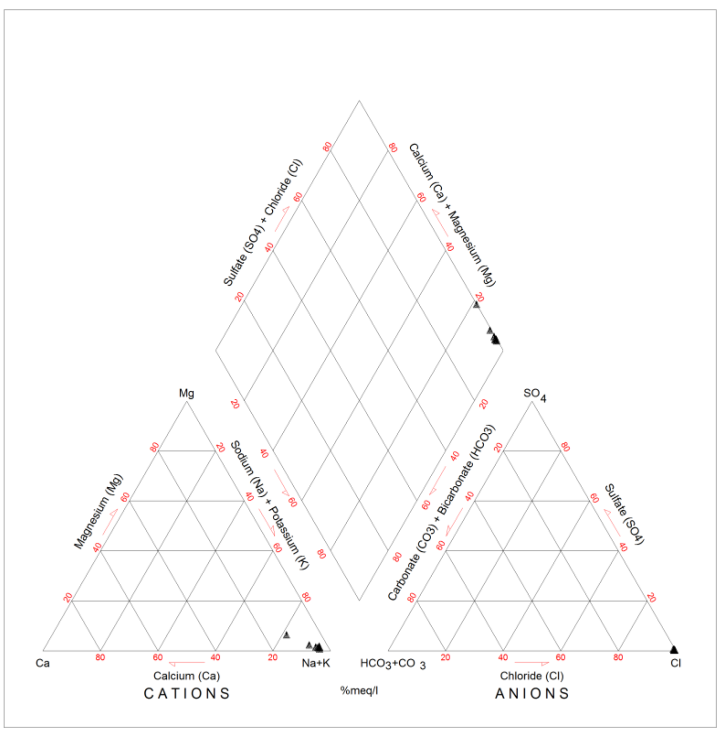

Figure 121. Piper plot for the Middle–Upper Triassic aquifer, west-central Alberta study area. Abbreviation: meq, milliequivalent.

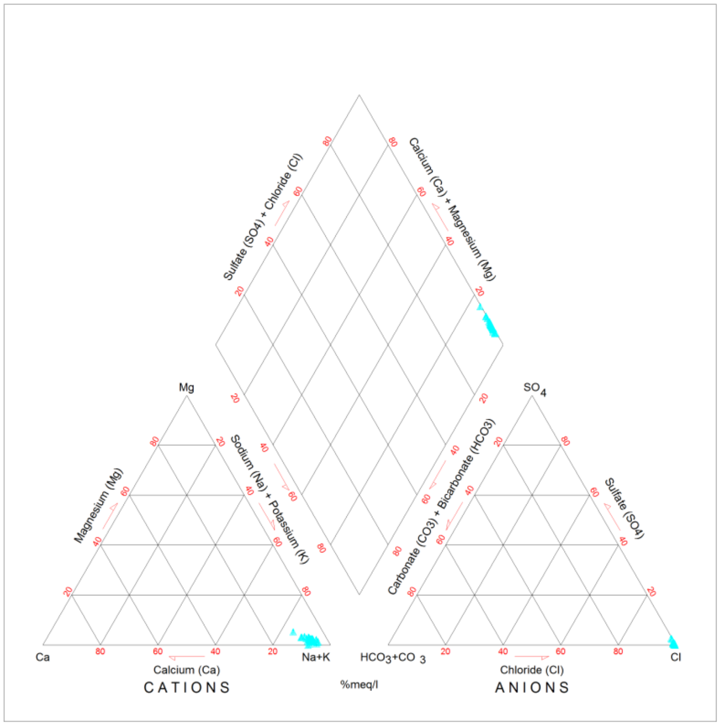

Figure 122. Piper plot for the Montney aquifer, west-central Alberta study area. Abbreviation: meq, milliequivalent.

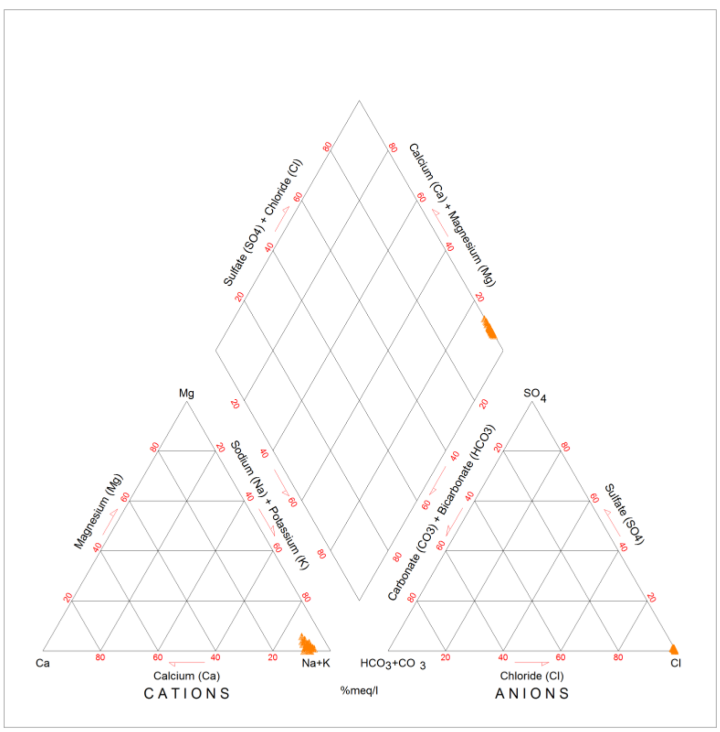

Figure 123. Piper plot for the Belloy aquifer, west-central Alberta study area. Abbreviation: meq, milliequivalent.

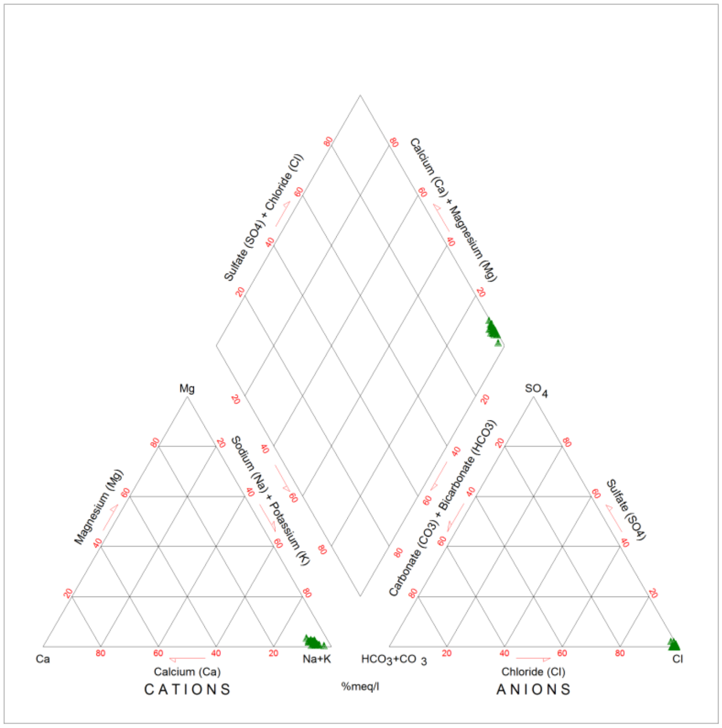

Figure 124. Piper plot for the Debolt aquifer, west-central Alberta study area. Abbreviation: meq, milliequivalent.

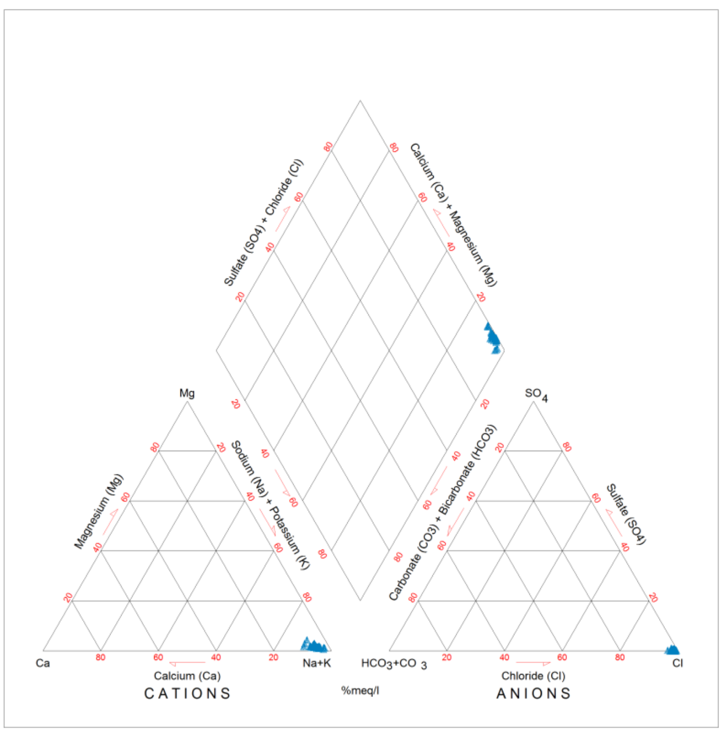

Figure 125. Piper plot for the Shunda aquifer, west-central Alberta study area. Abbreviation: meq, milliequivalent.

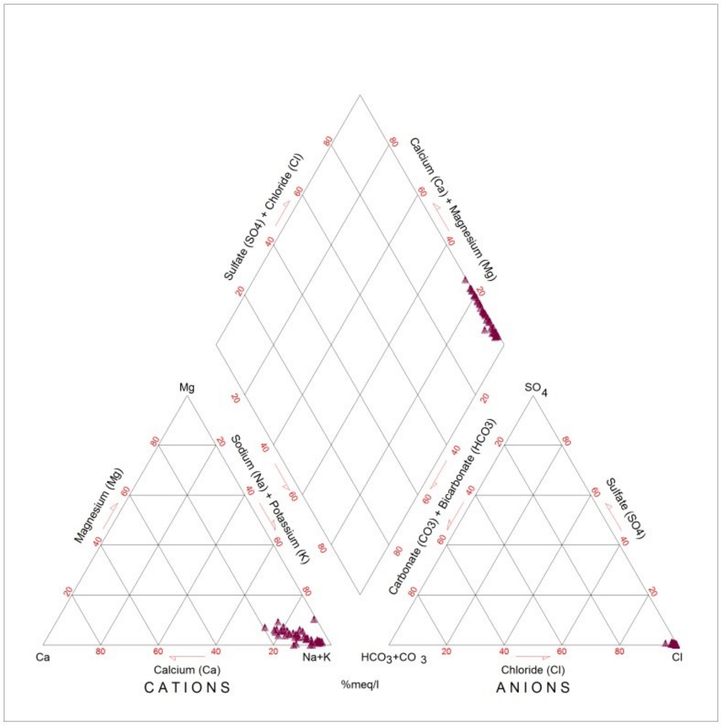

Figure 126. Piper plot for the Pekisko aquifer, west-central Alberta study area. Abbreviation: meq, milliequivalent.

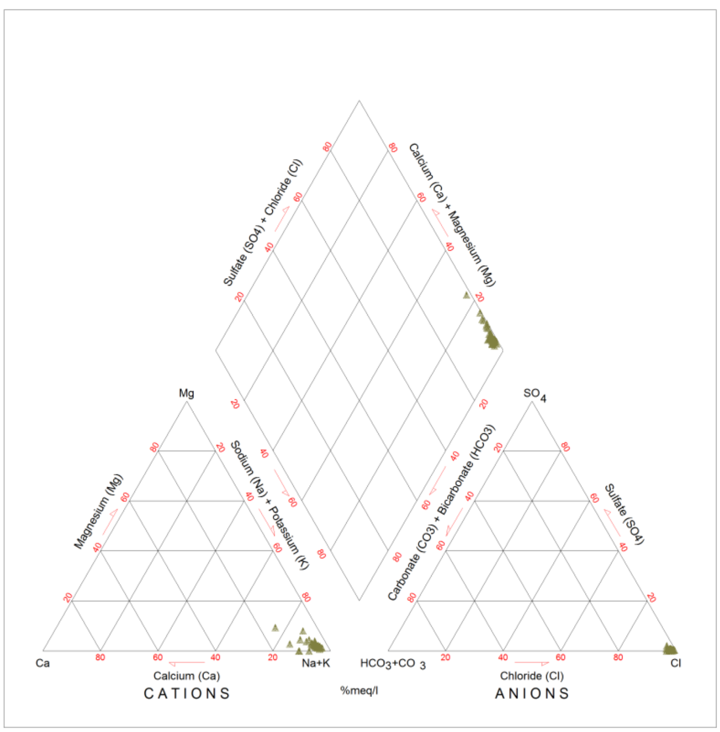

Figure 127. Piper plot for the Banff aquifer, west-central Alberta study area. Abbreviation: meq, milliequivalent.

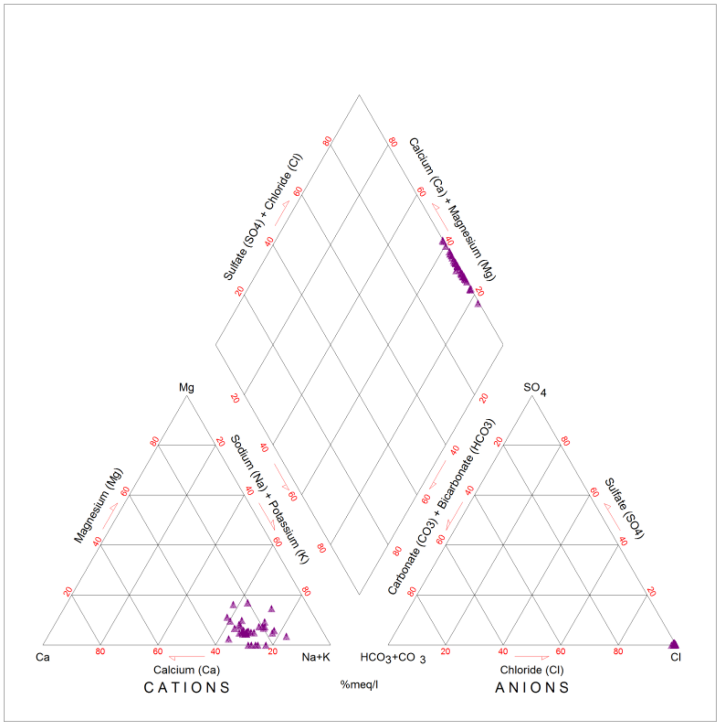

Figure 128. Piper plot for the Wabamun aquifer, west-central Alberta study area. Abbreviation: meq, milliequivalent.

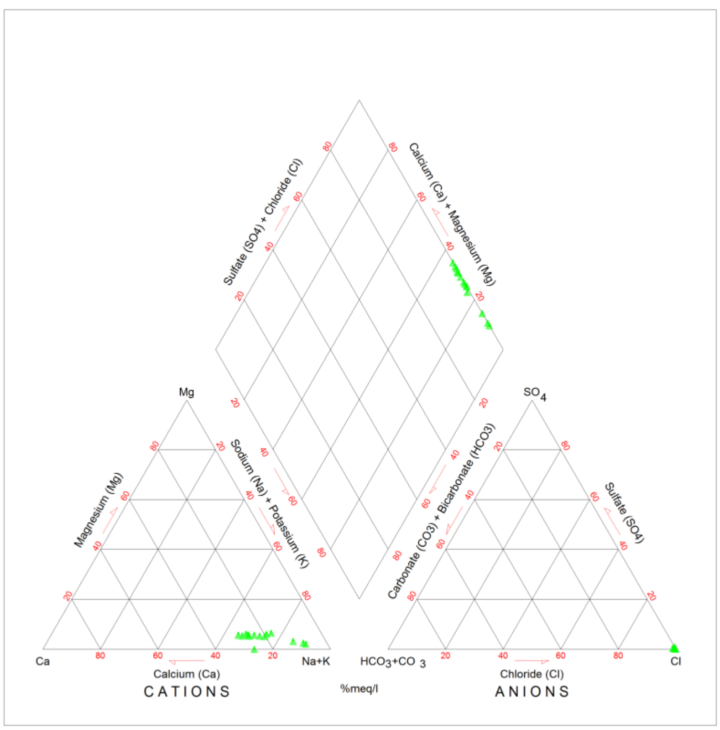

Figure 129. Piper plot for the Blue Ridge aquifer, west-central Alberta study area. Abbreviation: meq, milliequivalent.

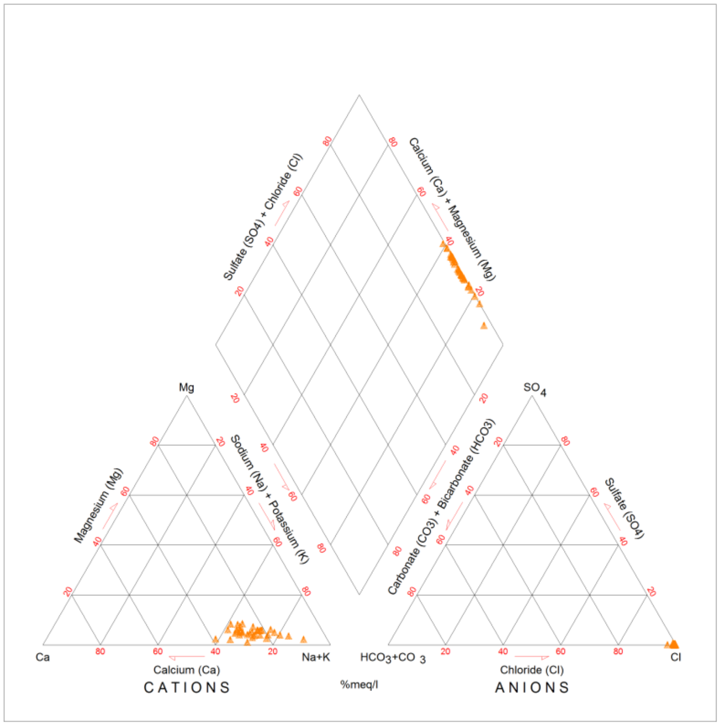

Figure 130. Piper plot for the Nisku aquifer, west-central Alberta study area. Abbreviation: meq, milliequivalent.

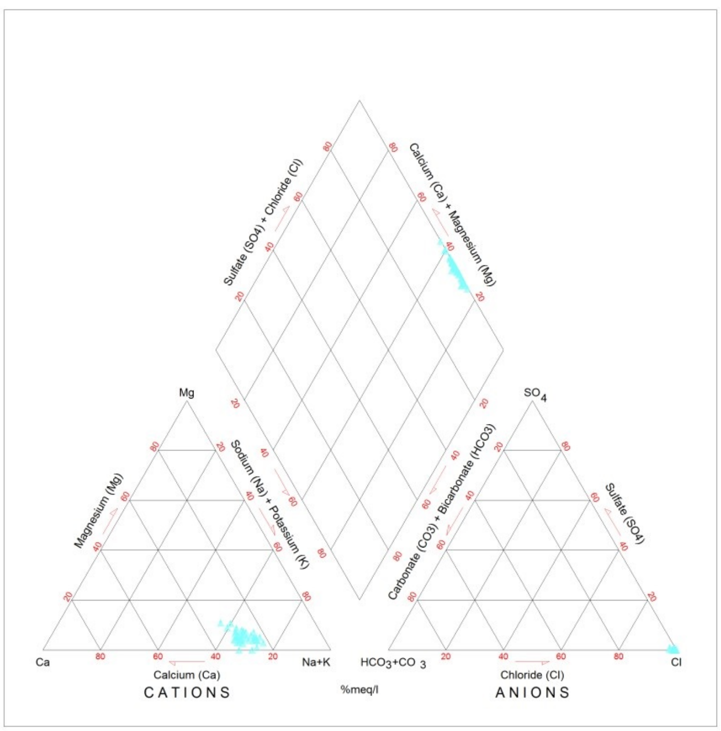

Figure 131. Piper plot for the Leduc aquifer, west-central Alberta study area. Abbreviation: meq, milliequivalent.

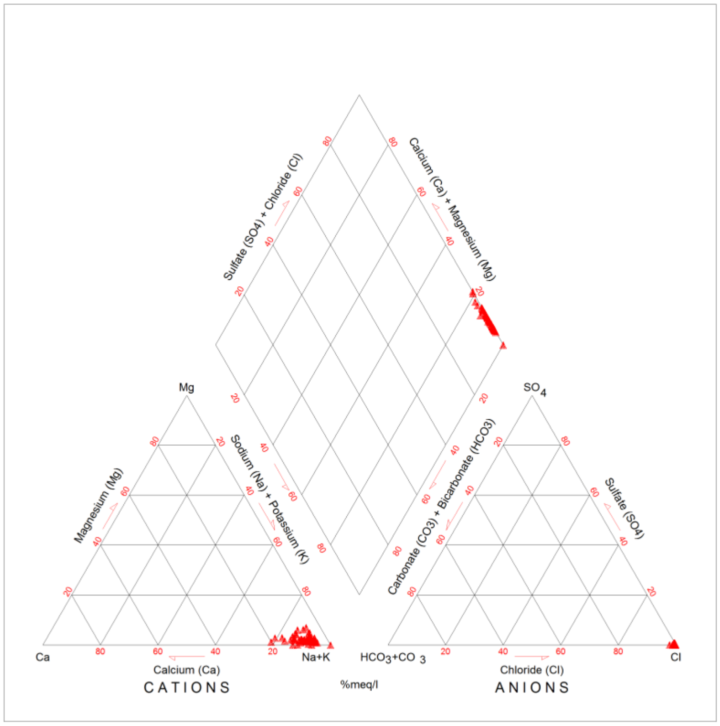

Figure 132. Piper plot for the Swan Hills aquifer, west-central Alberta study area. Abbreviation: meq, milliequivalent.

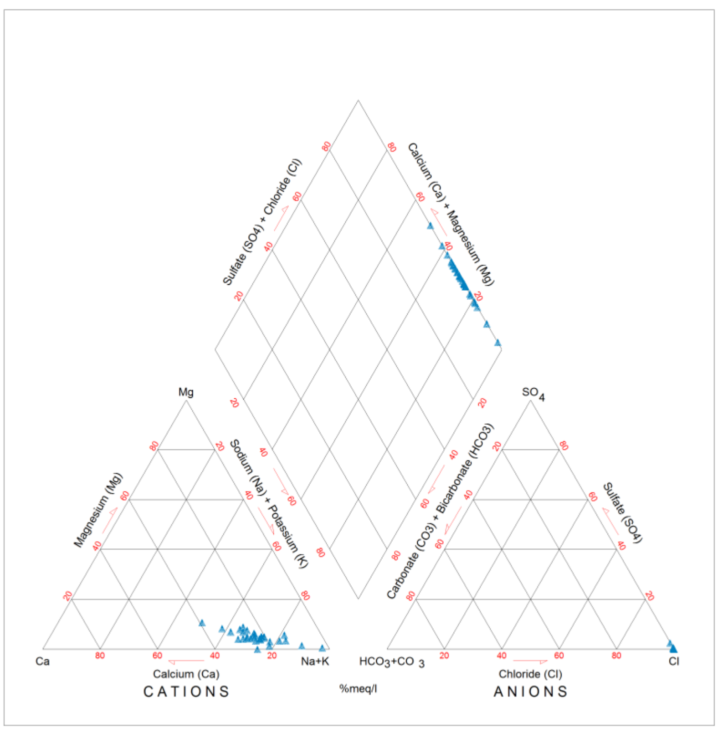

Figure 133. Piper plot for the Elk Point aquifer, west-central Alberta study area. Abbreviation: meq, milliequivalent.

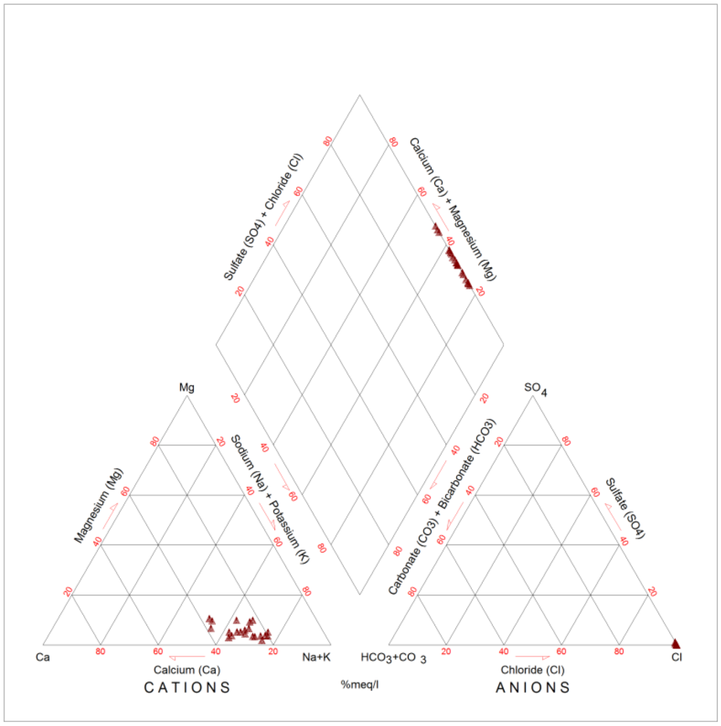

Figure 134. Piper plot for the Cambrian aquifer, west-central Alberta study area. Abbreviation: meq, milliequivalent.

2.2 Major Ion Plots

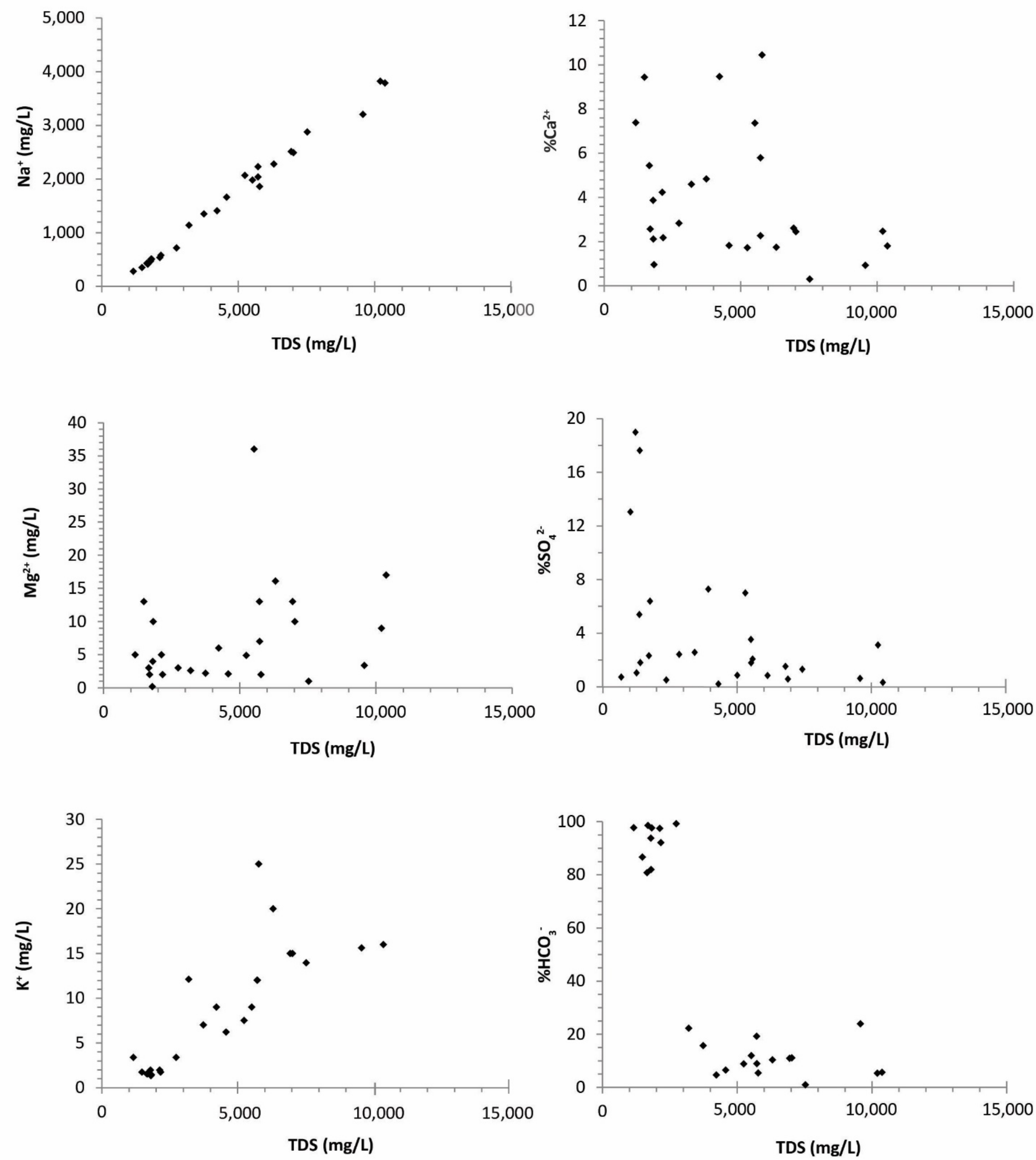

Figure 135. Major ion plots for the Wapiti aquifer, west-central Alberta study area. Abbreviation: TDS, total dissolved solids.

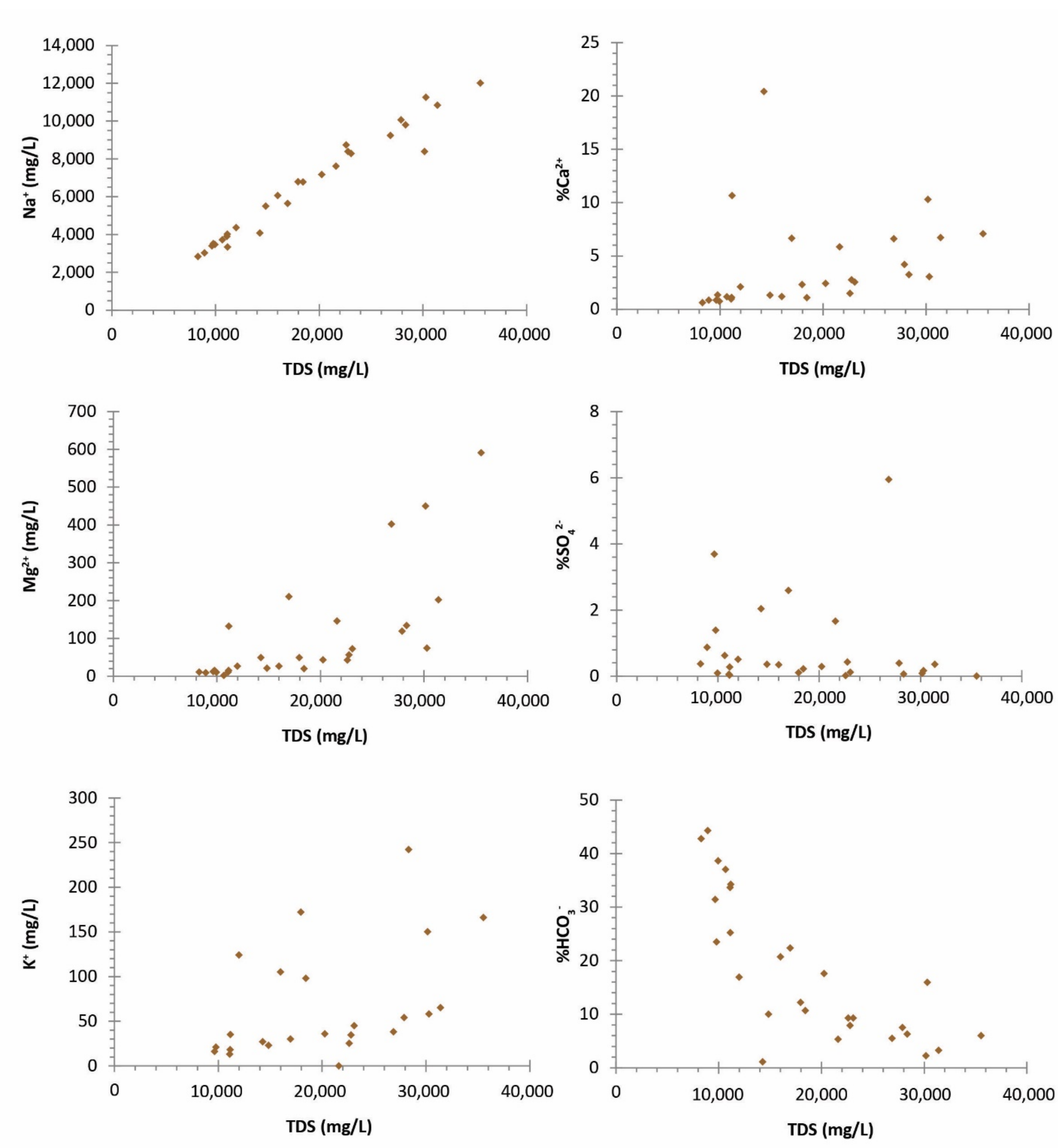

Figure 136. Major ion plots for the Cardium aquifer, west-central Alberta study area. Abbreviation: TDS, total dissolved solids.

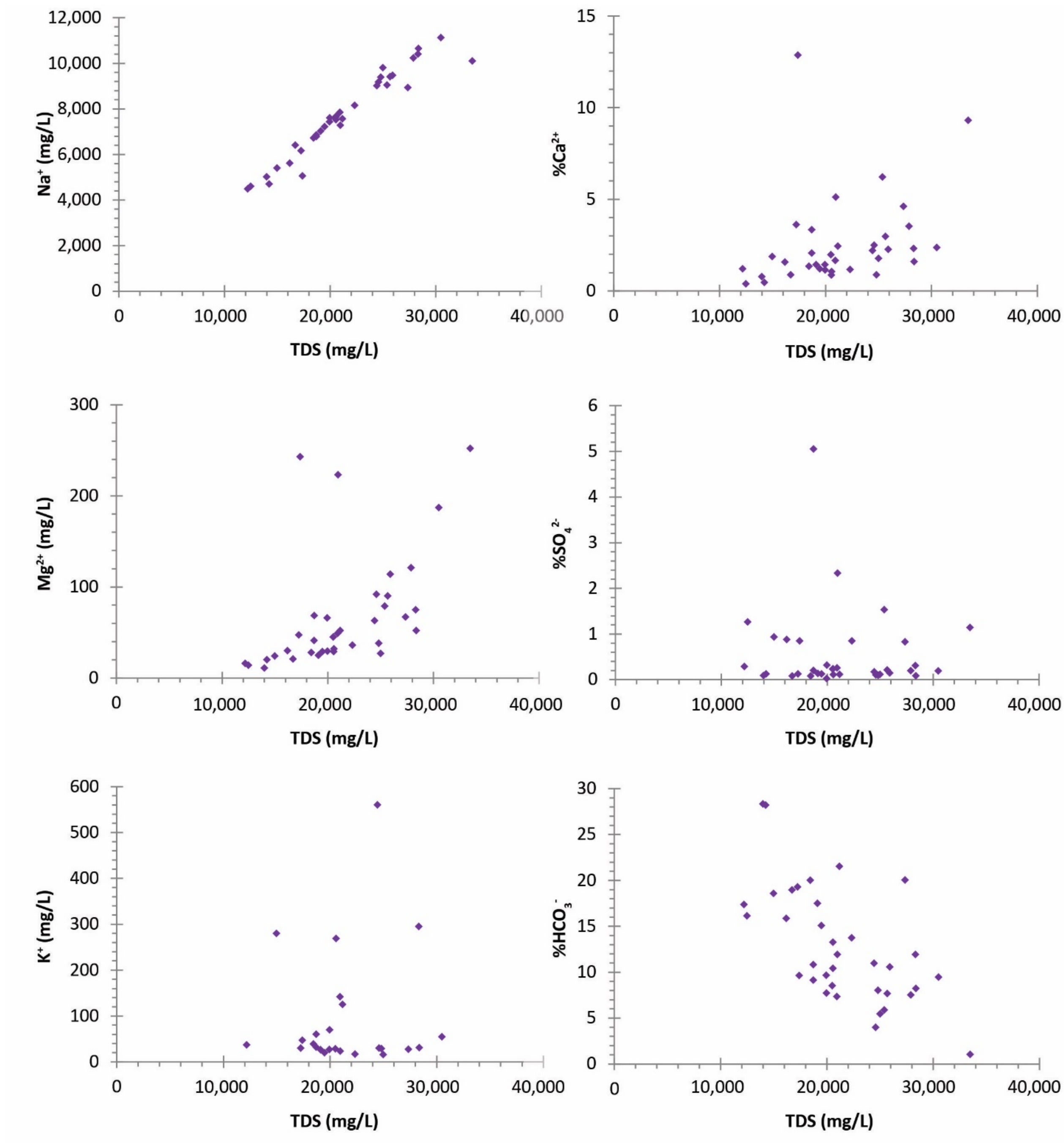

Figure 137. Major ion plots for the Viking aquifer, west-central Alberta study area. Abbreviation: TDS, total dissolved solids.

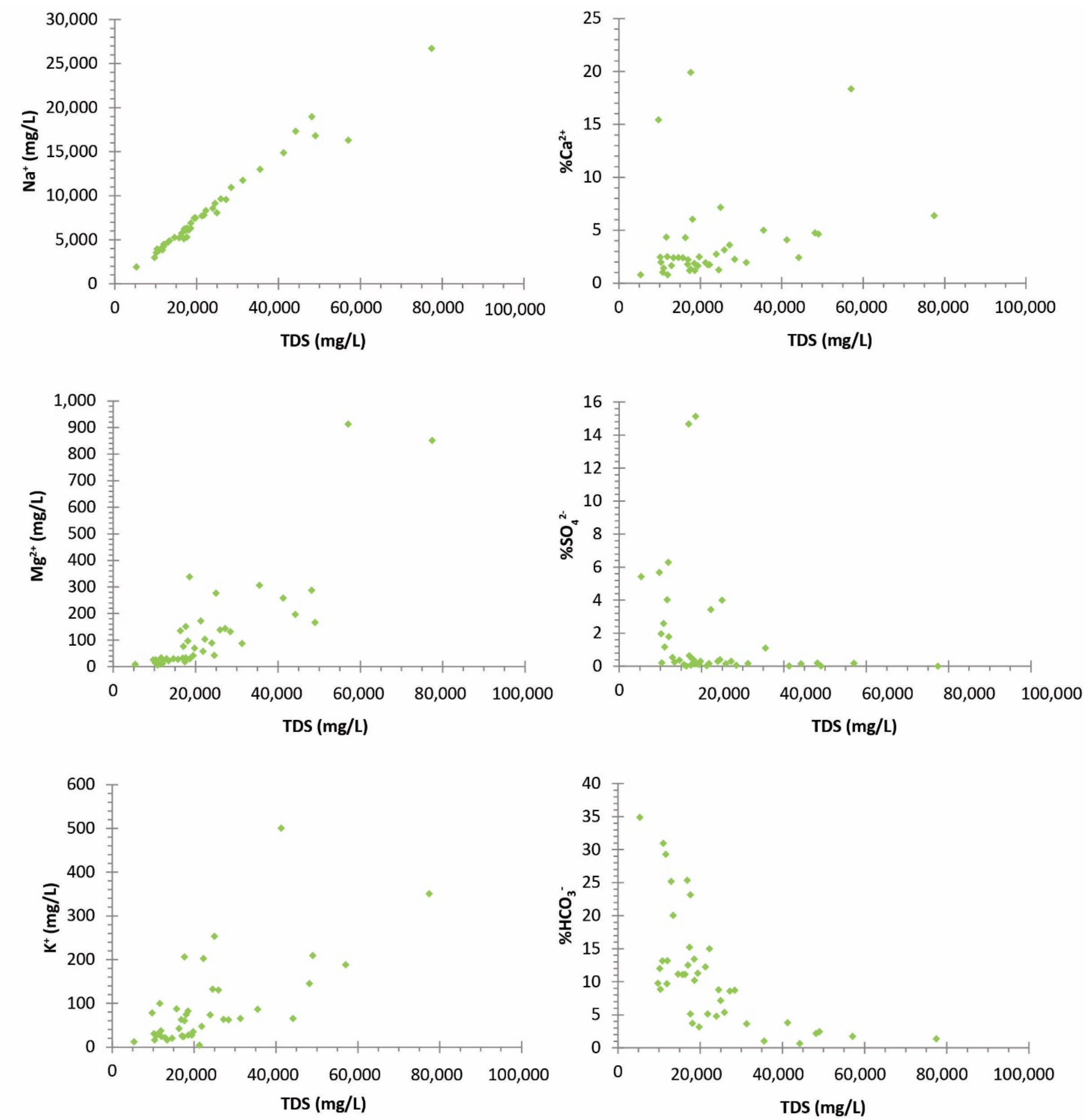

Figure 138. Major ion plots for the Spirit River aquifer, west-central Alberta study area. Abbreviation: TDS, total dissolved solids.

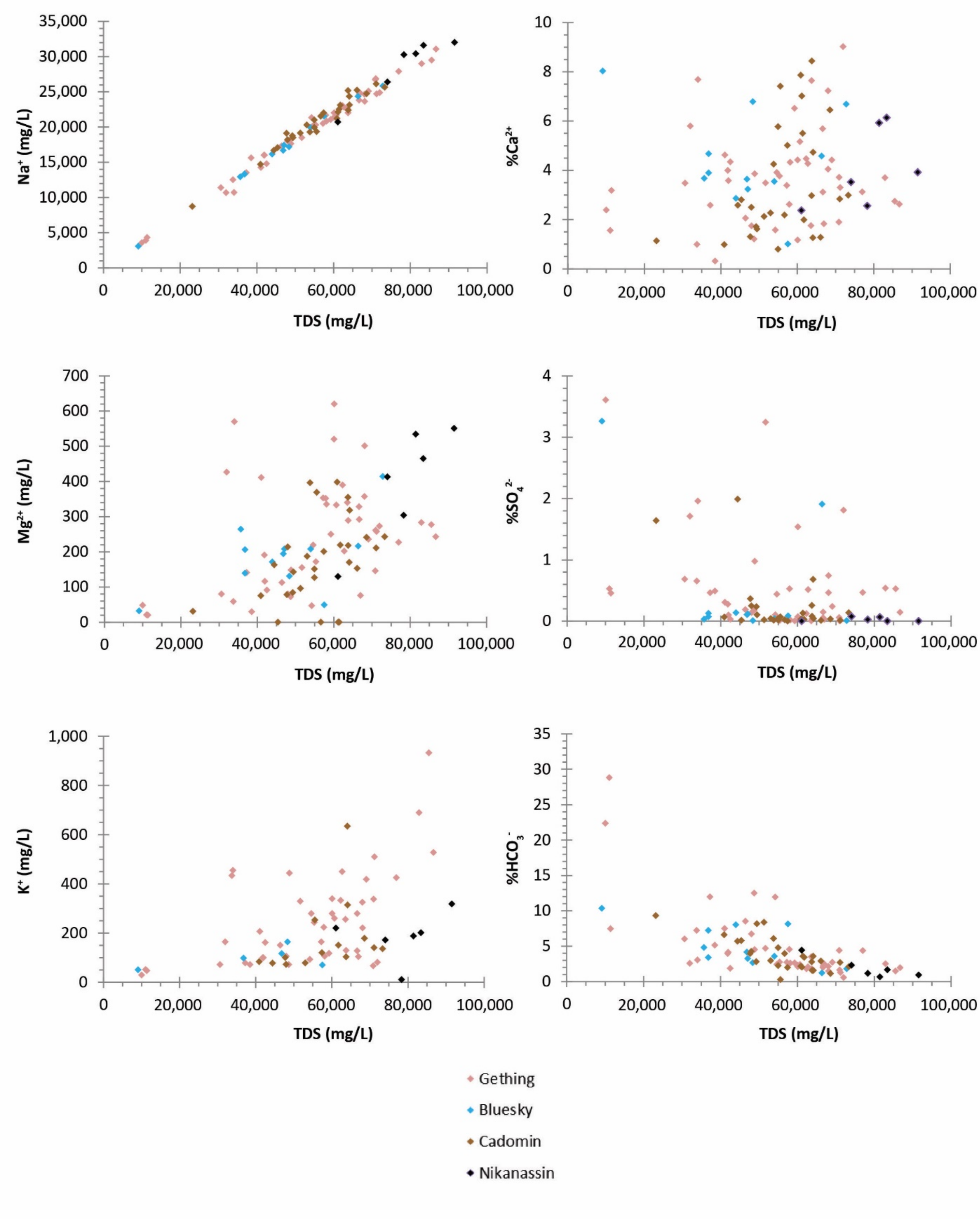

Figure 139. Major ion plots for the Bluesky, Gething, Cadomin, and Nikanassin aquifers, west-central Alberta study area. Abbreviation: TDS, total dissolved solids.

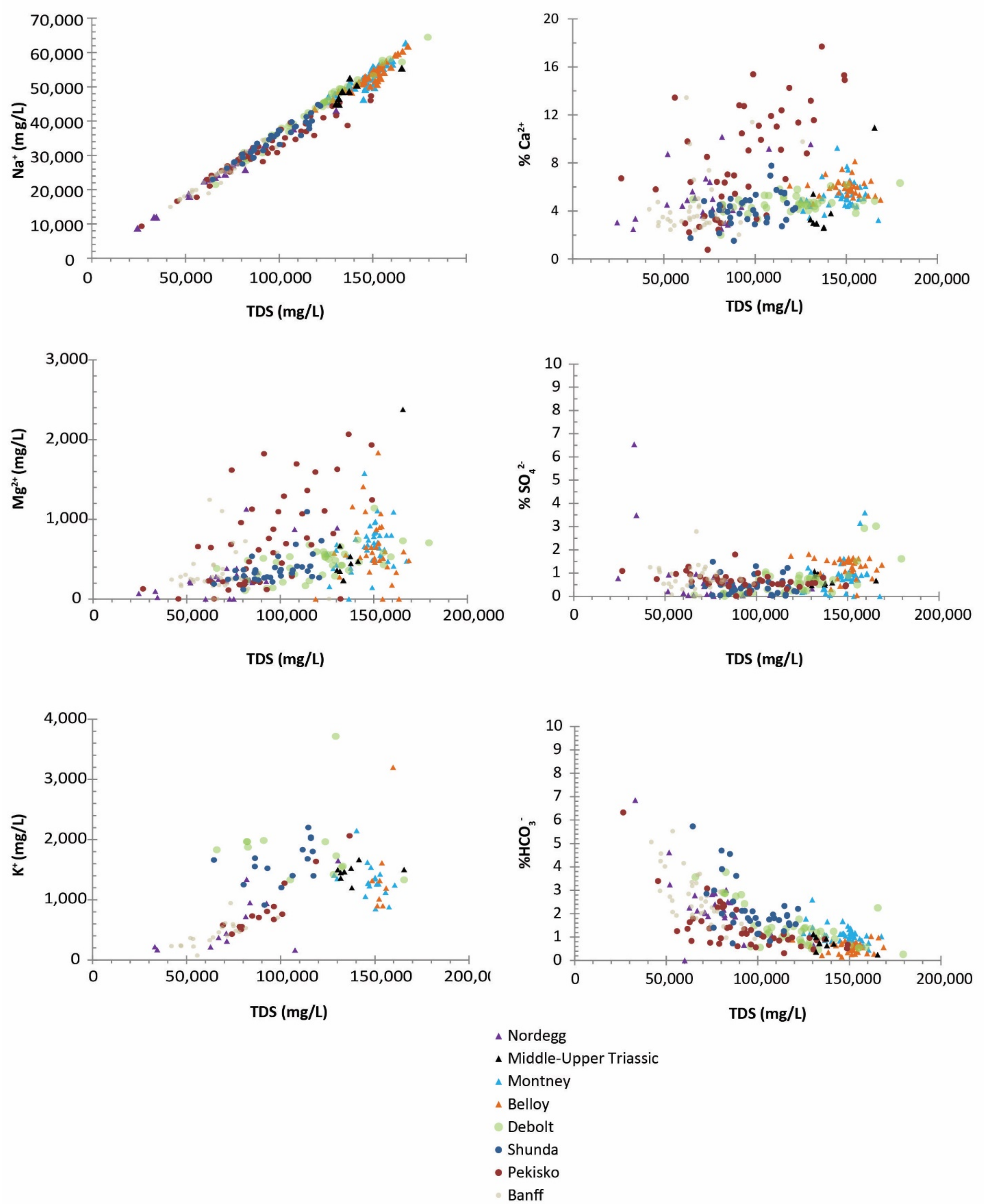

Figure 140. Major ion plots for the Mississippian–Jurassic aquifers, west-central Alberta study area. Abbreviation: TDS, total dissolved solids.

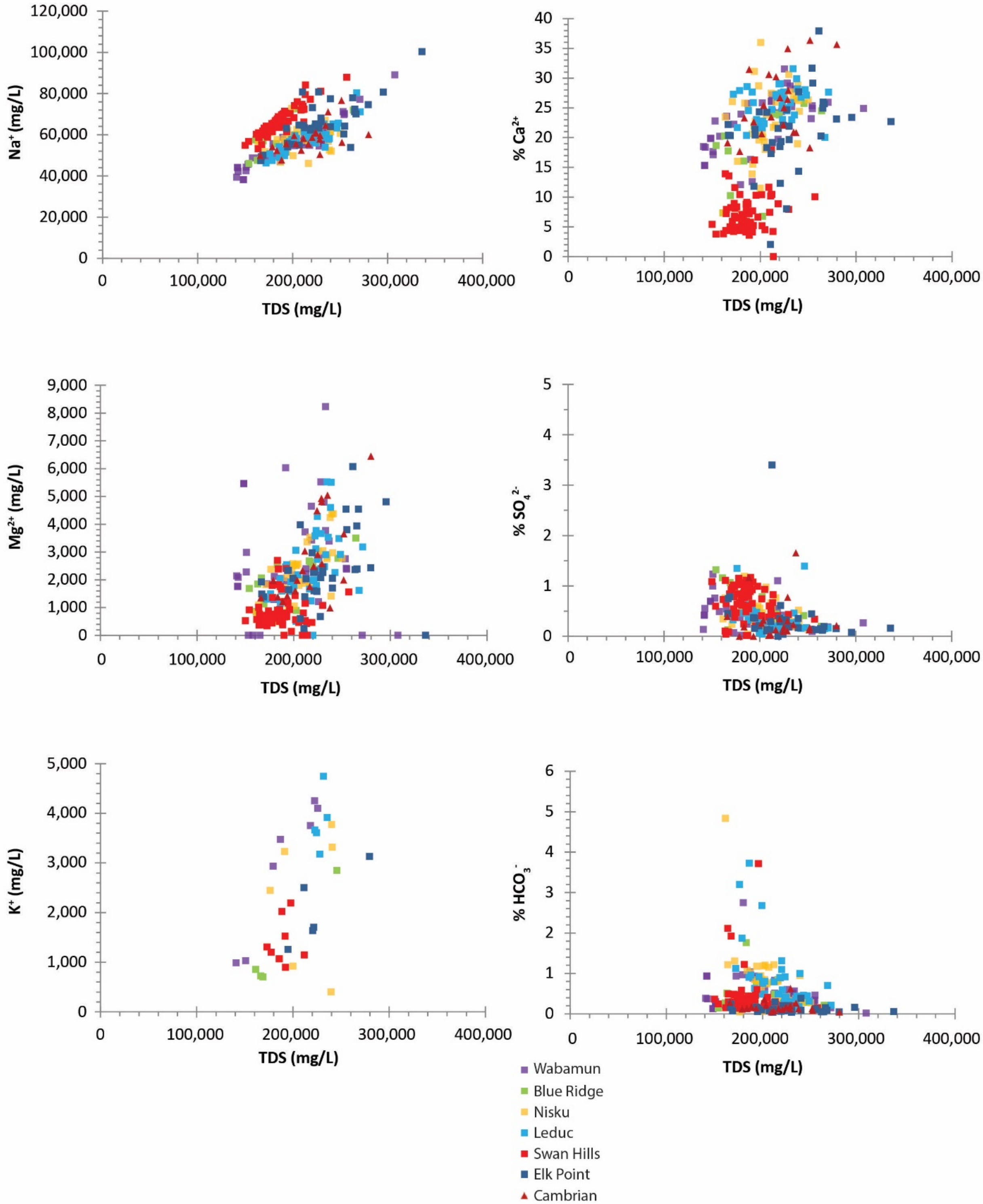

Figure 141. Major ion plots for the Cambrian–Devonian aquifers, west-central Alberta study area. Abbreviation: TDS, total dissolved solids.

Appendix 3 – Summary Tables of Results

Table 2. Results summary from the water recovery and total dissolved solids (TDS) mapping, west-central Alberta study area.

	Water Recovery Mapping				TDS Mapping						
Aquifer	**Figure**	**Number of DSTs**	**% with Water**	**Maximum Recovery (m)**	**Figure**	**Initial Points**	**Final Points**	**TDS Range (mg/L)**	**Gridding Method**	**Mean Error (mg/L)**	**RMSE (mg/L)**
Wapiti*	28	754	54	1332	73	N/A	N/A	662–8294	N/A	N/A	N/A
Cardium	29	78	20	1348	74	173	28	8 425–29 541	EBK	-54	3332
Dunvegan	30	30	15	1082	N/A	129	1	N/A	N/A	N/A	N/A
Viking	31	207	50	1463	75	286	31	14 855–29 171	OK	-56	4009
Spirit River	32	162	36	1950	76	730	43	10 965–58 224	EBK	252	8881
Bluesky	33	43	17	1460	N/A	96	12	9019–72 839	NA	NA	NA
Gething	34	290	35	1950	77	856	46	17 357–81 661	EBK	445	15 748
Cadomin	35	50	40	1737	78	155	28	31 614–70 789	EBK	20	9018
Nikanassin	36	7	28	1460	N/A	35	6	N/A	N/A	N/A	N/A
Nordegg	37	57	12	2165	79	1445	25	24 339–130 396	IDW	3935	16 388
Middle–Upper Triassic	38	66	8	1678	N/A	83	9	N/A	N/A	N/A	N/A
Montney	39	92	14	1992	80	535	42	125 125–167 496	IDW	302	9109
Belloy	40	98	40	1844	81	146	34	143 570–153 103	SK	52	10 191
Debolt	41	88	43	2273	82	343	42	70 755–174 813	SK	-1054	17 351
Shunda	42	80	9	1966	83	413	35	65 160–121 948	IDW	290	10 451
Pekisko	43	74	15	1725	84	566	37	34 892–148 388	IDW	-1657	29 160
Banff	44	69	9	1118	85	533	40	42 539–125 999	IDW	-1449	13 967
Wabamun	45	130	76	3125	86	552	38	148 655–240 482	SK	572	11 953
Blue Ridge	46	72	61	2557	87	292	15	154 189–264 406	SK	567	19 754
Nisku	47	127	52	3658	88	638	36	161 745–250 223	IDW	2016	17 265
Leduc	48	106	74	4370	89	516	40	175 590–271 485	IDW	403	17 756
Swan Hills	49	136	62	2747	90	1879	73	158 015–254 665	IDW	-2160	13 843
Elk Point	50	60	39	2801	91	213	69	166 883–336 478	IDW	205	30 659
Cambrian	51	45	48	3159	92	77	15	188 566–279 921	IDW	-5644	23 032

*See Nakevska and Singh (2017) for details.

Abbreviations: DST, drillstem test; EBK, empirical Bayesian kriging; IDW, inverse distance weighting; N/A, not available; OK, ordinary kriging; RMSE, root mean square error; SK, simple kriging

Table 3. Results summary from the hydraulic head (HH) mapping, west-central Alberta study area.

Aquifer	Figure	Initial Points	Final Points	HH Range (m asl)	Gridding Method	Mean Error (m asl)	RMSE (m asl)
Wapiti*	52	N/A	N/A	614-921	N/A	N/A	N/A
Cardium	53	243	40	383–809	IDW	-0.2	22.0
Dunvegan	N/A	109	14	N/A	N/A	N/A	N/A
Viking	54	407	83	366–509	SK	0.8	39.0
Spirit River	55	299	75	366-681	SK	0.12	42.0
Bluesky	56	70	28	592-721	EBK	-0.6	24
Gething	57	1046	90	401–790	EBK	3.0	68.0
Cadomin	58	75	31	574-604	EBK	0.1	12.0
Nikanassin	N/A	13	5	N/A	N/A	N/A	N/A
Nordegg	59	274	11	365–757	EBK	13.3	127.2
Middle–Upper Triassic	N/A	29	5	N/A	N/A	N/A	N/A
Montney	60	190	50	573–674	EBK	0.2	24.8
Belloy	61	74	40	556–707	EBK	0.7	16.9
Debolt	62	79	61	526–698	EBK	0.0	28.2
Shunda	63	79	29	563–682	EBK	0.2	65.2
Pekisko	64	153	21	385–708	EBK	1.5	45.1
Banff	65	185	17	434–694	EBK	3.4	58.4
Wabamun	66	154	53	356–1102	EBK	0.7	50.7
Blue Ridge	67	89	27	385–1083	EBK	-5.1	76.6
Nisku	68	155	19	414-1182	EBK	33.2	130.3.6
Leduc	69	112	24	811–1068	EBK	-0.4	70.1
Swan Hills	70	361	23	921-986	EBK	2.3	69.0
Elk Point	71	72	36	762–1070	EBK	2.5	37.0
Cambrian	72	33	17	789–981	EBK	0.9	26.1

[1]see Singh and Nakevska (2017) for details

Abbreviations: DST, drillstem test; EBK, empirical Bayesian kriging; IDW, inverse distance weighting; N/A, not available; OK, ordinary kriging; RMSE, root mean square error; SK, simple kriging

Table 4. Results summary from the water driving force mapping, west-central Alberta study area.

Aquifer	Figure	Hydraulic Head Gradient Dominated Areas	Buoyancy Gradient Dominated Areas
Wapiti	93	Throughout	None
Cardium	94	Throughout	None
Dunvegan	N/A	N/A	N/A
Viking	95	Throughout	None
Spirit River	96	Throughout	None
Bluesky	N/A	Throughout	None
Gething	97	Throughout	Isolated areas
Cadomin	98	Some	Some
Nikanassin	N/A	N/A	N/A
Nordegg	99	Throughout	None
Middle-Upper Triassic	N/A	N/A	N/A
Montney	100	Northern portion	Southern portion
Belloy	101	Majority	Some areas
Debolt	102	Majority	Isolated areas
Shunda	103	Majority	Small area
Pekisko	104	Throughout	None
Banff	105	Majority	Small area
Wabamun	106	Western portion	Eastern portion
Blue Ridge	107	Western portion	Eastern portion
Nisku	108	West/central portion	Eastern portion
Leduc	109	Minor	Throughout
Swan Hills	110	Minor	Throughout
Elk Point	N/A	N/A	N/A
Cambrian	111	Small areas	Majority

Abbreviation: N/A, not available

Appendix 4 – Culling Steps

Pressure Culling

Useful drillstem tests (DSTs) were selected based on the following selection criteria:

- DST had information on the top and bottom of the tested interval
- DST was conducted over a reasonably defined interval (<50 m)
- tested interval did not straddle multiple formations
- DST recovered water
- DST was mechanically sound (i.e., no misruns)
- DST pressure had stabilized or was close to stabilization (Pmax was provided)
- flow and shut-in times were reported

Outliers were investigated with an emphasis on the following conditions:

- small water recoveries (less than 100 to 300 m, depending on the formation)
- final shut-in and final flow times less than 30 minutes
- difference between final and initial shut-in pressures was more than 25%

The DSTs passing the above culling criteria were subsequently examined using the cumulative interference index methodology (Singh et al., 2017), to determine if the pressure was influenced by production/injection activities.

Total Dissolved Solids Culling

Useful formation water samples were selected based on the following selection criteria:

- charge balance error was between -10% and 10%
- sampled interval was <50 m
- sampled interval did not straddle multiple formations
- DST recovered water

Additional culling was performed in order to identify contaminated samples. The ratios are mass-based unless indicated otherwise. Samples were excluded if

- pH <5 or >8 (indication of acid water, or corrosion-inhibitor completion fluid),
- CO_3^- or OH^- reported (only a concern if pH <8.3, in which case CO_3^- should not exist or if pH <10.2 in which case OH^- should not exist, both indicative of drilling-fluid contamination or mud recovery),
- density <1 g/cc (indication of alcohol contamination),
- Ca/Cl >0.3 and pH <5.7 (indication of acid water completion fluid),
- Na/Ca <1.2 (indication of acid water completion fluid),
- Na/Cl >1 (characteristic of a large mud recovery),
- sampling locations such as a separator, pressure/mud tank, stock, swab, gas meter, meter run, manifold, sight glass, treater, frack manifold, flare line, rig tank, tubing, choke manifold indicate higher chance of contamination,
- Na/K <20 and Na/Cl (milliequivalents/litre) <0.6 and ‘water type’ field shows KCl.

Outliers were examined with an emphasis on the following conditions:

- small water recoveries (less than 100 to 300 m, depending on the formation)
- various criteria can’t be examined because of missing information, including missing major ions (Ca^{2+}, Mg^{2+}, Na^+, K^+, CO_3^-, HCO_3^-, Cl^- and SO_4^{2-}), pH, or density values
- analyses show <80% milliequivalents/litre of total anions present as Cl^-
- indication of contamination in the ‘remarks’ or ’recovery/description’ fields, such as the terms alcohol, acid, ammonium, condensate, coloured sample
- Stiff diagram indicates mud filtrate or acid

Appendix 5 – Sources of Errors, Uncertainties, and Limitations

Efforts were made throughout the study to reduce potential sources of error. However, it is acknowledged that potential errors and uncertainties exist, which are described below.

Errors in Pressure Data

The drillstem tests (DSTs) used in this study have undergone a documented culling process so only the tests with the most representative pressures were used. However, certain errors in the recorder and calculation of reservoir pressures are possible.

Relative errors in DST pressure gauge readings are in the range of 0.05% (Reid, 2011). This relative error typically has a minimal effect on the results of pressure determinations within lower pressured formations but could have a more substantial impact on pressure determinations in higher pressure (deeper) formations.

The data comes from DSTs conducted over multiple decades. Some of the pressures were recorded in relation to ambient atmospheric pressure (i.e., gauge pressure) and others in relation to an absolute pressure. The difference in reference could lead to an approximate error of 101.325 kPa in the pressure, which is equivalent to an error of 10.3 m in hydraulic head.

Although recorded DST pressures are related to a specific recorder at a specific depth, this information was not readily available. To overcome this lack of information, the pressure data was allocated to the midpoint between the top and bottom packer of the test interval. The average error for this varies depending on the length of the DST interval and the placement of recorders.

The DSTs that do not reach reservoir pressure during a shut-in period require a Horner plot extrapolation to determine the reservoir pressure. This extrapolation assumes radial flow in the reservoir. Due to the number of DSTs in the project, individual analysis of every published extrapolation was not completed.

Errors in Chemistry Data

The chemical analysis data were subjected to culling criteria in order to select the most representative formation water samples, however, errors may still exist in the reported concentration of constituents. Possible errors in reported values may come from the various techniques used for sample preservation, collection, and analysis. As data originate from different laboratories, detection limits for parameters may be different or have changed over the years.

Error in Data Allocation

Pressure and salinity data were assigned to a specific geological unit based on the reported test interval and the structural geology framework grids created for the west-central Alberta study area (Corlett et al., 2019). The structural framework grids are based on picks from wells, modelled to create a continuous surface. A geological unit top pick is not made in every well for each geological unit included in the geological model. There may be a discrepancy between DST or water sample collection depth, the geological unit top pick for that given location, and the structural framework grids. The net result could be some error in allocation of data to geological units, especially where located near to a unit top or bottom. However, the utmost care was taken for hydrogeological data located near the vertical boundary between units. For more information on the error and assumptions related to the stratigraphic surfaces, the reader is referred to Corlett et al. (2019). The DSTs that appeared to straddle multiple formations were not used in this study. It is acknowledged that valid data may have been omitted in certain cases. Towards some subcrop edges, DSTs with a packer set in an above formation or where the gridding process placed the top of the DST interval in another formation were considered straddles and were not included in the study area.

Data Limitation and Interpolation Error

Hydraulic head and TDS maps have uncertainties associated with the spatial distribution of data. Areas lacking data inherently have higher uncertainties than data-dense areas.

Hydraulic head and TDS grids are associated with interpolation errors. A root mean square error (RMSE) is reported to provide a measure of the grid interpolation error. The RMSE is used to show how similar interpolated grid values are to the original input data for the entire grid.

In general, all maps and analyses for this study have been completed at a regional scale and show generalized trends over the west-central Alberta study area. A more local-scale analysis of the hydrogeology and hydrochemistry is required for site-specific studies.